The development of optogenetic tools for investigations into mammalian circadian organisation

A thesis submitted to the University of Manchester for the degree of

Doctor of Philosophy

in the Faculty of Life Sciences

2013

Ling Zhuang

Table of Contents

Word Count: 37165 words

Table of Figures

Abstract

Many biological oscillators are perpetuated by an autonomous molecular clockwork that generates rhythmic expression of clock genes. Whilst the periods of these endogenous rhythms deviate from 24h, daily cues in the natural environment synchronise all internal rhythms precisely to 24h. Molecular signals, such as the principle intracellular messenger cAMP, are amplified by the $G\alpha_s$ signalling pathway upon activation of GPCRs and regulate a diverse array of physiological processes, one of which is entrainment of the mammalian circadian clock. cAMP conveys environmental cues to the molecular oscillatory network by interacting with the autonomous feedback loop of genes and proteins, thereby resetting their rhythmic expression. Many pharmacological studies have shown that the cAMP signalling cascade is relevant to the entrainment of the mammalian clock. However, due to inherent complications arising from lack of target and subtype specificity, pharmacological agents are known to elicit confounding side-effects in *in vivo* models. Indeed, there is still ambiguity about the relevance of physiological cAMP signalling in regulating circadian dynamics.

Opsin photopigments offer a powerful and drug free platform to initiate signalling cascades under temporally controlled parameters. The $G\alpha_s$-coupled *Carybdea rostonii* opsin (JellyOp) robustly activates cAMP signalling in functional studies, and is thus suitable for addressing the contributions of cAMP to circadian regulation. Furthermore a $G\alpha_s$-decoupled opsin variant (F139A JellyOp) was engineered which, despite being deficient in $G\alpha_s$ interactions, retained the ability to modulate the MAPK pathway in fibroblasts, comparably to JellyOp. Both the wildtype and F139A JellyOp photopigments were therefore employed for investigating contributions of GPCR triggered cAMP dependent pathways to regulating the mammalian circadian clock over background signals.

Upon stimulating wildtype or F139A JellyOp photopigments with equivalent irradiances and durations of ultraviolet and infra-red filtered light, both $G\alpha_s$ dependent and independent signalling impacted on the phasing of the fibroblast clock respectively. However, the two JellyOp signalling profiles produced divergent phase response curves in the fibroblast clock, which reflected inherent differences in the phase-responsiveness of the clock to cAMP dependent and independent cascades. A strong relationship was reported between the magnitude of a JellyOp triggered circadian response and the duration of photostimulation, a correlation that was been previously described though *in vivo* studies of photo-entrainment. These studies have confirmed that mammalian circadian dynamics are responsive to temporally controlled cAMP signalling in a phase and duration dependent manner. Thus, JellyOp and F139A JellyOp are suitable opsin photopigments for investigating the influences of $G\alpha_s$ dependent and independent mechanisms on mammalian clock dynamics.

Declaration

I declare that no portion of the work referred to in the thesis has been submitted in support of an application for another degree or qualification of this or any other university or other institute of learning.

Copyright Statement

i. The author of this thesis (including any appendices and/or schedules to this thesis) owns certain copyright or related rights in it (the “Copyright”) and she has given The University of Manchester certain rights to use such Copyright, including for administrative purposes.

ii. Copies of this thesis, either in full or in extracts and whether in hard or electronic copy, may be made only in accordance with the Copyright, Designs and Patents Act 1988 (as amended) and regulations issued under it or, where appropriate, in accordance with licensing agreements which the University has from time to time. This page must form part of any such copies made.

iii. The ownership of certain Copyright, patents, designs, trademarks and other intellectual property (the “Intellectual Property”) and any reproductions of copyright works in the thesis, for example graphs and tables (“Reproductions”), which may be described in this thesis, may not be owned by the author and may be owned by third parties. Such Intellectual Property and Reproductions cannot and must not be made available for use without the prior written permission of the owner(s) of the relevant Intellectual Property and/or Reproductions.

iv. Further information on the conditions under which disclosure, publication and commercialisation of this thesis, the Copyright and any Intellectual Property and/or Reproductions described in it may take place is available in the University IP Policy (see http://www.campus.manchester.ac.uk/medialibrary/policies/intellectual-property.pdf), in any relevant Thesis restriction declarations deposited in the University Library, The University Library’s regulations (see http://www.manchester.ac.uk/library/aboutus/regulations) and in The University’s policy on presentation of Theses

Acknowledgements

I would firstly like to thank my supervisor, Professor Robert J Lucas for his invaluable guidance, support and encouragement throughout the 4 years of my PhD. I am ever so grateful for all his creative and thoughtful contributions from each lab experiment to every piece of data analysis conducted. The investment of time, ideas and advice has been instrumental in the completion of my project. It has been a privilege to work with all members of the Lucas Lab. In particular, I owe my sincerest gratitude to Dr Helena J Bailes for her generous assistance and training in all the lab techniques I have practised. I have benefited greatly from her advice and encouragement in nearly every aspect of my project. I would also like to thank Dr Tim Brown for his assistance and guidance with data analysis, Dr Annette E Allen for all her support and Jonathan Wynne for his kindness. I also appreciate his assistance with liquid nitrogen duty. I wish to thank Dr Zoher Kapacee for training me in the techniques of cell culture and molecular biology. I would also like to give my thanks to Dr Qing Jun Meng for his generous donation of cell lines and reporter mice. My gratitude also goes to Dr Vanja Pekovic-Vaughan for her assistance with cell culture techniques. I would also like to thank Professor Hugh Piggins for his kind donations of mice, and also for kindly allowing me to use his bioluminescence imaging equipment. I am also grateful to Dr Alun T Hughes and Dr Claire Guilding for their time and supervision in the lab. I am most grateful to the BBSRC and MRC for funding my PhD studies.

I dedicate my thesis to my family, who have blessed me with their love and support. I am also very grateful to my fiancé Thomas Wales, for keeping my spirits up during the long periods of toil towards the end of my thesis writing.

Abbreviations

Word	Abbreviation
Adenosine Triphosphate	ATP
Brain and Muscle ARNT-Like Protein	BMAL1
Bioluminescence Resonance Energy Transfer	BRET
Cyclic adenosine monophosphate Response Element-Binding Protein	CREB
Cyclic adenosine monophosphate Response Elements	CRE
Carboxy-Terminus	COOH
Casein Kinase	CK1
Charge-Coupled Device	CCD
Circadian Time	CT
Clozapine-N-Oxide	CNO
Connexin 43	Cx43
Cryptochrome	CRY
Cyclic Adenosine Monophosphate	cAMP
Cyclic Guanosine Monophosphate	cGMP
Complementary Deoxyribonucleic Acid	cDNA
Designer Receptors Exclusively Activated By A Designer Drug	DREADD
Encephalopsin	OPN3
Enzyme Linked ImmunoSorbent Assay	ELISA
Extracellular Signal-Regulated Kinase	ERK

Free-Running Period	FRP
G Protein Coupled Receptor	GPCR
Gamma-Aminobutyric Acid	GABA
Green Fluorescent Protein	GFP
Guanine Nucleotide Exchange Factor	GEF
Guanine nucleotide-binding protein subunit 1	GNAT1
Guanosine Diphosphate	GDP
Guanosine Triphosphate	GTP
Human Embryonic Kidney Cells	HEK293
Inositol Phosphate	IP_3
JellyOp K68F, Y132G, F139A, Y219A	JellyOp KYFY
JellyOp Y132G Y219A	JellyOp YY
JellyOp Y132G, F139A, Y219A	JellyOp YFY
Light Dark	LD
Luciferase	luc
Lysophosphatidic Acid	LPA
Mdl-12,330A Hydrochloride	MDL
Melanopsin	OPN4
Messenger Ribonucleic Acid	mRNA
Mitochondrially targeted Aequorin	mtAeq
Mitogen Activated Protein Kinase	MAPK
Neuropsin	OPN5
Passage Number	P
Period	per

Phase Response Curve	PRC
Phorbol Myristate Acetate	PMA
Protein Kinase B	PKB
Receptors Activated Solely By Synthetic Ligands	RASSL
Regulator Of G-Protein Signalling 16	RGS16
Retinal Pigment Epithelium	RPE
Retinal pigment epithelium -retinal G Protein-Coupled Receptor	RGR
Rhodopsin Epitope Tag	ID4
Rod Outer Segment	ROS
Sarcoma	Src
Small Interfering RNA	siRNA

1. General introduction

1.1.1 G Protein coupled receptors

Mammalian cellular physiology is constantly shaped by local environmental cues including photons, hormones, neurotransmitters and growth factors (Oldham and Hamm, 2008). Such information is captured by protein receptors, many of which are present on a cell's surface, and subsequently relayed across the cell membrane. The vast and diverse families of cell surface receptors thus form a signalling platform between a cell and its environment. This allows extrinsic cues to be coupled to intracellular effectors, consisting of countless ion channels, enzymes and gene transcription factors.

G protein coupled receptors (GPCRs) are a diverse family of cell surface receptors distinguished by their conserved topology of seven hydrophobic membrane spanning helices joined by three intracellular loops and three extracellular loops (Rosenbaum et al. 2009). Upon activation, these monomeric proteins couple extracellular cues into a range of intracellular targets via signal transducer proteins including heterotrimeric G-proteins and β-arrestins (Oldham and Hamm. 2008, Miller and Lefkowitz. 2001). Such interactions lead to an amplification of the external signal though signalling cascades which eventually result in a cellular response (Ronnet and Moon. 2002, Pierce et al. 2002, Rosenbaum et al. 2009). Phylogenetic classification of GPCRs has produced at least five receptor classes based on conversed motifs and residues (Fredriksson et al. 2003). Class A represents the largest group consisting of at least 700 members, distinguished by the presence of conserved "signature" amino acid residu es in the transmembrane helices, such as the highly conserved (E/D) RY motif on Helix 3 and NPxxY motif on Helix 7 (Figure 1.1).

1.1.2 GPCR primary and secondary structure

All members of the GPCR receptor family are monomeric proteins which share a common topology of seven transmembrane α-helices joined by three extracellular and intracellular loops (Pierce et al. 2002). The N and C termini are typically extracellular and intracellular respectively but in the case of light sensitive GPCRs such as mammalian rhodopsins and cone opsins, where receptors are translocated into intracellular membrane disks of photoreceptor outer segments, the C-terminus is cytoplasmic whereas the N terminus is intradiscal (Garriga et al. 1996, Figure 1.1). The α-helices of GPCRs form a tight, ring-shaped central core that is

highly hydrophobic. Within the core, helix-helix interactions contribute to the functional tertiary structure of the GPCRs necessary for receptor stability, ligand binding and ligand-induced conformational changes (Rosenbaum et al. 2009). Ligand binding pockets involve multiple amino acid motifs on extracellular loops and transmembrane domains (Venkatakrishnan et al. 2013). Amino acid residues within the intracellular loops interact with effector targets such as G proteins (Moro et al. 1993). A high density of serine and threonine residues is often present on the C-terminus of GPCRs, which undergo reversible phosphorylation following ligand binding and is important in signal desensitisation and receptor internalisation (Hata and Koch. 2003).

GPCRs undergo a variety of post-translational modifications. The N terminus and extracellular loops of receptors are often glycosylated, which can be critical for correct cell-surface localisation (Chen et al. 2010). Extracellular Cysteine residues in the first two loops form disulfide bonds which can influence the stability of the receptor structure. In the case of bovine rhodopsin, the disulphide bond is formed between Cysteine residues at position 110 and 187 (Karnik and Khorana. 1990). Some GPCRs contain cysteine residues in the C-terminal domain, which can serve as site for palmitoylation (Figure 1.1). Palmitoylated cysteines become attached in the plasma membrane as palmitate groups penetrate into the lipid bilayer.

1. General introduction

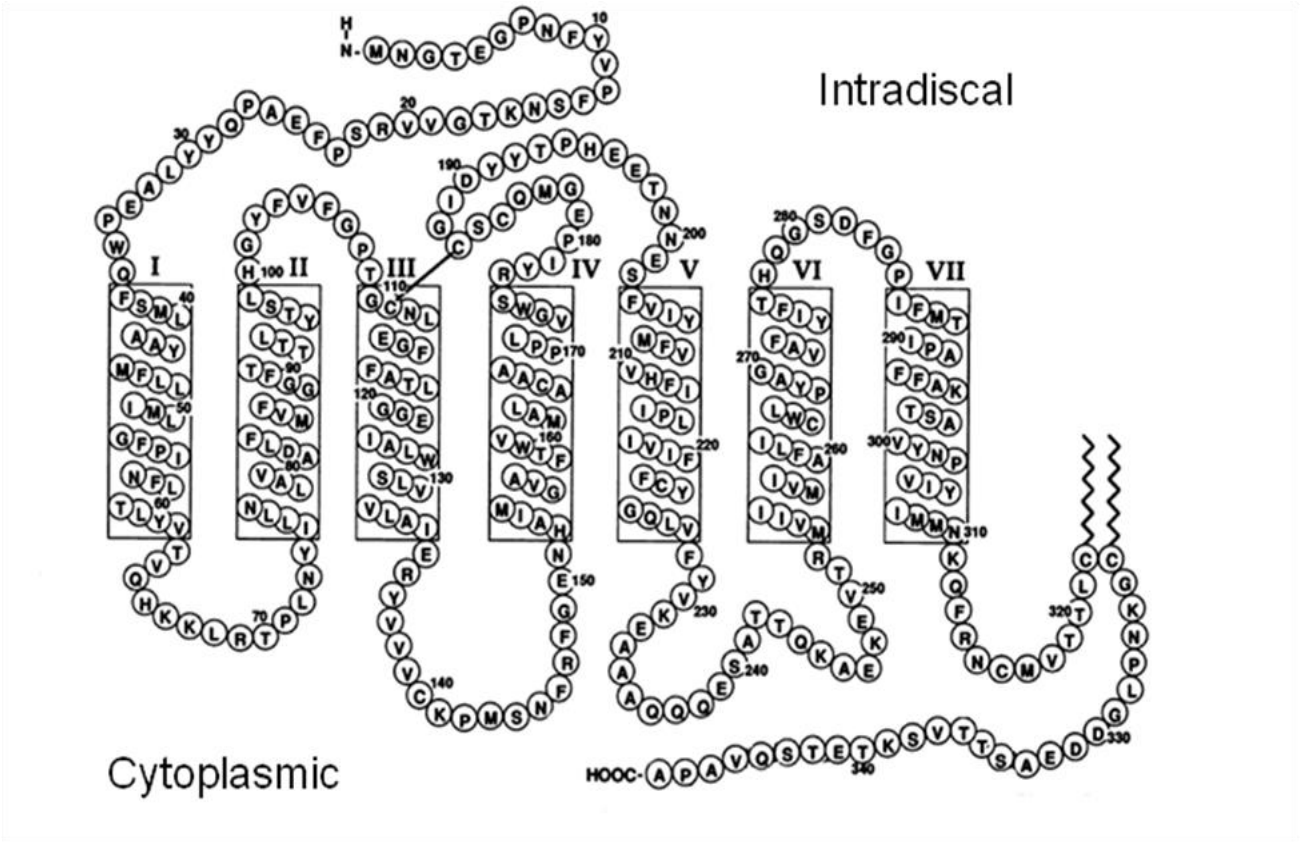

Figure 1.1 Schematic of membrane topology and key structural features of bovine rhodopsin, a typical Class A GPCR.

The receptor consists of seven transmembrane domains (as highlighted in rectangles and numbered in roman numerals) are connected by three extracellular and three intracellular loops. Structural elements such as the DRY motif at the cytoplasmic end of TM3 and NPXXY motif in TM7 are highly conserved. The C-terminus of bovine rhodopsin also contains two cysteine residues which undergo palmitoylation and extracellular cysteine residues, C110 and C187 form disulphide bonds. Every 10th amino acid residue is numbered. (Adapted from Hargrave and McDowell. 1992)

1.1.3 Ligand binding interactions on GPCRs

GPCRs can be modulated by a vast range of stimuli including photons, ions, amines and proteins (Shiraishi et al. 2013). Prior to signal transduction, ligand binding involves distinct interactions of the ligand with several domains of the receptor. Receptors for small ligand molecules such as biogenic amines, typically bind the ligand through a pocket involving conserved residues located in transmembrane helices and the second extracellular loop (Shi and Javitch. 2002). In particular, mutation of a highly conserved Aspartate residue in the third transmembrane helix fully abolishes binding affinities of several receptors such as serotonin and acetylcholine receptors from their cognate ligands without compromising receptor expression levels (Kristiansen et al. 2000, Page et al. 1995).

Ligand binding interactions are substituted by another mechanism in light sensitive GPCRs such as opsin photopigments. Visual pigments such as bovine rhodopsin are composed of a 11-*cis*-retinal chromophore bound to an opsin apoprotein via Schiff base on a converved lysine residue in the 7th transmembrane helix (Govardhan and Oprian. 1994). In the *cis* configuration, the chromophore promotes an inactive receptor configuration, preventing spontaneous activation (Cohen et al. 1992). Photon absorption induces isomerisation of 11-*cis*-retinal to all-*trans*-retinal, which functions as a receptor agonist, promoting a conformational change which leads to receptor activation. Mutation of this lysine residue with a non-polar amino acid such as alanine or methionine has been shown to abolish affinity of opsins to chromophores. Mutagenesis studies have shown that mutation of lysine 296 results in constitutively active protein (Cohen et al. 1992) which is able to interact with its cognate G protein, transducin. Furthermore, mutations of the Lys296 residue in rhodopsin have been associated with retinal diseases such as autosomal dominant retinitis pigmentosa (Rao and Oprian. 1996).

1.1.4 Conformational changes following agonist binding

GPCRs are thought to spontaneously fluctuate between various conformational states, but stabilised towards a state upon binding ligand (Baker and Hill. 2007). This hypothesis accounts for the different basal levels of constitutive G protein stimulation by various GPCRs, even in absence of ligands (Milligan. 2003). Traditionally, ligands were classified by their ability to influence coupling dynamics of GPCRs with G proteins. Ligands which suppressed basal levels of G protein activation were defined as inverse agonists. In contrast, partial and full agonists were assigned to ligands which favoured intermediate or maximal G protein responses respectively (Seifert et al. 2001). In addition, a neutral antagonist was defined as a ligand that bound and shielded the receptor from the action of agonists, but did not exert influence on G protein interactions.

Investigations into the structural-functional relationship of GPCR and G protein interactions have been greatly advanced by highly resolved structures of bovine rhodopsin and human β2 Adrenergic receptors (Palczewski et al. 2000, Rasmussen et al. 2007, Cherezov et al. 2007, Rasmussen et al. 2011). In these GPCRs, agonist binding induces movements between transmembrane helical domains. This movement is thought to expose G-protein-binding sites within cytoplasmic loops of the receptor (Konig et al. 1989) and promote interactions with cognate G proteins (Ballesteros et al. 2001, Rasmussen. 2011).

1.1.5 G protein coupling

Heterotrimeric G proteins were the first family of effector proteins discovered to mediate the physiology of GPCRs (Wess. 1997). In an inactive state, the membrane bound complex is composed of three subunits: α-GDP, β and ɣ (Wittinghofer. 1996). However, interaction with an activated GPCR promotes the release of guanosine diphosphate (GDP). The GDP is subsequently replaced by a diffuse guanosine triphosphate (GTP), which activates and liberates the Gα protein subunit from the βɣ dimer. The diffuse but membrane bound Gα protein associates with downstream enzyme effectors to elicit specific signalling cascades depending on the target enzyme (Marinissen and Gutkind. 2001). At least 6 different Gα protein paralogues are presently known to be participate in GPCR signalling; $G\alpha_i$, $G\alpha_o$, $G\alpha_s$ and $G\alpha_q$, $G\alpha_t$ and $G\alpha_{12/13}$. Gα proteins are auto-regulated by their intrinsic GTPase activity which catalyses the hydrolysis of GTP to GDP. As this occurs, the subunit becomes deactivated and reassociated with the βɣ dimer.

Many amino acid residues which reside in the intracellular loops of the GPCR play a critical role mediating interactions with G protein families. Within class A GPCRs, a conserved lipophilic amino acid located at the 3' end of the 2nd intracellular loop is strongly involved in G protein interactions. In the β2 adrenergic receptor and human Muscarinic 1 receptor, this residue corresponds with phenylalanine 139 (Moro et al. 1993). The authors showed that replacement of the phenylalanine with non-polar amino acids in both GPCRs did not compromise receptor expression or agonist affinities relative to the wildtype receptor, but caused marked attenuation of agonist induced secondary messenger production. As previously mentioned, there are at least six different subgroups of Gα proteins subunit presently known to be participate in GPCR signalling; $G\alpha_i$, $G\alpha_o$, $G\alpha_s$ and $G\alpha_q$, $G\alpha_t$ and $G\alpha_{12/13}$. These subunits are distinguished by the manner of interactions on effector targets.

1.1.5.1 Gαs and Gαi protein signalling

$G\alpha_s$ proteins interact with membrane bound isoforms of adenylate cyclase, causing activation of the enzyme (Taussig and Gilman. 1995). The enzyme catalyses the conversion of ATP to cAMP (Figure 1.2), a small soluble diffusible messenger which activates many effector proteins including PKA, EPAC and CNG channels (Ishikawa and Homcy. 1997, Kaupp and Seifert. 2002, Rooij et al. 2000). PKA is well studied heterotetrameric kinase, composed of two catalytic and regulatory subunits. cAMP binds to the regulatory subunit and induces

conformational changes that lead to the dissociation of the enzyme catalytic and regulatory subunits (Cheng et al. 2009). The active catalytic subunit can then elicit a range of diverse cellular events by phosphorylating various enzymes and transcription factors. EPAC, a cAMP dependent guanine nucleotide exchange factor exchange protein contains an evolutionally conserved cAMP-binding domain and is directly activated by the messenger (Cheng et al. 2009). EPAC is known to regulate the Ras superfamily small GTPases Rap1 and Rap2 (De Rooij et al. 2000). HCN channels function as voltage-gated channels which require bound cAMP for channel to open (Kaupp and Seifert. 2002). cAMP is negatively regulated by phosphodiesterase, an enzyme which catalyses the metabolism of cAMP to AMP, thereby inactivating the signaling cascade to basal levels. Some isoforms of cyclc nucleotide phosphodiesterases are upregulated by PKA (Keravis and Lugnier. 2012).

The $G\alpha_i$ subunit also interacts with adenylate cyclase but in an antagonistic manner to $G\alpha_s$ (Figure 1.2), whereby it reduces the basal activity of the enzyme (Taussig et al. 1993). Activation of $G\alpha_i$ therefore reduces intracellular levels of cytosolic cAMP. The $G\alpha_i$ subunit is susceptible to inactivation by pertussis toxin (Gunther et al. 2000) and is also regulated internally by Regulators of G proteins such as RGS4 (Doi et al. 2011).

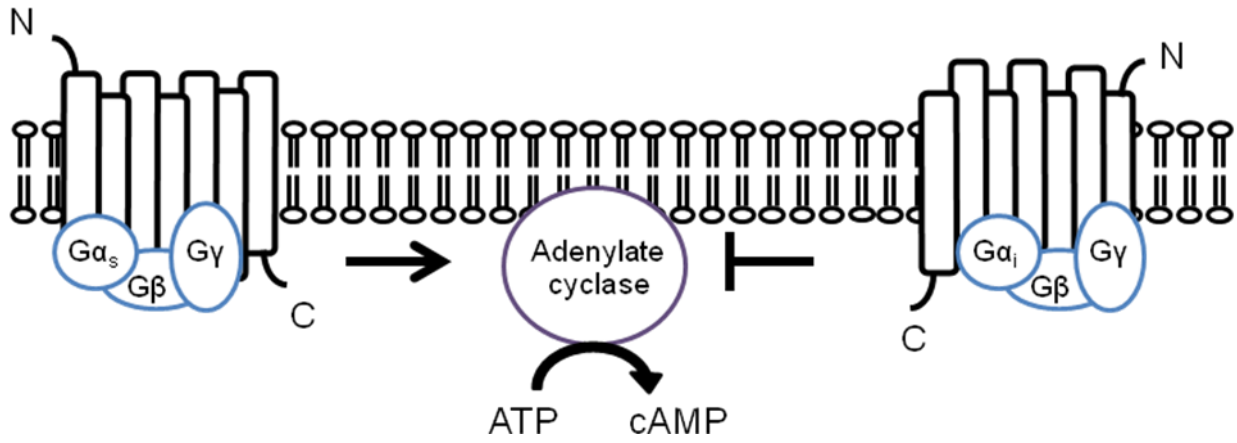

Figure 1.2 Schematic of $G\alpha_s$ and $G\alpha_i$ protein signalling

GPCRs activate their cognate Gα proteins by promoting the exchange of GTP for GDP. Activated $G\alpha_s$ dissociate from the βγ subunits and activate membrane bound adenylate cyclase, an enzyme that catalyses the production of cAMP from ATP. In contrast, $G\alpha_i$ protein inhibits adenylate cyclase to inhibit formation of cAMP.

1.1.5.2 $G\alpha_q$ protein signalling

$G\alpha_q$ subunit is a ubiquitous subunit which activates PLCβ (Lee et al. 1992), a membrane bound enzyme which catalyses the hydrolysis of the membrane lipid phosphatidylinositol 4,5-bisphosphate (PIP_2), producing inositol 1,4,5-triphosphate (IP_3) and diacylglycerol (DAG) (Figure 1.3). Both products act as independent diffusible messengers. IP_3 is water-soluble and diffuses across the cytoplasm to the endoplasmic reticulum where it activates IP_3 receptors, thereby releasing calcium from within the endoplasmic reticulum into the cytoplasm (Akimzhanov and Boehning. 2011). This leads to a rapid induction in cytosolic calcium levels. Calcium signaling is mediated by a wide range of proteins including calcineurin, calmodulin and PKC (Clapham et al. 2007). The latter is capable of modulating the behaviour of downstream transcription factors such as CREB through its kinase activity as well as interact with other signaling pathways such as the MAPK cascade (Mao et al 2007, Fan et al. 2004).

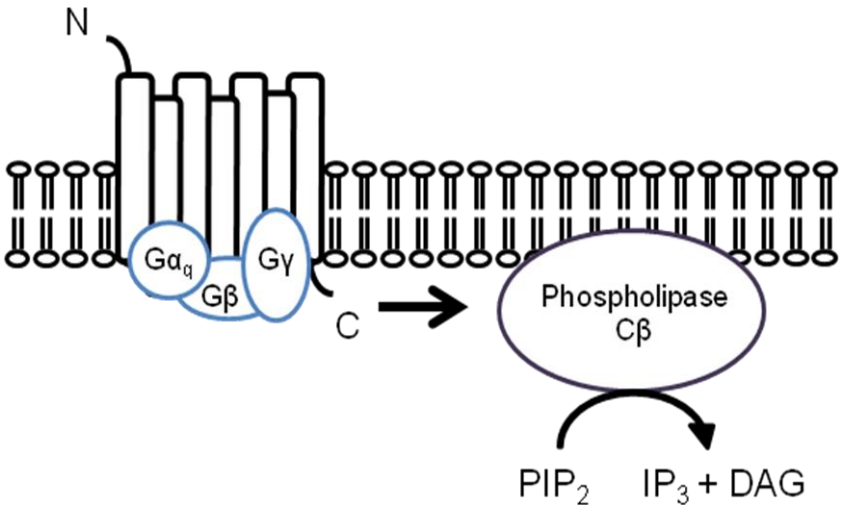

Figure 1.3 Schematic of $G\alpha_q$ protein signalling

$G\alpha_q$ protein activates phospholipase Cβ. PLCβ in turn catalyses the hydrolysis of PIP_2 to DAG and IP_3. DAG remains bound to the membrane, and IP_3 is released as a soluble structure into the cytosol. IP_3 then diffuses through the cytosol to bind to IP_3 receptors, particular calcium channels in the endoplasmic reticulum (Clapham et al. 2007). These channels are specific to calcium and only allow the passage of calcium to move through. This causes the cytosolic concentration of calcium to increase, causing a cascade of intracellular signalling.

1.1.5.3 $G\alpha_o$ protein signalling

The $G\alpha_o$ subunit is classified as a member of the $G\alpha_i/G\alpha_o$ family based on its homology to $G\alpha_i$ proteins (Won and Ghil. 2009), and like $G\alpha_i$, it is susceptible to inactivation by pertussis toxin. Direct effectors of $G\alpha_o$ are not well established, although studies by Nakata and Kozasa 2004 have identified that G protein-regulated inducer of neurite outgrowth 1 and 2 (GRIN1 and GRIN2, respectively) as a novel effector candidates for $G\alpha_o$. GRIN1 exhibits domains that are required for $G\alpha_o$ binding in its carboxyl-terminal region. In addition, $G\alpha_o$-GRIN1 interactions have been confirmed by GST pull-down experiments.

A study by Kojima et al. 1997 revealed the expression of $G\alpha_o$ that was colocalised with visual pigment SCOP2 in hyperpolarising ciliary photoreceptors of the scallop retina. Subsequent studies have suggested that either $G\alpha_i$ or $G\alpha_o$ protein is involved in initiating a hyperpolarizing phototransduction cascade in the scallop ciliary eye photoreceptors (Gomez and Nasi, 2000) via the activation of guanylate cyclase.

1.1.5.4 $G\alpha_t$ protein signalling

The $G\alpha_t$ subunit, transducin, is expressed abundantly in specialized sensory cells such as ciliary photoreceptors of the retina and pineal photoreceptors (van Veen et al. 1986). Transducin links the photoactivation of rhodopsin with activation of a type VI cGMP phosphodiesterase in rod photoreceptors (Clack et al. 2006). The effector phosphodiesterase catalyses the conversion of cGMP to GMP. In the absence of light, cGMP levels are sufficient to open cGMP-gated cationic channels in the membranes of rod outer segments. These channels allow positively charged ions such as sodium and calcium to diffuse into the photoreceptor cell, resulting in a depolarized membrane (Fu and Yau. 2007). Upon exposure to light, and subsequent activation of cGMP phosphodiesterase, the reduction in intracellular cGMP leads to closure of the cationic channels and thus reduces the entry of sodium and calcium ions into the photoreceptor cell outer segments, but not the extrusion of Ca^{2+}. This gives rise to a transient, hyperpolarisation of the rod photoreceptor membrane, a critical step to visual perception. $G\alpha_t$ shares a high level of sequence similarly with Gi and is also susceptible ribosylation by pertussis toxin (West et al. 1985).

1.1.5.5 $G\alpha_{12/13}$ protein signalling

$G\alpha_{12}$ and $G\alpha_{13}$ subunits impact a wide variety of cellular processes such as growth and proliferation, cytoskeleton rearrangement, cell–cell adhesion, migration and invasion (Kurose, 2003, Kelly et al., 2007). $G\alpha_{12}$ and $G\alpha_{13}$ subunits directly activate a family of Rho-specific guanine nucleotide exchange factors (RhoGEFs), which include p115RhoGEF, PDZ-RhoGEF and leukaemia-associated RhoGEF (Fukuhara et al. 1999, Hart et al. 1998).

Upon activation, these exchange factors in turn activate the Rho family of small monomeric GTPases (Spiering and Hodgson. 2011). One of the best recognized members of the Rho GTPase family is RhoA, which targets and activates Rho kinase. The RhoA/ROCK pathway has been implicated in a wide variety of human diseases including cardiovascular disease, glaucoma and Alzheimer's disease (Loirand et al. 2006, Wang et al. 2013, Kubo et al. 2008). Other proteins that directly interact with $G\alpha_{12/13}$ include cadherins, protein phosphatases, the tight junction protein zonula occludens-1 and regulators of G protein signalling RGS16 (Sabath et al. 2008, Johnson et al. 2003

1.1.6 Termination of G protein signalling pathways

The responsiveness of cells to the constant pounding of environmental cues is subject to damping through homeostatic mechanisms. Upon chronic agonist stimulation, GPCRs become phosphorylated (Sibley et al. 1987) which reduces the affinity of GPCRs to G proteins (Gibson et al. 2000). The pioneering studies of Bouvier et al. 1988 demonstrated that the C-terminus of GPCRs functioned as a critical modulator of desensitisation. By employing site directed mutagenesis of serine and threonine residues on the β2 adrenergic receptor C-terminus, the authors showed that the point mutated β2 adrenergic receptor resulted in delayed onset of agonist induced desensitisation, when compared to the wildtype receptor. Furthermore, the authors showed that agonist induced receptor internalisation was substantially reduced in the mutated receptor compared when to WT.

1.1.7 Arrestins

Arrestins are a family of soluble proteins that regulate the signalling of different GPCRs (Alvarez. 2008). Based on phylogeny and function, the vertebrate arrestin family can be further divided into two subfamilies: visual arrestins, and non-visual or β-arrestins. (Gurevich and Gurevich. 2006).

1.1.8 β-arrestins

β-arrestins are expressed ubiquitously in all cells and tissues of vertebrates and regulate the inactivation and internalisation of GPCRs. These proteins exhibit several functional domains such as a phosphate sensor domains in the N-terminus (Nobles et al. 2007), and a motif for interactions with AP-2, an adaptor protein for clathrin-mediated endocytosis (Laporte et al. 2000). Many studies have consistently reported that the stimulation of GPCRs, such as β2 adrenergic receptors, angiotensin receptors and dopamine receptors, lead to a robust translocation of β-arrestin from the cytoplasm to the phosphorylated receptor (Azzi et al. 2003, Krasel et al. 2008, Gesty-Palmer et al. 2006). Upon binding to GPCRs, β-arrestins reduce the level of G protein signalling. Furthermore, β-arrestins also function as adaptor proteins to facilitate vesicle-mediated endocytosis, thereby reducing the number of receptors of the cell surface (Laporte et al. 2000).

Studies by Marion et al. 2006 have also identified sites on GPCRs which facilitate β-arrestin recruitment, including one proline residue which resides in the 2nd intracellular loop, 9 amino acids from the DRY motif. Substitution of the proline with a neutral amino acid in the β2 adrenergic receptor has been shown to enhance isoproterenol induced cAMP accumulation coupled with delayed onset of β-arrestin recruitment, relative to the wildtype receptor. Introduction of the equivalent proline residue into GPCRs such as the α2 adrenergic receptor and NPY receptor led to a higher level of β-arrestin recruitment upon activation with noradrenealine or NPY respectively. These point mutation studies further implicate the proline residue as a common mediator of arrestin outside the C-terminus

In the past decade, it has become increasingly clear that the GPCR signalling repertoire is more dynamic and complex than GPCR-G protein interactions (Figure 1.4) An increasing body of evidence suggests that GPCRs are capable of initiating signal transduction upon interacting solely with β-arrestins, and thus challenges the traditional view that activated GPCRs couple principally to heterotrimeric G proteins (Shenoy and Lefkowitz. 2011). These studies have revealed that receptor bound β-arrestins serve as signal transducers, coupling the receptor to numerous signalling protein including extracellular signal-regulated kinase, c-Src tyrosine kinase and the Akt kinase (Cervantes et al. 2010).

A comprehensive study by Shenoy et al. 2006 illustrated the ability of the β2 adrenergic receptor to recruit β-arrestins upon agonist induced activation, independently of G proteins. The authors employed site-directed mutagenesis on the β2 adrenergic receptor to create 3 amino acid substitutions T68F, Y132G, and Y219A which rendered the receptor incapable of G protein activation, whilst preserving the interactions with arrestin and subsequent MAPK signalling. In cell based assays, it was shown that GPCR induced activation of MAPK signalling is co-ordinated by at least two parallel signal cascades with different temporal kinetics; a rapid transient induction between 2-5 minutes as well as a latent and sustained induction peaking at 15 minutes (Shenoy et al. 2006, Gesty-Palmer et al. 2006). By employing a combination of mutagenic and pharmacological techniques, the same authors successfully identified G protein dependent and β-arrestin dependent pathways that underlie rapid and delayed MAPK activation profiles respectively.

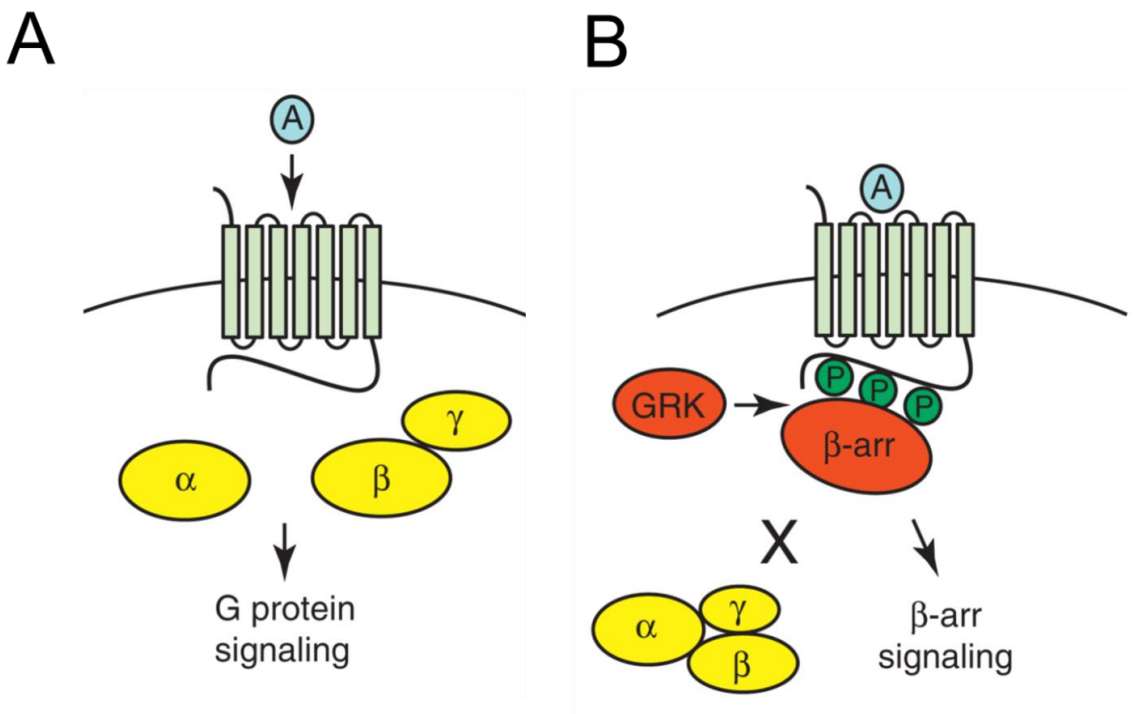

Figure 1.4 GPCR signalling repertoire consists of G proteins and β-arrestins

GPCR signalling and regulation by the GRKs and β-arrestins. (A) Agonist binding to a GPCR induces protein mediated signalling cascades. (B) Subsequently, phosphorylation and binding of β-arrestin to activated GPCR hinders agonist induced G protein signalling, but activates β-arrestin-mediated signals. Adapted from Whalen et al. (2011).

1.1.9 Visual arrestins

Vertebrate visual arrestin regulating the activities of light sensitive GPCRs. Like β-arrestins, it contains a phosphate sensor domain (Lutrell and Lefkowitz. 2002), and terminates the G protein signalling of activated rhodopsin. However, visual arrestins display enhanced affinity for activated rhodopsin than β2 adrenergic receptors in cell-based assays (Oakley et al. 2000). Although the AP-2 binding motif is not well characterised in visual arrestin, a recent study by Moaven et al. 2013 revealed that visual arrestin is indeed also capable of binding AP-2.

1.1.10 Novel tools in GPCR research-RASSLS and DREADDs

The progression of many diseases is commonly attributed to an imbalance of homeostatic signals. The considerable impact of GCPRs on health is reflected in the pharmaceutical industry, as 35-50 % of the world's pharmaceuticals are aimed at manipulating GPCR signalling (Kristiansen, 2004, Wise et al. 2002). Thus, in order to delineate the molecular basis of disease, an understanding of the biological significance of each signalling pathway is required, on a collective as well as individual basis. However, as GPCRs can induce multiple pathways at the same time (Rajagopal et al. 2010) it can be difficult to decipher the consequences of an individual pathway. In addition, current efforts to elucidate the connection between a single GPCR receptor and a physiological response profile *in vivo* are complicated by many factors such as the lack of specific agonists, inverse agonists and antagonists (Chang et al. 2007).

Another confounding issue with pharmacology is the lack of temporal and spatial control. Pharmacological compounds cannot distinguish between different receptor subtypes, or different cell types and therefore tend to create confounding side effects in *in vivo* models. This deficit in spatial and subtype resolution has been addressed by converting endogenous GPCRs into 'Receptors Activated Solely by Synthetic Ligands' (RASSLS) and 'Designer Receptors Exclusively Activated by a Designer Drug' (DREADDs) (Masseck et al. 2011). These engineered receptors retain a comparable signalling interface to endogenous GPCRs, but lack affinity for its cognate ligand. Instead they are exclusively activated by a synthetic inert compound (Scearce-Levie et al. 2005, Chang et al. 2007). When placed into specific tissues within an *in vivo* model, the advantages of these engineered GPCRs are two-fold: it allows for greater temporal and spatial control of GPCR signalling without undesirable endogenous signals and also allows the researcher to isolate physiological response caused by the GPCR of interest without impacting on endogenous receptors and subtypes in the background. Thus the physiological outcome following ligand application to a system can be solely attributed to that GPCR of interest.

A novel series of DREADDS and RASSLS which are unable to interact with G proteins, but retain interactions with β-arrestins have also been developed to study the physiology of these signal transducers without interference from G proteins. Nakajima and Wess 2012 introduced a single amino acid substitution of R165L to the M3 muscarinic receptor based DREADD, which rendered the receptor incapable of $G\alpha_q$ protein dependent signalling in mammalian expression

systems. Instead the M3 muscarinic receptor-based DREADD (Rq(R165L) exclusively interacted with arrestins-2 and 3 upon activation by CNO, without coupling to cognate $G\alpha_q$ proteins. The authors showed by conducting a BRET assay, that CNO treatment promoted interactions between β-arrestin and Rq(R165L) as well as arrestin dependent ERK phosphorylation. This allowed the authors to demonstrate the exclusive role of β-arrestins in regulating the secretion of insulin; when expressed in a MIN6 cell line derived from pancreatic beta cells, the DREADD mediated activation of β-arrestin was sufficient to upregulate insulin secretion in an arrestin-3 siRNA dependent manner.

Despite the advantages of ligand exclusivity that RASSLs and DREADDs offer in GPCR research these engineered receptors, along with endogenous GPCRs, rely on chemical ligands for activation. Thus the resolution of agonist mediated DREDD and RASSL activation is still limited by the speed of drug delivery, washout and degradation within animal models (Miesenbock, 2004).

1.2.1 Photoreception in metazoan organisms

Light perception allows organisms to detect electromagnetic radiation emitted or reflected from objects in their environment. Photic information is captured by a variety of light absorbing pigments and processed is many ways; visual organs such as camera-like or compound eyes capture light to produce a visual representation of these objects in the environment, commonly referred to as image forming vision (Fu et al. 2007). Mammals also perform various non-visual functions such as entrainment of the endogenous clock to the daily light dark cycle, and pupil constriction (Brown and Robinson. 2004, Lucas et al. 2003)

Detection of light in metazoans tends to employ ciliary photoreceptors or rhabdomeric photoreceptors (Plachetzki et al. 2005), both of which utilise opsin photopigments. These are GPCRs consisting of an opsin protein moiety covalently linked to a photosensitive retinaldyhyde chromophore (Palczewski et al. 2000). Despite the large diversity of metazoan opsins, all intracellular cascades are mediated by 5 Gα protein paralogues ($G\alpha_i$, $G\alpha_o$, $G\alpha_s$ and $G\alpha_q$ and $G\alpha_t$) and ultimately act upon cyclic nucleotide gated or transient receptor potential ion channels, causing the photoreceptor membrane to hyperpolarise or depolarise. This mechanism of photoreceptor activation is conserved across all animal phyla from prebilateral invertebrates to mammals (Plachetzki et al. 2010).

1. General introduction

Opsins are activated by certain wavelengths of light and transduce the photic signal by G proteins in specialised photoreceptor cells (Shichida and Imai. 1998). Vertebrate rhodopsin was one the first GPCRs to be characterised by X-ray crystallography, thereby allowing extensive characterisation of its structure-function relationship (Porter et al. 2012, Palczewski. 2006). The endogenous co-factor for rhodopsin, 11-*cis*-retinal, is covalently bound via a protonated Schiff-base linkage to rhodopsin in the dark state, and locks the receptor into an inactive state preventing interactions with its cognate $G\alpha_t$ protein, transducin.

The opsin bound chromophore optimally absorbs light around 500 nm (Wald. 1968) and upon absorption of a photon, 11-*cis*-retinal isomerises to all-*trans*-retinal. The *trans*-isomer functions as an agonist which causes a series of conformational changes in the opsin moiety to form meta-rhodopsin II. The new configuration favours activation of transducin and thereby initiates the phototransduction cascade, as depicted in Figure 1.5 (Schoenlein et al. 1991, Stryer, 1986, Zhukovsky et al. 1991, Baylor. 1996). Light-activated rhodopsin promotes the exchange of GDP for GTP on the $G\alpha_t$ subunit transducin. GTP bound transducin activates phosphodiesterase (Chen. 2005), which then catalyses the hydrolysis of cGMP into 5-GMP. This leads to a rapid decline in intracellular cGMP concentration, resulting in the closure of the cyclic nucleotide-gated channels in the plasma membrane and causing membrane hyperpolarisation.

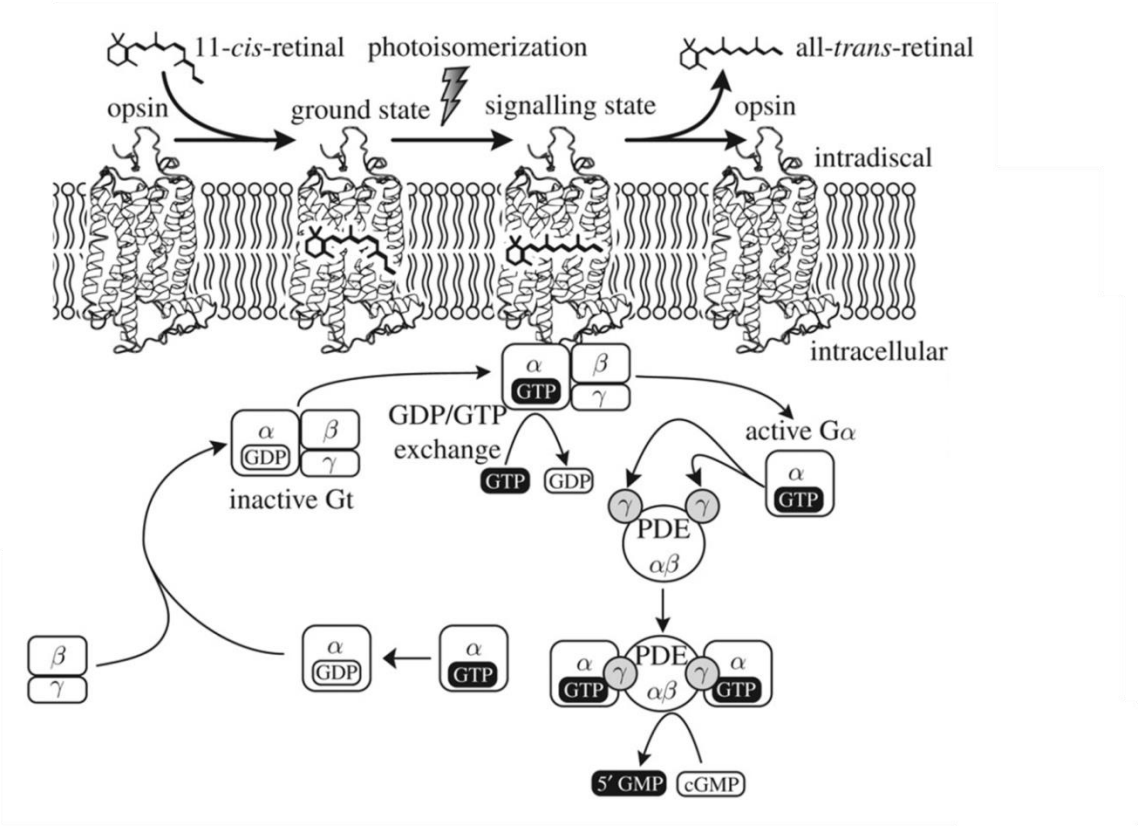

Figure 1.5 Vertebrate rhodopsin phototransduction cascade

A diagram showing the mechanism of phototransduction in mammalian eyes. Photons are captured by 11-*cis*- retinal bound opsins which can bind to and activate the G protein, transducin. Rhodopsin catalyses the exchange of GDP to GTP. The GTP-bound Gα dissociates from Gβγ exposing its active site. Activated Gα binds to its effector, cyclic nucleotide phosphodiesterase and activates it. PDE catalyses the conversion of cGMP to 5-GMP and the decrease in the concentration of cGMP causes cyclic nucleotide gated channels to close, results in hyperpolarisation of the photoreceptor cells. Photoactivated vertebrate rhodopsin is thermally unstable, and subsequent hydrolysis of the Schiff base liberates the chromophore. Adapted from Shichida and Matsuyama. (2009).

1.2.2 Termination of phototransduction

The temporal resolution of the mammalian retina is determined by the ability to inactivate electrical responses between sequentially arriving stimuli. Phototransduction systems have evolved efficient regulatory mechanisms that rapidly shut off activated rhodopsin intermediates created during the signalling process to avoid saturation. Indeed, metarhodopsin is functionally inactivated within milliseconds *in vivo* (Richard and Lisman, 1992) despite constant illumination. The thermal instability of the active receptor configuration therefore allows for rapid regeneration of the receptor molecules in order to maintain fast transduction kinetics

The activated Meta II conformation of vertebrate rhodopsin favours the phosphorylation of exposed serine residues on the C-terminus by specific G-protein receptor kinases (GRKs)

(Maeda et al. 2003). Phosphorylated Meta-rhodopsin II has reduced affinity towards transducin (McBee et al. 2001) but greater affinity for arrestins. In the mammalian retina, photoreceptor specific isoforms of arrestins (visual arrestin) directly interact with the phosphorylated opsins, analogous to β arrestins 2 and 3 in non-visual cells. Binding of visual arrestin to the phosphorylated active metarhodopsin-II further hinders G-protein binding and thereby suppresses activated rhodopsin activity (Xu et al. 1997). The same authors showed that mice which lack arrestin expression develop wildtype retinal morphology and photosensitive rods and cones when raised in the dark. However, upon photoactivation with 500 nm light flashes across 3 log range of intensities (1-1000 photons/m^2), the profile of electrical activity in rods and cones was abnormally sustained over time and did not recover as quickly as arrestin expressing mice (Xu et al. 1997), which is indicative of impaired signal termination.

1.2.3 Chromophore regeneration in monostable and bistable opsin pigments

Metazoan opsin pigments are divided into two classes based on their visual cycle: bistable and monostable pigments (Tsokomoto and Terakita. 2010). Whilst both monostable and bistable opsins covalently bound to 11-*cis*-retinal are thermally stable in the dark state, monostable opsins become unstable in the meta state resulting in hydrolysis of the Schiff base and liberation of all-*trans*-retinal from the opsin moiety (Borhan et al. 2000, Palczewski, 2006, Smith, 2010, Wald, 1968). This causes the opsin to bleach, and requires another 11-*cis*-retinal to reconstitute a functional pigment (Figure 1.6). Mechanisms must therefore be in place to regenerate rhodopsin by constant provision of 11-*cis*-retinal.

In vertebrate rod and cones, the all-*trans*-retinal is exchanged with underlying RPE cells for regenerated 11-*cis*-retinal chromophore, known as the visual cycle. Following hydrolysis of the Schiff base, all-*trans*-retinal is transported across the outer segment disc membrane into the cytoplasm, reduced to all-*trans*-retinol (Rattner et al. 2000) and translocated from the photoreceptor outer segments to the RPE (Edwards and Adler. 1994). Subsequently, all-*trans*-retinol is esterified into a fatty acid retinyl esters (Imanishi et al. 2004), and undergo isomerisation and hydrolysis to form 11-*cis*-retinol (Moiseyev et al. 2003). Upon oxidation to 11-*cis*-retinal, the regenerated chromophore is translocated to the photoreceptors allowing the regeneration of rhodopsin from Metarhodopsin (Mata et al. 1992).

In bistable pigments such dissociation between the chromophore and protein moiety does not occur, even following photoactivation (Yau and Hardie, 2009). Metarhodopsin is thermally stable and can bind *trans* isoforms of retinaldehyde. Subsequent absorption of a second photon photoisomerizes the all-*trans*-retinal back to 11-*cis*-retinal thus enabling regeneration of the dark state pigment (Figure 1.6) The bistable nature is associated with opsin pigments which possess the Glutamine 181 counterion, a negatively charged amino acid residue that stabilizes a positive charge on the retinylidene chromophore (Terakita et al. 2004). These include invertebrate rhodopsins, parietopsins, peropsins as well as vertebrate melanopsins and parapinopsins (Tsukamoto and Terakita. 2010, Terakita et al. 2004).

1. General introduction

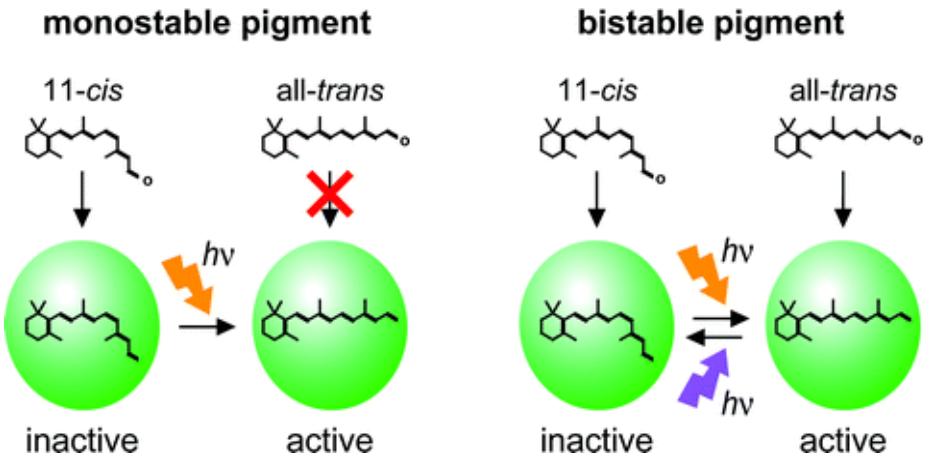

Figure 1.6 Monostable and bistable photopigments

Comparison of photoactivation between monostable and bistable pigments. Monostable pigments can only bind to 11-*cis*-retinal but not all-*trans*-retinal whereas bistable pigments can bind both to 11-*cis*- and all-*trans* retinals. Upon absorption of a photon, the conversion of 11-*cis*- to all-*trans* retinal leads to activation of monostable and bistable opsins. However in bistable pigments, further photon absorption reverts the *trans* isomer to *cis*. Adapted from Tsukamoto and Terakita. (2010).

1.3.1 Optogenetics

The field of optogenetics describes a range of optical techniques to elicit a physiological response in targeted biological systems in the absence of pharmacology and electric stimulation (Deisseroth et al. 2006, Miller. 2006). This technology utilises light sensitive proteins which are capable of transducing light into biological processes, such as enzyme activation, induction of secondary messengers and electrical currents in cells, and targets their expression in cells which lack such intrinsic photosensitivity (Stierl et al. 2006, Zemelman et al. 2002, Boyden et al. 2005).

Cells which are engineered to express these proteins are rendered responsive to visible-spectrum light with biologically well-tolerated intensities (Stierl et al. 2006, Bailes et al. 2012, Yizhar et al. 2011). Targeted expression of the light sensitive protein thus allows for control of physiology within a complex tissue or organism at high temporal resolution. Indeed, remote activation of such light sensitive proteins overcomes the limits of drug distribution and washout *in vitro* and *in vivo* as the speed of light delivery can exceed that which has been achieved through pharmacological manipulation.

1.3.2 Optogenetic applications of microbial opsins

Among the vast array of naturally occurring light transducers, bacterial light gated ion channels with an all-*trans*-retinal chromophore have proven to be highly adaptable optogenetic manipulators in a wide range of host cells. These microbial type I opsins are seven-transmembrane spanning proteins which bear no sequence homology to metazoan opsin photopigments. Microbial opsins including bacteriorhodopsins, halorhodopsins, and channelrhodopsins can transduce light to regulate the influx of protons, chloride balance, and monovalent cations respectively, and therefore alter the membrane current (Yizhar et al. 2011).

Whilst bacteriorhodopsins and halorhodopsins have both been adapted to optically regulate mammalian physiology, Channelrhodopsin-2 from the green alga *Chlamydomonas reinhardti,* was the first light gated ion channels to be applied for light-triggering action potentials in non-visual cells. Indeed, studies by Boyden et al. 2005 and Nagel et al. 2005 first demonstrated that Channelrhodopsin-2 was able to depolarize genetically targeted neurons that lack intrinsic photosensitivity, simply by heterologous expression and illumination. Many subsequent have consistently reported that Channelrhodopsin-2 can be stably robustly expressed in neurons of in-tact and freely mobile invertebrate models, and impact on animal behaviour (Zhang et al. 2007).

1.3.3 Photoactivated enzymes as optogenetic actuators

In various eukaryotic organisms, phototaxic responses are triggered by flavoprotein conjugated photoactivated adenylyl cyclases (Iseki et al. 2002, Ntefidou et al. 2003). It is thought that positive phototaxis allows organism to migrate to a light source for photosynthesis and negative phototaxis protects the cells from damage induced by excessive solar radiation at the water surface. In addition to light activated ion channels, flavin bearing phototransducers are also suitable for optogenetic applications because they are small in size, soluble, and spontaneous incorporate flavin chromophores into apoproteins (Stierl et al. 2006).

Eukaryotic photoactivated adenylate cyclases (PACs) represent a family of blue-light receptor consisting of two α-subunits PACα and two β-subunits PACβ. Each subunit contains two flavin-binding domains and two adenylyl cyclase catalytic domains (Iseki et al., 2002). RNAi studies by Ntefidou et al. 2003 give strong evidence that knockdown of PACα or PACβ abolishes any photophobic swimming in response to bright light (800 Wm^{-2}). Bacterial homologues have also been discovered (Stierl et al. 2006). Although it is not clear how bacterial PACs (bPACs) contribute to light responses in addition to light gated ion channels, studies by Stierl et al. 2006 demonstrated that photoactivated adenylate cyclase from *Beggiatoa* species of bacteria can be expressed in a wide variety of host cell including Xenopus oocytes, rat hippocampal pyramidal cells, and *Drosophila* neurons, and also elicit non-invasive control cAMP production.

1.3.4 Optogenetic applications for metazoan opsins

Optogenetic techniques which utilise metazoan opsins are most suitable for the optical regulation of principle intracellular messengers including cyclic AMP, cyclic GMP, calcium and MAPK, as the heterologous expression of opsin photopigments in non-photoreceptor cells recapitulates many aspects of the phototransduction cascade from native photoreceptors.

1.3.5 Optogenetic manipulation of the $G\alpha_s$ pathway Opto-Xrs

Kim et al. 2005 were the first to distil the photosensitive nature of human Rhodopsin and the $G\alpha_s$ signalling properties of bovine β2 and α1 adrenergic receptors into a single chimeric GPCR, later referred to as Opto-Xrs (Airan et al. 2009). The construction required splicing of all 3 cytoplasmic regions of the β2 adrenergic receptor to the transmembrane and extracellular regions of rhodopsin to create a GPCR with the capacity to bind a retinoid chromophore. When expressed in HEK cells, illumination of the β2 adrenergic opto-Xr at 504 nm light for 60 seconds created an elevation in cAMP compared to dark controls (Airan et al. 2009). These chimeric receptors also allowed for light regulated electrical activity in accumbens neurons and also behavioural conditioning in mouse models (Airan et al. 2009).

1.3.6 Optogenetic manipulation of the $G\alpha_s$ pathway with a Jellyfish photopigment

The box jellyfish *Carybdea rostonii* is a cnidarian invertebrate endowed with specialised photosensory organs for visual perception. Despite being considered the most primitive of metazoan organisms, it utilises a complex repertoire of various lens and non-lens eyes. Koyanagi et al. 2008 were the first to purify an opsin photopigment from the lens eye, which upon reconstitution with 11-*cis*-retinal, exhibited an absorption maximum of 500 nm. Upon photobleach at 500 nm, the photopigment absorption maximum was blue-shifted to 455 nm. However, it is noteworthy that further illumination of 455 nm did not regenerate the 11-*cis*-retinal. This initially raised questions about whether the opsin photopigment truly was a bistable pigment (Koyanagi et al. 2008).

Immunohistochemical studies in jellyfish lens eyes highlighted exclusive co-localisation of $G\alpha_s$ subunits and endogenous opsins in the ciliary-type photoreceptor cells, inferring that Jellyfish opsin triggered a $G\alpha_s$ mediated phototransduction cascade, as represented in Figure 1.7 (Koyanagi et al. 2008). Interestingly, light irradiated rhopalia exhibited a higher concentration of cAMP than dark adapted rhopalia. These observations collectively favour the role of the $G\alpha_s$ subunit in mediating box jellyfish phototransduction.

When expressed in mammalian cells, stimulation of the opsin with bright white light lead to a robust induction in cAMP levels, reflecting interactions with mammalian $G\alpha_s$ subunits to activate endogenous adenylate cyclase (Koyanagi et al. 2008, Bailes et al. 2012). In addition, cell based assay performed by Bailes et al. 2012 demonstrated that unlike the β2-OptoXr, exposing JellyOp to repetitive light flashes did not compromise the amplitude of signal transduction even after 15 minutes of stimulation. This study was the first to highlight bleach resistant properties of JellyOp, a highly desirable property for optogenetic tools. Although direct evidence of instability is currently lacking, it is noteworthy that JellyOp, as the opsin, also possesses the equivalent Glu 181 counterion, a negatively charged amino acid that is strongly associated with invertebrate bistable opsins (Terakita et al. 2004)

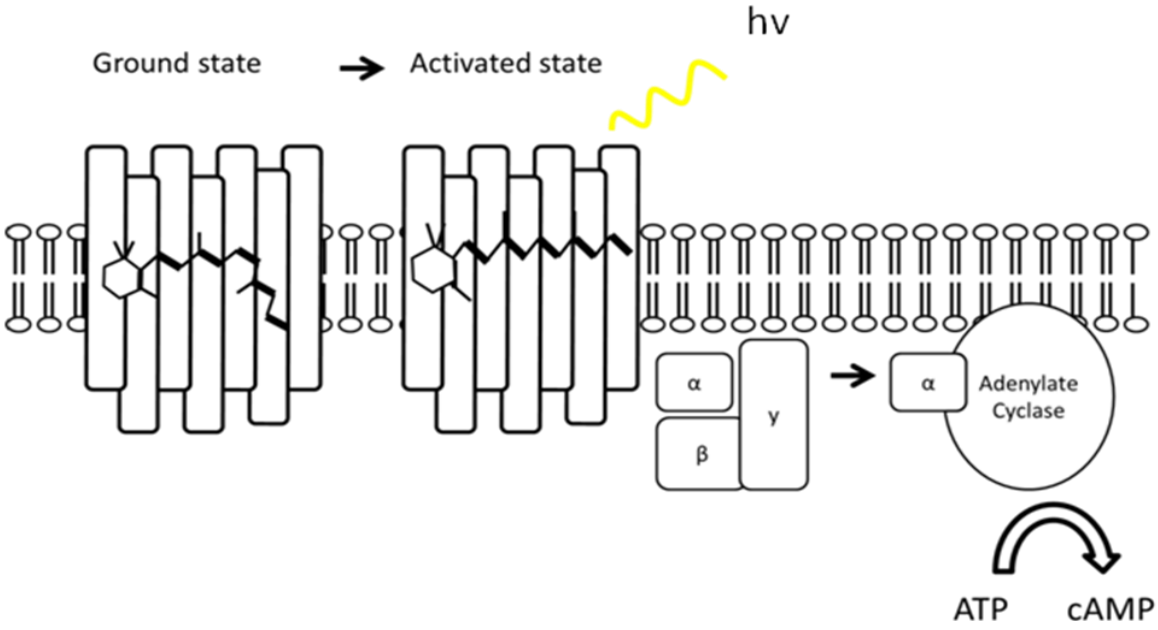

Figure 1.7 Schematic of JellyOp mediated $G\alpha_s$ signalling

Activation of JellyOp leads to interactions with $G\alpha_s$ subunit of heterotrimeric G proteins (Koyanagi et al. 2008, Bailes et al. 2012). This leads to activation and liberation of the $G\alpha_s$ subunit allowing it to activate membrane bound adenylate cyclase, the enzyme that catalyses the metabolism of ATP to cAMP (Cassel and Selinger. 1978)

1.3.7 Optogenetic control of the $G\alpha_{i/o}$ with vertebrate rhodopsin

In its native rod environment, vertebrate rhodopsin mediates phototransduction cascade via transducin (Heck and Hofmann. 1993). However, heterologous rhodopsin is capable of coupling to $G\alpha_i$ proteins in transducin deficient cell systems (Tsai et al. 1984, Stryer and Bourne. 1986), and has been subsequently implemented for optogenetic manipulation of $G\alpha_i$ proteins (Gutierrez et al. 2011).

Gutierrez et al. 2011 demonstrated that tissue specific expression of vertebrate rhodopsin in cerebellar purkinje neurons can be used to facilitate light dependent silencing of host neurons. By using a laser to access the neurons, the authors showed that delivery of 473 nm light for 26 seconds resulted in a 30.8 ± 4.5 % reduction in baseline spontaneous rate which persisted for 30 seconds after light offset. This was comparable to pharmacological inhibition of the $G\alpha_i$ coupled $GABA_B$ receptor in purkinje cells, in which 26 seconds infusion of baclofen at 1 mM to the cerebellum of mice also induced a 33.6 ± 12.3 % reduction in firing. In contrary, laser treatment of control mice, which lacked vertebrate rhodopsin, did not affect the firing rate with the same potency.

Bovine rhodopsin has also been used for optical manipulation of neurons in *Caenorhabditis elegans* models (Cao et al. 2012). The worm model is particularly useful for studying effects of rhodopsin photoactivation as the animal itself does not respond to blue light (488 ± 20 nm), even at 1000 lux (Cao et al. 2012). This is particularly relevant to bovine rhodopsin as its absorption maximum *in vitro* is 490nm when reconstituted in 11-*cis*-retinal (Nathans et al. 1989). Upon expression of bovine rhodopsin in CNS neurons, the transgenic worms showed a 9-*cis*-reitnal dependent and irradiance dependent diminution of mobility after 1s illumination of blue light (488 ± 20 nm). Motility was not affected in the absence of 9-*cis*- retinal or even all-*trans*-retinal, demonstrating the inability of bovine rhodopsin to function without a suitable chromophore supply

Such light driven inhibition of motility in the worms was transient as they were able to recover upon transfer to darkness. Upon characterisation of the action spectrum, peak defects in mobility were observed at approximately 490 nm, which matches the absorption maximum of native bovine rhodopsin *in vitro* (Nathans et al. 1989). To test whether the light induced inhibition of motility was truly $G\alpha_i$ dependent, the authors constructed a strain of PTX and bovine rhodopsin co-expressing worms. These worms showed no response to 1000 lux blue light, confirming that rhodopsin manipulation required only the $G\alpha_i$ subunit.

1.3.8 Optogenetic manipulation of the Gαi/o pathway with Opto-Xrs

Oh et al. 2010 also adapted vertebrate rhodopsin to study the $G\alpha_{i/o}$ coupled serotonin ($5\text{-}HT_{1A}$) receptor in *in vitro* and *in vivo* models. In order to mimic the subcellular targeting of the endogenous $5\text{-}HT_{1A}$ receptor as well as regulatory mechanisms, the authors generated a chimeric opsin photopigment constituting vertebrate rhodopsin with a C-terminus of the $5\text{-}HT_{1A}$ receptor.

Introduction of the chimeric GPCR (Rh-CT5-HT_{1A}) to HEK cells expressing G protein-coupled inwardly-rectifying potassium channels lead to inward currents upon exposure to 10 seconds light at 485 nm. In addition, such currents matched the profile of $5\text{-}HT_{1A}$ receptor upon activation with agonist 8OH-DPAT. In addition, expression of the Rh-CT5-HT_{1A} receptor in hippocampal neurons lead to light induced hyperpolarisation and reduced the spontaneous action potential firing rate.

The authors proceeded to demonstrate that Rh-CT5-HT$_{1A}$ was capable of modulating serotonergic neurons of the dorsal raphe nucleus in a manner comparable to the 5-HT$_{1A}$ receptor. Lentiviral expression of the chimera into the dorsal raphe nucleus lead to a light triggered reduction in spontaneous firing activity within neurons of mice irrespective of whether the 5-HT$_{1A}$ receptor was present. Whilst application of the 5-HT$_{1A}$ agonist, 8OH-DPAT (1 µm), onto brainstem slices failed to elicit a hyperpolarisation response in the dorsal raphe nucleus neurons of KO mice, the light activation of the Rh-CT5-HT$_{1A}$ chimera was able to compensate for lack of response to serotonin (Oh et al. 2010).

1.3.9 Optical control of the Gα$_q$ pathway by invertebrate rhodopsin

In a single *Drosophila* rhabdomere, there are multiple types of rhodopsins which collectively sense a wide spectrum of light by a common phototransduction cascade. Photon absorption triggers rhodopsin isomerisation into an active state, which stimulates GDP/GTP exchange in the α subunit of heterotrimeric G-protein, Gα$_q$ (Montell. 2012). The Gα$_q$-protein then activates phospholipase C, an enzyme that catalyses the hydrolysis of phosphatidylinositol biphosphate (PIP$_2$) into inositol trisphosphate (IP$_3$) and diacylglycerol (DAG) (Montell. 2012). This signaling cascade has been widely implicated in the activation of ion channels TRP and TRPL, which eventually lead to depolarisation of the photoreceptor cell.

Zimelman et al. 2002 first identified the minimal combination of phototransduction components required to render a *Drosophila* rhodopsin 1 signalling cascade in heterologous expression systems. These consisted of NinaE (a *Drosophila* rhodopsin), Arrestin-2 and Gα subunit. Transient co-expression of all three components in *Xenopus* oocytes lead to a light triggered inward current in presence of all-*trans*-retinal. The dependence on *Drosophila* rhodopsin on the presence of all-*trans*-retinal is consistent with the functional requirement of opsin photopigment to bind to a retinal chromophore. Also, the ability of rhodopsin to utilise all-*trans*-retinal, unlike vertebrate rhodopsins, is further testament to its bistable nature.

Such light induced inward rectifying currents observed in transfected cells were also sensitive to 20 µM xestospongin C, an antagonist of calcium-releasing inositol-1,4,5-triphosphate receptor (Zemelman et al. 2002). This further indicates that *Drosophila* rhodopsin drives an IP$_3$ cascade in endogenous photoreceptors as well as oocytes, causing the release of calcium which subsequently activates potassium channels in the oocyte membrane (Bauer et al. 1996).

In addition, expression of the three proteins in primary mouse hippocampal neurons increases the frequency of action potentials in transfected neurons, a response which was absent from mock transfected cells (Zimelman et al. 2002). To further ensure that these responses were not due to cross talk between neurons in culture, the authors inhibited neuronal glutamate receptors by application of 50 µM d,l-2-amino-5-phosphonovaleric acid (and 10 µM 6-cyano-7-nitroquinoxaline-2,3-dione. However, this did not prevent light from stimulating action potentials in the hippocampal neurons.

1.3.10 Optical control of the $G\alpha_q$ pathway by vertebrate melanopsin

Mammalian melanopsin is expressed in a subset of retinal ganglion cells within the retina and lends intrinsic photosensitivity to its host cell. This group of light sensitive cells constitutes the third class of mammalian photoreceptors and contributes to a wide range of light responses including pupillary reflexes and photoentrainment of mammalian circadian clock (Ruby et al. 2002, Berson et al. 2002). Spectral studies of melanopsin physiology *in vivo* and *in vitro* by Hattar et al. 2003, have revealed that these melanopsin induced pupil constrictions to light were maximally induced at around 480 nm at (log irradiances of 9-15). Similarly, upon physical isolation of retinal ganglion cells from the retina, light induced depolarisations was strongest upon irradiation at 484 nm compared to other wavelengths of light.

The bistable nature of mouse melanopsin has been described as a purified pigment and also in *in vitro* functional studies. Upon purification of C-terminally truncated mouse melanopsin and reconstitution with 11-*cis*-retinal, the opsin photopigment exhibited an absorption maximum of 467 nm (Matsuyama et al. 2012). The peak sensitivity is slightly dissimilar from the action spectrum of murine intrinsically photosensitive rationally ganglion cells (Hattar et al. 2003) within *in vivo* models. However, the difference may be attributed to many factors such as the C-terminal truncation or the lack of purity. Upon irradiation of the pigment with 448 nm light for 640 seconds, the composition of opsin bound retinal showed a mixture of 11-*cis*-retinal and all-*trans*-retinal, thus implying a mixture of ground state melanopsin and photoactivated metamelanopsin. Both resting state and photoactivated pigments shared overlapping absorption spectra, with maximum absorptions of 467 nm and 476 nm respectively. The similarity in spectral sensitivities may allow for the conversion of metamelanopsin to melanopsin with wavelengths that also drive photoactivation, resulting in an equilibration of photoactivation and regeneration at any time during saturating light stimulation. However, the bistable nature of mouse melanopsin *in vivo* has yet to be in established (Mawad and Van Gelder. 2008).

The bistable nature of human Melanopsin in cell based assays was also demonstrated by Melyan et al. 2005. Transfection of neuro-2A cells with full length human melanopsin cDNA yielded an opsin photopigment that triggered a G protein dependent modulation of membrane current, when incubated in 20 µM 11-*cis*-retinal. Interestingly, the greatest deviations in melanopsin induced membrane current were elicited with 360 nm and 420 nm of monochromatic light whereas longer wavelengths such as 480 nm yielded suboptimal membrane currents. Again, this deviation in optimal light absorption may reflect differences in the micro-environment of the opsin photopigment. However, when heterologous melanopsin was pre-exposed to 540 nm, a wavelength that did not discernibly affect membrane current, subsequent stimulation with 420 nm yielded an even greater induction of membrane current; another hint of the bistable properties of melanopsin. In light of these findings, it is conceivable that human Metamelanopsin strongly absorbs light at 560 nm, thus resulting in conversion to ground state melanopsin.

Functional expression of human and mouse melanopsins have been successfully demonstrated in several mammalian cell lines and primary cultures where upon photoactivation, the opsin photopigment induces inositol phosphate and calcium levels in host cells (Giesbers et al. 2008, Melyan et al. 2005). The phototransduction cascade in heterologous cell systems is also akin to endogenous retinal ganglion cells, implying robust coupling to $G\alpha_q$ proteins. Mouse melanopsin has recently been placed in fibroblast oscillators to generate light entrainable cell based models of the mammalian clock (Ukai et al. 2007, Pulivarthy et al. 2007).

1.4.1 Genetically encoded bioluminescent reporters

Optical reporter technology employs genetically encoded proteins which modulate optical properties in accordance with the dynamics of the intact cellular environment. Such biosensors offer a photic and thus, non-invasive readout of the microenvironment over time without the inconvenience of conducting end point assays (Binkowsky et al. 2009, Fan et al. 2008). This is particularly useful for visualising the temporal dynamics of cellular processes which occur at wide ranging time scales, from seconds to days, without resorting to invasive end-point assays (Fan et al. 2008).

1.4.2 Luciferase based cAMP reporters

Protein-based biosensors often utilize protein fragment complementation, where the reporter protein, such as a luciferase enzyme, is split into two fragments but physically tethered (Binkowsky et al. 2009). The sensor is functional when the two partners interact and conversely, the loss of interaction between the two halves renders the sensor inactive. Thus, these sensors can be reversibly activated depending on its environment.

Complementation based cAMP reporters have been successfully engineered from firefly (*Photinus pyralis)* luciferase (Binkowsky et al. 2009), thereby allowing for real-time surveillance of intracellular cAMP signalling. These luciferase proteins have been engineered to incorporate a RIIβB cAMP binding domain from protein kinase A in between two halves of the luciferase. Binding of cAMP to the PKA domain modulates the configuration resulting in a functional luciferase with functional catalytic domain for the catalysis of luciferin. This reporter has been utilised in cell based assays to capture real-time changes in intracellular cAMP levels triggered by a $G\alpha_s$ coupled Jellyfish opsin (Bailes et al. 2012). The authors calibrated the maximal bioluminescence responses of the Glosensor™20F to different log concentrations of forskolin (log_{10} -8 to -3M) , and illustrated a close relationship between the dose response curves of ELISA and Glosensor™20F assays (Bailes et al. 2012).

1.4.3 Aequorin based calcium reporters

Aequorin is a common bioluminescent reporter for monitoring intracellular calcium signaling in live cells. It is a protein complex comprised of apoaequorin and co-factor coelenterazine, first isolated from the luminescent jellyfish *Aequorea* (Shimomura et al. 1990). When calcium binds, a chemical reaction is initiated that involves the oxidation of coelenterazine to coelenteramide, the production of CO_2 and emission of blue light. This reaction effectively inactivates aequorin but with the addition of coelenterazine, the active complex can be regenerated. The dynamic range of Aequorin is dependent on the structure of the coelentrazine, which exists in many forms (Dupriez et al. 2002).

Aequorin assays have been validated for many GPCRs such as melanocortin receptors, serotonin (5-HT_{2B}) and orexin 2 receptors (Stables et al. 1997, Le Poul et al. 2002). The main challenge for adapting aequorin in cell based assays is capturing the rapid luminescence kinetics. A typical aequorin signal is emitted in an interval of less than 30s (Le Poul et al. 2002), although such kinetics can be modulated by various coelentrazine variants. Other groups including Bailes and Lucas 2013 have utilised aequorin to visualise $G\alpha_q$ signalling pathways in real-time. Upon transiently expressing mitochondrial aequorin and human or mouse melanopsin in HEK293 cells, exposure to a flash of light induced a robust transient induction in bioluminescence.

1.4.4 Luciferase based transcriptional reporters

Prior to the use of bioluminescence or fluorescence reporters, the study of circadian genes relied heavily upon techniques in molecular biology such as RT-PCR and immunoassays to sample real-time clock mRNA and protein levels respectively multiple times across consecutive days. Such approaches are time-consuming and require large numbers of experimental specimens. The development of real-time reporters offers a less invasive approach for live-reporting of clock genes in living tissues cultures and also significantly reduces the demand for organisms in each assay.

The luciferase reporter system allows us to measure real-time changes in gene transcription (Yamazaki and Takahashi. 2005). By fusing the open reading frame of luciferase to either the promoter or the C-terminus of a gene, transgenic luciferase can be heterologously expressed in the cells allowing quantification of gene and protein expression indirectly through luciferase activity. It is noteworthy that the luciferase protein must be sufficiently unstable such that its activity reflects changes in gene expression of live samples with high temporal resolution. In addition, the recent development of the cooled charge-coupled device (CCD) camera allows for highly sensitive imaging of tissue cultures at single cell level (Yamazaki and Takahashi. 2005). The single-cell bioluminescence imaging technique is a strong tool for quantifying spatiotemporal dynamics of individual cellular oscillators in complex tissues.

1.5.1 The mammalian circadian clock

Many organisms exhibit a rhythmic pattern of behaviour which is aligned to the 24 hour cycle. These circadian rhythms of behaviour also persist under constant conditions cycling approximately every 24 hours, but environmental time cues or “Zeitgebers” such as light and temperature can synchronise the clock to that of the environment. Thus, the daily resetting of rhythm allow organisms to accurately keep time and adjust to environmental changes. In mammals, the daily timing of behaviour is driven principally by the suprachiasmatic nucleus (SCN), a cluster of neurons in the hypothalamus of the brain (Moore and Eichler. 1972, Stephan and Zucker. 1972). The molecular clock is based on an autoregulatory feedback loop of interacting core “clock” proteins, secondary messengers and cytoplasmic kinases (Figure 1.8). Timely interactions between components produce transcriptional oscillations with a period of about 24 hours (Lowrey and Takahashi. 2004, Takahashi et al. 2008). Clock genes were first discovered from genetic analysis of mutants which exhibited abnormal circadian phenotypes, such as *clock*, *ck1ε*, *per* and *fbox13* (Konopka and Benzer. 1971, Ralph and Menaker, 1988, Vitaterna et al. 1994, Godinho et al. 2007). Transcription factors CLOCK and BMAL1 dimerise and activate transcription of repressor genes *per and cry*. Upon translation, these repressor proteins subsequently accumulate to form complexes later in the day and upon nuclear entry inhibit CLOCK/BMAL1-driven transcription. This leads to auto-suppression of *per* and *cry* repressor genes. The subsequent reduction in levels of PER and CRY protein disinhibits BMAL1 and CLOCK, allowing another cycle of transcriptional activation.

The contributions of the casein kinase 1 epsilon to regulating circadian period was discovered from a tau mutant strain of golden hamster which exhibited an accelerated free-running period of 22 h with respect to wheel running behaviour, compared to wildtype periods (24.1h) (Ralph and Menaker. 1988). The gene that was responsible for this phenotype was mapped and identified as a mutation in a gene encoding the enzyme casein kinase 1ε (CK1ε) (Lowrey et al. 2000), where a single- base-pair mutation resulted in an amino acid substitution in CK1ε.

Based on mathematical modelling and experimental studies, Gallego et al. 2006 proposed that the tau mutation in *ck1ε* resulted in a gain of function with respect to PER phosphorylation. Furthermore, mice which were engineered to express the tau allele within the *ck1ε* gene instead of the wildtype *ck1ε* exhibited significantly shortened of circadian period (Meng et al. 2008). Consistently, studies have also shown that delaying the degradation pathways of clock proteins CRY and PER prolongs the circadian period (Reischl et al. 2007, Godinho et al. 2007). β-

1. General introduction

TrCP1 and β-TrCP2 functions as part of the E3 ubiquitin ligase complex SCF (Skp1/Cdc-53-Cullin/F-box) for proteosome mediated degradation of phosphorylated PER2. Perturbation of the β-TrCP1 mediated degradation pathway in fibroblasts results in lengthening of the circadian period (Reischl et al. 2007). Similarly, dysfunction of Skp1/cullin/F-box protein ubiquitin ligase complex, which targets CRY, produces significantly longer free-running periods of wheel-running activity (23.9-24.3 hours) than the average population (23.63 hours) (Godinho et al. 2007).

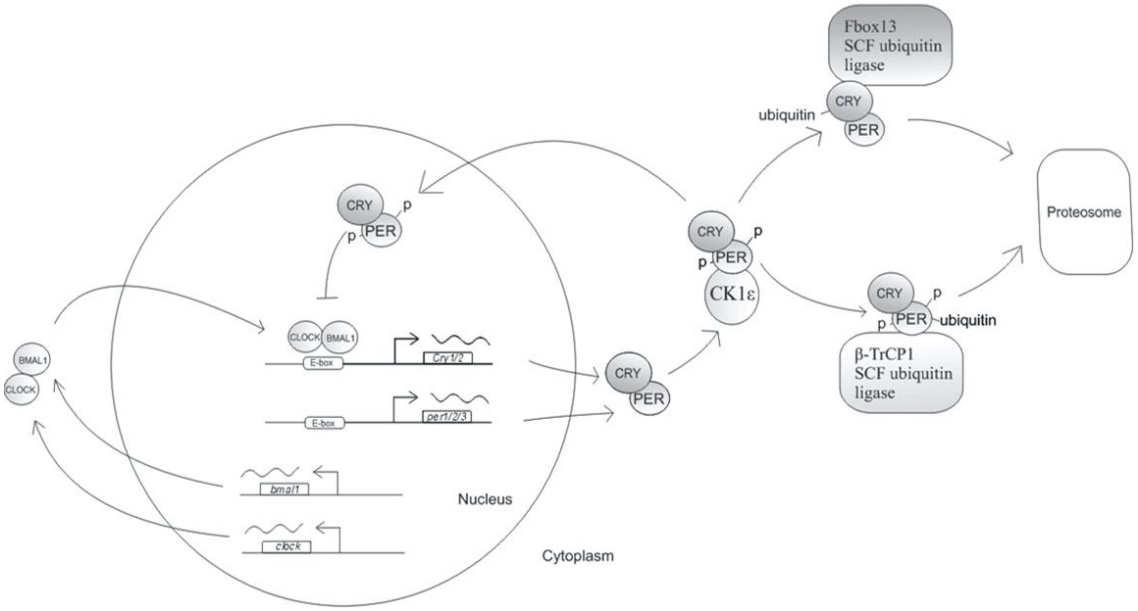

Figure 1.8 The transcriptional translational feedback loop of the mammalian clock.

The mammalian circadian rhythms core clock is a transcriptional–translational negative-feedback loop with a delay between transcription and the negative feedback. It is initiated by a heterodimeric transcription factor that consists of CLOCK and BMAL1, which drive the expression of their own negative regulators, the PERIOD and CRYPTOCHROME proteins. Over the course of the day, the PER and CRY proteins accumulate and dimerise in the cytoplasm, where they are phosphorylated by casein kinase Iε (CKIε). They then translocate to the nucleus in a phosphorylation-regulated manner where they interact with the CLOCK–BMAL1 complex to repress their own activator. In addition, degradation of PER and CRY proteins are releases the repression of the transcription and allows the next cycle to start (Godinho et al. 2007, Reischl et al. 2007, Fan et al. 2009, Takahashi et al. 2008).

1.5.2 Rhythmic activation of clock genes downstream of E-box regulatory motifs

E-box sites are defined as mainly 6-bp DNA elements and are recognized by Basic helix-loop-helix family transcription factors (Malik et al. 1995) and facilitate the transcription of various genes, including clock genes *per* and *cry*. The E-box is a palindromic sequence distinguished by consensus bases CANNTG. Subsequent studies have revealed a number of non-canonical E-box elements which also regulate rhythmic gene expression of genes in suprachiasmatic nuclei, the liver and the heart (Wang et al. 2013, Yoo et al. 2005, Storch et al. 2002). One such example is the non-canonical E-box (CACGTT), which participates in mammalian *per2* gene oscillation (Yoo et al. 2005).

Studies by Nahakata et al. 2008 demonstrated that E-box and E-box-like elements form tandem repeats separated by 6 base pairs, upstream of all 3 *per* genes in the human, rhesus, rat,

mouse genome. When incorporated into a reporter construct, the presence of these tandem sequences (CACTGT and TGTGTG for *per1*, CACGTT and TATGTG for *per2*, and CACGCG and CTCGAG for *per3*) upstream of a SV40 promotor and luciferase coding sequence was sufficient to drive rhythmic luciferase expression in transfected mouse fibroblast cell lines.

Interestingly, recent studies of the crustal structure of CLOCK/BMAL1 complexed to a canonical E-box DNA fragment CACGTG have unveiled a hydrophobic contact between an Isoleucine residue at position 80 in the BMAL1 protein and a thymine nucleotide flanking the E-box sequence, suggesting that CLOCK-BMAL1 may actually read a 7-bp DNA sequence.

1.5.3 Circadian photoentrainment

Circadian entrainment represents a mechanism for temporal adaptation endogenous clocks to the environment. “Zeitgebers” trigger the clock to adjust their period and phase, ensuring that the organism maintains synchrony with the 24 hour cycle of the earth (Golombek and Rosenstein. 2010). Light is a potent Zeitgebers for photosensitive organisms; during the subjective night short light pulse can elicit non-parametric entrainment in mammalian models, characterised by a rapid change in period and phasing. When the light stimulus is delivered during the early subjective night, this can delay the phasing of the clock, whereas a pulse during the late subjective night can advance the phasing of the clock (De Coursey. 1960). Equivalent light pulses during the day fail to modulate clock period and phase parameters but regulate the amplitude of behavioural rhythms. Thus, entrainment to light is temporally gated such that light can only incur changes in the kinetics of the clock during certain phases of the day.

At the molecular level, molecular signals triggered by light perception intersect the transcriptional translational feedback loop in SCN neurons by inducing acute expression of immediate early response genes such as *c-fos, per1* and *per2* (Kornhauser et al. 1996, Nagano et al. 2009). When rodent models are exposed to light during the subjective night, CREB is rapidly phosphorylated at several serine residues including ser133 and ser142. Light dependent CREB phosphorylation is also temporally gated and only receptive to light during the subjective night (such as CT14 and CT23) but not during the subjective day (CT10). It is likely that the multiple actions of calcium and cAMP, and MAPK pathways individually or collectively contribute to the stimulation of full CREB dependent transcription in a phase dependent manner.

1.5.4 Role of cAMP in circadian regulation

Pharmacological upregulation of cAMP signalling is frequently associated with acute induction of clock genes *per1* and *per2* via CREB activation in SCN neurons (Figure 1.9, O'Neill and Reddy. 2012). Previous studies have also reported that application of synthetic cAMP analogues to SCN explant cultures trigger robust phase advances in neuronal firing of the SCN when delivered during the subjective day (CT3-7) (Prosser and Gillette. 1989). This suggests that cAMP signalling impacts on the phasing of the clock though acute induction of clock genes.

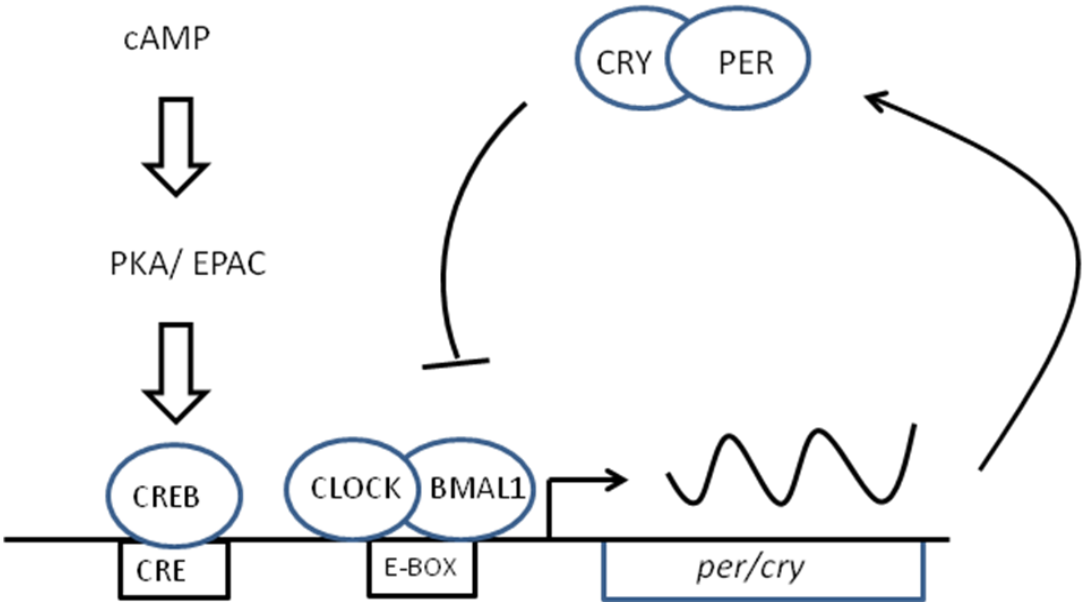

Figure 1.9 Schematic representation of the convergence between cAMP signalling and the transcriptional-translational feedback loop of core clock genes.

Schematic representation of the *per* promoter and its regulation by CLOCK/BMAL1 and CREB. While the E-boxes are targets of the clock-controlled CLOCK/BMAL1 regulation, the CRE is essential for responses to various signaling pathways. Increased cytosolic cAMP signalling is driven by $G\alpha_s$-coupled GPCRs thereby activating CREB, which then binds to CRE elements. This leads to the activation of transcription of *per* and *cry*, independently of E-box activity.

Endogenous levels of cAMP have been shown to oscillate in SCN and peripheral clocks across the circadian day (Prosser and Gillette. 1991, Doi et al. 2011), however, the physiological role of oscillatory cAMP remain to be elucidated. Whilst O'Neill et al. 2008 showed that chronic pharmacological disruption of endogenous cAMP rhythms suppressed circadian rhythms of clock gene expression, studies by Doi et al. 2011 presented compelling evidence that oscillatory cAMP was not required for rhythmic clock gene expression. The authors showed that genetic ablation of *rgs16*, which yielded loss of cAMP circadian rhythmicity, did not affect rhythmic clock genes expression in the SCN or rhythmic behaviour under free-running conditions.

There is much evidence for the role of Vasointestinal Peptide (VIP) and the $G\alpha_s$ coupled $VPAC_2$ signalling in mediating photic entrainment and mediating intercellular synchrony (Harmar et al. 2002, Piggins and Cutler. 2003). Mice which lack the $VPAC_2$ receptor also exhibited low amplitude rhythms of locomotor activity when placed under constant darkness or light dark cycles relative to wildtype. Studies by Harmar et al. 2002 demonstrated that a lack of $VPAC_2$ receptor also impaired the magnitude of acute clock gene induction upon exposure to light in the

subjective night; when exposed to a 6 hour period of light at ZT14, nocturnal induction of *mper1* and 2 were severely attenuated compared the wildtype. Consistently, application of VIP to SCN neurons has been shown to upregulate clock genes *per1* and *per2* expression and phase shift clock genes in a phase and dose dependent manner (Reed et al. 2001, An et al. 2011).

1.5.5 CREB independent mechanisms of entrainment

Several mechanisms of mammalian circadian entrainment have been described where CREB does not directly participate. These pathways are triggered by glucocorticoids, PMA and inhibitors of Casein Kinase in a CREB independent manner (Shim et al. 2007, Badura et al. 2007, Lee et al. 2010). Shim et al. 2007 demonstrated that exposure of fibroblasts to phorbol myristate acetate (PMA) induced rapid phosphorylation of CLOCK, subsequent redistribution from the cytoplasm to the nucleus and acute induction of the *per1* gene. Furthermore, pre-incubation of fibroblasts with inhibitors of PKC suppressed the effects of PMA mediated *per1* induction, whilst CREB phosphorylation remained unaffected, indicating a minimal role of CREB phosphorylation in PMA induction of *per1*. Furthermore, pre-incubation of fibroblasts with the MAPK inhibitor PD98059 which successfully prevented CREB phosphorylation, minimally attenuated the aforementioned effects of PMA on *per1* induction and CLOCK phosphorylation. Thus, despite PMA induced phosphorylation of CREB, the physiological consequences remain inconclusive as it cannot account for the PMA mediated *per1* induction.

Meng et al. 2010 reported that inhibition of $CK1_{\delta}$ in the SCN of *vipr*$^{-/-}$mice, where molecular pace making was compromised, was able to induce robust rhythms of clock gene expression. Furthermore, daily injections of the isoform specific inhibitor PF-670462 was successful in entraining the free-running behaviour in mice under free-running conditions. In contrast, saline injected mice failed to entrain, which showed that the injections themselves did not significantly contribute to the circadian response.

1.5.6 Phase response curves

The phase response curve (PRC) provides a description of the phase responsiveness to a stimulus, such as light, by plotting the phase shift as a function of the circadian phase at which light was delivered. By convention, phase advances and delays are represented by positive and negative values (Johnson. 1999). Two types of phase response curves have been described characterised by distinctive amplitudes and waveforms; a Type 1 PRC is typically described for photic entrainment in mammals, where short light pulses (15 minutes -1 hour) induce relatively small phase advances and delays during the early and late subjective night respectively with a contiguous transition in the middle of the night (Johnson. 1999).

Type 0 phase response curves are characterised by high amplitude phase advances and delays and a point of discontinuity between the transitions for delay to advance. When these phase shifts of up to 12 hours are plotted as advances and delays, a discontinuity often appears at the transition between phase delays to advances. The type of phase response curve elicited is intrinsically dependent on several factors such as the strength of the stimulus and the robustness of the endogenous oscillator to external perturbations. In mammalian models, Comas et al. 2006 examined the phase responses of free-running mice to light pulses varying between 1-18 hours in duration and reported that light pulses shorter than 3 hours generated Type 1 PRC, whereas exposures longer than 3 hours elicited Type 0 PRC, which lacked a dead zone. The robustness of the circadian oscillator can also determine the waveform. Mammalian models lacking components of the transcriptional translational feedback loop are more susceptible to high amplitude photoentrainment compared to wildtype strains (Vitaterna et al. 2006, Jud et al. 2010).

Such models include the *clock* mutant, where these mice are able to entrain to LD cycles, and retain a rhythmic behaviour, although dampened under free-running conditions. However, upon exposure to light during the subjective night, the magnitude of the phase shifts were enhanced compared the wildtype mice to the same light stimulus. Thus, large amplitude responses can be attributed to deficiencies in transcriptional translational feedback loop which may render the cycle more susceptible to changes. In contrast, Type I phase response curves are associated a more rigid transcriptional translational feedback loop is likely to impose a limit on the degree of acute induction of clock genes and phase shifting.

1. General introduction

Non-parametric entrainment of the mammalian clock is principally characterised by acute induction of clock genes and abrupt changes in period, leading to a stable shift in phase (Pittendrigh and Takamura. 1989). The changes in free-running period (FRP) correlate strongly with phase shifts; where acceleration and deceleration of the clock lead to phase advances and delays respectively. However, the molecular basis of such transient changes remains to be elucidated (Johnson et al. 2003).

1.5.7 Intercellular synchronisation of the mammalian clock

Under free-running conditions, synchronisation of cellular oscillators within the SCN tissue relies on intercellular coupling mechanisms consisting of multiple neurotransmitters, paracrine signalling molecules and gap junctions (Shirakawa et al. 2001, Aton et al. 2005, Maywood et al. 2011). Despite the abundance of such molecules, they are by no means redundant, as pharmacological blockade or genetic ablation of individual signalling pathways between neurons are sufficient to compromise the intercellular synchrony of rhythmic neurons in SCN cultures. Hughes et al. 2008 demonstrated using a *per1*::*gfp* reporter vipr2$^{-/-}$ mouse model, that the rhythmic expression of *per1* in SCN neurons showed a wider variation of peak times in culture than those in wildtype mice. Furthermore, application of the $VPAC_2$ inhibitor PG 99-465 at 10 nM to SCN cultures of wildtype mice resulted in a circadian phenotype similar to that of the *vipr2*$^{-/-}$ mouse, with respect to phase clustering.

Many types of peripheral cells such as fibroblasts express the same complement of clock genes as neurons of the SCN *in vitro* and *in vivo*, however, individual oscillators appear to be much less coupled (Izumo et al. 2003, Stratmann and Schibler. 2006, Leise al. 2012). Nagoshi et al. 2004 reported that cultured fibroblast cells oscillated independently of others within the same culture and were unable to influence the rhythm parameters of neighbouring cells. This was first demonstrated in co-cultures of BMAL1-luciferase reporter NIH3T3 cells, an immortalised fibroblast cell line derived from cultured embryonic mouse fibroblast (Rittling. 1996), and feeder fibroblast cells which exhibited different circadian properties. Following exposure to 10 nM dexamethasone for 15 minutes, rhythms of clock gene expression in rat1 fibroblasts were normally phase advanced by 6h compared to NIH3T3 cells. In a co-culture of 20:1 rat1 fibroblasts and baml1-luciferase reporter NIH3T3 cells, NIH3T3 cells did not show a significant deviation in phasing of baml1-luciferase activity. Similarly, when co-cultured with mutant *per1* Knockout primary fibroblasts, which exhibit a relatively short free-running period of 20 hours, the pace of the feeder cells did not impact the period of the rhythmic bioluminescence.

However, other reports claim that in the retina, a rhythmic tissue with complex anatomical organisation and circuitry, circadian rhythm parameters are indeed governed by intercellular communication. When Ruan et al. 2008 examined the impact of activation of GABA signalling in the SCN, they reported dose dependent manner suppression in rhythm amplitude of PER2::LUC reporter. Conversely, pharmacological blockade of $GABA_A$ and $GABA_B$ receptors with antagonist SR 95552 and TPMPA enhanced the rhythm amplitude of the PER2::LUC bioluminescence.

1.5.8 Singularity

Light induced arrhythmia and sustained diminution of behavioural rhythms is commonly reported in mammals whereupon a photic stimulus is delivered near the transition point of the phase response curve (Grone et al. 2011). This phenomenon has also been recapitulated in cell based models of the mammalian clock in pioneering studies by Ukai et al. 2007. The authors engineered *per2::luc* reporter fibroblasts to express melanopsin, thereby enabling direct photoentrainment from light pulses. It was subsequently reported that activation of melanopsin expressing cells at CT17 of the *per2* rhythm, where light induced phase responses were maximal, lead to a marked reduction in overall rhythmic amplitude of *per2.* Recordings of individual cells revealed that the critical light stimulus did not impact on intracellular rhythm amplitude, but instead, diversified the phasing of individual rhythmic cells. These findings have also been mirrored by Pulivarthy et al. 2007, who also reported light induced damping of rhythmic *per2* protein expression at the multi-cell level but not within individual cells.

1. Thesis aims

1.6 Thesis aims

Delineating the contributions of cAMP to the regulation of the mammalian pacemaker has traditionally relied on experimental manipulation of components by pharmacological or genetic techniques. However, the use of pharmacological agents to manipulate cellular physiology is accompanied with many practical limitations such as off-target responses, slow kinetics of drug distribution and clearance, and a lack of receptor subtype specificity. Such limitations reduce the validity of pharmacological agents for studying the physiological role of the $G\alpha_s$ signalling cascade in a biological system with multiple receptors and cell types.

Optogenetic tools can potentially overcome these practical limitations. By replacing chemical ligands with light for activation, the resolution of signalling is no longer hampered by drug delivery and washout mechanisms (Miesenbock, 2004). Light can be administered consistently over time, whereas drug doses fluctuate over time due to metabolism and excretion. In addition, optogenetic tools enable manipulation of cell types expressing orphan receptors or where pharmacological agents are lacking. Thus, tissues which currently cannot be influenced by drug application can be instead by modulated by introducing optogenetic tools (Farrel and Roth. 2013).

By allowing timely manipulation a desired signalling pathway within a complex but drug free-system, optogenetics has further enabled researchers to dissect the functional relationship between a single receptor and a cellular output in the midst of other cellular processes (Deisseroth. 2011). Due to the selectivity of the photoreceptor protein to light, other endogenous receptors are not activated by light and the photoreceptor is mutually insensitive to endogenous signals. Thus, cellular responses can be solely attributed to the phototransduction cascade of the optogenetic tool. Overall, optogenetic tools can substitute or even complement current pharmacological tools by allowing the investigator to study the role of an individual receptor in an *in vitro* or *in vivo* model without disrupting or being disrupted by other cellular processes.

1. Thesis aims

In this study, I thus sought to develop and utilise an optogenetic tool which could mimic robust GPCR mediated cAMP signalling within the mammalian clock. The $G\alpha_s$-coupled *Carybdea rostonii* opsin, JellyOp, robustly activates cAMP signalling in functional studies, and is thus suitable for addressing the contributions of temporally controlled cAMP signalling to circadian regulation. Previous studies by Bailes et al. 2012 have demonstrated many desirable properties of heterologous JellyOp including stability, robust $G\alpha_s$ interactions and bleach resistance which I intended to exploit for the investigation.

Another critical objective was to investigate whether the JellyOp signalling interface could also contribute to the regulation of circadian regulation independently of cAMP. The main focus of the thesis (as described in chapter 3 and 4) is dedicated towards designing and implementing JellyOp based optogenetic tools for investigating $G\alpha_s$ dependent and independent mechanisms of circadian organisation, in the context of GPCR signalling. My investigations, as described in chapter 5, attempt to characterise the role of light in regulating RPE circadian physiology, and also investigates the contributions of tissue integrity on the intercellular synchrony of RPE clocks.

1.6.1 Chapter 3

The initial aim of this study was to develop a suitable optogenetic tool for investigating G protein independent signalling cascades of JellyOp. To achieve this, I sought to modify the signalling profile of JellyOp so that it was unable to interact with endogenous G proteins. The process of decoupling the JellyOp from the $G\alpha_s$ signalling pathway would allow for the receptor to exclusively promote G protein independent signalling cascades. Intrinsic to this aim was the desire to advance my understanding of the functional structural relationship of JellyOp in relation to other $G\alpha_s$-coupled GPCRs through identifying critical residues that are implicated in G protein interactions. Given the $G\alpha_s$ coupling capacities of JellyOp, I hypothesised that this was principally due to individual amino acid residues in the intracellular loops of the receptor that were involved in direct interactions with downstream effector G proteins, and that substitution of those residues would abolish G protein interactions

To address this hypothesis I first sought to identify these functional amino acids, by comparing the amino acid sequence of JellyOp with the human β2-Adrenergic receptor, a well characterised $G\alpha_s$ coupled GPCR. Previous mutagenic studies on the β2-adrenergic receptor

have identified several amino acids involved in G protein interactions. If present in JellyOp amino acid sequence, it is plausible that they also contribute to interactions between JellyOp and G proteins. Upon identification of conserved amino acids from the sequence alignment, I sought to modify those residues by site directed mutagenesis in order to create G protein decoupled structural mutants, and evaluate the functional expression of those variants in cell based assays with respect to G protein signalling. This was conducted by assessing the ability of JellyOp mutant variants to manipulate intracellular messengers, cAMP, calcium and MAPK in a range of end-point assays as well as real-time cell based reporter assays. A qualitative investigation into the interactions between β-arrestins and JellyOp was assessed using a fluorescently tagged GFP construct, which enabled me to track the distribution of the GFP reporter within subcellular locations. The second aim of this investigation was to characterise the functional expression of JellyOp and structural variants in rat1 fibroblasts, with respect to $G\alpha_s$ dependent and independent signalling cascades. The hypothesis for this study was that JellyOp would be able trigger the $G\alpha_s$ pathway in rat1 fibroblasts in light dependent manner, as previously observed in HEK283 cells (Bailes et al. 2012), and elicit induction of intracellular cAMP.

1.6.2 Chapter 4

In this study, I sought to characterise the contributions of time-delimited $G\alpha_s$ dependent and independent pathways, triggered by wildtype and $G\alpha_s$ decoupled JellyOp photopigments respectively, in regulating the rat1 fibroblast circadian clock. I hypothesised that JellyOp would be able to perturb the kinetics of the mammalian transcriptional-translational feedback loop in a phase and dose dependent manner. In addition, my second hypothesis was that JellyOp mediated responses are predominantly dependant on the $G\alpha_s$ pathway, irrespective of other intracellular cascades, and that in the absence of cAMP signalling, a $G\alpha_s$ decoupled JellyOp photopigment would be less able to impact on all aspects of the mammalian clock such as rhythm amplitude and phasing. To observe these circadian responses, the oscillatory dynamics of *per2* gene expression was surveyed in rat1 fibroblasts before and after activation of JellyOp based pigments.

1.6.3 Chapter 5

In this chapter, I sought to investigate the role of tissue organisation in mediating intercellular synchrony of individual peripheral oscillators, in particular RPE cells. I hypothesised that due to the recently discovered intercellular mechanisms that regulate overall circadian rhythms of retinal tissues, factors such as tissue anatomy and structure could also play a role in regulating intercellular synchronisation of individual RPE oscillators. To this end I aimed to conduct a comparative analysis of RPE rhythm parameters, including phase and period, between explant cultures and dispersed cell cultures.

Another aim was to investigate whether RPE circadian physiology was influenced by photostimulation. Due to the reported presence of endogenous melanopsin photopigments in RPE cells, my hypothesis was that this pigment could render the RPE cells light responsive that was akin to fibroblasts engineered to express heterologous melanopsin. In particular, I aimed to explore whether RPE oscillators were susceptible to synchronisation and entrainment to light, presumably due to well characterised phototransduction pathways of melanopsin. To probe for entrainment, rhythms of luciferase activity were captured from RPE tissue cultures of PRE2::LUC reporter mice, in between exposure to a pulse of bright white light. To probe for acute light responses in the RPE, I also assayed for acute induction of the immediate-early gene *c-fos* following exposure of dark adapted mice to bright light.

2. Materials and methods

2.1 Construction of the pIRES-JellyOp-GFP expression vector

The coding sequence of full length JellyOp was tagged downstream with extra bases to encode a 9 amino acid epitope of C-terminal bovine rhodopsin (1D4) (designed by Dr Helena Bailes and manufactured by Genscript Corp, USA). The JellyOp-1D4 construct was subcloned from the original pUC57 vector into a bicistronic pIRES-AcGFP expression vector (kindly donated by Dr Jim Bellingham, University of Manchester). Briefly, the pUC57-JellyOp-1D4 and pIRES-AcGFP vectors were double digested with EcoR1 (Life Technologies, USA) and BamH1 (Life Technologies) at 37°C for 1½ hours. Following electrophoretic separation, the digested JellyOp-1D4 fragment and linearised pIRES-Ac-GFP vector backbone were purified from a 1 % SeaKem® LE agarose (Lonza, Switzerland)–TAE (Sigma Aldrich) gel containing 0.01 % Ethidium Bromide (Promega, USA), using a Gel Extraction Kit (Qiagen, USA). The JellyOp-1D4 construct was ligated into pIRES-AcGFP vector with T4 ligase (Life Technologies) at room temperature overnight, and purified to be endotoxin-free before transfecting mammalian cells.

2.2 Site-directed mutagenesis of JellyOp

All primers for site directed mutagenesis of JellyOp were purchased from Sigma Aldrich.

Mutagenesis	Primer sequences	
F139A	Forward sequence	tcacagtgtgcagacctgccgtggcaactgcgattca
	Reverse sequence	tgaatcgcagttgccacggcaggtctgcacactgtga
Y192A	Forward sequence	gttcttttgatggtggctactgccgtgttggttcaaggagagatg
	Reverse sequence	catctctccttgaaccaacacggcagtagccaccatcaaaagaac

Y105G	Forward sequence	tctcgccttagatcgaggcttcacagtgtgcagac
	Reverse sequence	gtctgcacactgtgaagcctcgatctaaggcgaga
K68A	Forward sequence	cttacgacataaattggcttttgcagatgctctcatggctagtatgg
	Reverse sequence	ccatactagccatgagagcatctgcaaaagccaatttatgtcgtaag
Upstream EcoR1	Forward sequence	gaagaattgtcggtggtaatgaattcgctccttccagtacggctgttga
	Reverse sequence	acagccgtactggaaggagcgaattcattaccaccgacaattcttccac
Downstream EcoR1	Forward sequence	aacagccgaatctgaattcacggagacgagccaggtggccccggcctaa
	Reverse sequence	ttaggccggggccacctggctcgtctccgtgaattcagattcggctgtt

Mutagenesis of each amino acid was carried out within the pIRES-JellyOp-1D4-GFP vector using QuikChange® Lightning Site-Directed Mutagenesis Kit (Agilent Technologies, USA) according to the manufacturer's instructions. PCR amplification was carried out in a Techne PCR machine (Bibby Scientific Limited). Following PCR amplification, the parental DNA plasmid was digested with 1 µl Dpn I at 37^{o}C for 15 minutes.

The mutagenised plasmid products were cloned in XL10-Gold® Ultracompetent Cells (Agilent Technologies) according to manufacturer's proctocol. Heat shock was performed in a 42°C water bath for 30 seconds, followed by incubation on ice for 2 minutes. The cells were suspended in 42°C preheated supplemented NZY+ broth (1 % NZ amine casein hydrolysate, Sigma Aldrich) , 0.5 % yeast extract, 0.5 % NaCl, 12.5 mM $MgCl_2$ (Sigma), 12.5 mM $MgSO_4$ (Sigma Aldrich), 20 mM glucose (Sigma) in dH_2O) and incubated in a 37°C shaking incubator at 225–250 rpm for 1 hours. Ultracompetent cells were concentrated by centrifugation 600xg for 2 minutes and resuspended in 200 µl NZY+ broth. The cells were plated onto 37°C pre-warmed LB agar plates containing 50 µg/ml kanamycin and incubated at 37°C overnight. Mutagenesis was confirmed by DNA sequencing.

2.3 FLP-IN™ cell culture and maintenance

Stable FLP-IN™-293 Glosensor™20F HEK cells and FLP-IN™-293 Glosensor™20F JellyOp HEK cells were kindly donated by Dr Helena Bailes, University of Manchester. FLP-IN™-293 Glosensor™20F HEK cell lines were maintained in supplemented Dulbecco's modified Eagle's medium (4,500 mg/l DMEM, D-glucose, sodium pyruvate and L-glutamine, 10 % foetal bovine serum (Sigma Aldrich), 1 % penicillin and streptomycin) as selective antibiotics including 100 µg/ml hygromycin (InvivoGen, USA) and 100 µg/ml blasticidin (InvivoGen) in a 37°C and 5 % CO_2 incubator (RS Biotech, UK). Similarly polyclonal stable FLP-IN™-293 Glosensor™20F JellyOp HEK cell lines were selectively maintained with 100 µg/ml hygromycin, 100 µg/ml blasticidin and 400 µg/ml G418 (InvivoGen) under dim red light. Cells were passaged at least once a week under sterile conditions.

2.4 Stable expression of JellyOp in rat1 fibroblasts

rat1 fibroblasts which express a minimal promoter of the mouse *period2 (per2)* gene fused to a luciferase gene, (kindly donated by Qing-Jun Meng, University of Manchester) were selectively maintained in supplemented DMEM media but without 100 µg/ml hygromycin. The minimal promotor consisted of 418 base sequence which lies 519 bases upstream from the start of the native mouse *per2* start codon (NM_011066.3). It contains double E-box-like elements (5'**cacgtt**ttccac**tatgtg**-3') 165 bases upstream of the start codon (See Appendix 1 for entire sequence). The pIRES-JellyOp-1D4-AcGFP vector was linearised with ApaL1 (Life Technologies) at 37°C overnight. Following plasmid purification with QIAGEN Plasmid Mini Kit (Qiagen), the pIRES-Ac-JellyOp-GFP was transfected into *per2::luc* RAT1 fibroblasts with

Lipofectamine 2000 (Life Technologies) as above and selected with 400 µg/ml neomycin (InvivoGen). Stable isogenic transfectants were then isolated with cloning rings (Sigma Aldrich). All fibroblast cell lines were passaged at ratio of 1:6 every 3-4 days under sterile conditions.

2.5 Quantification of GFP expression in stably transfected rat1 fibroblast cell lines

4 x 10^4 *per2::luc* rat1 fibroblasts from stable lines were seeded as triplicates into a white, clear bottom 96 well plate (Greiner Bio-one, Austria) overnight. Following 200 50 Hz flashes of 485 nm light, 520-30 nm fluorescence was recorded at 27°C through a topread 2 mm lens in a FLUOstar OPTIMA platereader (BMG Labtech, Germany) at a gain of 2000. The data were collected with Optima data collection software (BMG Labtech). The averaged background autofluorescence from the culture media and 96-well plate was subtracted from total average fluorescence values to obtain cellular fluorescence from each monoclonal line. Statistical significance was calculated with a one way ANOVA with Bonferroni's post-hoc test using GraphPad Prism (GraphPad Software, USA).

2.6 Immunohistochemical labelling for the 1D4 epitope in mammalian cells

Under dim red light, 10^5 *per2::luc* rat1 fibroblasts or FLP-IN™-293 Glosensor™20F JellyOp HEK cells were seeded onto glass coverslips (VWR International, USA) in a 24 well plate (Corning, USA) overnight. The cells were rinsed in DPBS (2.69 mM KCl, 1.47 mM KH_2PO_4, 136.8 mM NaCl, 8 mM NaH_2PO_4, Sigma Aldrich) and incubated in 1 ml 4 % paraformaldyhyde (Sigma Aldrich) in DPBS for 2 hours at room temperature, and washed 3 x 5 minutes. The fixed cells were incubated in 2 % glycine (Fisher Scientific, USA) in DPBS for 5 minutes, washed 3 x 5 minutes in DPBS and blocked in 2 % normal goat serum (Vector laboratories, USA), 5 % BSA (Sera Laboratories International, UK), 0.1 % TX-100 (Sigma Aldrich) in DPBS for 30 minutes at room temperature. Autofluorescence was quenched with a 5 minutes incubation of cells in 0.25 % NH_4Cl (Sigma Aldrich) in DPBS, followed by 3 x 5 minutes washes in DPBS. Incubation in primary monoclonal mouse anti-rhodopsin antibody (1:500 in 2 % BSA/DPBS, Affinity BioReagents, USA) was performed for 1 hour at room temperature, followed by 3 x 5 minutes washes of 0.1 % Tween-20 (Sigma Aldrich) in DPBS. Goat anti-mouse antibody conjugated to Alexa 555 Fluor® (1:1000 in 0.1 % Tween-20/ DPBS, Molecular

Probes) was added to the cells for 90 minutes, followed by 3 x 50 minutes washes of 0.1 % Tween-20 in DPBS. The cells were post-fixed with 4 % PFA in DPBS for 30 minutes at room temperature and coverslips were mounted onto poly-Lysine coated glass slides (VWR International, USA) with DAPI containing mounting medium (Vector Laboratories) in the dark overnight. The cells were examined on an Olympus BX51 fluorescence microscope (Olympus, Japan) and images were acquired with on a Coolsnap ES camera (Photometrics, USA) using MetaVue Imaging Software (Molecular Devices, USA).

2.7 Western blot for the ID4 epitope in mammalian cells expressing JellyOp

$3x10^6$ cells were plated into two wells of a 6 well plate overnight. For protein extraction, the cells were rinsed in ice cold DPBS and lysed with 150 µl ice cold RIPA buffer (1 % sodium deoxycholate (Sigma Aldrich), 0.1 % SDS (Fisher Scientific), 1 % Triton X-100, 10 mM Tris-HCl (Sigma Aldrich) pH6.8, 140 mM NaCl (Sigma Aldrich) in dH_2O) with PhosSTOP Phosphatase Inhibitor Cocktail Tablet (Roche) and Complete Phosphatase Inhbitor Cocktail Tablets. The cell lysates were collected with cell scrapers into eppendorf tubes (Starlab, USA) gently triturated using a 1 ml syringe (BD Biosciences, USA) with reducing gauge needles (25G x 5/8", 23G x 1.25", 21G x 2", 19G x 15", BD Biosciences). Samples were stored at -80°C freezer until needed for western blotting. 20 µg of protein made up in 20 µl Milli Q and heated on a 100°C dry block with 10 µl 2x Laemmli sample buffer (2.5 % SDS (Fisher Scientific), 125 mM pH 6.8 Tris-HCl (Sigma Aldrich), 20 % glycerol (Fisher Scientific), 0.5 % β-mercaptoethanol (Sigma Aldrich) in dH_2O) for 5 minutes. 30 µl samples were loaded into individual wells of a NuPAGE® Novex® 4-12 % Bis-Tris Gels (Life Technologies) alongside 10 µl Protein plus ladder (Life Technologies) and run with 1x MOPS running buffer (100 mM MOPS (Fisher Scientific), 100 mM Tris-base (Sigma Aldrich), 7 µM SDS (Sigma Aldrich), 2 µM EDTA (Sigma Aldrich) at 100 V for 90 minutes. The protein was transferred to Amersham Hybond™-P polyvinylidene difluoride (PVDF) membrane (GE healthcare, USA) in 1x transfer buffer (38.7 mM Glycine (ThermoFisher Scientific, USA), 48 mM Tris-base, 1.28 mM SDS, 20 % Methanol) for 90 minutes at 90 V. The membrane was washed with 1x TBST (43.8 g/ml NaCl and 3.025 g/ml Tris base, 1 % Tween 20 in dH_2O) for 3x 5 minutes and rinsed in amidoh black (ThermoFisher Scientific) to confirm protein sample transfer. The membrane was blocked in 5 % Marvel milk powder in TBS/T for 1 hour at RT. Membrane was incubated with primary anti-rhodopsin mouse monoclonal antibody (1:500 in blocking buffer) at 4ºC overnight on a shaker at 100rpm and washed 3x 10 minutes in 1x TBST. Membrane was incubated with 1:1000 goat anti-mouse in blocking buffer at room temperature for 1 hour, followed by 3 washes in 1xTBST. The membrane was soaked in 2 ml SuperSignal West Dura Extended

Duration Substrate (ThermoFisher Scientific) for 2 minutes, then developed on Kodak Biomax light film (Sigma Aldrich).

2.8 Maintenance of mPER2::LUC mice

Adult mPER2::LUC knockin mice were housed in the at the University of Manchester, under a 12 hour light:dark (LD) cycle with *ad libidum* access to standard lab chow (B&K Universal) and water. Temperature was maintained at 18°C and humidity at 40 %. All procedures were carried out in accordance with the UK Animals (Scientific Procedures) Act 1986.

2.9 RPE culture medium

Culture medium for primary RPE cells consisted of Dulbecco's modified Eagle's medium/F12 (Sigma Aldrich) to a ratio of 1:1, supplemented with 20 % foetal calf serum and 1 % penicillin and 1 % streptomycin.

2.10 RPE tissue dissection and primary culture preparation

The PER2::LUC reporter mice were culled by cervical dislocation, their eyeballs were immediately removed after cull with spring scissors (World Precision Instruments, USA) and incubated in chilled HBSS (Sigma Aldrich) supplemented with 0.75 % sodium bicarbonate, 100 mM HEPES buffer (Sigma Aldrich) and 1 % penicillin and 1% streptomycin. The eye balls were dissected with the aid of a dissecting microscope in a laminar flow hood. The cornea of the eyeball was sliced open with a razor blade (Swann Morton, UK) to release the intraocular pressure. The anterior ocular tissues including the cornea, iris pigment epithelium and ora serrata were subsequently removed with Vannas scissors and forceps (World Precision Instruments). The eye cup was then incubated in filter sterilised 2.5 U/ml Dispase II (Sigma Aldrich) in Ca^{2+}/Mg^{2+} free PBS at 37°C for 30 minutes before wash in Ca^{2+}/Mg^{2+} free PBS (Sigma Aldrich). Dissociated RPE cells were then lifted from the choroid and sclera with a paintbrush, collected in 200 µl RPE medium and aspirated with a 200 µl micropipettor (Gilson, USA), followed by centrifugation at 300 g for 5 minutes. Pelleted cells were resuspended in RPE culture medium and plated into 35 mm cell culture dishes containing 2 ml RPE culture. Cells were cultured at 37°C in a 5 % CO_2 atmosphere, with culture medium replaced every 2 days.

2.11 Photomicroscopy of RPE primary cultures

Cells were visualised with a Leica DM LED inverted microscope (Leica Microsystems, Switzerland) through a phase contrast filter. Images were captured with a fitted Canon Powershop S70 digital camera (Canon, USA) using Canon Zoombrowser EX image browser software and processed on Corel photoshop X3 (Corel, Canada).

2.12 Immunocytochemical labelling for RPE65 in primary RPE cells.

RPE primary cells cultured on glass coverslips (VWR international, USA) were fixed with 4 % PFA (Sigma Aldrich) at 4^{o}C for 30 minutes in between washings in ice cold PBS. Cells were permeablised in 0.025 % Triton-X 100 in PBS at room temperature for 10 minutes, and blocked in 1 ml BSA, 10 % normal goat serum (Vector Laboratories) in PBS for 30 minutes and then incubate in anti-RPE65 Ig (1:1000, Abcam, UK) in 1 % BSA for 2 hours at room temperature. After 3 washings in PBS, cells were incubated in 2 µg/ml goat anti-mouse Ig conjugated to Alexa 555 Fluor® (Life Technologies) in 1 % BSA for 90 minutes in the dark at room temperature. After rinsing in PBS, coverslips were mounted on a poly-L-lysine slide using vectashield mounting medium with DAPI. Stained cells were observed with a fluorescence microscope with DAPI and Texas red filters. All images were captured with a digital camera (Canon) and processed using the bio-imaging software MetaVue Imaging system (Molecular Devices).

2.13 Bioluminescence recordings of JellyOp FLP-IN™-293 Glosensor™20F cells

5 x 10^{4} FLP-IN™-293 Glosensor™20F cells were plated as triplicates in solid white 96 well plates (Greiner BioOne) for bioluminescence recordings. To allow for measurable expression of the Glosensor™20F 20 cAMP biosensor, cells were then incubated for another 16 hours in the presence of 300 ng/ml tetracycline and 10 µM 9-*cis*- retinaldehyde, Sigma Aldrich) in CO_2 independent medium without phenol red, L-15, (Life Technologies), with 10 % foetal calf serum. Beetle luciferin (Promega) reconstituted in 10 mM HEPES buffer (Sigma Aldrich) was added for a final concentration of 2 mM luciferin to each well and allowed to equilibrate at 37°C for 2 hours. Raw luminescence units in cells were recorded at 37°C with 1 second resolution at 30 second intervals with a topread 3 mm lens in a BMG Labtech Fluostar Optima plate reader, at a gain of 3600. Following 30 minutes equilibration inside the platereader, cells were subjected to light flashes delivered from a camera flash bulb (Jessops). Luminescence recordings were analysed with Optima software (BMG), Microsoft Office Excel (2010,

Microsoft) and GraphPad Prism 4 (GraphPad). All data from each well were normalised to baseline measurements captured prior to the initial photo-stimulation. For MDL-12330 A (MDL) titration, MDL was delivered to cells in each well at a final concentration of 5, 10, 25, 50, 100, and 200 nM after 15 minutes of platereader equilibration. Photoactivation by camera bulb and platereader recordings were performed as described above.

2.14 Transient expression of JellyOp mutant variants in FLP-IN™-293 Glosensor™20F cells

5 x 10^4 FLP-IN™-293 Glosensor™20F cells were plated in duplicate in solid white 96 well plates, and transfected with 0.2 µg pIRES plasmid vectors bearing the various mutagenic JellyOp constructs as described above, using Lipofectamine 2000 (Life Technologies) according to the manufacturer's instructions for 6 hours. Cells were incubated in L-15 (Life Technologies) supplemented with 10 % foetal calf serum for 16 hours and 10 µM 9-*cis*-retinal at 37°C and 5 % CO_2. Platereader recordings were conducted as described in the previous paragraph.

2.15 ELISA based quantification of cAMP in FLP-IN™-293 Glosensor™20F cells transiently expressing JellyOp and F139A JellyOp

5x10^4 FLP-IN™-293 Glosensor™20F cells and FLP-IN™-293 Glosensor™20F JellyOp cells were plated in 12 well plates overnight at 37°C and 5 % CO_2 , and then incubated in Dulbecco's modified Eagle's medium lacking phenol red, but supplemented with 10 % foetal calf serum and 10 µM 9-*cis*-retinal for 2 hours. Dark control cells were lysed with 300 µl 0.1 µM HCl (Sigma Aldrich) in the dark for 10 minutes at room temperature whereas experimental samples were flashed with light from the camera bulb and lysed at 2 minutes post-stimulation. Cell lysates were collected from the culture dishes using cell scrapers (Greiner BioOne) and centrifuged at 600 xg for 10 minutes.

To determine the cAMP increase in light exposed cells, enzyme-linked immunoassay was conducted using a direct cAMP Enzyme Immunoassay Kit (Sigma Aldrich) according to the manufacturer's instructions. Optical measurements were conducted using a platereader at 405 nm. The protein content was determined with Fluka protein quantification kit (Sigma Aldrich) according to the manufacturer's instructions and optical measurements performed at 455 nm.

2.16 Bioluminescence recordings in *per2::luc* rat1 fibroblasts stably expressing JellyOp and F139A JellyOp

5 x 10^4 *per2::luc* fibroblasts were plated in triplicate in solid white 96 well plates, and transfected with 0.2 µg pGlosensor™20F using Lipofectamine 2000 (Life Technologies) according to the manufacturer's instructions for 6 hours. Cells were incubated in L-15 (Life Technologies) supplemented with 10 % foetal calf serum for 16 hours and 10 µM 9-*cis*-retinal at 37^{o}C and 5 % CO_2. Following 30 minutes platereader equilibration at 37^{o}C, cells were exposed to 2 flashes of light with 10 minutes recovery times per flash. Cells were then flashed approximately every 30 seconds for 15 minutes. For investigating the effects of MDL on JellyOp activity, the agent was delivered to cells in each well at a final concentration of 5, 10, 25, 50, 100, and 200 nM after 15 minute of platereader equilibration. Photoactivation by camera bulb and platereader recordings were performed as described above.

2.17 ELISA based quantification of cAMP in JellyOp and F139A JellyOp *per2::luc* rat1 fibroblasts

5x10^5 *per2::luc* fibroblasts were treated with 200 nM dexamethasone for 2 hours prior to bioluminescence recordings. On the second day of recording, fibroblast cultures were removed from the lumicycle at various times of the circadian day lysed in 300 µl of 0.1 M HCl solution for 10 minutes at room temperature. Cell lysates were collected from the culture dishes using cell scrapers (Greiner BioOne) and centrifuged at 600 xg for 10 minutes. 100 µl of supernatant treated with 5 µl acetylation reagent (1:2 acetic anhydride: triethylamine) before determination of cAMP level by direct EIA (10µl/well) according to the manufacturer's instructions (Sigma Aldrich). Optical measurements were conducted using a platereader at 405 nm. The protein content was determined with Fluka protein quantification kit (Sigma Aldrich) and optical measurements performed at 455 nm.

2.18 Bioluminescence recordings of HEK cells transiently expressing Glosensor™22F and opsin photopigments

5 x 10^4 HEK293 cells were plated in triplicate in solid white 96 well plates, and co-transfected with 0.2 µg pcDNA5/ FRT/TO Glosensor™ 22F and 0.2 µg pcDNA3 –JellyOp, pcDNA3 –F139A JellyOp, pcDNA3 –human Melanopsin or pcDNA3 –human Rhodopsin, using 0.5 µl Lipofectamine 2000 (Life Technologies) according to the manufacturer's instructions for 6 hours. Cells were incubated in L-15 (Life Technologies) supplemented with 10 % foetal calf serum for 16 hours and 10 µM 9-*cis*-retinal at 37°C and 5 % CO_2. Beetle luciferin was reconstituted in 10mM HEPES buffer was added for a final concentration of 2 mM to each well and allowed to equilibrate at room temperature for 3 hours. Cells were treated with 3 µM forskolin for 2 minutes before exposure to a flash of light. Luminescence was measured with a topread 3 mm lens in a Fluostar Optima plate reader (BMG Labtech) at a gain of 3600, 1 second, every 20 seconds intervals.

2.19 Bioluminescence recordings of HEK293 cells transiently co-expressing aequorin and opsin photopigments

Calcium mobilisation was detected using an encoded mitochondrially targeted aequorin (mtAeq) reporter, adapted from Bailes and Lucas (2013) (See Appendix 2). 5x10^4 HEK293 cells in each well of solid white 96 well plates were co-transfected with 0.2 µg pcDNA5/FRT/TO mtAeq and pcDNA3-JellyOp or pcDNA3-melanopsin using Lipofectamine 2000 (Life Technologies) in serum-free Dulbecco's modified Eagle's medium (Sigma Aldrich) for 6 hours. Cells were then incubated for 16 hours at 37°C in the presence of 300 ng/ml tetracycline and 10 µM 9-*cis*-retinal (Sigma Aldrich) in CO_2 independent medium lacking phenol red (L15), but supplemented with 10% foetal calf serum. Coelentrazine H (Biotium, USA) reconstituted in 10 mM HEPES buffer was added for a final concentration of 2 mM coelentrazine to each well and allowed to equilibrate at room temperature for 3 hours. Bioluminescence from each well was recorded at room temperature with a topread 3 mm lens in a BMG Labtech Fluostar Optima plate reader at a gain of 3600, for 0.5 seconds, at 2 second intervals,

2.20 Western blotting for phosphorylated MAPK and total MAPK in FLP-IN™-293 Glosensor™20F cells and rat1 fibroblasts

3x 10^6 FLP-IN™-293 Glosensor™20F cells or FLP-IN™-293 Glosensor™20F JellyOp cells were plated into two 25cm^2 cell culture flasks, serum starved in 0.5 % foetal calf serum for 24 hours and further incubated with L15 with 0.5 % foetal calf serum and 10 µM 9-*cis*-retinal for 3 hours. 5x 10^5 *per2::luc* fibroblasts expressing wildtype JellyOp, F139A JellyOp or lacking photopigments were plated in 6 well plates, and similarly serum starved and incubated with 10 µM 9-*cis*-retinal. White light from a halogen light source (Fiber-Lite® DC950, Dolan-Jenner Industries, USA) was fed into the incubator through a liquid light guide (Knight photonics) with a UV and infrared cut-off. Light-treated cells were subject to 2 or 15 minutes exposure of light at 37°C with irradiance levels of 28.40 mW/cm^2. For protein extraction, the cells were rinsed in ice cold DPBS and 150 µl ice cold RIPA buffer per flask or well (1 % sodium deoxycholate (Sigma Aldrich), 0.1 % SDS (Thermo Fisher Scientific), 1 % Triton X-100, 10 mM Tris-HCl (Sigma Aldrich) pH 6.8, 140 mM NaCl (Sigma Aldrich) in dH_2O) with PhosSTOP Phosphatase Inhbitor Cocktail Tablet (Roche) and Complete Phosphatase Inhbitor Cocktail Tablets. The cell lysates were collected with cell scrapers into eppendorf tubes (Starlab) gently triturated using a 1 ml syringe (BD Biosciences) with reducing gauge needles (25G x 5/8”, 23G x 1.25”, 21G x 2”, 19G x 15”, BD Biosciences). Samples were stored at -80°C freezer until needed for western blotting.

20 µg of protein made up in 20µl Milli Q and heated on a 100°C dry block with 10 µl 2x Laemmli sample buffer (2.5 % SDS (Fisher Scientific), 125 mM pH 6.8 Tris-HCl (Sigma Aldrich), 20 % glycerol (Thermo Fisher Scientific), 0.5 % β-mercaptoethanol (Sigma Aldrich) in dH_2O) for 5 minutes. 30 µl samples were loaded into individual wells of a 4-12 % Life Technologies Bis-Tris gel (Life Technologies) alongside 10 µl Protein plus ladder and run with 1x MOPS running buffer (100 mM MOPS (Thermo Fisher Scientific), 100 mM Tris-base (Sigma Aldrich), 7 µM SDS (Sigma Aldrich), 2 µM EDTA (Sigma Aldrich) at 100 V for 90 minutes. The protein was transferred to Amersham Hybond™-P polyvinylidene difluoride (PVDF) membrane (GE healthcare) in 1x transfer buffer (38.7 mM Glycine (Thermo Fisher Scientific), 48 mM Tris-base, 1.28 mM SDS, 20 % Methanol) for 90 minutes at 90 V. The membrane was washed with 1x TBST (43.8 g/ml NaCl and 3.025 g/ml Tris-base, 1 % Tween 20 in dH_2O) for 3x 5 minutes and rinsed in amidoh black to confirm protein sample transfer. The membrane was blocked in 5 % Marvel milk powder (Premier Foods, UK) in TBS/T for 1 hour at RT. Membrane was incubated with 1:1000 rabbit monoclonal phospho-ERK Ig (New

England Biolabs, UK) at 4°C overnight on a shaker at 100 rpm. After 3 x 10 minutes washes in 1x TBST, membrane was incubated with 1:1000 goat anti-rabbit Ig conjugated horse radish perioxidase (Life Technologies) in blocking buffer at room temperature for 1 hour. After another 3 washes in 1xTBST, the membrane was soaked in 2 ml SuperSignal West Dura Extended Duration Substrate (ThermoFisher Scientific) for 2 minutes, then developed on Kodak Biomax light film (Sigma Aldrich).

The membrane was stripped at 50°C for 30 minutes in 100 mM β -mercaptoethanol (Sigma Aldrich), 62.5 mM Tris-HCl, 2 g/ml SDS in dH_2O followed by washes in TBS/T. The membrane was blocked in 5 % Marvel milk powder in TBS/T for 1 hour at room temperature, and then incubated in 1:1000 rabbit monoclonal ERK Ig (New England Biolabs, UK) at 4°C overnight on a shaker followed by in 3x 10 minute washes in 1x TBST. Membrane was then incubated with 1:1000 goat anti-rabbit in blocking buffer at room temperature for 1 hour, followed by 3 washes in 1xTBST. For investigating the effects of MDL on light induced MAPK responses, MDL was delivered to cells in each well at a final concentration of 100 nM at 15 minutes prior to photoactivation.

2.21 Automated photostimulation and bioluminescence recordings of JellyOp and JellyOpΔCOOH expressing FLP-IN™-293 Glosensor™20F cells

To capture luciferase bioluminescence from FLP-IN™-293 cells continuously over a period of over 10 hours within the platereader, a script was programmed by Krystopher Procyk and Dr Helena Bailes (University of Manchester) to automate JellyOp photostimulation with the internal xenon light source. Each loop with the script consisted of three functions; baseline luminescence readings of 2 minutes with a topread 3 mm lens at a gain of 3600, a 45 seconds light stimulation protocol (200 flashes on a 3x3 matrix) followed by post-stimulation luminescence readings of 7 minutes. The programme was then looped 48 times, such that each well was light pulsed and recorded for 10 minutes, every 30 minutes.

4x 10^4 FLP-IN™-293 Glosensor™20F cells were plated into three wells on a 96 well plate, of which two were transfected with pIRES vectors bearing JellyOp or JellyOp Δ COOH, whilst the third was mock transfected. Bioluminescence was recorded as described above at 37°C. All data were recorded on Optima Data Analysis (BMG Labtech) and analysed in Microsoft Excel 2007 (Microsoft, USA).

2. Materials and methods

2.22 β-arrestin2-GFP mobilisation assay in HEK cells

Under dim red light, 10^5 FLP-IN™-293 Glosensor™20F or FLP-IN™-293 Glosensor™20F JellyOp HEK cells were seeded onto glass coverslips (VWR International) overnight. All cells were transfected with pcDNA3 vector bearing β-arrestin-2-GFP for 6 hours using lipofectamine 2000 according to the manufacturer's instructions. Cells were incubated in L15 supplemented with 10 % foetal calf serum with 10 µM 9-*cis*-retinal for 16 hours. Dark control cells were fixed in 4 % paraformaldyhyde (Sigma Aldrich) under dim read light, whereas light treated cells were exposed to 30 minutes of bright white light at 28.40 mW/cm^2 at 37°C. For a pharmacological control, 10 µM isoproterenol (Sigma Aldrich) was added to cells in the dark for 30 minutes before fixation in paraformaldehyde and immunolabelling as described above. Images were acquired on a Delta Vision deconvolution microscope (Applied Precision, USA) using a 60 x Plan Apo objective magnification and numerical aperture magnification of 1.42 x with FITC, Texas red and FITC filters. The images were collected using a Coolsnap HQ (Photometrics, USA) camera with a Z optical spacing of 0.35 µm and deconvolved using the Softworx software (Applied Systems).

2.23 Recording medium for fibroblasts

The recording medium for bioluminescence recordings of fibroblast cultures consisted of 10 g/l Dulbecco's modified Eagle's medium supplemented with 3.5 g/l D- Glucose (Sigma Aldrich), 350 mg/ml Sodium Bicarbonate (Sigma Aldrich), 10 mM Hepes buffer, 2 % B27 (Life Technologies), 20 U/ml Penicillin and 25 µg/ml Streptomycin (Sigma Aldrich), 200 µM beetle Luciferin (Promega, USA) and 10 µM Forskolin (Sigma Aldrich).

2.24 Bioluminescence recordings for *per2::luc* fibroblasts

Prior to recording, cells were synchronised with 200 nM dexamethasone (Sigma Aldrich) for 1 hour, after which medium was replaced with recording medium. Cell dishes were then sealed with glass coverslips using high vacuum grease (Dow Corning, USA) and bioluminescence recordings were conducted within a Lumicycle machine (Actimetrics, USA) housed in a 37°C incubator. The photon count was sampled from each well with 75 seconds resolution at 10 minute intervals. Following 3 days of luminescence recordings, dishes were exposed to 4 hours of 5 second light steps every 30 seconds whilst placed underneath a light source adjacent to the lumicycle within the same incubator. White light from a Fiber-Lite® DC950 Illuminator (Dolan-Jenner Industries) was fed into the incubator through a liquid light guide

(Knight photonics, USA) with a UV and infrared cut-off and controlled via a programmable shutter (Cairn, UK). Irradiance at the level of the cells was 28.40 mW/cm^2.

The 24 hour running average was first deducted from the raw data to filter out baseline deviations in the *per2::luc* rhythm. Detrended data were then averaged over 2 hours to filter out high frequency fluctuations in bioluminescence signal. The oscillatory amplitude was measured as the peak to trough difference from the processed rhythm data. Relative amplitude changes were calculated as the percentage difference in amplitude between the oscillation following light treatment and the 2nd (unperturbed) oscillation of the recorded rhythm. Changes in amplitude were plotted as a function of the circadian time at which the light pulse was delivered. The troughs and peaks of the fibroblast rhythm were assigned CT0 and CT12 respectively. To measure light induced phase responses in the *per2::luc* rhythm, a continuous sine wave was modelled over the unperturbed rhythm prior to treatment and used to extrapolate the theoretical phase of the unperturbed fibroblast rhythm. Assigning the peaks and troughs as reference markers, the phase shift was deduced as the time lag between actual bioluminescence rhythm and projected sine wave following light treatment. The phase shifts were plotted as a function of the circadian time at which the light pulse was delivered.

2.25 Methods for processing rhythm data

The raw data were exported to Microsoft Excel (Microsoft) where analysis of rhythm parameters was performed. Prior to analysis, the 24 hours running average was deducted from the raw data to filter out baseline deviations in the *per2::luc* rhythm. Furthermore, the detrended data were averaged over 2 hours to filter out high frequency fluctuations in bioluminescence signal.

2.26 Phase shift and period analysis

To measure light induced phase responses in the *per2::luc* rhythm, a continuous sine wave was modelled over the unperturbed rhythm prior to treatment. The sine wave was used to extrapolate the theoretical phase of the unperturbed fibroblast rhythm. Assigning the peaks and troughs as reference markers, the phase shift was scored as the temporal difference between the sine wave and the processed rhythm data following light treatment. The phase shifts were plotted as a function of the circadian time at which the light pulse was delivered. Period duration of bioluminescence oscillations was measured by calculating the time lag

between consecutive phase markers (peaks and troughs). The oscillatory rhythm during which the light pulse occurred was thus measured and subtracted from the average free-running period to capture immediate light induced period changes. In addition, period changes were also measured in the subsequent oscillatory cycle to assess latent changes.

2.27 Amplitude analysis

The amplitude of the *per2::luc* oscillation was measured as the peak to trough difference from the processed rhythm data. Relative amplitude changes were calculated as the percentage difference in amplitude between the oscillation following light treatment and the 2nd (unperturbed) oscillation of the recorded rhythm. Changes in amplitude were plotted as a function of the circadian time at which the light pulse was delivered. The toughs and peaks of the fibroblast rhythm were assigned CT0 and CT12 respectively.

2.28 Bioluminescence recordings for PER2::LUC RPE explant cultures and primary cultured cells

Mice which harboured the PER2::LUC reporter were culled by cervical dislocation and the eyes enucleated as described above. Upon dissection of the eye, the lens and retina was gently removed with a fine paintbrush and the remaining eye cup was flattened with radial slits on a Millicell-CM low height culture insert (Millipore, USA) within a 35 mm culture dish (corning) containing 1 ml recording medium supplemented with 200 µM beetle. The culture dish was sealed air-tight with a 40 mm coverslip (VWR international) and high vacuum grease (Dow Corning).

All RPE samples, including explant cultures and confluent P0 primary RPE cells were recorded from the lumicycle (Actimetrics) housed in a light tight incubator at 37°C. The average photon count was sampled for 75 seconds per sample. To change the recording medium, the samples were removed from the lumicycle and transferred to a Class I tissue culture hood. The coverslip was lifted from the culture dish and the old medium was removed with a P1000 pipette (Gilson). 1 ml fresh medium was placed into the culture dish and resealed with the original coverslip and the culture dish protected from light, and returned to their respective wells in the lumicycle.

2. Materials and methods

2.29 Bioluminescence imaging for PER2::LUC RPE explant cultures

RPE explants were prepared and cultured as mentioned above, and recorded in the lumicycle for free-running PER2:LUC expression. The tissue and transwell insert were transferred to a glass bottom culture dish (Sigma Aldrich) containing 1.2 ml recording medium, and re-sealed with the original coverslip. The sample was placed under the microscope and focussed onto the x20 lens firstly with brightfield microscopy. Bioluminescence imaging was performed using a self-contained Olympus luminoview LV200 luminescence microscopy system (Olympus Japan) fitted with a cooled Hamamatsu ImageEM C9100-13 EM-CCD camera and a 20 x 0.4 NA Plan Apo objective (Olympus, Japan). Time-lapse images were captured with an exposure time of 30 minute per frame over for 8 days consecutively at 37^{o}C in darkness and transferred to IMAGEJ software (National Institute of Health, USA) for analysis.

3. Developing a selective signalling interface for JellyOp

3.1 Introduction

A combination of pharmacological and genetic techniques has been highly successful in enhancing spatial and temporal control of GPCR signalling in *in vivo* models. In particular, site-directed mutagenesis of functional amino acid motifs have enabled modifications in GPCR characteristics such as ligand sensitivity, selectivity for G protein subtypes and signalling kinetics (Scearce-Levie et al. 2005, Chang et al. 2007). Prime examples are Engineered receptors, known as 'Receptors Activated Solely by Synthetic Ligands' (RASSLs) and 'Designer Receptors Exclusively Activated by a Designer Drugs (DREADDs), which allow for the study if GPCRs in *in vivo* models, without the confounding influences of endogenous ligands, multiple receptor subtypes and cell types (Alvarez-Curto et al. 2011, Nakajima and Wess. 2012).

Optical control of signalling molecules is currently accessible through the targeted expression of optogenetic manipulators such as opsin photopigments (Melyan et al. 2005, Bailes et al 2012). These techniques offer a more sophisticated method of cellular manipulation over pharmacological or electrical stimulation. Similar to RASSLs and DREADDs, optogenetic manipulators provide the opportunity to further understand the relationship between a single receptor signalling pathway and a specific physiological response. However, these tools do not require the use of multiple ligands that might have differential effects on the signal and the regulation of receptors (Deisseroth. 2011)

Optogenetic tools have been successfully adapted from microbial opsins and light sensitive ion channels, the most prominent in neuronal systems being the light-sensitive channelrhodopsin-2 (Nagel et al. 2003). In response to light stimulation on a millisecond time scale, these channels produce an ion flux, which modulates the membrane potential of the host cell, and is thus suitable for targeting excitable cells such as neurons with unprecedented temporal control (Fenno et al. 2011). Yet, most of the perturbations described with light gated ion channels lack the signalling specificity required to manipulate individual intracellular pathways and are therefore not always a relevant tool for dissecting the functional roles of a GPCR. In contrast, optogenetic tools based on eukaryotic opsins transduce light through G proteins, and thus compatible for interrogation of specific intracellular cascades (Porter et al. 2012).

3. Developing a selective signalling interface for JellyOp

Several studies have shown that heterologously expressed opsin photopigments confer light sensitivity to host cells by activating G proteins (Giesbers et al. 2008, Cao et al. 2012, Gutierrez et al. 2011). Opsins such as vertebrate rhodopsin have already been used to overcome the spatiotemporal limits of ligand pharmacology in *in-vivo* models (Cao et al. 2012, Gutierrez et al. 2011). Several groups have adapted naturally occurring and chimeric GPCRs for this purpose. $G\alpha_{i/o}$ studies have relied on vertebrate and bovine rhodopsin (Cao et al. 2012, Gutierrez et al. 2011, Oh et al. 2012) whereas mammalian melanopsin and invertebrate rhodopsin have also been utilised for initiating inositol and calcium signalling pathways in various mammalian cells from RPE cells to rat hippocampal neurons (Zemelman et al. 2002, Giesbers et al. 2008).

Chimeric GPCR based optogenetic tools have been synthesised by fusing transmembrane regions and extracellular domains derived from bovine rhodopsin, and intracellular loops of G protein coupled receptors to mimic natural GPCR signalling functions (Kim et al. 2005). The first chimeras were based on bovine rhodopsin and hamster β2 adrenergic receptor which enabled optical control of $G\alpha_s$. The optogenetic potential of these chimeras *in vivo* was first demonstrated by Airan et al. 2009 who utilised chimeric rhodopsin-α1 adrenergic and rhodopsin β2 adrenergic OptoXRs to control calcium and cAMP signalling respectively in neurons.

A naturally occurring $G\alpha_s$ coupled opsin pigment in the box jellyfish *Carybdea rostonii* has also demonstrated great potential as an optogenetic tool (Koyanagi et al. 2008, Bailes et al. 2009). When purified and reconstituted with 11-*cis*-retinal, JellyOp is spectrally tuned to 500 nM lambda max, which allows for convenient excitation with blue-green light. Studies on the functional expression of this opsin in mammalian cells have revealed robust control of $G\alpha_s$ protein signalling and also unprecedented resistance to bleaching (Bailes et al. 2012). The same authors were the first to compare the signalling properties of JellyOp and human Rhodopsin-β2 adrenergic OptoXRs in cell based cAMP reporter assays, and subsequently demonstrated superior signalling activity from JellyOp with the same light stimulus (Bailes et al. 2012). Unlike the β2-OptoXr, exposing JellyOp to repetitive light flashes did not compromise the response amplitude even after 15 minutes of stimulation. Based on these *in vitro* assays, the non-bleach feature of JellyOp may imply that it is bistable. Although direct evidence of this remains lacking, it is noteworthy that JellyOp, as the opsin, also possesses the equivalent Glu 181 counterion, a negatively charged amino acid residue that stabilizes a positive charge on the retinal chromophore. Furthermore, Terakita et al. 2004 have shown that the counterion Glu181 and is strongly associated with invertebrate bistable opsins.

3. Developing a selective signalling interface for JellyOp

The study of β-arrestin signalling has been of great interest in GPCR research; in addition to their role in terminating G protein signalling and GPCR internalisation, β-arrestins serve as signal transducers coupling the receptor to numerous signalling proteins including extracellular signal-regulated, c-Src, and Akt kinases (Cervantes et al. 2010, Rapacciuolo et al. 2003). In addition, arrestins have been shown to mediate a wide range of cellular processes including proliferation, stress response and insulin secretion (Kong et al. 2010, Hara et al. 2011, Butcher et al. 2012, Shenoy and Lefkowitz. 2011).

Receptor engineering has also been successful in isolating G protein independent signalling pathways, and thus enabling the study of β-arrestin signalling without interference from G proteins. Several groups have aimed at elucidating the physiological roles of B-arrestin dependent signalling, by developing GPCRs that can exclusively recruit arrestins following activation by agonists. Shenoy et al. 2006 developed and validated a β2 adrenergic receptor with three amino acid substitutions T68F, Y132G and Y219A (β2AR TYY) that rendered the receptor incapable of G protein recruitment, but could still couple to arrestins upon agonist stimulation. Other groups including Nakajima and Wess et al 2012 have engineered a M3 muscarinic receptor-based DREADD (Rq(R165L)) which exclusively interacted with arrestins-2 and 3 upon activation by CNO, without coupling to cognate $G\alpha_q$ proteins. This signalling interface was achieved with a single amino acid substitution of R165L within the DRY motif conserved in Class A GPCRs (Rq(R165L)).

Thus, a combination of optogenetics and receptor engineering for selective signalling may prove to be highly useful in dissecting the roles of GPCR mediated signalling pathways in mammalian physiology (Armbruster et al. 2007, Guettier et al. 2009). The mammalian circadian system is a mechanism which forms an internal representation of local time, and enables an organism to anticipate environmental transitions and perform biological activities at optimal times. GPCR signalling cascades play a critical role in mediating external influences on multiple clock parameters including amplitude, phase and free-running period. Indeed, numerous pharmacological studies have shown that cAMP is an intrinsic component of the molecular clockwork operating both as inputs as well as output of the clock (O'Neill and Reddy 2012, O'Neill and et al. 2008). Given that JellyOp exhibits robust and reproducible G protein

signalling capacities, it is well placed as an optogenetic tool for my investigations into the role of GPCR mediated cAMP signalling in circadian organisation. My initial aim was thus to develop optogenetic tools based on JellyOp to investigate cAMP dependent mechanisms of circadian organisation, and evaluate whether circadian influences of temporally controlled JellyOp mediated cAMP correlate with previous pharmacological studies.

Given the recently established functional roles of β-arrestin in mediating GPCR physiology, I sought to investigate whether these G protein independent pathways could also impact on the mammalian circadian system. Given the $G\alpha_s$ coupling capacities of JellyOp, i hypothesised that this was principally due to individual amino acid residues in the intracellular loops of the receptor that were involved in direct interactions with downstream effector G proteins, and that substitution of those residues would abolish G protein interactions. To address this hypothesis I first sought to identify these functional amino acids, by comparing the amino acid sequence of JellyOp with the human β2- Adrenergic receptor, a well characterised $G\alpha_s$ coupled GPCR. Based on previous mutagenic studies on the β2- adrenergic receptor, identify of several amino acids involved in G protein interactions have been revealed. If present in JellyOp amino acid sequence, it is plausible that they also contribute to interactions between JellyOp and G proteins.

I thus sought to apply mutagenic techniques to JellyOp to generate a mutant variant that was unable to interact with G proteins such that activation would promote G protein independent interactions. For validation of mutant signalling properties, the functional expression of all engineered structural variants was characterised with respect to principle secondary messengers such as cAMP, calcium and MAPK. To further examine whether JellyOp signalled via a G protein independent pathway, cell based assays were performed to visualise recruitment of β-arrestin to photoactivated JellyOp. In addition, I conducted mutagenic studies to develop a mutant form of JellyOp which lacked a C-terminus, a site which has previously implicated in β-arrestin recruitment and probed the physiological consequences of truncation with respect to kinetics of light induced $G\alpha_s$ coupling.

3. Developing a selective signalling interface for JellyOp

Another important aim was to discern whether functional expression of JellyOp and structural variants were compatible in rat1 fibroblasts, as this would enable me to generate a light entrainable cell based model of the mammalian clock. The hypothesis for this study was that JellyOp would be able trigger the $G\alpha_s$ pathway in rat1 fibroblasts in light dependent manner, as previously observed in HEK283 cells (Bailes et al. 2012), and elicit induction of intracellular cAMP whereas a $G\alpha_s$ decoupled JellyOp variant would be unable to induce cAMP pathway. To this end, I stably expressed JellyOp and mutant variants in rat1 fibroblasts to validate the functional expression of each opsin variant by testing whether JellyOp signalling was compatible in mammalian oscillatory cells.

3. Developing a selective signalling interface for JellyOp

3. Developing a selective signalling interface for JellyOp

3.2 Materials and methods

3.2.1 Cloning and mutagenesis of JellyOp

The coding sequence of full length JellyOp was tagged downstream with extra bases to encode a 9 amino acid epitope of C-terminal bovine rhodopsin (1D4) (designed by Dr Helena Bailes and manufactured by Genscript Corp, USA). The JellyOp-1D4 construct was subcloned from the original pUC57 vector into a bicistronic pIRES-AcGFP expression vector (kindly donated by Dr Jim Bellingham, University of Manchester). All primers for site directed mutagenesis of JellyOp were purchased from Sigma Aldrich. The full sequence of each primer is displayed in Chapter 2, Materials and Methods, chapter 2.2), Mutagenesis of each amino acid was carried out within the pIRES-JellyOp-1D4-GFP vector using QuikChange® Lightning Site-Directed Mutagenesis Kit (Agilent Technologies, USA) according to the manufacturer's instructions, and confirmed by DNA sequencing (DNA Sequencing Facility, University of Manchester).

3.2.2 Maintenance of *per2::luc* rat1 fibroblast and FLP-IN™-293 Glosensor™20F cell lines

rat1 fibroblasts which express a minimal promoter of the mouse *period2 (per2)* gene fused to a luciferase gene, (kindly donated by Qing-Jun Meng, University of Manchester) were selectively maintained in supplemented Dulbecco's modified Eagle's medium (4,500 mg/l DMEM, D-glucose, sodium pyruvate and L-glutamine, 10 % foetal bovine serum, 1 % penicillin and streptomycin) with selective antibiotics including 100 µg/ml hygromycin (InvivoGen) in a 37°C and 5 % CO_2 incubator (RS Biotech, UK). The pIRES-JellyOp-1D4-AcGFP vector was linearised with ApaL1 (Life Technologies) at 37°C overnight. Following plasmid purification with QIAGEN Plasmid Mini Kit (Qiagen), the pIRES-Ac-JellyOp-GFP was transfected into *per2::luc* RAT1 fibroblasts with Lipofectamine 2000 (Life Technologies) as above and selected with 400 µg/ml neomycin (InvivoGen). Stable isogenic transfectants were then isolated with cloning rings (Sigma Aldrich). Monoclonal stable JellyOp and F139A JellyOp expressing cell lines were selectively maintained with 100 µg/ml hygromycin, and 400 µg/ml G418 (InvivoGen) under dim red light. All fibroblast cell lines were passaged at ratio of 1:6 every 3-4 days under sterile conditions.

Stable FLP-IN™-293 Glosensor™20F HEK cells and FLP-IN™-293 Glosensor™20F JellyOp HEK cells were kindly donated by Dr Helena Bailes, University of Manchester. FLP-IN™-293 Glosensor™20F HEK cell lines were maintained in supplemented Dulbecco's modified Eagle's medium (4,500 mg/l DMEM, D-glucose, sodium pyruvate and L-glutamine, 10 % foetal bovine serum, 1 % penicillin and streptomycin) with selective antibiotics including 100 µg/ml hygromycin (InvivoGen, USA) and 100 µg/ml blasticidin (InvivoGen) in a 37°C and 5 % CO_2 incubator (RS Biotech, UK). Similarly polyclonal stable FLP-IN™-293 Glosensor™20F JellyOp HEK cell lines were selectively maintained with 100 µg/ml hygromycin, 100 µg/ml blasticidin and 400 µg/ml G418 (InvivoGen) under dim red light. Cells were passaged at least once a week under sterile conditions.

For transient expression of JellyOp structural variants in FLP-IN™-293 Glosensor™20F, 5 x 10^4 FLP-IN™-293 Glosensor™20F cells were plated in duplicate in solid white 96 well plates, and transfected with 0.2 µg pIRES plasmid vectors bearing the various mutagenic JellyOp constructs as described above, using Lipofectamine 2000 (Life Technologies) according to the manufacturer's instructions for 6 hours. Cells were incubated in L-15 (Life Technologies) supplemented with 10 % foetal calf serum for 16 hours and 10 µM 9-*cis*-retinal at 37°C and 5 % CO_2. Platereader recordings were conducted as described in the previous paragraph.

3.2.3 Assays for stable transgene expression in rat1 fibroblasts

For the GFP reporter assay, 4 x 10^4 *per2::luc* rat1 fibroblasts from stable lines were seeded as triplicates into a white, clear bottom 96 well plate (Greiner Bio-one) overnight. Following 200 50 Hz flashes of 485 nm light, 520-30 nm fluorescence was recorded at 27°C through a topread 2 mm lens in a FLUOstar OPTIMA platereader (BMG Labtech) at a gain of 2000. The data were collected with Optima data collection software (BMG Labtech). The averaged background autofluorescence from the culture media and 96-well plate was subtracted from total average fluorescence values to obtain cellular fluorescence from each monoclonal line. Statistical significance was calculated with a one way ANOVA with Bonferroni's post-hoc test using GraphPad Prism (GraphPad Software).

JellyOp expression was determined with ICC techniques. Under dim red light, 10^5 *per2::luc* rat1 fibroblasts or FLP-IN™-293 Glosensor™20F JellyOp HEK cells were seeded onto glass coverslips (VWR International) in a 24 well plate (Corning) overnight.

The cells were rinsed in DPBS (2.69 mM KCl, 1.47 mM KH_2PO_4, 136.8 mM NaCl, 8 mM NaH_2PO_4, Sigma Aldrich) and incubated in 1 ml 4 % paraformaldyhyde (Sigma Aldrich) in DPBS for 2 hours at room temperature, and washed 3 x 5 minutes. The fixed cells were incubated in 2 % glycine (Fisher Scientific, USA) in DPBS for 5 minutes, washed 3 x 5 minutes in DPBS and blocked in 2 % normal goat serum (Vector laboratories, USA), 5 % BSA (Sera Laboratories International, UK), 0.1 % TX-100 (Sigma Aldrich) in DPBS for 30 minutes at room temperature. Autofluorescence was quenched with a 5 minutes incubation of cells in 0.25 % NH_4Cl (Sigma Aldrich) in DPBS, followed by 3 x 5 minutes washes in DPBS. Incubation in primary monoclonal mouse anti-rhodopsin antibody (1:500 in 2 % BSA/DPBS, Affinity BioReagents, USA) was performed for 1 hour at room temperature, followed by 3 x 5 minutes washes of 0.1 % Tween-20 (Sigma Aldrich) in DPBS. Goat anti-mouse antibody conjugated to Alexa 555 Fluor® (1:1000 in 0.1 % Tween-20/ DPBS, Molecular Probes) was added to the cells for 90 minutes, followed by 3 x 50 minutes washes of 0.1 % Tween-20 in DPBS. The cells were post-fixed with 4 % PFA in DPBS for 30 minutes at room temperature and coverslips were mounted onto poly-Lysine coated glass slides (VWR International, USA) with DAPI containing mounting medium (Vector Laboratories) in the dark overnight. The cells were examined on an Olympus BX51 fluorescence microscope (Olympus, Japan) and images were acquired with on a Coolsnap ES camera (Photometrics, USA) using MetaVue Imaging Software (Molecular Devices, USA).

Western blotting was also employed to identify the molecular mass of JellyOp. $3x10^6$ cells were plated into two wells of a 6 well plate overnight. For protein extraction, the cells were rinsed in ice cold DPBS and lysed with 150 µl ice cold RIPA buffer (1 % sodium deoxycholate (Sigma Aldrich), 0.1 % SDS (Fisher Scientific), 1 % Triton X-100, 10 mM Tris-HCl (Sigma Aldrich) pH6.8, 140 mM NaCl (Sigma Aldrich) in dH_2O) with PhosSTOP Phosphatase Inhibitor Cocktail Tablet (Roche) and Complete Phosphatase Inhbitor Cocktail Tablets. The cell lysates were collected with cell scrapers into eppendorf tubes (Starlab, USA) gently triturated using a 1 ml syringe (BD Biosciences, USA) with reducing gauge needles (25G x 5/8”, 23G x 1.25”, 21G x 2”, 19G x 15”, BD Biosciences). Samples were stored at -80°C freezer until needed for western blotting. 20 µg of protein made up in 20 µl Milli Q and heated on a 100°C dry block with 10 µl 2x Laemmli sample buffer (2.5 % SDS (Fisher Scientific), 125 mM pH 6.8 Tris-HCl (Sigma Aldrich), 20 % glycerol (Fisher Scientific), 0.5 % β-mercaptoethanol (Sigma Aldrich) in dH_2O) for 5 minutes. 30 µl samples were loaded into individual wells of a NuPAGE® Novex® 4-12 % Bis-Tris Gels (Life Technologies) alongside 10 µl Protein plus ladder (Life Technologies) and run with 1x MOPS running buffer (100 mM MOPS (Fisher Scientific), 100 mM Tris-base (Sigma Aldrich), 7 µM SDS (Sigma Aldrich), 2 µM EDTA (Sigma Aldrich) at 100 V for 90 minutes.

The protein was transferred to Amersham Hybond™-P polyvinylidene difluoride (PVDF) membrane (GE healthcare, USA) in 1x transfer buffer (38.7 mM Glycine (ThermoFisher Scientific, USA), 48 mM Tris-base, 1.28 mM SDS, 20 % Methanol) for 90 minutes at 90 V. The membrane was washed with 1x TBST (43.8 g/ml NaCl and 3.025 g/ml Tris base, 1 % Tween 20 in dH_2O) for 3x 5 minutes and rinsed in amidoh black (ThermoFisher Scientific) to confirm protein sample transfer. The membrane was blocked in 5 % Marvel milk powder in TBS/T for 1 hour at RT. Membrane was incubated with primary anti-rhodopsin mouse monoclonal antibody (1:500 in blocking buffer) at 4ºC overnight on a shaker at 100rpm and washed 3x 10 minutes in 1x TBST. Membrane was incubated with 1:1000 goat anti-mouse in blocking buffer at room temperature for 1 hour, followed by 3 washes in 1xTBST. The membrane was soaked in 2 ml SuperSignal West Dura Extended Duration Substrate (ThermoFisher Scientific) for 2 minutes, then developed on Kodak Biomax light film (Sigma Aldrich).

3.2.4 Bioluminescent Glosensor™20F recordings and light stimulation

5 x 10^4 FLP-IN™-293 Glosensor™20F cells were plated as triplicates in solid white 96 well plates (Greiner BioOne) for bioluminescence recordings. To allow for measurable expression of the Glosensor™20F 20 cAMP biosensor, cells were then incubated for another 16 hours in the presence of 300 ng/ml tetracycline and 10 µM 9-*cis*- retinaldehyde, Sigma Aldrich) in CO_2 independent medium without phenol red, L-15, (Life Technologies), with 10 % foetal calf serum. Beetle luciferin (Promega) reconstituted in 10 mM HEPES buffer (Sigma Aldrich) was added for a final concentration of 2 mM luciferin to each well and allowed to equilibrate at 37°C for 2 hours. Raw luminescence units in cells were recorded at 37°C with 1 second resolution at 30 second intervals with a topread 3 mm lens in a BMG Labtech Fluostar Optima plate reader, at a gain of 3600. Following 30 minutes equilibration inside the platereader, cells were subjected to light flashes delivered from a camera flash bulb (Jessops). Luminescence recordings were analysed with Optima software (BMG), Microsoft Office Excel (2010, Microsoft) and GraphPad Prism 4 (GraphPad). All data from each well were normalised to baseline measurements captured prior to the initial photo-stimulation.

For the MDL-12330 A (MDL) titration assays, MDL was delivered to cells in each well at a final concentration of 5, 10, 25, 50, 100, and 200 nM after 15 minutes of platereader equilibration. Photoactivation by camera bulb and platereader recordings were performed as described above.

To capture luciferase bioluminescence from FLP-IN™-293 cells continuously over a period of over 10 hours within the platereader, a script was programmed by Krystopher Procyk and Dr Helena Bailes (University of Manchester) to automate JellyOp photostimulation with the internal xenon light source. Full details of the protocol is displayed in Chapter 2, Materials and Methods, chapter 2.21)

4x 10^4 FLP-IN™-293 Glosensor™20F cells were plated into three wells on a 96 well plate, of which two were transfected with pIRES vectors bearing JellyOp or JellyOp Δ COOH, whilst the third was mock transfected. Bioluminescence was recorded as described above at 37°C. All data were recorded on Optima Data Analysis (BMG Labtech) and analysed in Microsoft Excel 2007 (Microsoft, USA).

3.2.5 ELISA based quantification of cAMP in FLP-IN™-293 Glosensor™20F cells transiently expressing JellyOp and F139A JellyOp

5x10^4 FLP-IN™-293 Glosensor™20F cells and FLP-IN™-293 Glosensor™20F JellyOp cells were plated in 12 well plates overnight at 37°C and 5 % CO_2 , and then incubated in DMEM lacking phenol red, but supplemented with 10 % foetal calf serum and 10 µM 9-*cis*-retinal for 2 hours. Dark control cells were lysed with 300 µl 0.1 µM HCl (Sigma Aldrich) in the dark for 10 minutes at room temperature whereas experimental samples were flashed with light from the camera bulb and lysed at 2 minutes post-stimulation. Cell lysates were collected from the culture dishes using cell scrapers (Greiner BioOne) and centrifuged at 600 xg for 10 minutes.

To determine the cAMP increase in light exposed cells, enzyme-linked immunoassay was conducted using a direct cAMP Enzyme Immunoassay Kit (Sigma Aldrich) according to the manufacturer's instructions. Optical measurements were conducted using a platereader at 405 nm. The protein content was determined with Fluka protein quantification kit (Sigma Aldrich) according to the manufacturer's instructions and optical measurements performed at 455 nm. The same protocol was used to measure light induced cAMP levels between stable JellyOp and F139A JellyOp expressing fibroblasts.

3.2.6 Bioluminescence recordings of HEK cells transiently expressing Glosensor™22F and opsin photopigments

For quantifying light induced $G\alpha_i$ signalling cascades, 5 x 10^4 HEK293 cells were plated in triplicate in solid white 96 well plates, and co-transfected with 0.2 µg pcDNA5/ FRT/TO Glosensor™ 22F and 0.2 µg pcDNA3 –JellyOp, pcDNA3 –F139A JellyOp, pcDNA3 –human Melanopsin or pcDNA3 –human Rhodopsin, using 0.5 µl Lipofectamine 2000 (Life Technologies) according to the manufacturer's instructions for 6 hours. Cells were incubated in L-15 (Life Technologies) supplemented with 10 % foetal calf serum for 16 hours and 10 µM 9-*cis*-retinal at 37°C and 5 % CO_2. Beetle luciferin was reconstituted in 10mM HEPES buffer was added for a final concentration of 2 mM to each well and allowed to equilibrate at room temperature for 3 hours. Cells were treated with 3 µM forskolin for 2 minutes before exposure to a flash of light. Luminescence was measured with a topread 3 mm lens in a Fluostar Optima plate reader (BMG Labtech) at a gain of 3600, 1 second, every 20 seconds intervals.

3.2.7 Bioluminescence recordings of HEK293 cells transiently co-expressing aequorin and opsin photopigments

Calcium mobilisation was detected using an encoded mitochondrially targeted aequorin (mtAeq) reporter, adapted from Bailes and Lucas (2013) (See Appendix 2). 5x10^4 HEK293 cells in each well of solid white 96 well plates were co-transfected with 0.2 µg pcDNA5/FRT/TO mtAeq and pcDNA3-JellyOp or pcDNA3-melanopsin using Lipofectamine 2000 (Life Technologies) in serum-free Dulbecco's modified Eagle's medium (Sigma Aldrich) for 6 hours. Cells were then incubated for 16 hours at 37°C in the presence of 300 ng/ml tetracycline and 10 µM 9-*cis*-retinal (Sigma Aldrich) in CO_2 independent medium lacking phenol red (L15), but supplemented with 10% foetal calf serum. Coelentrazine H (Biotium, USA) reconstituted in 10 mM HEPES buffer was added for a final concentration of 2 mM coelentrazine to each well and allowed to equilibrate at room temperature for 3 hours. Bioluminescence from each well was recorded at room temperature with a topread 3 mm lens in a BMG Labtech Fluostar Optima plate reader at a gain of 3600, for 0.5 seconds, at 2 second intervals.

3.2.8 Western blotting for phosphorylated MAPK and total MAPK in FLP-IN™-293 Glosensor™20F cells and rat1 fibroblasts

3x 10^6 FLP-IN™-293 Glosensor™20F cells or FLP-IN™-293 Glosensor™20F JellyOp cells were plated into two 25cm^2 cell culture flasks, serum starved in 0.5 % foetal calf serum for 24 hours and further incubated with L15 with 0.5 % foetal calf serum and 10 µM 9-*cis*-retinal for 3 hours. 5x 10^5 *per2::luc* fibroblasts expressing wildtype JellyOp, F139A JellyOp or lacking photopigments were plated in 6 well plates, and similarly serum starved and incubated with 10 µM 9-*cis*-retinal. White light from a halogen light source (Fiber-Lite® DC950, Dolan-Jenner Industries, USA) was fed into the incubator through a liquid light guide (Knight photonics) with a UV and infrared cut-off. Light-treated cells were subject to 2 or 15 minutes exposure of light at 37°C with irradiance levels of 28.40 mW/cm^2. For protein extraction, the cells were rinsed in ice cold DPBS and 150 µl ice cold RIPA buffer per flask or well (1 % sodium deoxycholate (Sigma Aldrich), 0.1 % SDS (Thermo Fisher Scientific), 1 % Triton X-100, 10 mM Tris-HCl (Sigma Aldrich) pH 6.8, 140 mM NaCl (Sigma Aldrich) in dH_2O) with PhosSTOP Phosphatase Inhbitor Cocktail Tablet (Roche) and Complete Phosphatase Inhbitor Cocktail Tablets. The cell lysates were collected with cell scrapers into eppendorf tubes (Starlab) gently triturated using a 1 ml syringe (BD Biosciences) with reducing gauge needles (25G x 5/8", 23G x 1.25", 21G x 2", 19G x 15", BD Biosciences). Samples were stored at -80°C freezer until needed for western blotting.

20 µg of protein made up in 20µl Milli Q and heated on a 100°C dry block with 10 µl 2x Laemmli sample buffer (2.5 % SDS (Fisher Scientific), 125 mM pH 6.8 Tris-HCl (Sigma Aldrich), 20 % glycerol (Thermo Fisher Scientific), 0.5 % β-mercaptoethanol (Sigma Aldrich) in dH_2O) for 5 minutes. 30 µl samples were loaded into individual wells of a 4-12 % Life Technologies Bis-Tris gel (Life Technologies) alongside 10 µl Protein plus ladder and run with 1x MOPS running buffer (100mM MOPS (Thermo Fisher Scientific), 100 mM Tris-base (Sigma Aldrich), 7 µM SDS (Sigma Aldrich), 2 µM EDTA (Sigma Aldrich) at 100 V for 90 minutes. The protein was transferred to Amersham Hybond™-P polyvinylidene difluoride (PVDF) membrane (GE healthcare) in 1x transfer buffer (38.7 mM Glycine (Thermo Fisher Scientific), 48 mM Tris-base, 1.28 mM SDS, 20 % Methanol) for 90 minutes at 90 V. The membrane was washed with 1x TBST (43.8 g/ml NaCl and 3.025 g/ml Tris-base, 1 % Tween 20 in dH_2O) for 3x 5 minutes and rinsed in amidoh black to confirm protein sample transfer. The membrane was blocked in 5 % Marvel milk powder (Premier Foods, UK) in TBS/T for 1 hour at RT. Membrane was incubated with 1:1000 rabbit monoclonal phospho-ERK Ig (New England Biolabs, UK) at 4°C overnight on a shaker at 100 rpm.

After 3 x 10 minutes washes in 1x TBST, membrane was incubated with 1:1000 goat anti-rabbit Ig conjugated horse radish perioxidase (Life Technologies) in blocking buffer at room temperature for 1 hour. After another 3 washes in 1xTBST, the membrane was soaked in 2 ml SuperSignal West Dura Extended Duration Substrate (ThermoFisher Scientific) for 2 minutes, then developed on Kodak Biomax light film (Sigma Aldrich).

The membrane was stripped at 50°C for 30 minutes in 100 mM β -mercaptoethanol (Sigma Aldrich), 62.5 mM Tris-HCl, 2 g/ml SDS in dH_2O followed by washes in TBS/T. The membrane was blocked in 5 % Marvel milk powder in TBS/T for 1 hour at room temperature, and then incubated in 1:1000 rabbit monoclonal ERK Ig (New England Biolabs, UK) at 4°C overnight on a shaker followed by in 3x 10 minute washes in 1x TBST. Membrane was then incubated with 1:1000 goat anti-rabbit in blocking buffer at room temperature for 1 hour, followed by 3 washes in 1xTBST. For investigating the effects of MDL on light induced MAPK responses, MDL was delivered to cells in each well at a final concentration of 100 nM at 15 minutes prior to photoactivation.

3.2.9 β -arrestin2-GFP mobilisation assay in HEK cells

Under dim red light, 10^5 FLP-IN™-293 Glosensor™20F or FLP-IN™-293 Glosensor™20F JellyOp HEK cells were seeded onto glass coverslips (VWR International) overnight. All cells were transfected with pcDNA3 vector bearing β-arrestin-2-GFP for 6 hours using lipofectamine 2000 according to the manufacturer's instructions. Cells were incubated in L15 supplemented with 10 % foetal calf serum with 10 µM 9-*cis*-retinal for 16 hours. Dark control cells were fixed in 4 % paraformaldyhyde (Sigma Aldrich) under dim read light, whereas light treated cells were exposed to 30 minutes of bright white light at 28.40 mW/cm^2 at 37°C. For a pharmacological control, 10 µM isoproterenol (Sigma Aldrich) was added to cells in the dark for 30 minutes before fixation in paraformaldehyde and immunolabelling as described above. Images were acquired on a Delta Vision deconvolution microscope (Applied Precision, USA) using a 60 x Plan Apo objective magnification and numerical aperture magnification of 1.42 x with FITC, Texas red and FITC filters. The images were collected using a Coolsnap HQ (Photometrics, USA) camera with a Z optical spacing of 0.35 µm and deconvolved using the Softworx software (Applied Systems).

3. Developing a selective signalling interface for JellyOp

3.3 Results

3.3.1 Sequence alignment between JellyOp and β2-adrenergic receptor reveals conserved amino acid residues implicated in G protein coupling

The principal aim of this investigation was to determine whether JellyOp can be adapted as an optogenetic tool for separable interrogation of intracellular cascades involved in regulation of the mammalian circadian clock. To this end, structural modifications were implemented on intracellular motifs of GPCRs that defined G-protein signalling. Although arrestin biased GPCRs have been previously designed to study β-arrestin signalling, an optogenetic tool is yet to be tested and validated. To this end, I attempted to design structural variants of JellyOp which were unable to couple to G proteins upon photoactivation, but instead could potentially interact with β-arrestin (Figure 3.1 A). I therefore conducted a series of amino acid substitutions to inactivate such motifs implicated in G protein coupling. Several amino acid motifs strongly implicated in G protein activation were conserved between mammalian GPCRs and JellyOp including Phenylalanine 139, Tyrosine 132 and Tyrosine 219 (Moro et al. 1988, Shenoy et al. 2006). Figure 3.1. B shows cartoons of mutants created, including F139A JellyOp, JellyOp YY, JellyOp YFY and JellyOp KYFY.

3. Developing a selective signalling interface for JellyOp

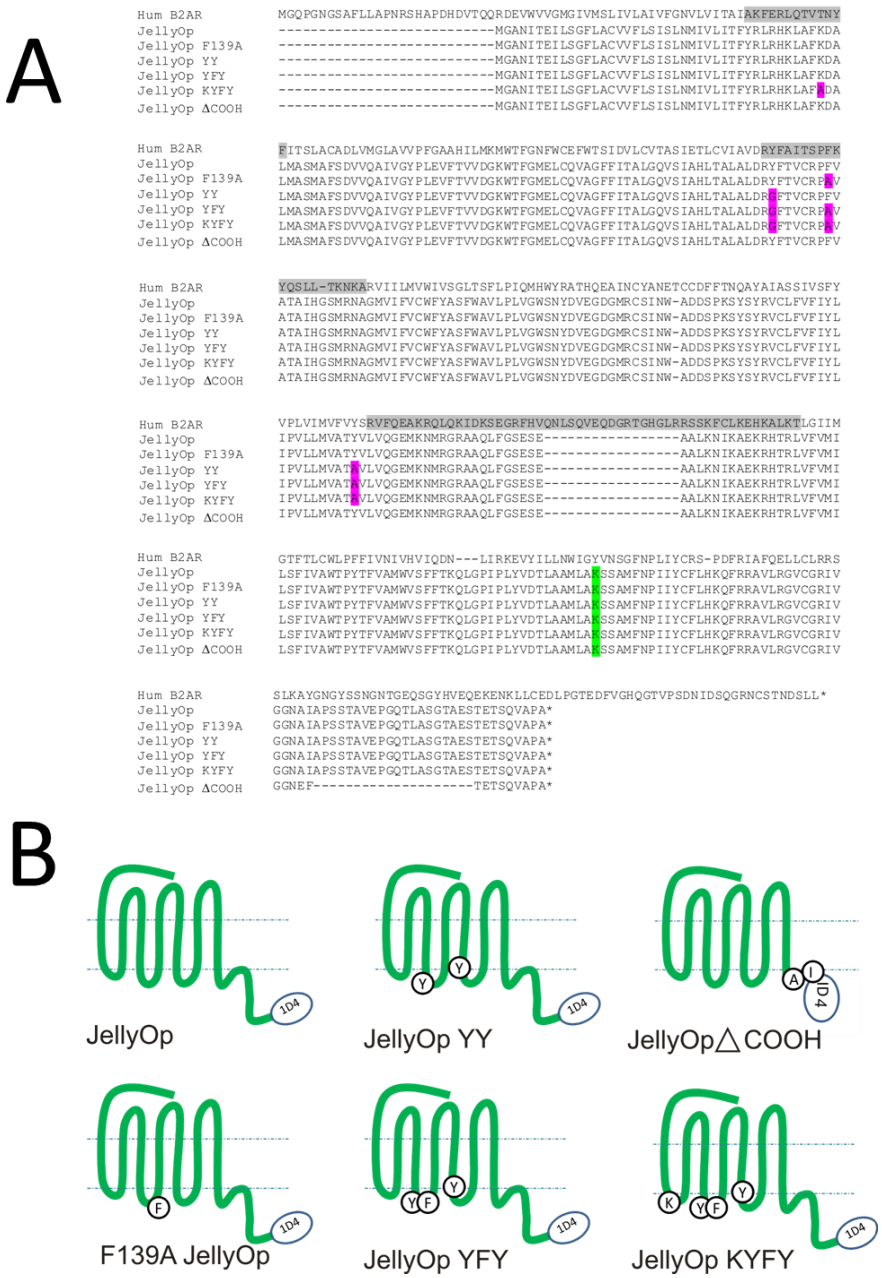

Figure 3.1 JellyOp based optogenetic tools for selective control of signal transduction

(A) An amino acid sequence alignment of JellyOp (Genbank AB435549) and structural variants including F139A JellyOp, JellyOp Y132G Y219A (JellyOp YY), JellyOp Y132G, F139A, Y219A, (JellyOp YFY), JellyOp K68F, Y132G, F139A, Y219A (JellyOp KYFY) and JellyOp ΔCOOH generated by site directed mutagenesis. The sequence of the human β2 adrenergic receptor (Genbank NM000539.3) was used as a model template for mutagenesis of JellyOp. The intracellular loops of the β2 adrenergic receptor, previously confirmed through structural studies, are highlighted in grey (Rasmussen et al. 2007). The terminal 9 amino acids of bovine rod opsin which forms an epitope tag (1D4) was fused to the Carboxyl terminus of all JellyOp variants used in the study. Furthermore, the lysine residue which forms the Schiff-base linkage with a retinoid chromophore is also highlighted in green. (B) Cartoons of JellyOp structural variants generated by site directed mutagenesis. Mutagenised amino acids are shown for F139A JellyOp, JellyOp YY, JellyOp YFY and JellyOp KYFY. The truncation mutant contains two amino acid substitutions (A354E and I355F), immediately followed by the 1D4 epitope.

3.3.2 Signalling properties of the wildtype JellyOp photopigment

Prior to testing the JellyOp mutants, I sought to establish the signalling properties of wildtype JellyOp photopigment in HEK 293 cells. Phototransduction kinetics were inferred from changes in levels of secondary messengers including cAMP and calcium. A cell-based reporter system was used which produced a bioluminescent readout of intracellular messengers over time in cells whilst minimising photoactivation of the opsin photopigment. For JellyOp photostimulation, a camera light was employed to deliver a flash of bright white light to the cells in between Glosensor™20F signal measurements over time. Following the light pulse, a robust induction in bioluminescence was observed in JellyOp expressing HEK 293 cells which peaked 2.5 minutes with a fold response amplitude of 24.9 ± 2.8 (Figure 3.2 A), and subsequently decayed back to baseline over 2 minutes. According to Bailes et al. 2012, one of the defining properties of JellyOp was its unprecedented resistance to bleach. Subsequently, I conducted a series of 30 light pulses and assayed for Glosensor™20F activity to further investigate this phenomenon. The maximal fold response was observed after 3 minutes light treatment was augmented to 29.8 ± 2.8, after which a gradual linear reduction in signal was observed throughout the course of light treatment to 17.2 ± 2.7. Nonetheless, the persistent elevation in Glosensor™20F activity suggests sustained cAMP responses, and supports the notion that JellyOp is bleach resistant (Bailes et al. 2012).

In HEK 293 cells which lacked JellyOp, transient spikes in baseline bioluminescence were immediately observed after the light pulse. These rapid responses, however, were too fast to reflect induction of cAMP reporter activity, and most likely reflect spontaneous reaction of luciferin to the light. Comparison of the fold response (Figure 3.2 B) or absolute response amplitude (Figure 3.2 C) between the two cell lines showed that only JellyOp expressing cells produced statistically significant responses in terms of Glosensor™20F activity. The ELISA data also complemented the Glosensor™20F assays by showing that optical stimulation yielded significant production of cAMP only in JellyOp expressing cells (Figure 3.2 D). The relevance of JellyOp-$G\alpha_s$ interactions in mediating Glosensor™20F responses was further examined by pre-incubating the cells with 100 µM MDL12330-A (MDL), an inhibitor of adenylate cyclase. It was noted that MDL suppressed light dependent peak fold bioluminescence in JellyOp expressing cells in a dose-dependent manner (Figure 3.2 E and F).

3. Developing a selective signalling interface for JellyOp

Despite the well-established $G\alpha_s$ affinity of JellyOp, I was interested in the functional consequences of heterologous JellyOp expression with respect to $G\alpha_q$ signalling. To investigate light induced calcium responses, I utilised a cellular bioluminescent reporter based on aequorin, a calcium dependent photo protein isolated from the jellyfish *Hydromedus aequorea* and subsequently adapted as a bioluminescent calcium biosensor (Dupriez et al. 2002). Transient co-expression of melanopsin reconstituted with 9-*cis*-retinal and mitochondrial aequorin in HEK 293 cells produced rapid induction of bioluminescence following the light (Figure 3.2. G). Due to the speed of the aequorin activity, the recording protocol was unable to capture the peak response, but rather on falling limb of the luminescence signal from the first read.

Nonetheless, a robust and significant 80 ± 2.7 fold response was captured from the aequorin biosensor in melanopsin expressing cells (Figure 3.2 H). In absence of any opsin photopigment, the baseline luminescence is heavily dampened to small rapid transients, presumably due to the intrinsic light responsiveness of the coelentrazine substrate. Photoactivation of JellyOp expression resulted in a 24.2 ± 8.7 fold induction of luminescence, suggesting a transient increase in intra-mitochondrial and cytosolic calcium levels. Maximal levels of absolute bioluminescence from mitochondrial aequorin were substantially greater with human melanopsin than JellyOp (Figure 3.2.I). Despite this, JellyOp expressing cells was able to produce a statistically significant induction in bioluminescence compared to mock transfected cells.

3. Developing a selective signalling interface for JellyOp

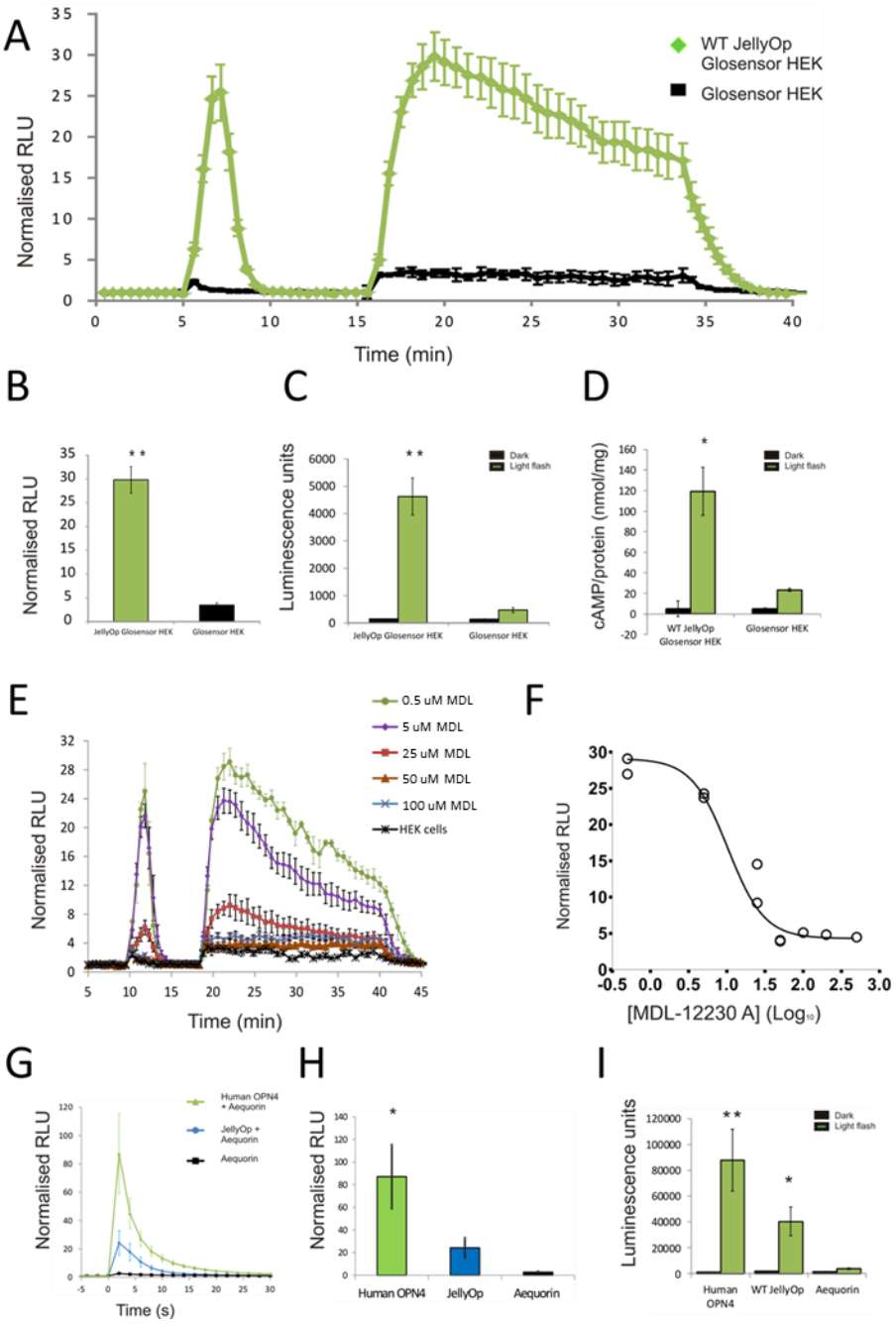

Figure 3.2 Characterisation of wildtype JellyOp phototransduction in HEK cells

(A) Light induced changes in Glosensor™20F luminescence of HEK293 cell line stably expressing JellyOp in the presence of 10 µM 9-*cis*-retinaldehyde. The data represent baseline normalised mean luminescence units ± SEM, from 3 independent repeats. Cells were pulsed with a single light flash at 5 minutes and 30 light flashes (at approximately 30 seconds intervals) from 16 to 34 minutes. Quantification of (B) normalised maximal response amplitude and (C) absolute response amplitude for the first light flash revealed that only the JellyOp expressing HEK cells produced a significant induction in reporter activity, based on one-way ANOVA with Dunnett's post hoc comparisons to *per2::luc* fibroblasts (**p<0.01). (D) A cAMP immunoassay shows that cAMP levels (normalized to total protein content) are elevated significantly within 2 minutes of light onset in JellyOp expressing HEK cells. Data correspond to the mean ± SEM from three independent experimental repeats, each performed in duplicate (based on an unpaired t-test with Welches' correction, *p<0.05). (E) When pre-treated with MDL 12330-A, maximal Glosensor™20F bioluminescence in JellyOp expressing HEK cells as suppressed in a dose dependent manner. Data represent mean luminescence units ± SEM from triplicate cell samples in a single experiment. (F) A dose response curve of MDL mediated suppression of JellyOp responses. Data are expressed as mean luminescence of individual replicates. (G) Real time analysis of a calcium influx into the mitochondria using Aequorin targeted to the mitochondrial matrix. Aequorin luminescence was captured in HEK293 cells transiently co-expressing aequorin reconstituted in coelentrazine H, and indicated opsin photopigment with 10 µM 9-*cis*-retinaldehyde. Maximal responses are presented as fold change in baseline bioluminescence prior to light treatment. Data are expressed as means ± SEM of 3 independent replicates. Statistical analysis of the relative change in (H) relative luminescence or (I) the absolute change in amplitude of aequorin luminescence yielded significant differences between cells transiently expressing aequorin alone or aequorin and human melanopsin (based on one-way ANOVA with Dunnett's post hoc comparisons to aequorin expressing cells, **p<0.01, *p<0.05). Data are expressed as means ± SEM of 3 independent replicates. The absolute response of JellyOp expressing cells is also statistically different from that of aequorin alone.

3.3.3 Signalling properties of JellyOp structural variants

The signal transduction cascades of mutant JellyOp variants were subsequently tested relative to wildtype JellyOp. Transient WT JellyOp produced 11.5 ± 2.7 fold change in luminescence, a response amplitude that was unmatched by other mutants (Figure 3.3 A and B). Among all mutants, residual Glosensor™20F activity was strongest in JellyOp Y132G and Y219A with a peak response of 8.5 ± 1.5 to a single flash of light, alluding to substantial interactions with $G\alpha_s$ proteins. A single amino acid substitution at F139A abolished Glosensor™20F responses to the extent that it was seemingly comparable to mock transfected HEK 293 cells. Interestingly, a mutant with a combination of Y132G, F139A and Y219A point mutations produced intermediate response amplitude (4.8 ± 0.9).

To probe for potential interactions between F139A JellyOp and $G\alpha_i$ proteins, I used a cell based cAMP luciferase reporter assay, developed and validated by Dr Helena Bailes at the University of Manchester. The assay required pharmacological elevation of endogenous cAMP without disrupting receptor and G protein interactions such that any $G\alpha_i$ mediated inhibition of adenylate cyclase would be represented more dramatically. Chronic elevation of cAMP with 3 µM forskolin treatment resulted in a sustained elevation in luminescence values which peaked at 13 minutes to 5.5 x 10^4 ± 1.2 x10^4 luminescence units in HEK 293 cells (Figure 3.3 C). Opsin pigments were transiently expressed in the reporter HEK293 cells and light pulsed 2 minutes after forskolin treatment.

Opsin photopigments JellyOp and human rhodopsin (hRH1) were utilised as controls for $G\alpha_s$ and $G\alpha_i$ signalling. Upon transient expression of JellyOp to HEK cells and light stimulation, Glosensor™20F luminescence was elevated to 1 x 10^5 ± 1.4 x 10^4 units at 13 minutes post-forskolin, which was much greater than that of HEK cells alone. This is presumably due to the combination of forskolin treatment and WT JellyOp signal transduction, both of which elevate cAMP in host cells (Figure 3.3 D). When hum RH1 expressing cells were assayed for Glosensor™22F activity in, a subdued level the luminescence signal (2.9 x 10^4 ± 6.3 x 10^3) was observed at 13 minutes. Thus is consistent with previous reports on the signalling capacity of Rh1 *in vitro,* in which $G\alpha_i$ proteins are activated (Tsai et al. 1984).

The response profile of F139A JellyOp resembled that of HEK 293 cells with a luminescence read of $4.8 \times 10^4 \pm 4.7 \times 10^3$ at 13 minutes. This suggests the mutant opsin does not contribute to cAMP regulation in either an active or inhibitory manner. The data appear to validate Glosensor™20F assays on F139A JellyOp performance in G protein signalling. In addition, when HEK 293 cells were co-expressed with F139A JellyOp and aequorin, light stimulation produced deviations in baseline bioluminescence that was comparable to aequorin expressing cells (Figure 3.3 E and F). Furthermore, the lack of physiological responses in HEK cells expressing F139A JellyOp with respect to cAMP and calcium are not due to poor levels of protein expression, as I was able to detect abundant and comparable levels of the ID4 immunoreactivity in cells transfected with JellyOp and F139A JellyOp (Figure 3.4 E).

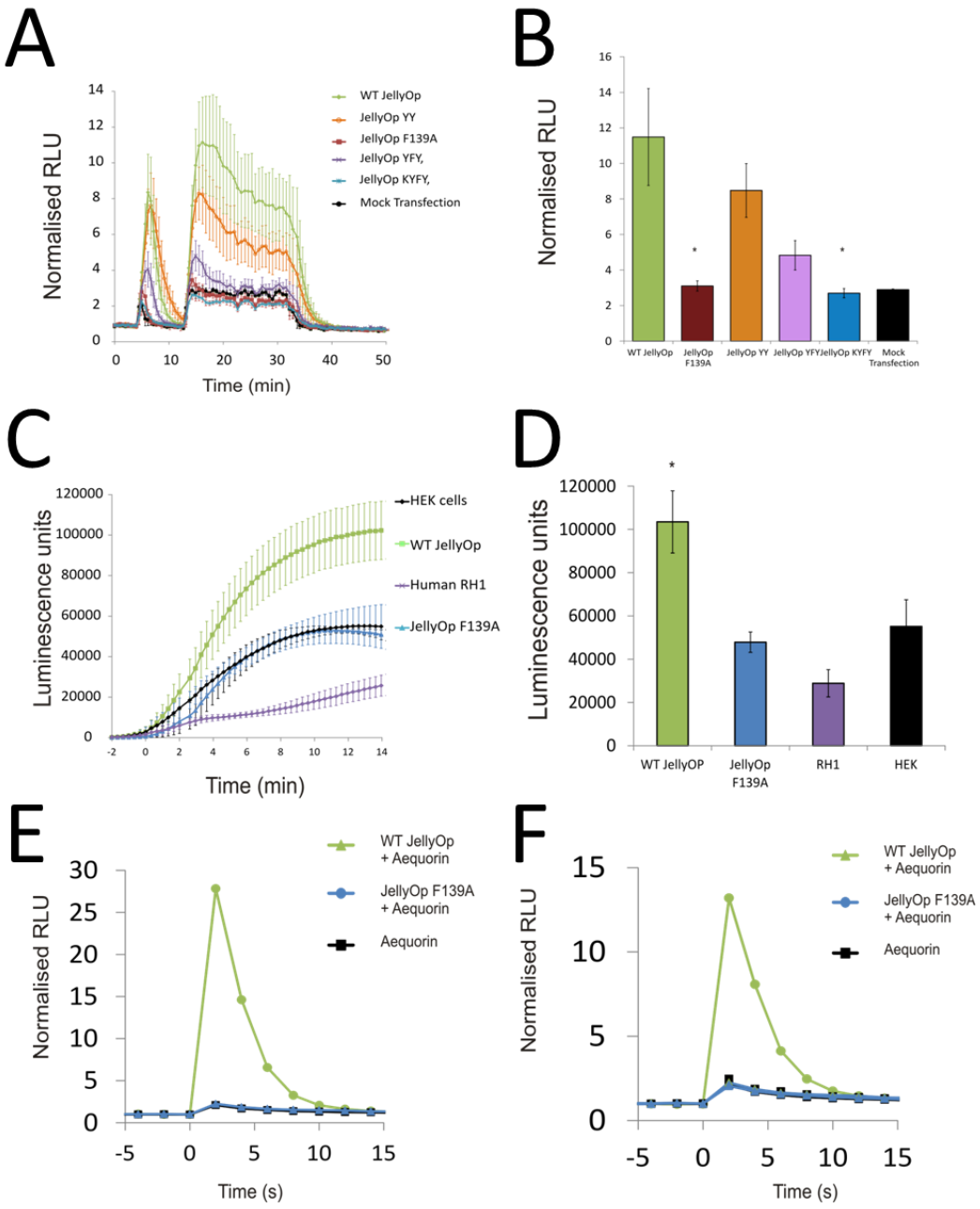

Figure 3. 3 Validation of $G\alpha_s$ decoupled JellyOp mutants

(A) Glosensor™20F reporter activity in HEK cells transiently expressing indicated structural variants, exposed to initial light flash at 5 minutes and 30 flashes at 12 minutes. (B) A one way ANOVA with Dunnett's comparison (*p<0.05) to WT JellyOp revealed significant deviation in maximal fold responses of F139A JellyOp and JellyOp KYFY. Data are expressed as mean ± SEM of three independent replicates. (C) Activation of endogenous adenylate cyclase activity was achieved with 3 µM forskolin at 2 minutes and cells transiently expressing indicated opsin photopigment were subsequently stimulated with light. Data are expressed as mean ± SEM of three independent replicates. A one way ANOVA with Dunnett's comparison (*p<0.05) to HEK cells revealed significant deviation in responses of JellyOp but not human RH1. (D) A comparison of absolute luminescence values between samples at 15 minutes following forskolin treatment (when forskolin response peaks for HEK cells). (E and F) Light dependent aequorin responses in HEK293 cells transiently expressing F139A JellyOp were abolished compared to WT JellyOp. Data are expressed as means ± SEM of duplicate cell samples in individual experiments.

3.3.4 Functional expression of JellyOp and structural variants in *per2::luc* rat1 fibroblasts

My next aim was to discern whether the signalling properties of heterologous JellyOp and JellyOp F139A, as characterised in HEK 293 cells, could be replicated in rat1 fibroblasts to generate a light entrainable cell based model of the mammalian clock. JellyOp and F139A JellyOp was thus stably in rat1 fibroblast cell lines. Due to the nature of polyclonal stable transfectants, I anticipated high levels of variability in transgenic expression of photopigment between individual clones. To overcome this potential inconsistency in protein expression, monoclonal transgenic lines were cultured to guarantee homogenous levels of transgene expression. This was achieved using a bicistronic expression vector which allowed simultaneous expression of opsin and GFP. The GFP served as an additional quantitative marker for transgene expression in fluorescence assays (Figure 3.4 A and B). Opsin expression was also confirmed by immunolabelling the monoclonal fibroblast cells for 1D4 epitope (Figure 3.4 C). Immunoreactivity was concentrated at the cell membrane, as well as in granules across the cytoplasm, but absent in the cell nuclei. A western blot of the 1D4 epitope showed that the JellyOp and JellyOp F139A formed a stable monomeric protein of approximate 35 KDa (Figure 3.4 D).

3. Developing a selective signalling interface for JellyOp

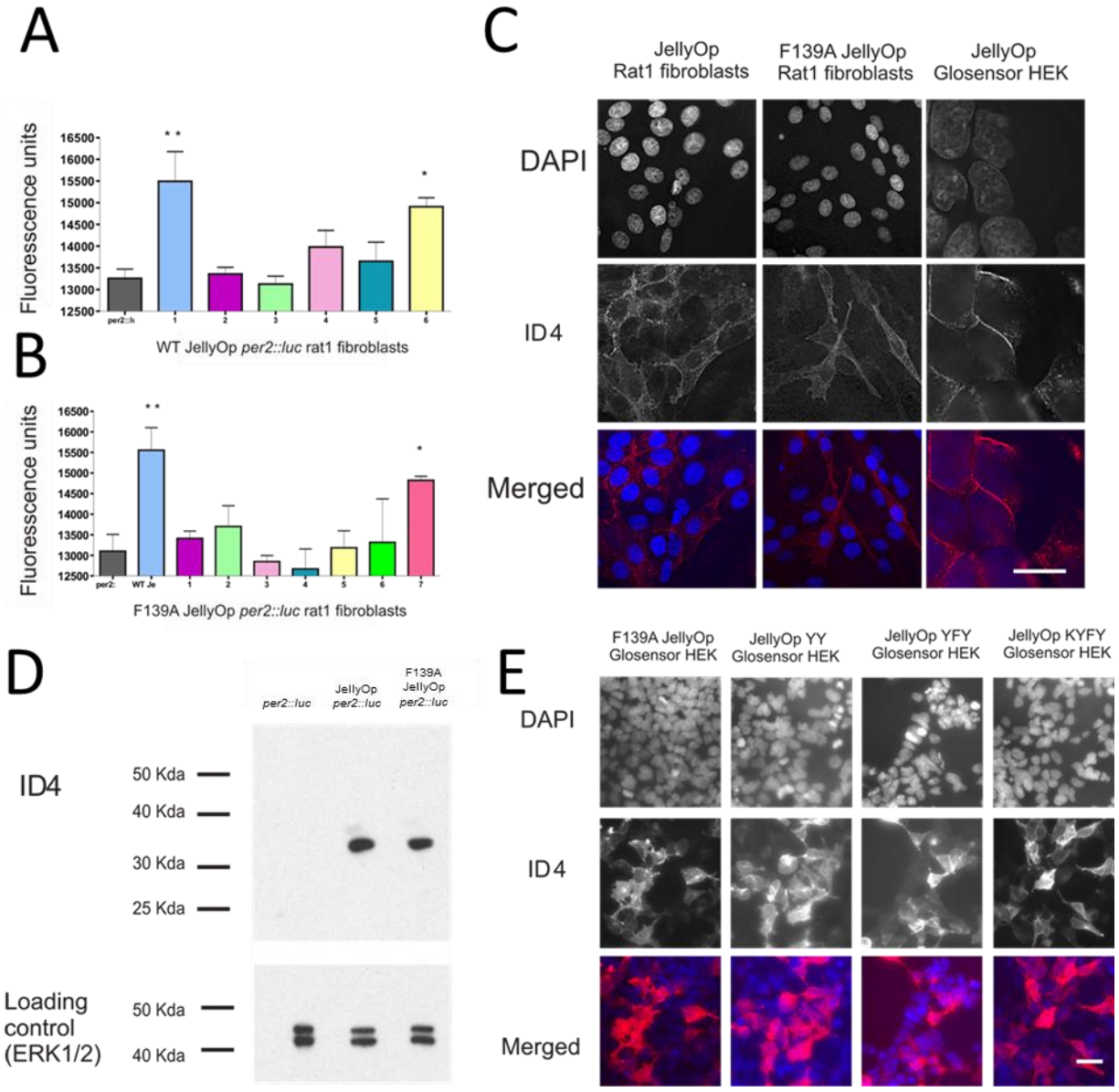

Figure 3.4 Construction of JellyOp expressing rat1 fibroblasts cell lines and immunocytochemical characterisation

(A) A comparison of GFP fluorescence between six monoclonal cell lines (labelled 1-6) of (A) JellyOp and (B) F139A JellyOp expressing *per2::luc* rat1 fibroblasts. Stable transfectants were isolated for homogenous levels of transgene expression and GFP fluorescence levels compared following excitation at 485 nm. Data correspond to the mean ± SEM of triplicate cell samples from a single assay. Statistical comparison of the values was performed by using a one-way ANOVA with Dunnett's post hoc comparisons to *per2::luc* fibroblasts (*p<0.05, **p<0.01). (C) Optical sections of JellyOp or F139A JellyOp expressing *per2::luc* rat1 fibroblast and JellyOp expressing HEK-293 cells, co-labelled with a fluorescent 1D4 antibody and visualized through deconvolution microscopy. All cells were also co-labelled with a DAPI, a fluorescent nuclear. Bottom panels contain merged images in which the red signal corresponds to ID4 fluorescence and the blue signal DAPI fluorescence. (Scale bar for fibroblasts: 20 µm, HEK cells: 10 µm) (D) JellyOp and F139A JellyOp protein expression was also confirmed with immunoblotting assays. (E) Fluorescence immunohistochemical labelling of the 1D4 epitope in Glosensor™20F HEK cells transiently expressing various JellyOp structural mutants. (Scalebar: 50 µm).

3. Developing a selective signalling interface for JellyOp

I tested the signal transduction cascade of JellyOp through Glosensor™20F recordings. Following the light pulse, a robust 1.8 ± 0.2 fold elevation in bioluminescence signal was reported which peaked within 3 minutes (Figure 3.5 A and B), with a subsequent decay back to baseline over 5 minutes. Such a response profile was slower than the one observed in JellyOp expressing HEK 293 cells, implying similar but delayed G protein signalling kinetics. The amplitude responses in fibroblasts were relatively lower, presumably due to transient expression of the cAMP biosensor and competition for the luciferin substrate by background *per2* luciferase. However, the baseline bioluminescence in rat1 fibroblasts which, lacking either Glosensor™20F or JellyOp, remained unchanged following light stimulation. Interestingly, background Glosensor™20F luminescence was markedly higher in *per2::luc* fibroblasts ($3.5 \times 10^3 \pm 1.9 \times 10^2$ units) compared to JellyOp *per2::luc* fibroblasts in the presence of 9-*cis*-retinaldehyde ($1.9 \times 10^3 \pm 9.9 \times 10^1$) (Figure 3.5 C). This is likely to be due to differences in level of background *per2::luc* activity.

I further investigated the reproducibility of the JellyOp signalling in fibroblast cells, by delivering repetitive light stimulation (every 30 seconds for 15 minutes). The Glosensor™20F signal was sustained throughout the intermittent light pulses, implying a resistance to bleach in fibroblast cells. Interestingly, the decay in signal following chronic stimulation was more gradual over time compared to HEK 293 cells. This may reflect cellular difference in desensitisation mechanisms for cAMP signalling (Figure 3.5 A).

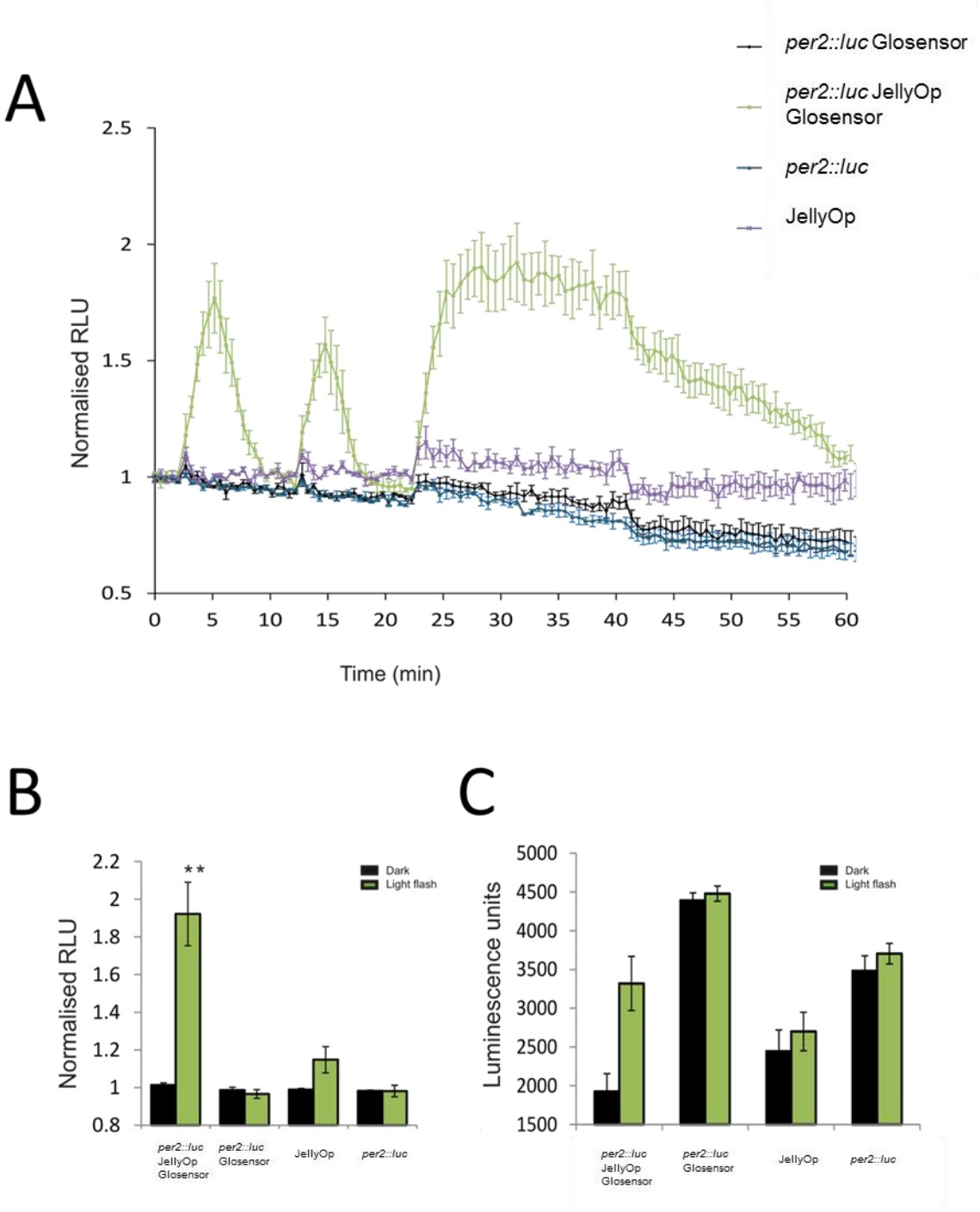

Figure 3.5 JellyOp mediated $G\alpha_s$ signalling in rat1 fibroblasts cells

(A) Light induced changes in luminescence of Glosensor™20F transfected *per2::luc* rat1 fibroblasts stably expressing WT JellyOp reconstituted in 9-*cis*-retinal. Fibroblasts expressing Glosensor™20F or JellyOp alone produced minimal fold changes in bioluminescence following light stimulation, with response profiles comparable to mock transfected fibroblasts. The data represent baseline normalised mean luminescence units ± SEM, from triplicate samples in a single assay. Cells were pulsed with a single light flash at 2 and 12 minutes, followed by 30 light flashes (at approximate 30 second intervals) at 22 minutes. (B) Quantification of normalised maximal response amplitude reveals that only the HEK cells expressing JellyOp shows a statistically significant induction in reporter activity. Statistical comparison of the values was performed by using a one-way ANOVA with a Dunnett's post hoc comparison (**$p < 0.01$). (C) High variability in the baseline luminescence between *per2::luc* and JellyOp expressing *per2::luc* cells is presumably due to variable background circadian *per2::luc* activity.

I then sought to confirm with MDL whether such light responses were due to activation of adenylate cyclase by JellyOp. Upon pre-incubation with 50 or 100 µM MDL, a dose-dependent reduction in dark baseline bioluminescence was reported as well as light driven bioluminescent changes (Figure 3.6 A and B). Indeed, this confirms that endogenous adenylate cyclase was activated by $G\alpha_s$ proteins under the influence of JellyOp.

I then evaluated the functional expression of F139A JellyOp in *per2::luc* rat1 fibroblasts. A stark reduction in baseline Glosensor™20F activity was reported in the mutant receptor cell line, which again may reflect a clonal difference in background *per2::luc* luciferase activity (Figure 3.6 A and B). The luminescence of F139A JellyOp expressing cells was comparable to 100 µM MDL pre-treatment of JellyOp *per2::luc* fibroblasts, whilst absolute changes in cAMP, assessed with a cAMP ELISA, revealed that F139A JellyOp was unable to induce discernible levels of cAMP following light treatment in fibroblasts (Figure 3.6 C).

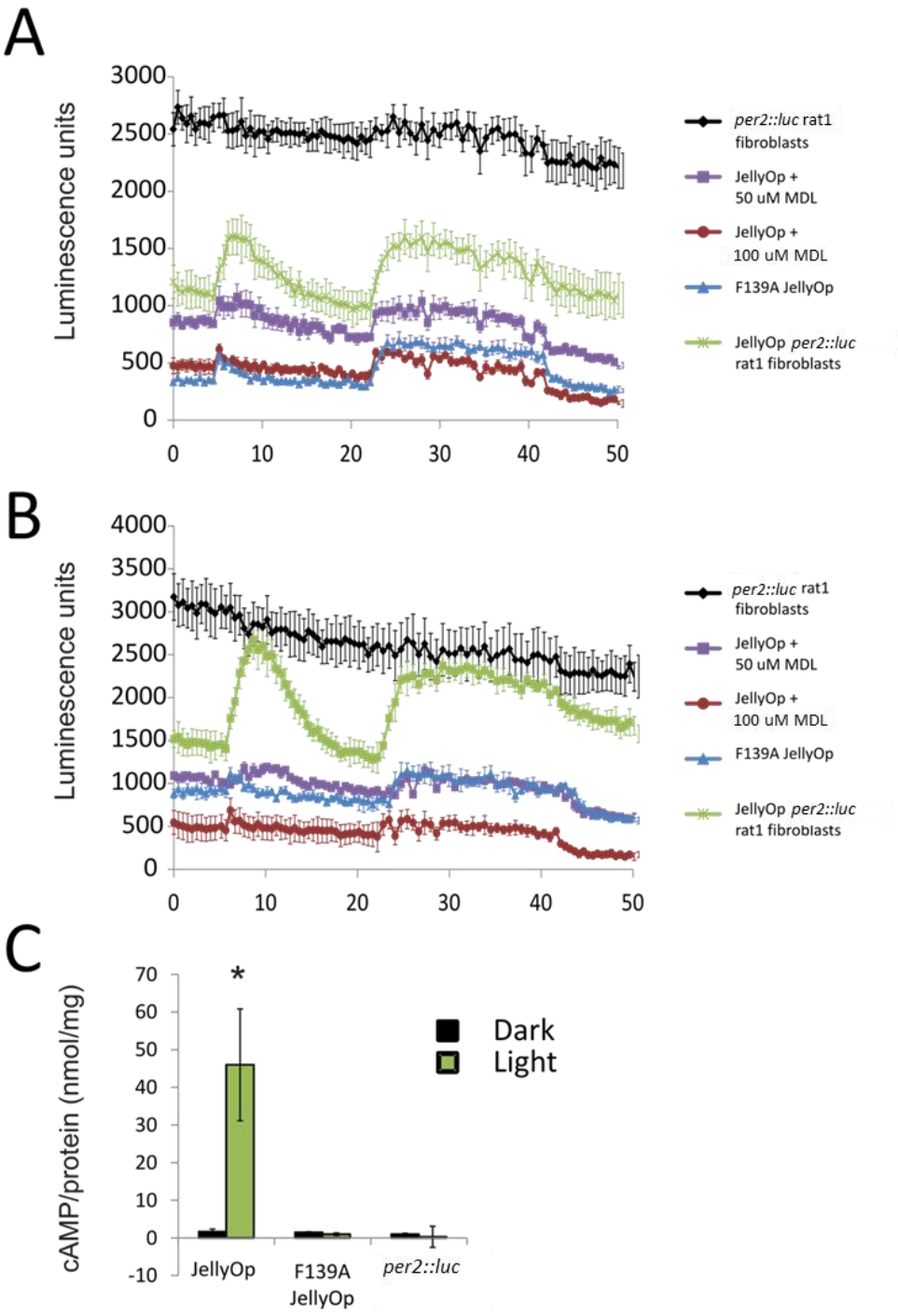

Figure 3.6 Functional expression of F139A JellyOp in rat1 fibroblasts

(A and B) Pre-treatment of WT JellyOp expressing rat1 fibroblasts with MDL 12330-A suppressed the baseline activity of Glosensor™20F in a dose dependent manner despite light stimulation. Data are expressed as means ± SEM of triplicate cell samples in individual experiments. F139A JellyOp expressing rat1 fibroblasts show minimal changes in Glosensor™20F activity following light stimulation. (C) A cAMP ELISA demonstrates that in contrast to WT JellyOp, F139A JellyOp expressing rat1 fibroblasts showed an indiscernible cAMP response to a light flash at 2 minutes. Data correspond to the mean ± SEM from three independent experimental repeats, each performed in duplicate (based on one way ANOVA with Dunnett's comparison to *per2::luc* fibroblasts, *p<0.05).

3.3.5 JellyOp dependent modulation of the MAPK signalling pathway in HEK 293 cells and fibroblasts

I sought to investigate the effect of JellyOp expression on MAPK signalling in HEK cells and fibroblasts. It appeared that exposure of JellyOp in HEK 293 cells to UV and infra-red filtered white light (28.40 mW/cm^2) drove a light dependent increase in ERK1/2 phosphorylation in a temporally defined manner. This was reflected in a marked increase in immunoreactivity for phospho-ERK1/2, which was observed at 2 minutes exposure to light (Figure 3.7 A). However, this appeared to be a transient response as elevated phospho-ERK levels returned to baseline within 15 minutes of light onset. The timing of this response matches the kinetics of the JellyOp induced cAMP signalling and is also typical of G protein mediated MAPK activation (Shenoy et al. 2006). I was therefore interested in isolating the pathway responsible for MAPK response profile in each cell type. Pre-treatment of HEK 293 cells with 100 µM MDL, previously shown to abolish all responses in Glosensor™20F activity to JellyOp photostimulation, severely attenuated ERK1/2 phosphorylation at 2 minutes (Figure 3.7 C). This strongly suggests that that production of cAMP following light activation of JellyOp is necessary for the acute induction MAPK.

In striking contrast to HEK 293 cells, there was a pronounced reduction of immunoreactivity for phosph-ERK1/2 in fibroblasts stably expressing JellyOp, between 2 and 15 minutes of light treatment (Figure 3.7 B). The divergent modulation of MAPK responses to the same stimulus and opsin suggests that the cellular background plays an important role in the nature of cAMP and MAPK crosstalk. JellyOp expressing fibroblasts, when pre-incubated with the same concentration of MDL, showed enhanced baseline levels of ERK1/2 phosphorylation (Figure 3.7 D). This suggests that 100 µM MDL may suppress baseline levels of cAMP sufficiently to disinhibit MAPK. At 2 minutes following a light flash, there were minimal deviations in MAPK phosphorylation compared to dark control fibroblasts. Nonetheless, a reduction in phosphorylated ERK immunoreactivity was observed at 15 minutes of light onset. This suggests that in MAPK activity may be influenced by JellyOp independently of cyclic AMP. However, one of the limitations of MDL-12330 A is the lack of target specificity as it also influences guanylate cyclase and phosphodiesterases (Hunt and Evans. 1980). There is a possibility that the residual response at 15 minutes may be due to the lack of cAMP hydrolysis such that levels gradually accumulate over time that is sufficient to inhibit MAPK.

I proceeded to investigate MAPK responses in fibroblasts stably expressing the mutant F139A JellyOp. Baseline MAPK phosphorylation levels were comparable between *per2::luc* fibroblasts expressing F139A JellyOp or lacking any exogenous pigments (Figure 3.7. E). Interestingly the extent of MAPK inhibition was comparable to wildtype JellyOp at 15 minutes but not 2 minutes (Figure 3.7. E). The current body of evidence suggests that the mutant receptor does not impact on endogenous cAMP, which alludes to the possibility that the delayed inhibition of MAPK may be driven by cAMP independent pathways. Upon quantification of optical densities, I observed that F139A JellyOp mediated inhibition of ERK phosphorylation is intermediate between JellyOp and MDL pre-treated JellyOp fibroblasts at both 2 and 15 minutes of light treatment (Figure 3.7. F).

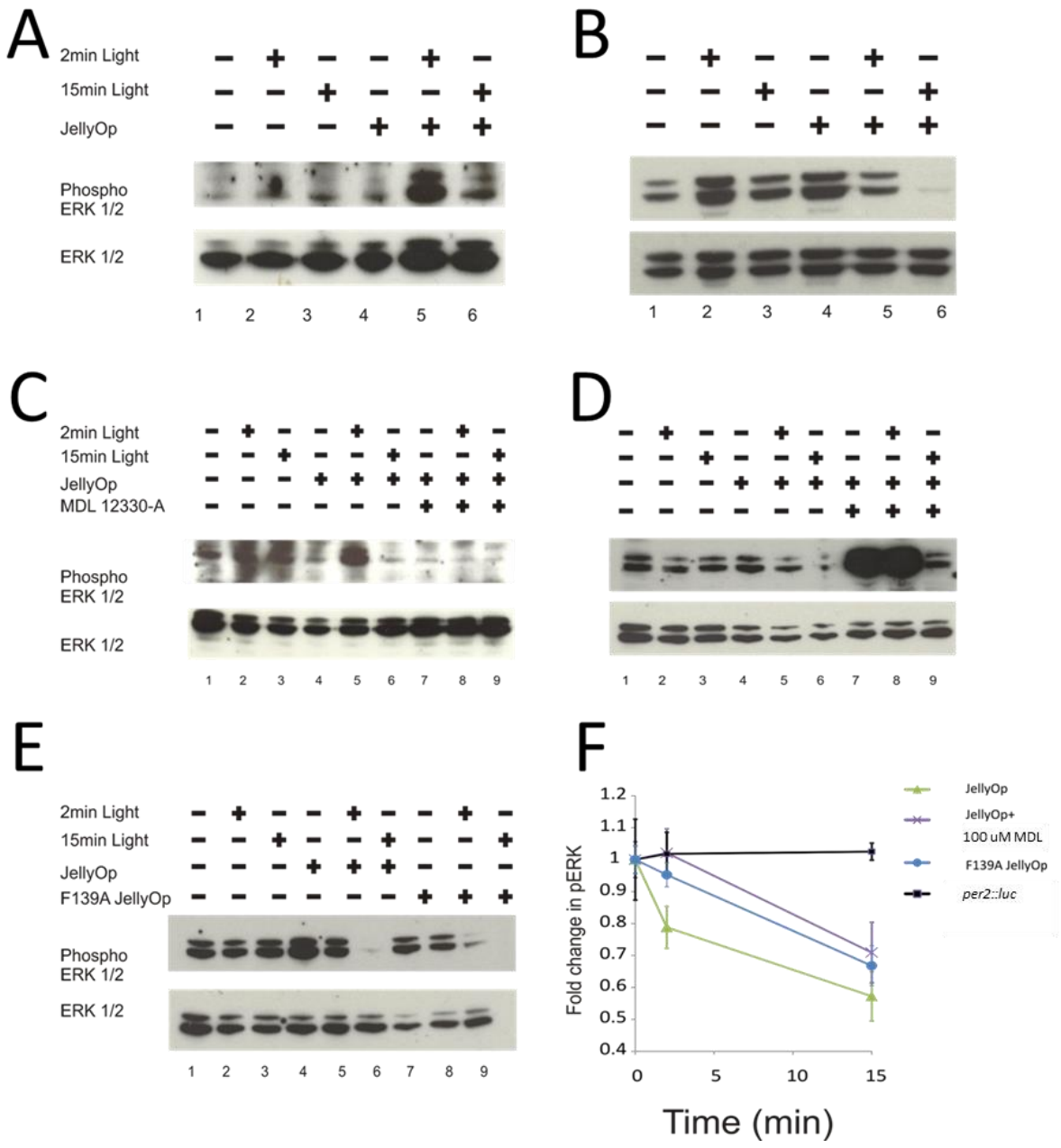

Figure 3.7 Pharmacological and optogenetic manipulation of the MAPK pathway

Time course of endogenous ERK1/2 phosphorylation in WT JellyOp expressing (A) FLP-IN™ HEK293 cells and (B) rat1 fibroblast cells stimulated with light for the indicated periods of time. Cells were stimulated with either 2 or 15 minutes light at 37°C and the level of endogenous ERK1/2 phosphorylation quantified by immunoblotting assay. In JellyOp expressing HEK cells, strong immunolabelling was detected at 2 minutes following light onset but not at 15 minutes. In contrast, rat1 fibroblasts show sustained and cumulative suppression of MAPK phosphorylation from 2 to 15 minutes of light treatment. (C) Pre-treatment of HEK cells with 100 µM MDL abolished the induction of MAPK signaling. (D) In contrast, the baseline level of ERK1/2 phosphorylation was augmented in MDL treated rat1 fibroblasts. Furthermore, light dependent inhibition of MAPK was abolished at 2 minutes but sustained at 15 minutes. (E) rat1 fibroblasts expressing F139A JellyOp retained light dependent MAPK responses similar to that of WT JellyOp. (F) Relative changes in optical density of immunolabelled pERK1/2 at 2 and 15 minutes following light stimulation compared to dark baseline levels, in the presence or absence of MDL. Data represent the mean ± SEM from at least three independent experimental replicates, each performed in triplicate. Statistical comparison of the values was performed by using a one-way ANOVA and a Dunnett's post hoc comparison to Glosensor™20F HEK cells at each of the time points (*$p < 0.05$), revealing significant suppression of ERK at 15 minutes based on a one-way ANOVA and a Dunnett's post hoc comparison to Glosensor™20F HEK cells at each of the time points (*$p < 0.05$, n=3).

3.3.6 Signalling properties of the C-terminally truncated JellyOp

It has been shown that the cytoplasmic terminus of a typical class A GPCR, such as the β2 adrenergic receptor, plays a crucial role in β-arrestin binding and subsequent receptor desensitisation (Bouvier et al. 1988, Shenoy et al. 2006). The C-terminus is enriched with multiple serine and threonine sites which are subject to phosphorylation by GRKs upon ligand binding. Furthermore, amino acid substitutions of these residues result in delayed onset of desensitisation compared to the wildtype receptor. Due to the presence of serine and threonine residues on the C-terminus of JellyOp, it was speculated that these residues could play a role in JellyOp desensitisation or even interacted with β-arrestins.

To address this speculation, a C-truncation mutant variant of JellyOp was which excluded all intracellular serine and threonine residues was constructed and subsequently evaluated whether this truncation changed the temporal kinetics of G protein interactions over time (Figure 3.1 A and B). Figure 3.8 A confirms the expected differences in molecular mass of the truncated opsin compared to the wildtype photopigment. It is conceivable that based on the findings of Bouvier et al. 1988, such modifications may compromise the ability of JellyOp to interact with β-arrestins and therefore be shielded from desensitisation mechanisms. I therefore conducted Glosensor™20F assays to capture any differences in temporal dynamics of cAMP signalling between the wildtype and truncation mutant, as a reflection of altered desensitisation.

Interestingly, a modest reduction in the dark baseline activity of Glosensor™20F was observed in truncated JellyOp expressing HEK 293 cells. However, following a light flash, there appeared to be very little, if any difference in the maximal Glosensor™20F in response to a single light stimulus or repetitive flashes (Figure 3.8 B and C). This demonstrates that the Δ COOH mutant was as efficient as the wild-type receptor in stimulating cAMP production under these experimental parameters. One possible interpretation is that the C terminus is responsible for sustaining a level of constitutive receptor activation. I then tested the ability of the WT opsins and truncation mutant to induce Glosensor™20F activity following light stimulation at 30 minute intervals over 10 hours (Figure 3.8 D). However, there were no qualitative differences between the reporter levels.

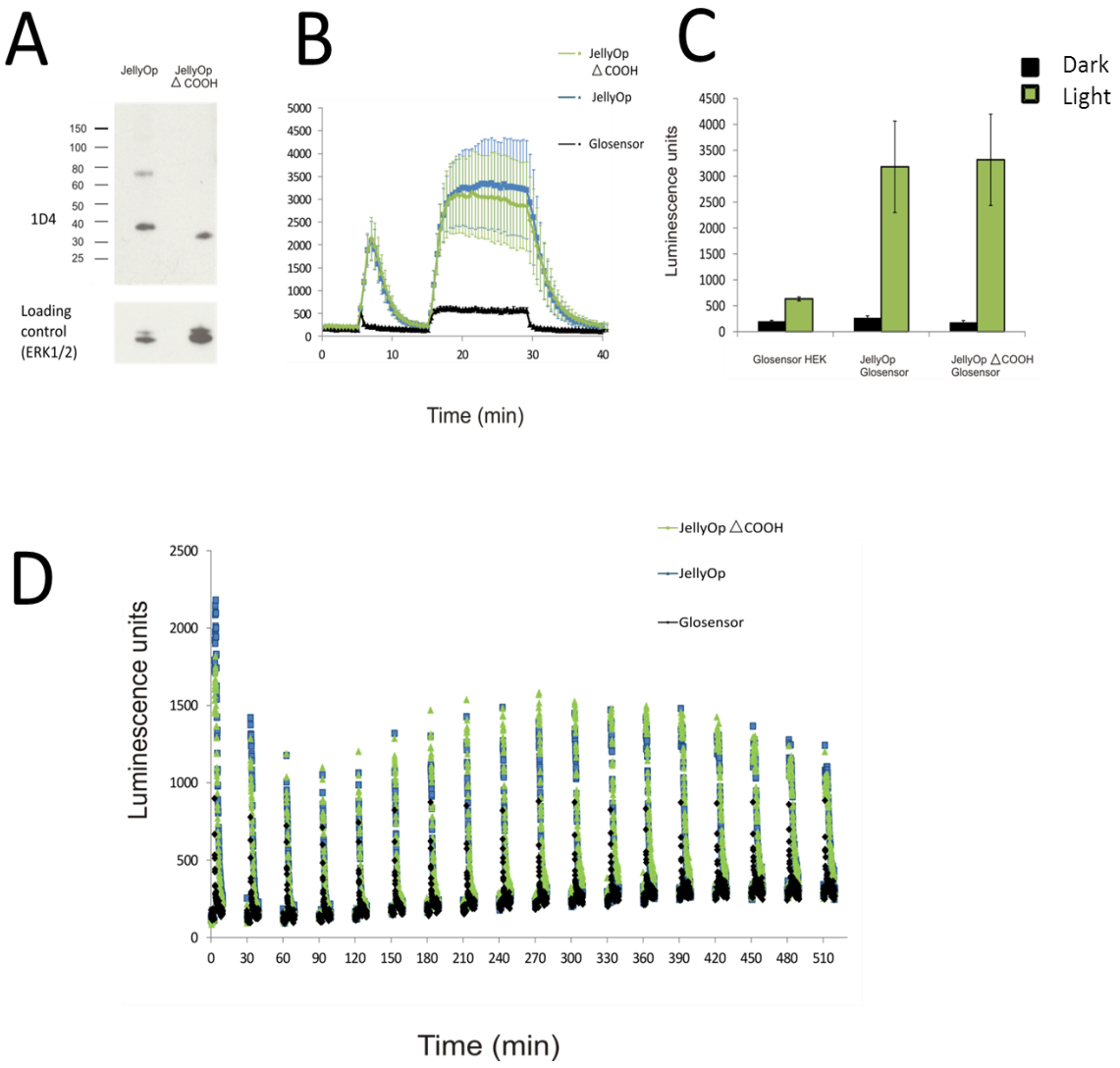

Figure 3.8 Indiscernible differences in physiological responses of WT JellyOp and JellyOp Δ COOH expressing HEK cells to light stimulation.

(A) A western blot of wildtype and truncated JellyOp to confirm the difference in molecular weight between the variants. (B) absolute mean luminescence units ± SEM, from 3 independent repeats. Cells were pulsed with a single light flash at 5 minutes and 30 light flashes (at 30 second intervals) at 15 minutes. Quantification of the (C) absolute maximal response revealed no significant differences in induction of reporter activity between the structural mutants, based on one-way ANOVA with Dunnett's comparison, $p<0.01$. (D) Light induced Glosensor™20F responses recorded in WT JellyOp and JellyOp Δ COOH expressing HEK cells pulsed for 45 seconds every 30 minutes over 10 hours. Data represent fold change in baseline bioluminescence units from a single assay.

3. Developing a selective signalling interface for JellyOp

Given the well-established role of β-arrestin in receptor desensitisation, I sought to probe for potential interactions of β-arrestin and endogenous or exogenous GPCRs such as the β2 adrenergic receptor and JellyOp respectively. Firstly I tested whether induce β-arrestin translocation could be induced to the membrane of HEK293 cells by pharmacological means. This involved transiently expressing the fluorescent tagged β-arrestin in HEK 293 cells and exposing them to 10 μM isoproterenol for 35 minutes. HEK 293 cells expressing β-arrestin2-GFP showed a strong fluorescent uniform signal throughout the cytosol (Figure 3.9 A). Even after 35 minutes of isoproterenol treatment, there was no discernible enhancement of membrane fluorescence or loss of cytosolic fluorescence. I next conducted a qualitative immunocytochemical assessment of 1D4 localisation in JellyOp and β-arrestin2-GFP co-expressing HEK 293 cells before and after light stimulation. Again, I did not observe a redistribution of the membrane receptor to distinct subcellular locations in response to light, or even a reduction in cell surface receptor expression (Figure 3.9 B). There appears to be little, if any, difference between the fluorescence signals from GFP tagged β-arrestin between light treated cells and dark controls.

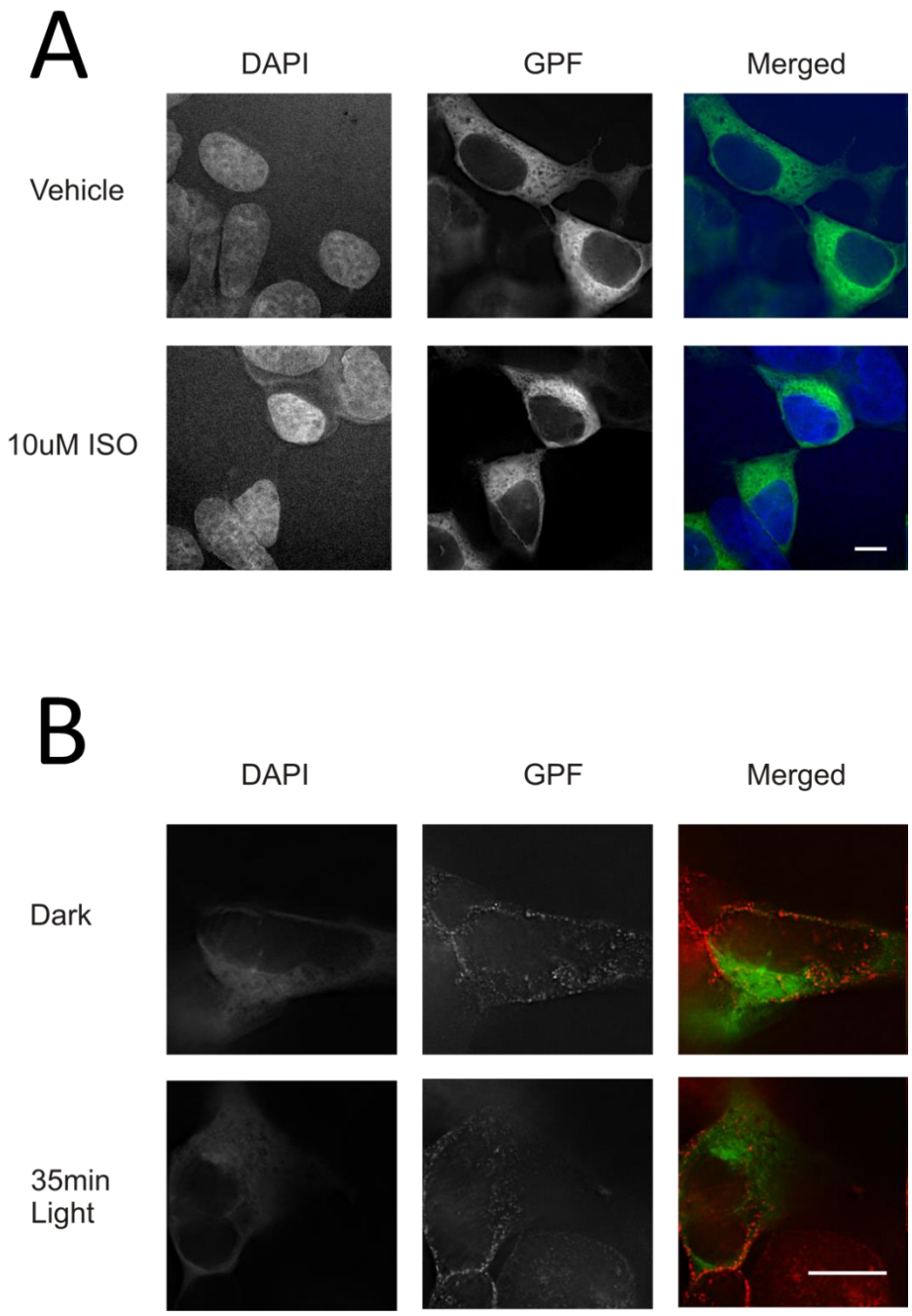

Figure 3.9 Immunocytochemistry for β-arrestin interactions

(A) A β-arrestin2–GFP based reporter was employed to study the effect of isoproterenol stimulation on the cellular mobilisation of β-arrestin2 in HEK cells. Cells were either non-stimulated (top panel) or treated with 10 μM isoproterenol for 35 minutes (bottom panel). Right panels contain merged images in which the green signal corresponds to β-arrestin2–GFP fluorescence and the blue signal DAPI fluorescence. β- arrestin2 -GFP was detected as a strong fluorescent signal in the cytosol. However, β-arrestin2 -GFP localisation did not show any discernible changes between the treated and untreated cell samples. (scalebar for HEK cells: 50 μm) (B) ID4 immunolabelling assays was conducted in JellyOp and β-arrestin2–GFP co-expressing HEK cells before (top panel) and after 35 minutes light treatment (bottom panel). Right panels contain merged images in which the green signal corresponds to β-arrestin2–GFP fluorescence and the red signal the bound ID4 antibody. (Scalebar for HEK cells: 50 μm)

3. Developing a selective signalling interface for JellyOp

3.4 Discussion

3.4.1 Development of a $G\alpha_s$-decoupled JellyOp photopigment

The discovery and validation of JellyOp is exciting from both evolutionary and optogenetic perspectives. It is the only naturally occurring opsin to induce a cAMP signalling cascade upon photoactivation and is expressed in a pre-bilateral organism which predates bilateral invertebrates (Koyanagi et al. 2008). In bilateral invertebrates, opsins are coupled to $G\alpha_q$ subunit but not $G\alpha_s$. I was also able to demonstrate the MDL-dependent $G\alpha_s$ interactions of JellyOp using a range of cAMP reporter and ELISA assays (Figure 3.2. E.). JellyOp also exhibits superior bleach resistance properties and phototransduction kinetics to β2 adrenergic OptoXRs when exposed to the equivalent light irradiances (Bailes et al. 2012). Taken together, JellyOp is suitable as an optogenetic tool for investigating $G\alpha_s$ signalling pathways in mammalian cells.

To complement the current range of tools for studying circadian physiology, I sought to develop optogenetic tools based on JellyOp for the selective activation of G protein dependent and independent pathways whilst overcoming the practical limitations of pharmacological agents. To this end, I aimed to abolish G protein signalling in JellyOp without compromising the stability and conformational diversity of the receptor. Thus, I attempted to introduce relevant point mutations in JellyOp to remove conserved amino acids that were implicated in G protein coupling (Figure 3.1 B). Several residues were identified based on an amino acid alignment of JellyOp and the human β2 adrenergic receptor, a well-studied Class A GPCR in which many functional motifs implicated in G protein mediated signal transduction have already been identified (Figure 3.1 A).

One such amino acid was a lipophilic amino acid conserved in over 60 mammalian GPCR sequences as either leucine, isoleucine, valine, methionine or phenylalanine (Moro et al. 1993). Mutagenic studies of this amino acid revealed its physiological significance in G protein dependent signal transduction of the β2 adrenergic receptor, where substitution of Phenylalanine 139 with alanine yielded a mutant receptor defective in agonist mediated intracellular cAMP accumulation. I therefore hypothesised that substitution of this amino acid with a small amino acid such as glycine or alanine would abolish such JellyOp mediated cAMP production in mammalian cells.

I also identified several other conserved amino acid residues in the primary structure of JellyOp, including Y132 and Y219, which are known to be implicated in G protein activation (Shenoy et al. 2006). The same authors have previously demonstrated through mutagenic studies that point mutations at K68, Y132 and Y219 abolished $G\alpha_s$ coupling abilities in the β2 adrenergic receptor. I thus proceeded to mutate these corresponding residues in JellyOp to generate a variety of structural mutants with different combinations of point mutations including JellyOp YY, JellyOp YFY and JellyOp KYFY (Figure 3.1 A).

Prior to characterising the signalling properties of G protein decoupled JellyOp mutants, the signalling diversity and kinetics of the wildtype JellyOp photopigment was investigated in mammalian HEK 293 cell lines, with regards to principal intracellular messengers cAMP, calcium and MAPK. Upon exposing JellyOp expressing cells to a flash of bright white light, a transient but significant increase in baseline bioluminescence was reported, peaking at 2.5 minutes before falling to pre-stimulus levels (Figure 3.2 A). Such response amplitudes in JellyOp expressing cells were comparable to the findings of similar studies by Bailes et al. 2012, who also showed that the level of JellyOp mediated Glosensor activation was comparable to forskolin induction. Cells lacking exogenous photopigment showed small and transient spikes in bioluminescence to light stimuli, but these were not sustained over 5 minutes.

The cAMP ELISA assays similarly showed a significant light dependent induction in intracellular levels of cAMP in JellyOp expressing HEK 293 cells at 2.5 minutes following a flash of bright light, thus validating the Glosensor™20F observations. Taken together, the Glosensor™20F and ELISA data on JellyOp are consistent with the findings of Koyanagi et al. 2008 who first demonstrated through ELISA assays that heterologously expressed the box jellyfish opsin in HEK 293S cells resulted in a light-dependent increase in intracellular cAMP compared to dark controls and mock transfected cells. Furthermore, the fold induction of light induced cAMP was comparable to pharmacological activation of the human β2-adrenergic receptor with to 10 nM isoproterenol agonist for 20 minutes.

3. Developing a selective signalling interface for JellyOp

I report that the light induced Glosensor™20F responses in JellyOp expressing HEK 293 cells were sensitive to the adenylyl cyclase inhibitor MDL, as addition of this agent caused a dose dependent reduction in maximal fold bioluminescence (Figure 3.2. E). This demonstrated the necessity of JellyOp-$G\alpha_s$ interactions in signal transduction and subsequent modulation of Glosensor™20F activity and confirms a $G\alpha_s$ signal transduction cascade for JellyOp.

As I was also interested in characterising JellyOp mediated $G\alpha_q$ signalling, I chose to assay calcium levels as a measure of phototransduction. For assaying calcium responses I employed a calcium reporter aequorin, a calcium sensitive photo protein when reconstituted with coelentrazine (Shimomura et al. 1990). The dynamic range of aequorin is dependent on the structure of the coelentrazine, which exists in many forms (Dupriez et al. 2002). Coelentrazine H renders aequorin highly sensitive to calcium and was therefore used in my study.

The dynamics of calcium signalling are also regarded as very different from cyclic nucleotide based messengers. In non-excitable cells, intracellular calcium is compartmentalised in various organelles including the endoplasmic reticulum, lysosomes and Golgi network and can be triggered by a variety of intracellular messengers (Galione et al. 2009). It has been shown that calcium induction in the cytosol leads to rapid transient redistributions into the mitochondria. COS-7 cells expressing mitochondrially targeted aequorin reported larger transient increases in calcium following LPA stimulation compared to cytoplasmic aequorin, demonstrating the importance of the organelle as an interactive component of calcium signalling (Dupriez et al. 2002).

When the aequorin was targeted into the mitochondrial matrix of JellyOp expressing cells, a light dependent induction in the bioluminescence of mitochondrial aequorin was captured (Figure 3.2 G). This is a promising suggestion that JellyOp transduction elicited an induction in mitochondrial calcium levels, presumably due to an elevation of cytosolic calcium. This alludes to upstream activation either through $G\alpha_q$ proteins or downstream targets of cAMP. Pharmacological inhibition of $G\alpha_q$ protein would help further elucidate whether JellyOp mediated calcium signalling is dependent on the phosphoinositol signalling cascade.

3. Developing a selective signalling interface for JellyOp

I subsequently conducted a comparative analysis of cAMP and calcium cascades between wildtype JellyOp and JellyOp mutants. All structural mutants exhibited reduced maximal Glosensor™20F activity compared to the wildtype form, which alluded to impairment of cAMP production (Figure 3.3 A). In particular, F139A JellyOp and JellyOp KYFY expressing HEK 293 cells elicited indiscernible Glosensor™20F activity upon photostimulation, which was comparable to that observed from JellyOp-expressing cells pre-treated with 100 µM MDL. Furthermore, the F139A JellyOp mutant was unable to induce discernible aequorin bioluminescence upon expression in HEK 293 cells compared to the WT receptor, which provides additional evidence for the lack of upstream G protein interactions (Figure 3.3 E and F).

I sought to investigate the signalling capacities of mutant F139A with respect to other $G\alpha_i$ proteins. Using a combination of pharmacological agents, opsins and Glosensor™22F, I was able to assay opsin mediated inhibition of adenylate cyclase in HEK 293 cells. Upon forskolin induced elevation of cAMP signalling, I showed that WT JellyOp augmented Glosensor™20F activity above that of forskolin, presumably due to $G\alpha_s$ activation (Figure 3.3 C). Activation of human Rhodopsin signalling was sufficient to negate forskolin induced cAMP levels in HEK 293 cells following light stimulation, inferring that $G\alpha_i$ activation was able to limit the magnitude and duration of pharmacologically induced cAMP signals. This is consistent with previous reports that vertebrate rhodopsin couples to $G\alpha_i$ protein *in vitro* (Gutierrez et al. 2012, Cao et al. 2012).

I further show that there is no significant difference between maximal Glosensor™20F activity of F139A JellyOp transfected HEK 293 cells and mock transfected cells (Figure 3.3 C). This indicates that F139A JellyOp was unable to suppress forskolin induced Glosensor™20F activity. I thus conclude that the F139A JellyOp mutant failed to modulate cAMP and calcium in the same way as the JellyOp, human Melanopsin or human Rh1. Thus, the minimal impact on intracellular signalling molecules by F139A JellyOp reflects indicate a lack of G protein responses.

I sought to investigate whether JellyOp mediated induction of cAMP was sufficient to modulate downstream signalling cascades such as MAPK in HEK 293 cells and fibroblasts. I showed that activation of JellyOp in HEK 293 cells elicited a rapid but transient induction in ERK1/2 phosphorylation (Figure 3.7 A) in a 100 µM MDL dependent manner (Figure 3.7 C), thus implicating the necessity of cAMP. This is consistent with previous studies which show that intracellular cAMP stimulates MAPK activity via the activation of rap-1 and B-raf activity in many cell types including kidney cortical collecting duct cells (Stork and Schmitt 2002, Laroche-Joubert et al. 2002). Other investigations in COS-7 and HEK 293 cells show that cAMP activation of MAPK is mediated through the actions of GEF (rasGRF1) (Norum et al. 2003). Generating a stable HEK 293 cell line expressing F139A JellyOp would allow for a comparative assessment of light induced MAPK signalling and also to test for cAMP independent effects on MAPK.

3.4.2 Application of JellyOp and F139A JellyOp in *per2::luc* rat1 fibroblasts

The second aim of the study was to generate light entrainable fibroblasts to enable the study of cAMP dependent and independent pathways in circadian clock regulation. Thus, I constructed a JellyOp *per2::luc* rat1 fibroblast line to study of effect of temporally controlled cAMP signalling on circadian organisation. In addition, as F139A JellyOp lacked $G\alpha_s$ protein capacities, I generated a F139A JellyOp *per2::luc* rat1 fibroblast cells line to investigate whether $G\alpha_s$ independent pathways of JellyOp were implicated in circadian regulation.

Robust light dependent increases in Glosensor™20F activity of JellyOp expressing fibroblasts, was reported in HEK 293 cells. However, the most confounding issue for the Glosensor™20F assay was highly variable levels of background *per2::luc* luminescence between the clonal lines. Nonetheless, robust changes in Glosensor™20F activity were only reported in JellyOp *per2::luc* fibroblasts, but not in F139A JellyOp fibroblasts (Figure 3.6 A and B). In addition, an ELISA assay confirmed significant production of intracellular cAMP in JellyOp expressing cells and lack thereof in fibroblasts expressing F139A JellyOp or lacking opsin photopigments (Figure 3.6 C). Thus, I was able to further confirm the divergent signalling interface between JellyOp and F139A JellyOp in rat1 fibroblasts.

To determine if JellyOp and F139A JellyOp could elicit modulation of ERK1/2 phosphorylation in fibroblasts I exposed serum starved rat1 fibroblasts stably expressing JellyOp or F139A JellyOp to 2 or 15 minutes of bright white light. Under dark control conditions, fibroblasts showed no significant change in immunoreactivity for phosphor-ERK at any time point sampled. JellyOp expressing fibroblasts showed a discernible reduction of in immunoreactivity at 2 minutes following light stimulus signal (Figure 3.7 B). At 15 minutes, the optical density was reduced further, suggesting cumulative inhibition of ERK phosphorylation under continuous light activation. Thus, it appears that JellyOp elicits divergent MAPK responses between HEK cells and fibroblasts. This could be attributed to the differences in the cellular background of the cell types (Stork and Schmitt. 2002).

Pre-treatment of cells with 100 µM MDL prevented light suppression of ERK phosphorylation at 2 minutes, which highlights the role of cAMP in down regulation of MAPK signalling (Figure 3.7 D). However, in spite of pharmacological inhibition of cAMP, a delayed onset of MAPK suppression at 15 minutes alludes to a cAMP independent mechanism of influencing MAPK signalling. This also suggests that MAPK activity is indeed influenced by JellyOp independently of cAMP. However, one of the limitations of MDL-12330 A is the lack of target specificity and also influences guanylate cyclase and phosphodiesterases (Hunt and Evans. 1980). There is a possibility that the residual response at 15 minutes may be due to the lack of cAMP hydrolysis such that levels gradually accumulate over time and become sufficient to trigger MAPK inhibition.

Interestingly, I observed a time dependent reduction in levels of phospho-ERK in F139A JellyOp expressing fibroblasts following exposure to light. Furthermore, the degree of MAPK inhibition between 2 and 15 minutes was intermediate between light treated JellyOp HEK cells and 100 µM MDL treated JellyOp HEK cells (Figure 3.7 E). Given the absence of cAMP induction in light irradiated F139A JellyOp expressing fibroblasts, as deduced from previous cAMP ELISA and biosensor assays, the data suggest that ERK modulation in fibroblasts is mediated by a cAMP independent mechanism. Taken together, WT JellyOp and F139A JellyOp differed significantly in their ability to stimulate secondary messengers including calcium and cAMP. However, both structural variants are capable of eliciting a suppression of MAPK signalling in rat1 fibroblasts.

3.4.3 Investigating regulatory mechanisms of JellyOp

I sought to further elucidate whether the C-terminus of JellyOp could contribute to the regulation of $G\alpha_s$ protein interactions, by mechanisms dependent on β-arrestin. Previous studies have shown that β-arrestin recruitment to the receptor is promoted by phosphorylation of serine and threonine residues of the C-terminus (Cervantes et al. 2010). It is noteworthy to mention that the C-terminus of JellyOp contains several serine and threonine residues which may be implicated in phosphorylation. As previously described, the presence of serine and threonine resides on the C-terminus of JellyOp raised speculation of interactions with kinases.

Thus I generated a truncated mutant variant of JellyOp which lacked all C-terminal serine and threonine residues (except for those on the 1D4 tag) and assessed its G protein kinetics in cell based assays. The effect of C-terminal ablation on JellyOp-$G\alpha_s$ signalling kinetics was investigated with respect to Glosensor™20F dynamics. When HEK 293 cells were transfected with the wild-type receptor and mutants and pulsed with light, the induction of Glosensor™20F activity was comparable in both opsins (Figure 3.8 B). Therefore, it appeared that the C-terminus contributes minimally to the kinetics of $G\alpha_s$ signalling under such experimental parameters. I further tested the ability of the WT opsins and truncation mutant to induce Glosensor™20F activity following light stimulation over 10 hours. However, there was no qualitative difference between the reporter levels (Figure 3.8 D). This also raises questions over the role of the C-terminus in regulating JellyOp signalling. However, it is also possible that the experimental paradigm may not be sufficient to distinguish between the signalling kinetics of the two structural variants.

The results of these findings deviate markedly from previous studies. Mutagenic studies by Bouvier et al. 1988 have demonstrated the importance of the intracellular C-terminus in regulating G protein signalling kinetics of β2 adrenergic receptor. To test the role of the C-terminus, the authors truncated the receptor after residue T365 and tested its ability to under desensitisation *in vitro*. When expressed in Chinese hamster fibroblasts, the mutant receptor exhibited similar ligand binding affinity and basal phosphorylation to the WT receptor. However, following 15 minutes exposure to 2 µM isoprenaline, only the WT receptor showed significant agonist induced phosphorylation, a hallmark of desensitisation.

The authors also showed that 2-180 minutes of 10 μM isoprenaline pre-treatment of HEK 293 cells expressing the wildtype receptor with resulted in a duration dependent reduction in adenylate cyclase activity from as early as 2 minutes. In contrast, the truncation mutant showed a delayed onset of desensitisation to at least 10 minutes pre-stimulation. Furthermore, a mutant version of the full length receptor where 11 serine and threonine residues were mutated to non-charged glycine and alanine residues showed even less susceptibility to desensitisation. This study highlights the importance of C-terminal serine and threonine residues in regulating G protein signalling.

Based on the Glosensor™20F assays of JellyOp and JellyOp Δ COOH, the comparable levels of assayed bioluminescence make it difficult to conclude the role of the JellyOp C-terminus. It may appear that the C-terminus contributes minimally to the signalling properties of the JellyOp. Alternatively, activation of photoactivation of JellyOp may not be sufficiently optimal so as to stimulate C-terminal phosphorylation and subsequent β2 arrestin interactions.

I further attempted to investigate possible interactions between β-arrestin-GFP and the endogenous β2 adrenergic receptor or with exogenous JellyOp in HEK293 cells. When expressed in HEK 293 cells, GFP expression showed an even distribution of fluorescence throughout the cytoplasm, without the subcellular localisation patterns. However, I was unable to detect B-arrestin movements in HEK 293 cells irrespective of pharmacological activation of endogenous receptors or light activation of JellyOp (Figure 3.9 A and B). This suggested strongly that the current experimental setup did not appear to be optimised for assessing B-arrestin mobilisation.

3. Developing a selective signalling interface for JellyOp

Within the current experimental paradigm I was unable to detect β-arrestin interactions. There may be several reasons for this. One of those is that JellyOp may not have affinity for β-arrestin and therefore does not interact favourably. If this were true however, this would imply that MAPK response elicited by $G\alpha_s$-decoupled F139A JellyOp could be due to alternative G protein independent pathways or even the G protein βγ subunits. However, it is also likely that these experimental paradigms were not suitable for assaying for β-arrestin mobilisation, and thus need further optimisation. This is the most likely explanation as the pharmacological control (isoproterenol) failed to elicit visible interactions between β-arrestin-GFP and β2 adrenergic receptor. An alternative way to investigate the role of β-arrestin would be to suppress the baseline expression levels of the protein in siRNA assays, and then explore the impact of JellyOp and F139A JellyOp on MAPK signalling.

3. Developing a selective signalling interface for JellyOp

4. Optogenetic manipulation of the mammalian clock

4.1 Introduction

The role of the $G\alpha_s$ in regulating mammalian circadian organisation has been extensively characterised by pharmacological studies. These investigations have employed a wide range of agents including cAMP analogues and modulators of GPCRs, adenylate cyclase and EPAC, all of which act on different components of the $G\alpha_s$ signalling cascade (Gillette and Prosser. 1988, O'Neill et al. 2008, An et al. 2011). Many of these studies have thus implicated cAMP in coupling extracellular signals to the molecular clock and regulating multiple clock parameters including period, phase and amplitude. Indeed, application of various cAMP analogues to SCN organotypic cultures have been shown to stimulate phase advances in electrical firing as well as clock gene expression in a temporally gated manner (Gillette and Prosser. 1988, O'Neill et al. 2008).

Long term pharmacological attenuation of cAMP levels in the SCN has been shown to impact on the free-running period of rhythmic clock genes as well as the locomotor activity of mouse models (O'Neill et al. 2008). It has been recently been shown that cAMP levels fluctuate with circadian rhythmicity in SCN neurons and peripheral cells (Doi et al. 2011, O'Neill et al. 2008). Furthermore, O'Neill et al. 2008 also claimed that these endogenous fluctuations in cAMP in the SCN were also required to sustain the molecular clock as pharmacological suppression resulted in damping of cellular rhythmicity. In contrast, Doi et al. 2011 have shown that intrinsic cAMP rhythms are not required for rhythm preservation as mice which lack the regulator of $G\alpha_i$, *Rgs16,* and consequently do not exhibit cAMP rhythms, retain rhythmic expression of clock genes in the SCN. Thus, there is still ambiguity about the contributions of cAMP signalling, within physiologically relevant parameters, to the clock.

In mammalian cells, cAMP signalling is initiated by GPCRs, which is regulated by external and internal mechanisms (Zhang et al. 2010, Doi et al. 2011, Piggins and Cutler. 2003). Studies have probed the role of the $G\alpha_s$ coupled $VPAC_2$ receptor in SCN neurons and shown that the receptor is important for maintaining high amplitude, synchronised rhythms between individual oscillatory neurons (Piggins and Cutler. 2003). Furthermore, genetic deletion of the $VPAC_2$ receptor is known to severely compromise the endogenous rhythmicity in clock gene expression but also accelerate kinetics of entrainment to LD cycles (Harmar et al. 2002).

4. Optogenetic manipulation of the mammalian clock

Activation of the receptor with Vasointestinal peptide (VIP) leads to robust induction in cAMP as well as dose dependent induction of *per2* in SCN organotypic slices (An et al. 2011). Due to the $G\alpha_s$ interactions of JellyOp, it is well placed to substitute the role of the $VPAC_2$ receptor and trigger cAMP signalling in the absence of pharmacological agents. My principal aim is thus to investigate whether temporally controlled $G\alpha_s$ signalling with JellyOp can reflect aspects of pharmacologically influences on mammalian clock dynamics, via the $VPAC_2$ receptor. This investigation will help to further establish the relevance of the $G\alpha_s$ pathway to circadian regulation.

Although less well studied, many other signalling pathways have been shown to influence the molecular clock by directly targeting components other than cAMP and CREB. Recent studies have also reported that Protein Kinase C (PKC) mediated phosphorylation of CLOCK is crucial to mediating entrainment to phorbol 12-myristate 13-acetate (PMA) stimulation (Shim et al. 2007, Lee et al. 2010). In addition to PKC other kinases such as Casein Kinase epsilon (CKε), which plays an important role in phosphorylation and nuclear translocation of clock proteins PER and CRY, are also implicated in entrainment (Badura et al. 2007). Also, Meng et al. 2010 have previously reported that inhibition of casein kinase δ (CKδ) in the SCN of *vipr*$^{-/-}$mice, in which molecular pacemaking was compromised, was able to induce robust rhythms of clock gene expression. In support of this, free-running behaviour in mice was entrainable to daily injections of the isoform specific inhibitor PF-670462, in contrast to saline injections. The membrane receptors which regulate these kinase activities are unknown, nonetheless, it is possible that given the complex signalling interface, GPCRs may be involved, especially in light of G protein independent signalling.

The physiological importance of G protein independent signals is becoming increasingly recognised, though little is known about their impact on mammalian circadian organisation. I thus sought to investigate this further with an optogenetic approach. The F139A JellyOp is an appropriate candidate tool for such investigations; although previous studies failed to identify β-arrestin interactions, they did demonstrate that this opsin photopigment could initiate a signalling pathway that substantially affected MAPK signalling without discernible induction of $G\alpha_s$, $G\alpha_i$ and calcium signalling. Such a cAMP-decoupled counterpart to JellyOp would allow me to explore $G\alpha_s$ dependent and independent influences on the mammalian clock.

4. Optogenetic manipulation of the mammalian clock

I hypothesised that JellyOp would be able to perturb the kinetics of the mammalian transcriptional-translational feedback loop in a phase and dose dependent manner. In addition, my second hypothesis was that JellyOp mediated responses was dependant on the $G\alpha_s$ pathway, irrespective of other intracellular cascades, and that in the absence of cAMP signalling, a $G\alpha_s$ decoupled JellyOp photopigment would be less able to impact on all aspects of the mammalian clock such as rhythm amplitude and phasing. To observe these circadian responses, the oscillatory dynamics of *per2* gene expression was surveyed in rat1 fibroblasts before and after activation of JellyOp based pigments.

For the experimental model, I utilised a *per2::luc* rat1 fibroblast model of the mammalian circadian clock. These cells harbour a minimal *per2* reporter which enables the surveillance of *per2* expression under the transcriptional influence of E-box elements in real-time, and thus captures the dynamics of rhythmic BMAL1/CLOCK mediated transcription with high resolution before and after JellyOp photoactivation. As shown in the previous chapter, I generated isogenic lines of fibroblasts stably expressing JellyOp and F139A JellyOp to enable activation of these divergent signalling pathways in a drug-free system.

4. Optogenetic manipulation of the mammalian clock

4.2 Materials and methods

4.2.1 Maintenance of isogenic JellyOp and F139A JellyOp expressing *per2::luc* expressing rat1 fibroblast lines

Monoclonal stable JellyOp and F139A JellyOp expressing cell lines were selectively maintained in supplemented Dulbecco's modified Eagle's medium (4,500 mg/l DMEM, D-glucose, sodium pyruvate and L-glutamine, 10 % foetal bovine serum, 1 % penicillin and streptomycin) with 100 µg/ml hygromycin, and 400 µg/ml G418 (InvivoGen) under dim red light. All fibroblast cell lines were passaged at ratio of 1:6 every 3-4 days under sterile conditions.

4.2.2 Recording medium for bioluminescence recording of *per2::luc* fibroblasts

The recording medium for bioluminescence recordings of fibroblast cultures consisted of 10 g/l Dulbecco's modified Eagle's medium supplemented with 3.5 g/l D- Glucose (Sigma Aldrich), 350 mg/ml Sodium Bicarbonate (Sigma Aldrich), 10 mM Hepes buffer, 2 % B27 (Life Technologies), 20 U/ml Penicillin and 25 µg/ml Streptomycin (Sigma Aldrich), 200 µM beetle Luciferin (Promega) and 10 µM Forskolin (Sigma Aldrich).

4.2.3 Bioluminescence recordings for *per2::luc* fibroblasts and light stimulation protocol

Prior to recording, cells were synchronised with 200 nM dexamethasone (Sigma Aldrich) for 1 hour, after which medium was replaced with recording medium. Cell dishes were then sealed with glass coverslips using high vacuum grease (Dow Corning) and bioluminescence recordings were conducted within a Lumicycle machine (Actimetrics) housed in a 37°C incubator. The photon count was sampled from each well with 75 seconds resolution at 10 minute intervals. Following 3 days of luminescence recordings, dishes were exposed to 4 hours of 5 second light steps every 30 seconds whilst placed underneath a light source adjacent to the lumicycle within the same incubator. White light from a Fiber-Lite® DC950 Illuminator (Dolan-Jenner Industries) was fed into the incubator through a liquid light guide (Knight photonics) with a UV and infrared cut-off and controlled via a programmable shutter (Cairn). Irradiance at the level of the cells was 28.40 mW/cm^2.

4.2.4 Methods for processing rhythm data

The raw data were exported to Microsoft Excel (Microsoft) where analysis of rhythm parameters was performed. Prior to analysis, the 24 hours running average was deducted from the raw data to filter out baseline deviations in the *per2::luc* rhythm. Furthermore, the detrended data were averaged over 2 hours to filter out high frequency fluctuations in bioluminescence signal. The troughs and peaks of the fibroblast rhythm were assigned CT0 and CT12 respectively.

4.2.5 Methods for rhythm amplitude analysis

The oscillatory amplitude was measured as the peak to trough difference from the processed rhythm data. Relative amplitude changes were calculated as the percentage difference in amplitude between the oscillation following light treatment and the 2nd (unperturbed) oscillation of the recorded rhythm. Changes in amplitude were plotted as a function of the circadian time at which the light pulse was delivered.

4.2.6 Methods for phase shift and period analysis

To measure light induced phase responses in the *per2::luc* rhythm, a continuous sine wave was modelled over the unperturbed rhythm prior to treatment. The sine wave was used to extrapolate the theoretical phase of the unperturbed fibroblast rhythm. Assigning the peaks and troughs as reference markers, the phase shift was scored as the temporal difference between the sine wave and the processed rhythm data following light treatment. The phase shifts were plotted as a function of the circadian time at which the light pulse was delivered. Period duration of bioluminescence oscillations was measured by calculating the time lag between consecutive phase markers (peaks and troughs). The oscillatory rhythm during which the light pulse occurred was thus measured and subtracted from the average free-running period to capture immediate light induced period changes. In addition, period changes were also measured in the subsequent oscillatory cycle to assess latent changes.

4.2.7 ELISA based quantification of cAMP in JellyOp and F139A JellyOp per2::luc rat1 fibroblasts

$5x10^5$ *per2::luc* fibroblasts were treated with 200 nM dexamethasone for 2 hours prior to bioluminescence recordings. On the second day of recording, fibroblast cultures were removed from the lumicycle at various times of the circadian day lysed in 300 µl of 0.1 M HCl solution for 10 minutes at room temperature. Cell lysates were collected from the culture dishes using cell scrapers (Greiner BioOne) and centrifuged at 600 xg for 10 minutes. 100 µl of supernatant treated with 5 µl acetylation reagent (1:2 acetic anhydride: triethylamine) before determination of cAMP level by direct EIA (10µl/well) according to the manufacturer's instructions (Sigma Aldrich). Optical measurements were conducted using a platereader at 405 nm. The protein content was determined with Fluka protein quantification kit (Sigma Aldrich) and optical measurements performed at 455 nm.

4.3 Results

4.3.1 Free-running rhythm periods of *per2:luc* fibroblasts lacking or expressing JellyOp or F139A JellyOp

Based on the findings of the previous chapter, JellyOp and F139A JellyOp elicited cAMP-dependent and independent signalling pathways in fibroblasts respectively but both pigments were able to modulate MAPK signalling in a comparable manner. Therefore, I sought to impose these differential signalling cascades on the fibroblast clock under a temporally controlled manner and observe their influence on various mammalian clock parameters such as period, phase and amplitude.

Prior to this, I characterised baseline circadian profiles of *per2* rhythmicity in the *per2::luc* fibroblasts which either express or lack exogenous opsin pigments. Thus, I recorded free-running rhythms of bioluminescence of all three fibroblast reporter lines following dexamethasone treatment over 8 days (representative traces shown in Figure 4.1 A, C, E). Upon baseline subtraction I deduced the average free-running period (FRP) of the bioluminescence rhythms from each clonal line, by measuring the temporal intervals between phase markers such as rhythm peak and trough (Figure 4.1 B, D and F). I report that the average FRP for *per2::luc* fibroblasts was 22.4 ± 0.4 hours, whereas both JellyOp and F139A expressing fibroblasts exhibited slightly shorter periods of 22.1 ± 0.6 hours and 22.3 ± 0.4 hours respectively. However, such clonal differences in free-running period were not significant.

I also report different rates of damping in free-running rhythms between clonal lines. In *per2::luc* and JellyOp *per2::luc* fibroblasts, rhythmic phase markers remained distinguishable despite damping of rhythm amplitude over 8 days (4.1 B and D). However, F139A JellyOp expressing fibroblasts exhibited the lowest rhythm amplitude overall (4.1 E and F), where after 4 consecutive oscillations, phase markers become difficult to identify from background noise.

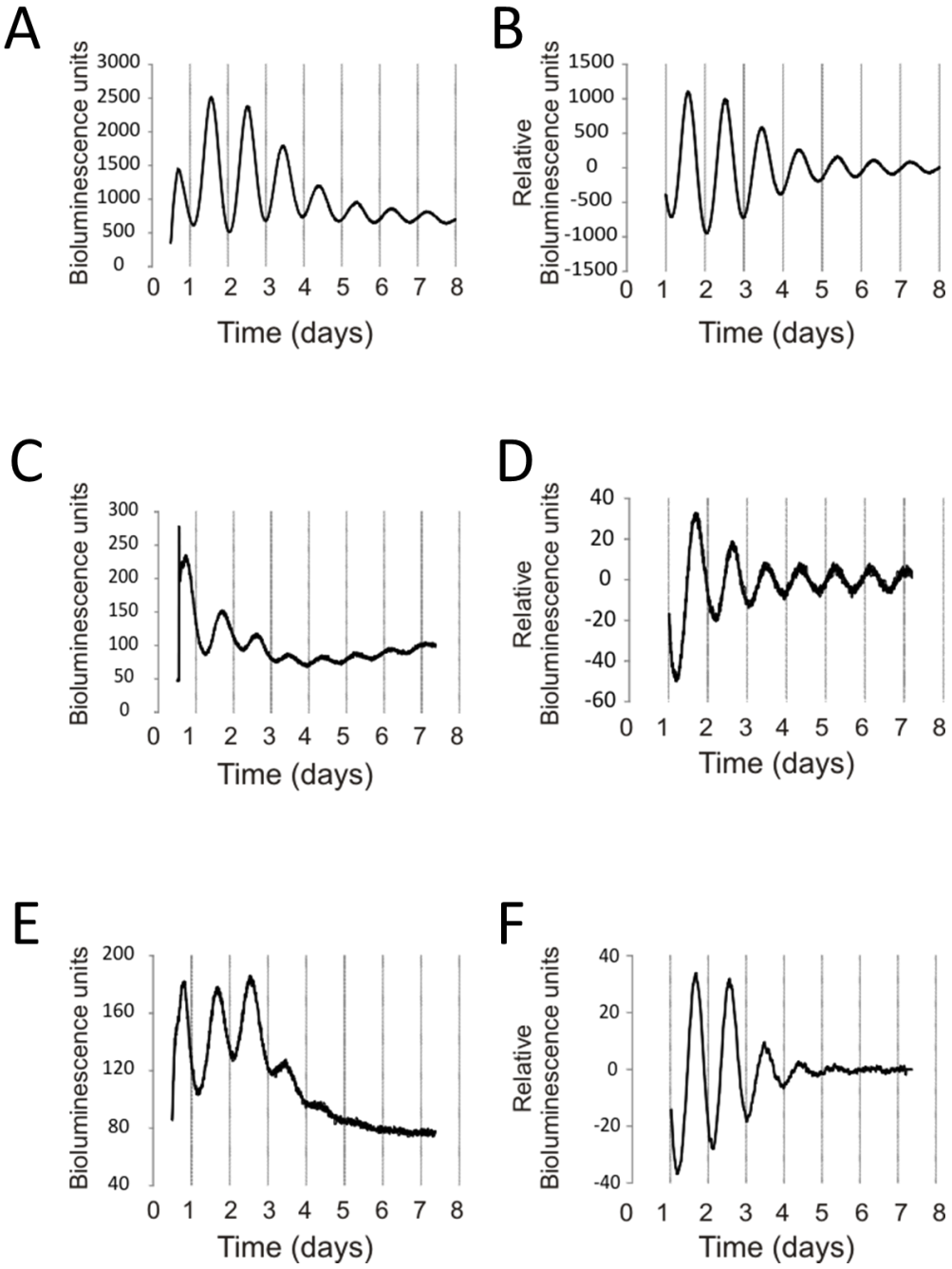

Figure 4.1 *per2::luc* rat1 fibroblasts stably expressing JellyOp photopigments sustain rhythm circadian oscillations of bioluminescence in culture

(A) Representative rhythms of bioluminescence recorded from isogenic cultures of *per2::luc* reporter fibroblasts cells presynchronised with 200 nM Dexamethasone. Horizontal lines correspond to 24 hours intervals along the x axis for all rhythm traces. (B) To correct for drifting baselines and enable quantification of rhythm amplitude, each bioluminescence value was subtracted from the 4 hours moving average. Representative trace of rhythmic bioluminescence captured from 200 nM Dexamethasone synchronised isogenic stable lines of (C) JellyOp and (E) F139A JellyOp expressing *per2::luc* fibroblasts, with corresponding detrended rhythm profiles (D and F).

4.3.2 Light dependent circadian responses in JellyOp and F139A JellyOp expressing fibroblasts

To determine whether JellyOp mediated fluctuations in cAMP could perturb the fibroblast clock, 5 second light pulses were delivered to all fibroblast cultures at every 30 second intervals over 4 hours across the circadian day. Immediately after light stimulation, the bioluminescence recording captured a transient spike and rapid exponential decline in bioluminescence from all three fibroblast lines (Figure 4.2 A, C, E). Given the rapidity of this response it is unlikely to reflect sudden changes in *per2::luc* transcription, and more likely to be due to the photo-reactivity of the luciferase substrate, luciferin, in the recording media.

Following light stimulation, I continued to measure the bioluminescence for another 3-4 days to quantify changes in phase and amplitude. I report that exposure of JellyOp expressing fibroblasts to 4 hours intermittent light elicited robust phase responses in a temporally gated manner. As shown in Figure 4.2 C and D, light treatment delivered on the rising and falling limbs of the bioluminescence rhythm elicited phase advances and delays respectively. In contrast, light administered near the circadian peak, CT12, produced minimal phase shifts. Thus the nature of the phase response was highly dependent on the circadian phase of application.

I proceeded to investigate the effect of F139A JellyOp photostimulation on circadian clock parameters, thus subjected F139A expressing fibroblasts to the same light treatment regime and recording protocols for JellyOp. As shown in Figure 4.2 E and F, F139A expressing cells do indeed respond to light through phase adjustments. Light treatments occurring just after the circadian peak of the *per2* rhythm yielded phase delays whereas light pulses delivered before the rhythmic trough produced phase advances.

Light treatment did not influence the phasing of *per2::luc* fibroblasts at any time of the circadian day (Figure 4.2 A and B), which supports the contributions of JellyOp and F139A JellyOp phototransduction in mediating robust light driven phase responses. Thus, I can be confident that JellyOp and F139A JellyOp expressing fibroblasts are directly entrainable to a 4h light pulse.

4. Optogenetic manipulation of the mammalian clock

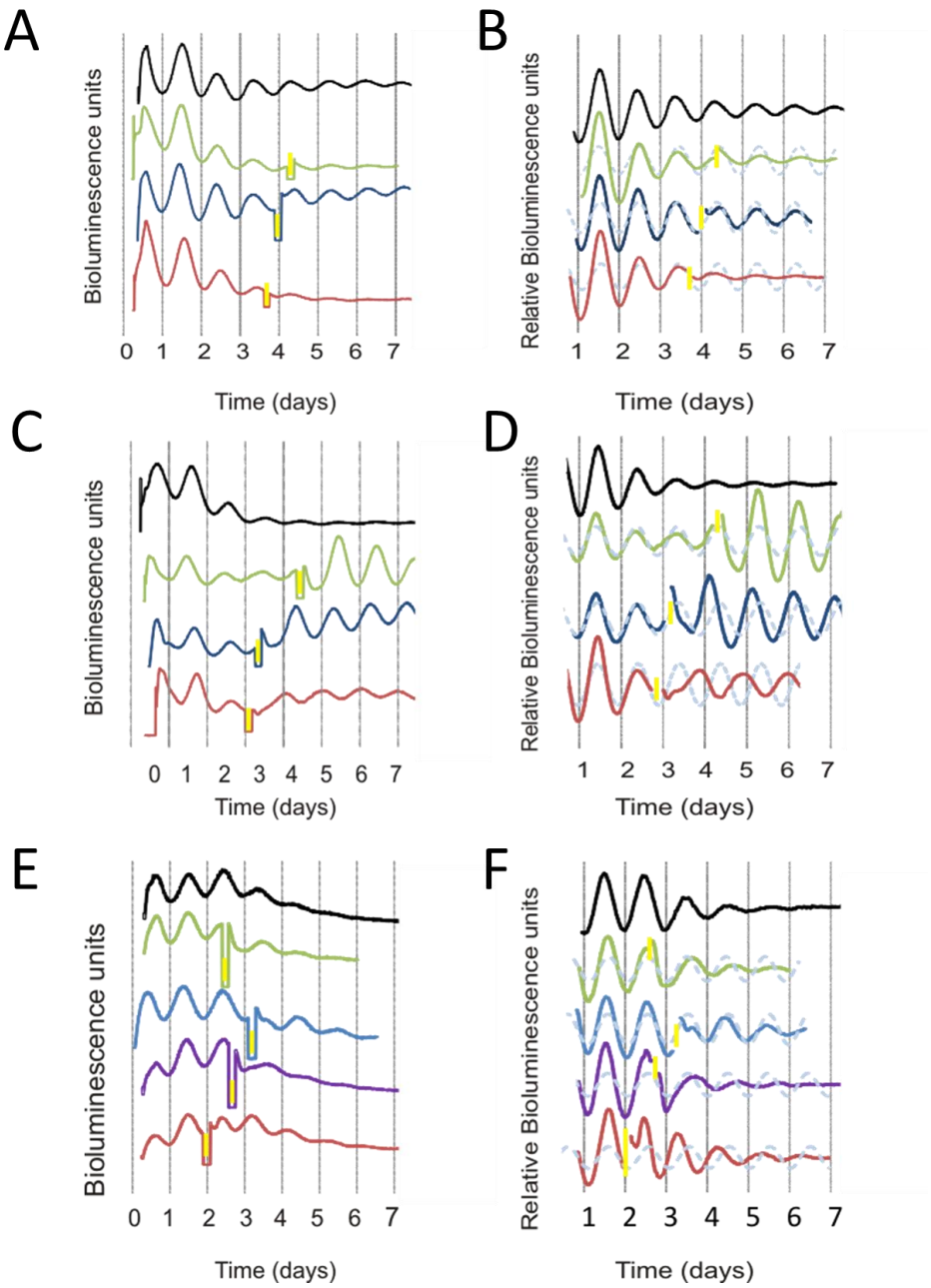

Figure 4.2 Light modulates the phasing and amplitude of *per2::luc* rhythm in JellyOp expressing cells in a phase dependent manner

(A) To explore the impact of opsin photoactivation on the phasing of the *per2* rhythm, cultures of (A) *per2::luc* fibroblast, (C) JellyOp WT and (E) F139A JellyOp *per2::luc* fibroblasts were exposed to 4h of intermittent, infra-red and ultraviolet filtered bright white light (28.40 mW/cm^2) at various phases of the *per2* rhythm (indicated by yellow arrows). In all panels, the black trace represents the rhythm captured from unperturbed cells. (A) Green, blue, and red traces represent bioluminescence rhythms captured from individual *per2::luc* fibroblast cultures pulsed at the circadian peak (CT11.2), rising limb (CT 2.1) and falling limb (CT 17.3) of *per2* rhythm respectively. (C) Green, blue and red traces represent bioluminescence rhythms captured from individual JellyOp WT *per2::luc* fibroblast cultures pulsed at the circadian peak (CT11.8), rising limb (CT 3.1) and falling limb (CT 19.6) of *per2* rhythm respectively. (E) Green, blue, purple and red traces represent bioluminescence rhythms captured from individual F139A JellyOp *per2::luc* fibroblast cultures pulsed at the circadian peak (CT12.5), rising limb (CT 2.6) and falling limbs (CT 16.9) and (CT22.4) of the *per2* rhythm respectively. (B, D, F) For phase analysis, baseline corrected bioluminescence rhythms prior to light treatment were modelled by a sine wave. The temporal deviation between the peaks and troughs of the sine wave and sampled bioluminescence over 3-4 days after the light pulse was quantified. Relative changes in rhythm amplitude were quantified for the cycle immediately following light treatment compare with that of dexamethasone pre-treatment.

To further describe the phase dependent responsiveness of the JellyOp and F139A JellyOp expressing fibroblasts to light, I constructed phase response curves for each opsin by plotting the phase shift as a function of the circadian time at which light exposure started (Figure 4.3 A and B). For WT JellyOp expressing fibroblasts, phase advances and delays were most prominent around CT0/24, giving maximal phase delays and phase advances of 8.6 and 11.2 hours respectively (Figure 4.3 A). Due of the scaling of the PRC, the waveform appears such that the transition from phase advances to phase delays is continuous at CT12, but the converse transition is abrupt at CT0. The response profile is reminiscent of a Type 0 resetting PRC, characterised by large phase responses and an absence of a dead zone. Light pulses appear to reset fibroblast clocks to a common phase around CT12 (corresponding to the point at which *per2::luc* reporter activity is maximal) irrespective of light stimulus timing, such that phase responses are greatest when light perturbation occurs towards the circadian trough (CT0).

Upon constructing the phase response curve for F139A JellyOp, I also report light induced Type 0 resetting with large phase advances and delays possible. However, the light pulses delivered before and after CT17-18 yielded the most prominent phase delays (11.8 h) and advances (8.7 h) respectively. In addition, light pulses around CT6 of the *per2* rhythm elicited minimal changes in phase (Figure 4.3 B). There was thus a clear divergence in the phase response curves for JellyOp and F139A JellyOp (Figure 4.3 C).

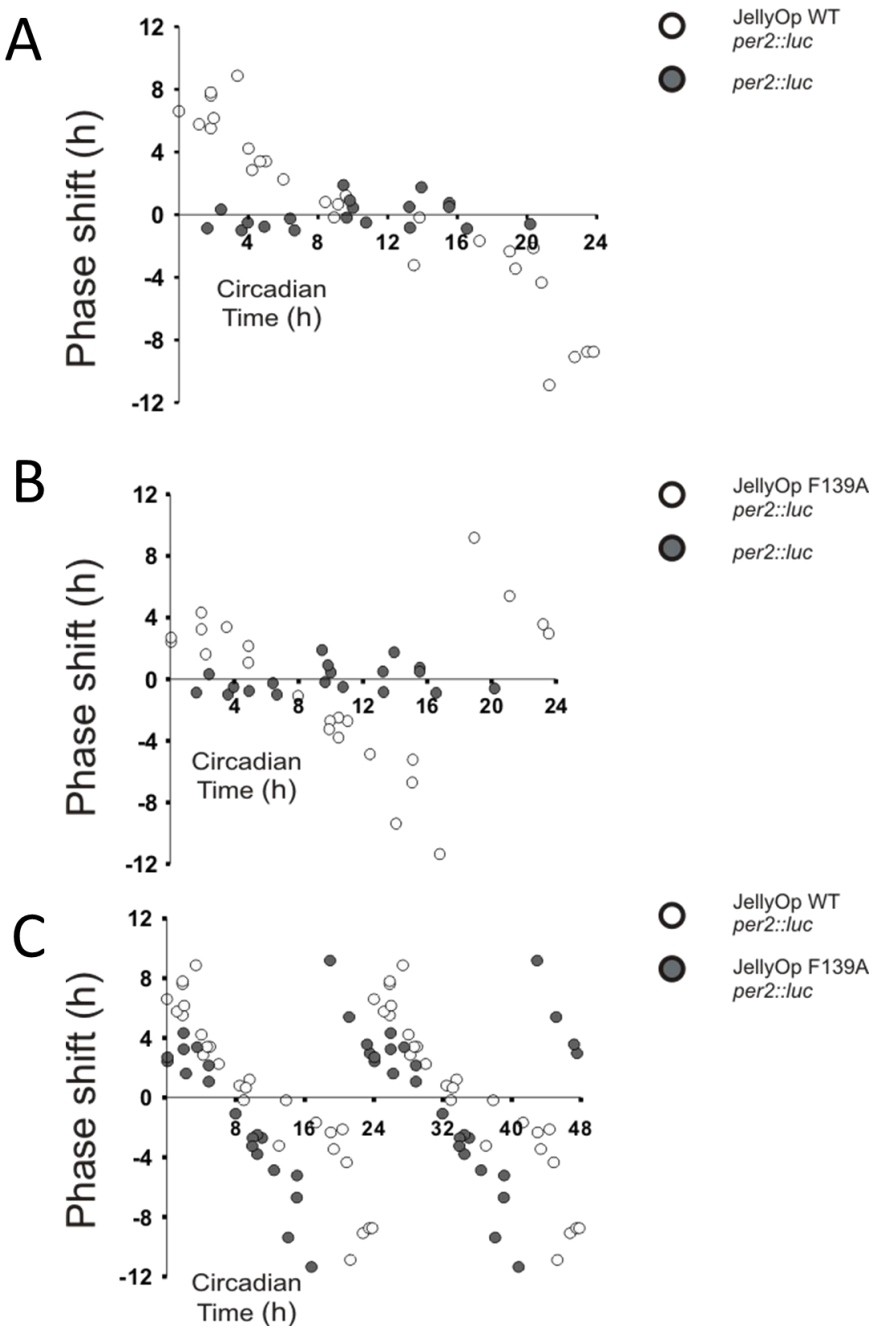

Figure 4.3 Phase response curves of JellyOp and F139A JellyOp

Phase response curve illustrating the relationship between the timing of light onset and magnitude of phase shifts in *per2* rhythm of fibroblasts (A) expressing JellyOp WT or (B) expressing F139A JellyOp. Data represent extent of phase shifts captured from individual light pulsed cultures and plotted on a y-axis where positive and negative values denote phase advances and delays respectively. The x-axis corresponds to the timing of light onset in circadian hours where CT0 and CT12 represent the free-running rhythm trough and peak respectively. Phase shifts were also measured in hours and represented as circadian hours, by multiplying the actual phase shift in hours by the ratio of 24/free-running period. (C) Double plotted phase response profiles for JellyOp and F139A JellyOp expressing fibroblasts.

4.3.3 Phase dependent induction of rhythm amplitude in light stimulated JellyOp fibroblasts

In addition to phase resetting, I also report that light stimulation impacted the relative amplitude of the post stimulated *per2* rhythm of JellyOp expressing fibroblasts in a phase dependent manner. Upon plotting the amplitude of post-stimulus oscillation as a function of circadian onset, I noted that when light onset occurring during between CT0-20 of the *per2* rhythm robustly induced oscillatory amplitude which was comparable to 200 µM dexamethasone pre-treatment (Figure 4.4). Interestingly, as light onset tended towards the circadian trough of *per2*, the maximal post-stimulus amplitude became progressively diminished. Indeed, the lowest amplitude changes were observed around CT22-24.

Augmentation in post-stimulus rhythm amplitude was also observed in many cultures of light pulsed F139A JellyOp fibroblasts. Post-stimulated amplitude ranged from 20 -70 % of dexamethasone pre-treatment but did not correlate strongly with the timing of light onset. Furthermore, maximal changes in amplitude were generally smaller than those reported in WT JellyOp fibroblasts (Figure 4.4 C). *per2:luc* fibroblasts without opsin expression showed minimal changes in amplitude when light pulsed across the circadian day, with post-stimulus amplitudes ranging from 10-30 % dexamethasone treatment (Figure 4.4 A and B).

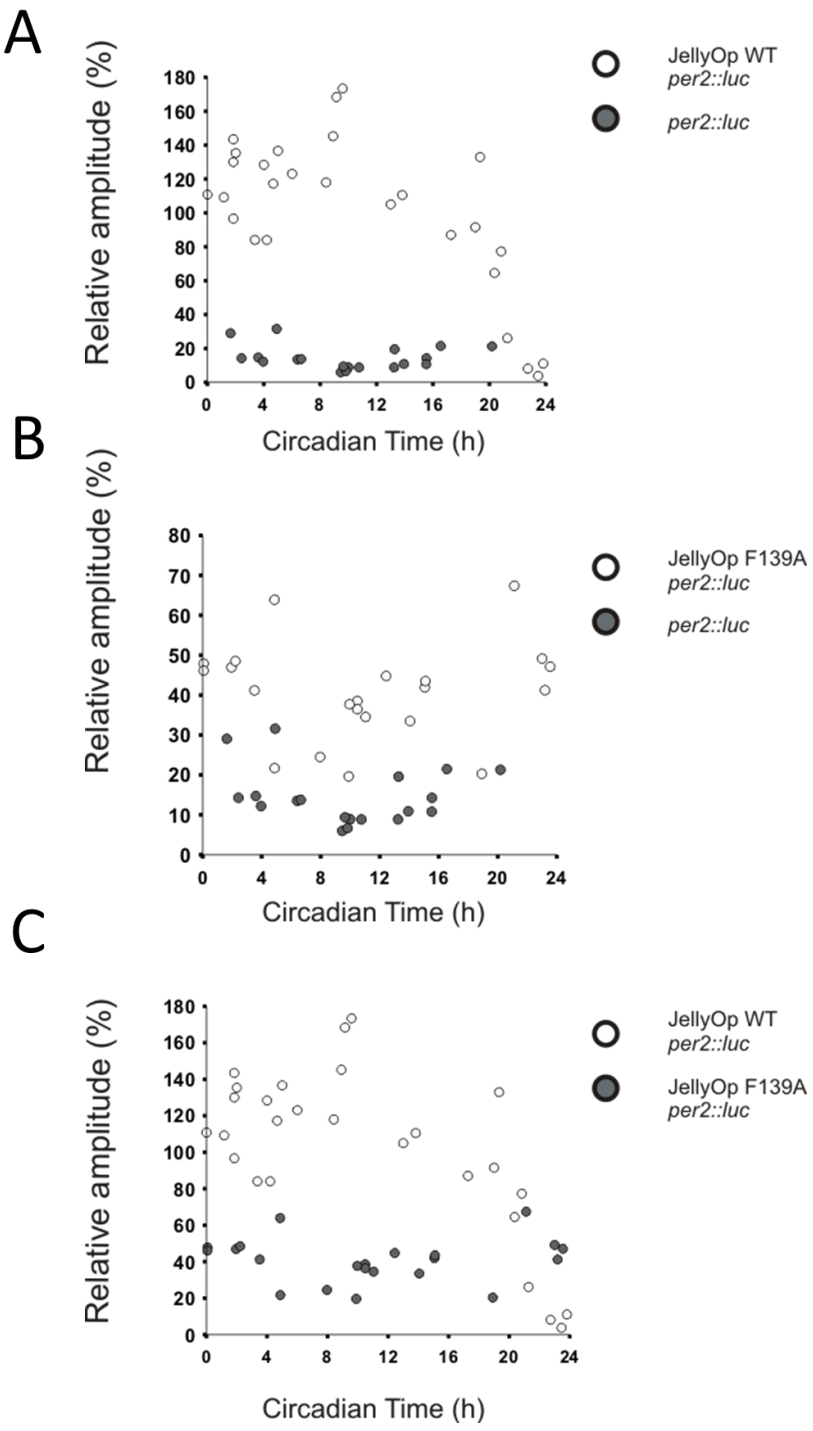

Figure 4.4 Amplitude response curves of JellyOp and F139A JellyOp

Amplitude response curves to illustrate the relationship between the timing of light onset and relative amplitude of *per2* rhythm in light treated fibroblasts (A) expressing JellyOp or (B) expressing F139A JellyOp. Data points relative amplitude of individual samples after a light pulse, plotted in the y axis. The x-axis corresponds to the timing of light onset in circadian hours. (C) A comparison of the amplitude response profiles between JellyOp WT and F139A JellyOp expressing *per2::luc* fibroblasts.

4.3.4 Divergent kinetics of phase adjustment between JellyOp and F139A JellyOp expressing fibroblasts

Upon comparing rhythms of JellyOp and F139A JellyOp expressing fibroblasts which attained similar phase responses, transient circadian responses which followed light stimulation were very divergent between the two cell lines, reflecting differences in kinetics of entrainment. Figure 4.5 A to C shows an alignment of comparably phase shifted rhythms between light stimulated JellyOp and F139A JellyOp fibroblast lines. In these phase shifted rhythms, light stimulation induced rhythm perturbation of divergent kinetics between the two lines such that rhythmic peaks and troughs were transiently misaligned. As phase changes stabilised, the same phase markers became synchronised between the two rhythms, as before light stimulation.

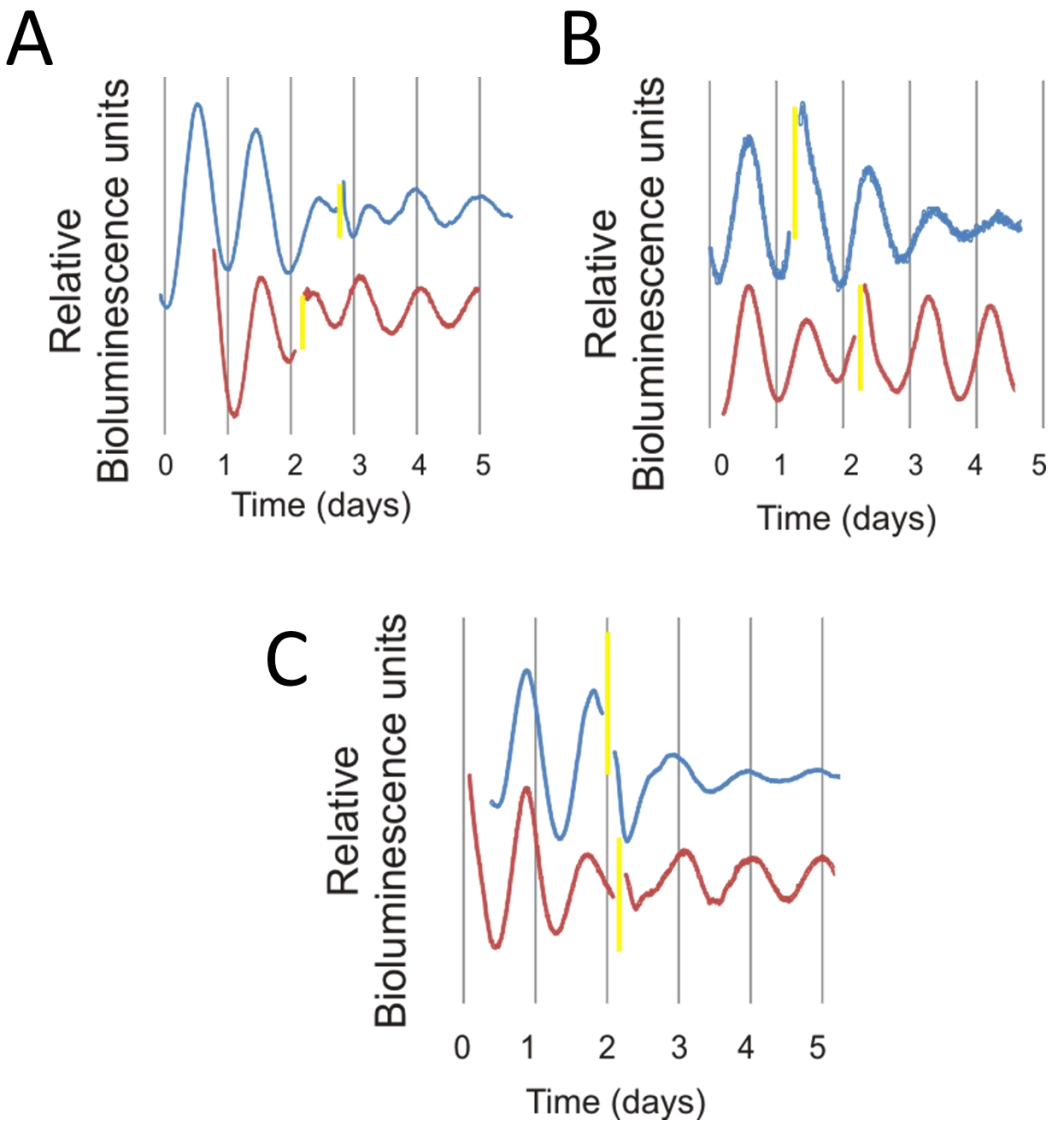

Figure 4.5 Transient perturbations in the rhythm of phase shifted JellyOp WT and F139A JellyOp expressing fibroblasts

Paired bioluminescence rhythms of WT JellyOp (red) and F139A JellyOp (blue) expressing fibroblasts both exhibiting phase advances of (A) 9.5 hours, (B) 1 hours, and delays of (C) 9.2 hours following exposure to 4 hours of light (indicated by yellow line).

I observed that in all phase shifted rhythms captured from wildtype and F139A JellyOp expressing cells, the period of the post-stimulus *per2* rhythm was transiently perturbed before a stable new phase was established. Thus, I proceeded to investigate the relationship between phase responses and transient changes in rhythm period. I plotted light induced deviations from the free-running period as a function of light onset for both JellyOp and F139A JellyOp expressing cells. In particular, I measured period deviations in two *per2* oscillations; to capture rapid changes in period immediately following light exposure I measured the oscillatory period which coincided with the onset of light pulse. Also, I measured the subsequent free-running period of the subsequent oscillation to determine any latent changes in period.

In doing so, I noted that for JellyOp expressing cells, light onset between CT0-4 immediately yielded a reduction in period duration, whereas light onset between CT4-24 elicited longer periods (Fig 4.6 A). Subsequent free-running oscillations showed less deviation from the average free-running period. Although period measurements were based on the temporal intervals between consecutive rhythm troughs, these temporal deviations were also reflected in the rhythm peaks.

An exception to this pattern was observed for 3 fibroblast cultures pulsed between CT22-24. These rhythms yielded high amplitude phase delays (Figure 4.3 A) as well as marked diminution in post-stimulus rhythm amplitude (Figure 4.4 A). Due the masking of the circadian trough during the light exposure, I measured the temporal intervals between rhythm peaks to capture changes in period. There were minimal disturbances in the timing of rhythm acrophase before and immediately after the light pulse. However, in the subsequent oscillation, there was a sudden shortening in the peak-to-peak interval.

In F139A expressing fibroblasts, light exposure across the phases did not immediately impact on the rhythm period. However, in the subsequent free-running rhythm, period deceleration became increasingly prominent as light was delivered from CT2-14 (Figure 4.6 B). In contrast, application of light at CT18-24 produced latent shortening in period.

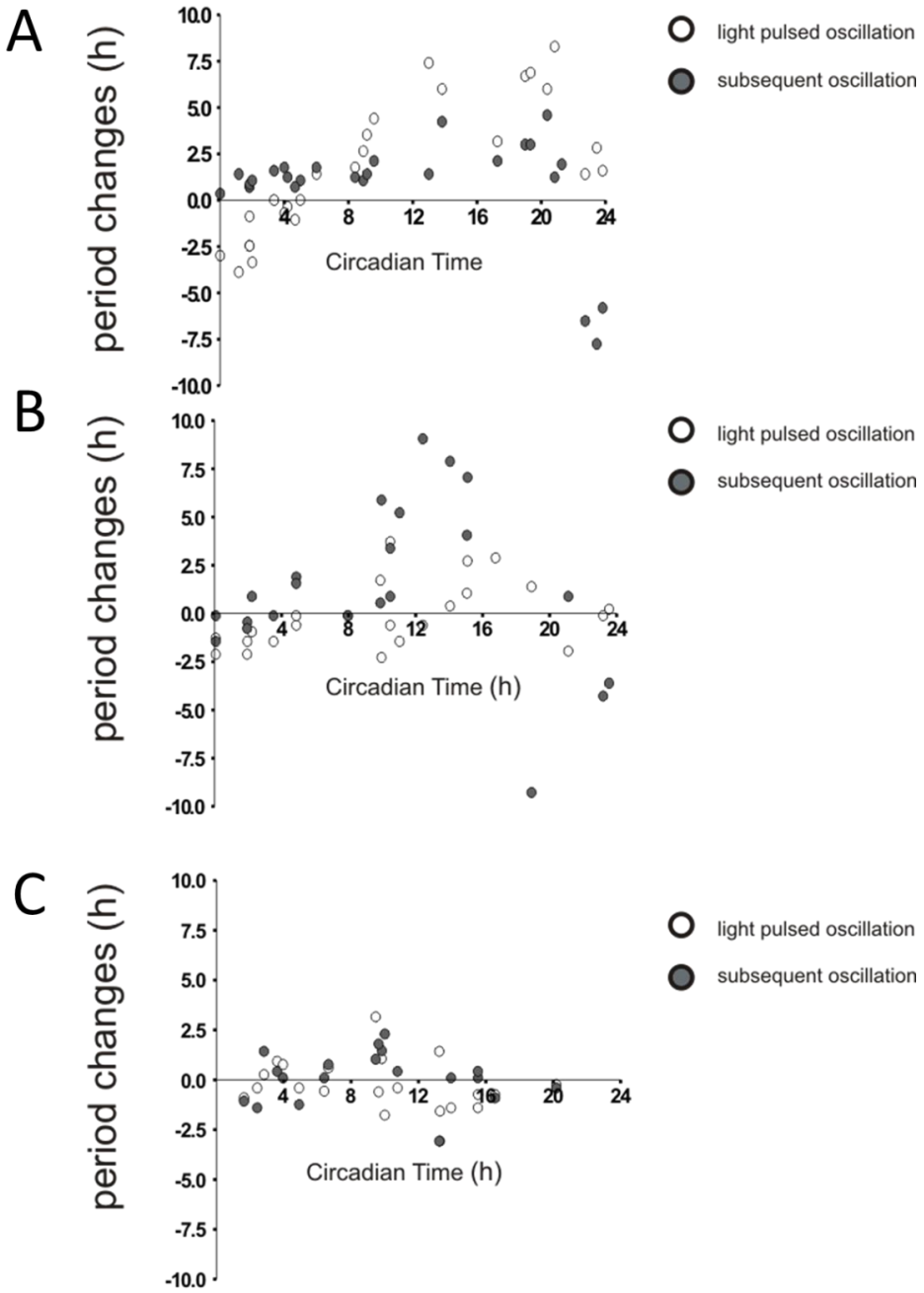

Figure 4.6 Phase dependent changes in rhythm period between JellyOp WT and F139A JellyOp expressing fibroblasts

Changes in circadian period for the circadian oscillation at which light was presented is plotted as a function of the circadian time of light exposure for (A) JellyOp *per2::luc*, (B) F139A JellyOp *per2::luc* and (C) *per2::luc* expressing fibroblasts (white circles). Also, changes in circadian period of the subsequent oscillation are plotted on the same axis for each cell line. Shortening and lengthening in period is represented by negative and positive values respectively. When a light pulse masks the timing of rhythm trough, the peaks were used as phase markers. White circles refer to period changes in which the light pulse occurred and black circles indicated period changes in subsequent consecutive oscillation.

When period changes were plotted as a function of phase adjustments for JellyOp expressing fibroblasts, I observed that overall, period lengthening correlated with phase delays (Figure 4.7 A). However, there is still the exception that the 3 phase delayed fibroblast rhythms (pulsed at CT22-24) produced a latent acceleration of period. For F139A JellyOp expressing fibroblasts, oscillations in which light pulse occurred did not deviate substantially irrespective of magnitude of phase response (Figure 4.7 B). However, subsequent oscillations exhibited a trend in which phase delays were associated with lengthening in rhythm period. *per2::luc* fibroblasts which lack exogenous pigments showed indiscernible period changes when light pulsed at any time of the *per2* rhythm, either during and after the light pulse (Figure 4.6 C).

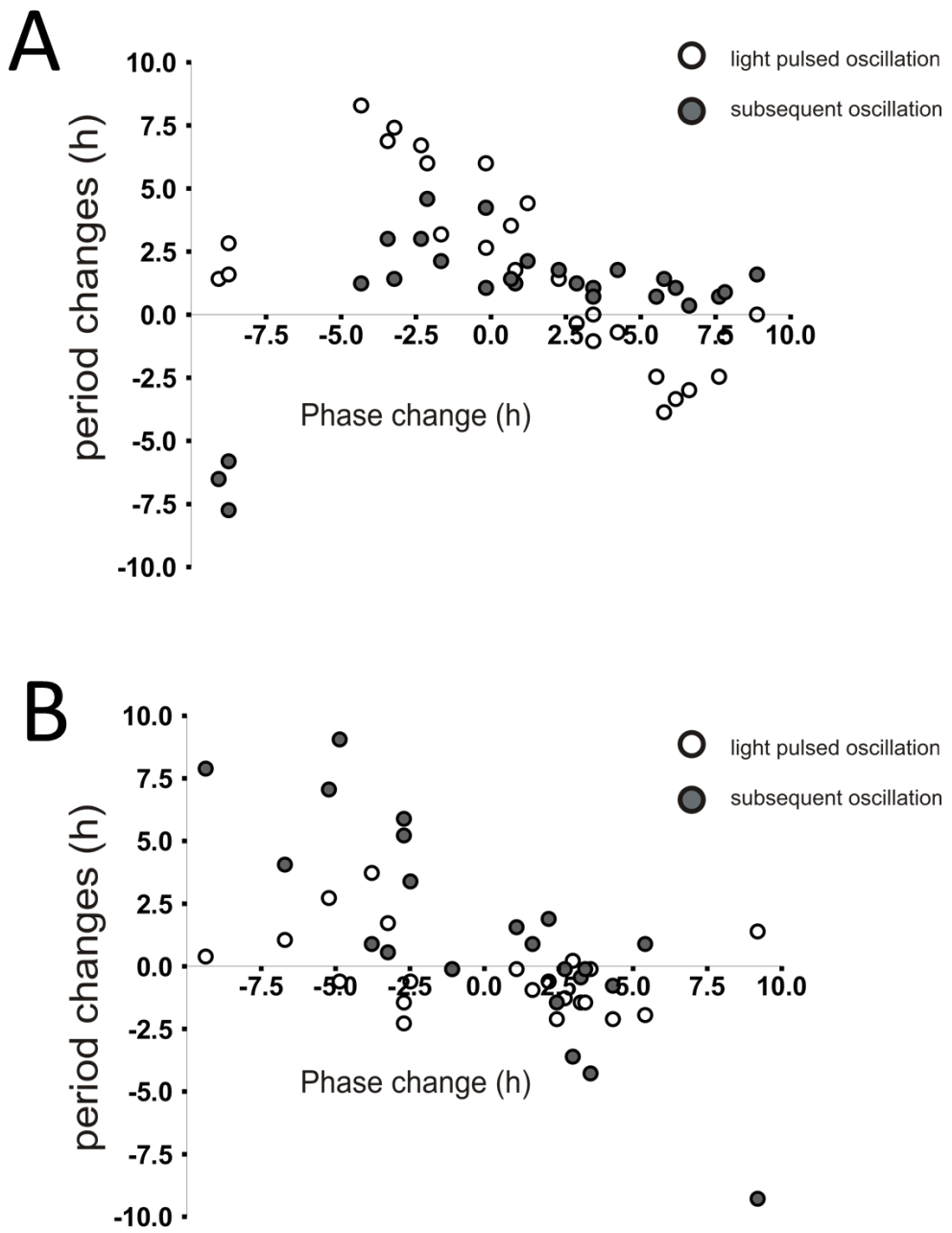

Figure 4.7 Differential kinetics of period adjustments between JellyOp WT and F139A JellyOp expressing fibroblasts

The relationship between the magnitude of phase shift and the period of the *per2::luc* luminescence rhythm quantified for (A) JellyOp and (B) F139A JellyOp expressing *per2::luc* fibroblasts. Data points represent the trough to trough intervals between the *per2* oscillation in which the light pulse was presented and subsequent circadian oscillation. Trough-to-trough intervals are plotted on the y axis in hours, whereas the x axis represents the magnitude of phase shifts in circadian hours. In JellyOp WT expressing fibroblasts, light rapidly elicited transient lengthening and shortening of period, whereas the period of subsequent oscillations were relatively stable. In F139A expressing fibroblasts however, light elicited modulation of circadian period strongly in the subsequent oscillation.

4.3.5 Circadian fluctuations of cAMP levels in fibroblasts

I sought to establish the relationship between cellular cAMP levels and the amplitude of phase response in fibroblast cultures. To this end, I quantified the concentration of cAMP in free-running *per2::luc* fibroblasts at different phases of the endogenous *per2* rhythm. Indeed, I reported a strong circadian deviation in cAMP concentration where the highest concentrations were observed between CT21-2 (Figure 4.8 A). It is noteworthy that peak cAMP levels occurred around the circadian trough of *per2* rhythm, whereas the lowest levels of baseline cAMP were located between CT8-16 of the *per2* rhythm, coinciding with high levels of *per2* expression. When the circadian profile of cAMP concentrations were superimposed over the phase response curve for JellyOp, I report that large and small phase responses coincided with relatively high and low basal levels of cAMP respectively (Figure 4.8 B).

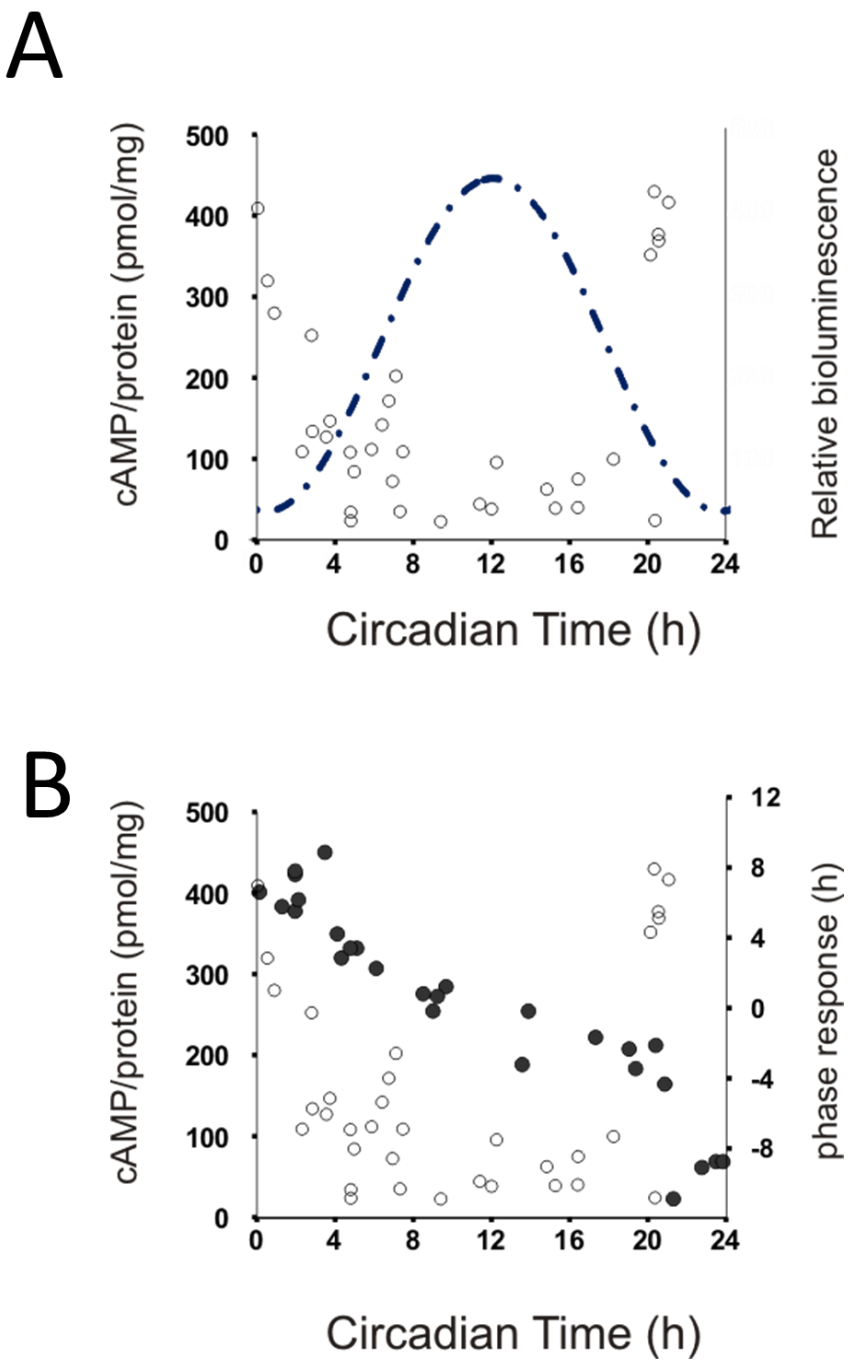

Figure 4.8 Circadian oscillations of intracellular cAMP levels in fibroblast cells

(A) *per2::luc* rat1 fibroblasts exhibit circadian rhythms in intracellular levels of cAMP. Data points represent quantities of cAMP normalised to total protein sampled from the lysate of fibroblast cultures at various phases of the *per2* rhythm with cAMP immunoassays. A circadian profile of the *per2* rhythm is transposed over the cAMP data points, on the right axis. (B) Circadian profile of cAMP levels in *per2::luc* fibroblasts over overlaid with phase response curve of JellyOp expressing fibroblasts on the right axis.

4.3.6 Dose dependent phase and amplitude responses to JellyOp phototransduction

It is likely that sustained JellyOp phototransduction is also accompanied by negative feedback mechanisms that could diminish the photosensitivity of JellyOp or attenuate downstream signalling components. Thus, I sought to assess the effective duration of JellyOp photoactivation on *per2* phase and amplitude. Upon exposing JellyOp expressing fibroblasts to various durations of light between 0-4 hours around circadian phases CT2-4, I reported duration dependent changes in rhythm phasing, period and amplitude (Figure 4.9, A and B). JellyOp expressing fibroblast rhythms exhibited progressively larger phase responses with increasing pulse durations. Similarly, transient accelerations in rhythm period were observed immediately after light pulse in a duration dependent manner. Rhythm amplitude was also induced, particularly with 4h of light compared to the other durations (Figure 4.9, B). In contrast, *per2::luc* fibroblasts showed minimal circadian changes with all durations of light stimulus (Figure 4.9 C and D).

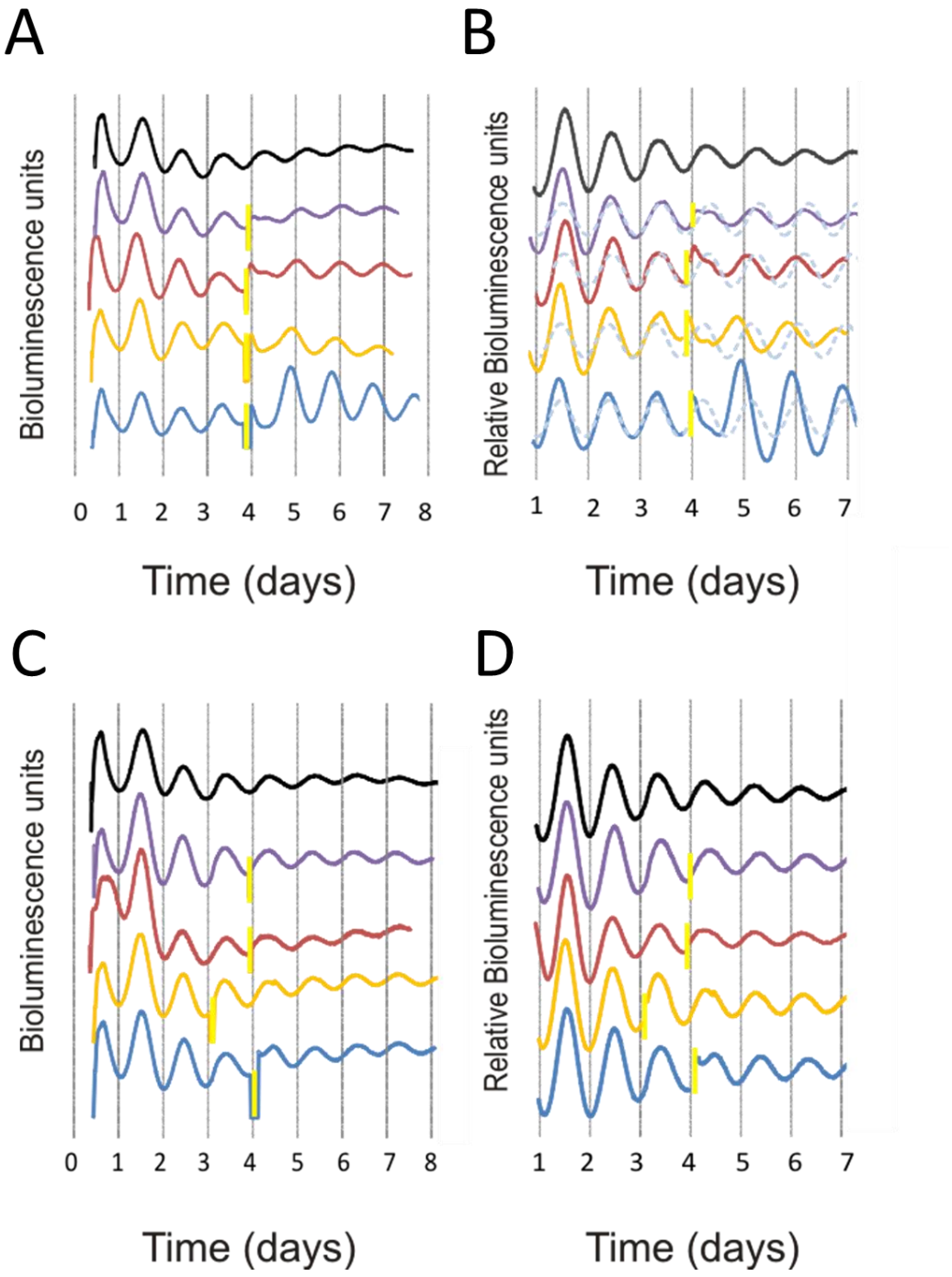

Figure 4.9 Duration dependent modulation of circadian parameters with JellyOp

(A) Representative traces of bioluminescence rhythms sampled from cultures of JellyOp WT rat1 fibroblasts and (C) *per2::luc* fibroblasts, exposed at CT2-4 to bright white light (28.40 mW/cm^2) for various durations of time. In all panels, the black trace represents the rhythm captured from unperturbed cells and purple, red, yellow and blue traces represent rhythms of fibroblasts subjected to 30 minutes, 1, 2 and 4 hours of light respectively. (B and D) Baseline corrected bioluminescence traces from respective samples, modelled with sine waves, show progressively greater temporal deviation between the sine wave and detrended trace of bioluminescence in JellyOp WT expressing fibroblasts, following increasing durations of light.

The magnitude of phase advances increased with light-stimulus duration between 0-2 hours, where 30 minutes of stimulation was sufficient to elicit a strong phase response of up to 3.2 hours (Figure 4.10 A). 2-4 hours of light produced comparable phase response magnitudes between 6-8 hours, thus implying that a saturated response could be achieved as early as 2 hours of light.

Rhythm amplitude was progressively enhanced with increasing light pulse durations only in JellyOp expressing fibroblasts. Unlike phase responses, 4h of light treatment triggered amplitude induction of up to 131 % of dexamethasone treatment, profoundly greater than that elicited by 2 hours of light, even when phase changes were saturated (Figure 4.10, A). In contrast, fibroblasts which lacked opsin photopigments showed minimal changes in amplitude (Figure 4.10, A and B). Thus I speculate that JellyOp photoactivation could also promote synchronisation of rhythms in individual fibroblasts, which collectively yields higher amplitude rhythms overall in culture.

Temporal compression of rhythm period was also reported with increasing duration of light. When period change was plotted as a function of light stimulus duration, compression of period of up to 6.3 hours was elicited with 2 hours of light, with no further noticeable enhancement after 4 hours of light (Figure 4.10, C). Interestingly, phase responses also saturated between 2-4 hours of light, which suggests a relationship between magnitude of transient period change and phase response. Thus, it would appear that period changes precede the establishment of a stable new phase, as previously described for light stimulation at other phases of the *per2* rhythm in both JellyOp and F139A JellyOp expressing fibroblasts.

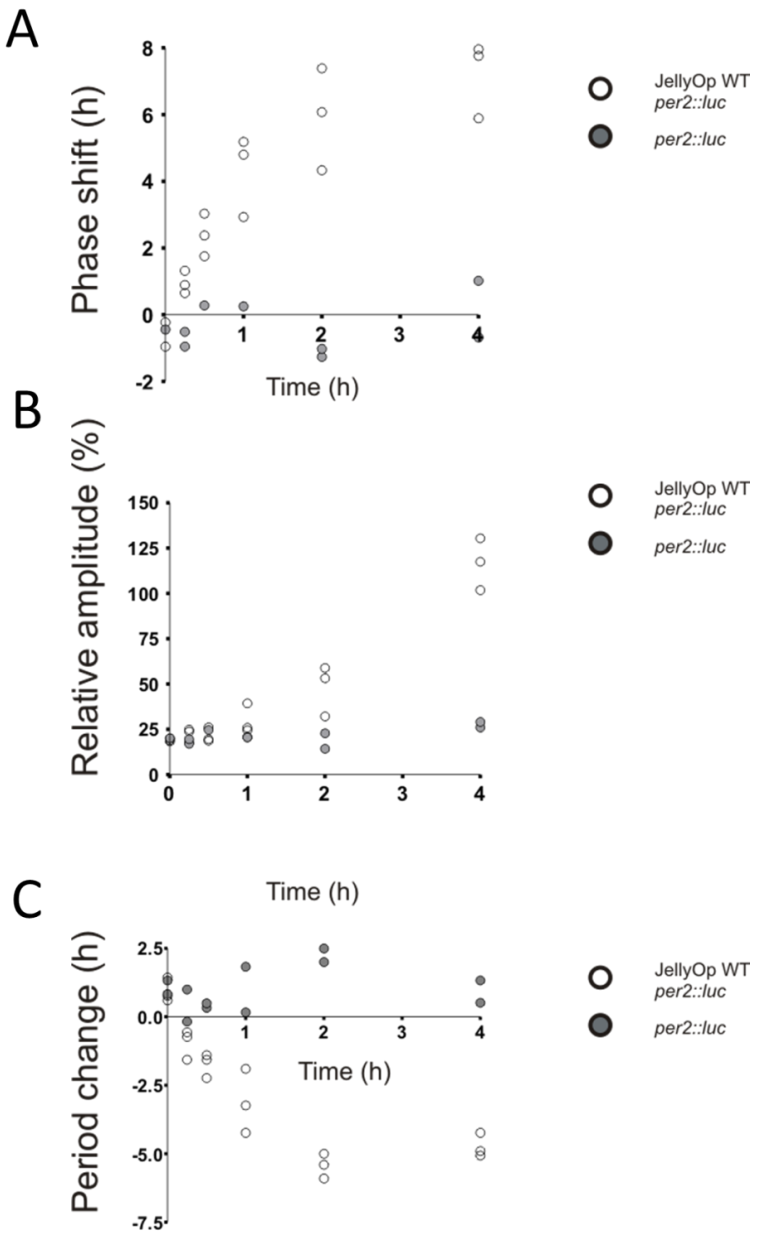

Figure 4.10 Circadian phase, period and amplitude of the *per2* rhythm is regulated by light in a duration dependent manner

(A) Relationship between light pulse duration and the magnitude of the phase response. Data points represents the magnitude of phase shift in circadian hours (y axis) captured from individual cell cultures, over duration of light pulse in hours (x axis). Advances in phase correlate with duration of light pulse, but begin to plateau after 2 hours, thus implicating the limit of entrainment under such experimental conditions. (B) Relationship between duration of light treatment and relative amplitude of the *per2* rhythm in WT JellyOp expressing fibroblasts. The relative amplitude of the *per2::luc* rhythm exhibited a logarithmic increase over linear increments in duration of light treatment between 5 minutes - 4 hours of light, suggesting that amplitude responses could be further augmented with longer durations of light. (C) The immediate impact of light treatment on circadian period of E-box transcriptional activity was quantified with respect to duration of light pulse. Trough-to-trough intervals are plotted on the y axis in hours whereas the x axis represents the duration of light pulse, in hours.

4.4 Discussion

One of my principle aims was to examine the importance of temporally controlled $G\alpha_s$ signalling in shaping mammalian circadian clock parameters such phase, period, amplitude and kinetics of entrainment. To this end, I utilised the ability of JellyOp trigger cAMP dependent signalling cascades in the fibroblast clock. I showed that *per2::luc* rat1 fibroblast cultures expressing JellyOp and F139A JellyOp produced circadian rhythms of bioluminescence, and exhibited free-running periods that were comparable to from rat1 fibroblasts lacking exogenous opsin pigments (Figure 4.1).

Rhythm damping was consistently observed in all cultured fibroblasts under free-running conditions. This is consistent with previous studies on peripheral oscillators (Welsh et al 2004, Nagoshi et al. 2004). In particular, Welsh et al 2004 investigated single-cell circadian oscillations in primary fibroblasts dissociated from mPER2::LUC-SV40 knockin mice and reported that rhythm damping consistently occurred after each medium change. In addition the authors reported a lack of significant phase clustering under free-running conditions, which suggests an absence of functional coupling among individual cellular oscillators. This indicates that fibroblasts functioned as cell autonomous independent oscillators which were unable to influence the circadian properties of neighbouring cells. Thus it is very likely that the decline in observed rhythm amplitude of *per2::luc* fibroblasts in my study is partly due to the consumption of luciferin in recording medium and the lack of synchronisation between individual oscillators which may exhibit intrinsically variable circadian periods. Although all opsin expressing fibroblasts exhibited circadian rhythms of clock gene expression, there were dramatically higher rates of rhythm damping in F139A JellyOp fibroblasts. This is likely to be due to lower expression levels of luciferase in comparison to the other lines, but is not likely to reflect differences in synchronisation.

4.4.1 Photostimulation of JellyOp and F139A JellyOp yielded differential phase responses in fibroblast rhythms

In order to test whether JellyOp mediated changes in cAMP were sufficient to modulate the fibroblast clock, a 4 hour pulse of bright white light was delivered to cells and the after-effects of stimulation on *per2* rhythm parameters monitored. Upon detecting light induced phase responses, I proceeded to characterise light responsiveness of the opsin expressing fibroblasts with respect to endogenous *per2* expression levels.

For JellyOp expressing fibroblasts, a Type 0 phase response curve was observed where maximal phase responses were observed around CT0 (or CT24) and minimal phase changes at CT12 (Figure 4.3 A). Thus, light exposure at all times of the circadian day consistently reset the fibroblast oscillator to the peak of the *per2* rhythm (CT12). The observed fibroblast phase responses largely agree with phase shifting data derived from pharmacological activation of cAMP effector protein Exchange protein activated by cAMP (EPAC) on SCN slices (O'Neill et al. 2008), where application of Sp-8-CPT-2′-O-Me-cAMP at CT6 and CT18 elicited a phase advances and delays in PER2 protein expression respectively. However, the experimental PRC was very different from the findings of Koinuma et al. 2009, who systematically applied forskolin, a cyclic adenylate cyclase activator, to the C6 glioma cell across the circadian day. They also reported that forskolin induced maximal phase responses during CT12 and minimal responses at CT0 or 24, coupled with phase delays and advances when treatment coincided on the rising and falling limbs of *per2* respectively. In addition, I noted that the phase response waveform also differed from VIP induced phase responses in SCN slices (An et al. 2011), which was characterised predominantly by phase delays.

The mechanism underlying the temporal gating of sensitivity is unknown but there are several hypotheses. Zhang et al. 2010 reported that high levels of CRY expression suppressed isoproterenol mediated induction of intracellular cAMP and CREB signalling in HEK293 cells. Therefore, cAMP signalling appears to be temporally gated such that strong induction of *pen* is only permissible during phases of low PER and CRY. Thus, it is conceivable that JellyOp signalling is also subjected to circadian inhibition. Alternatively, acute induction of clock genes may also be temporally gated such that as the *per2* rhythm approaches CT12, acute induction of clock genes is increasingly suppressed, which results in dampened phase responses. I are therefore keen to investigate whether high amplitude responses, which occur near the circadian trough of *per2,* is associated with relatively high levels of acutely induced *per* and *cry* genes. It would be useful to quantify the levels of acutely induced *per* and *cry* between CT12 and CT0 to verify whether the level of acute induction reflects overall phase responses.

I also speculate that acute upregulation of clock genes *per* and *cry* at phases 0-12 may lead to premature accumulation of clock proteins in the cell, which could then result in accelerated inhibition of CLOCK and BMAL1. In this scenario, rate of auto-inhibition would be accelerated and therefore shorten the rhythm periods of *per* and *cry*. In contrast, acute induction of genes between 12-24 hours, where clock proteins are already accumulated in the cell, could lead to an excessive accumulation of PER and CRY into the cell. This over-accumulation could mean that it takes longer for levels clock proteins to be degraded, but also the high levels of PER and CRY could sustain the repression of BMAL1 and CLOCK for longer, and the delay the disinhibition of these transcriptional activators. This would lead to a transient lengthening in period, and thus produce phase delays in the post-stimulus rhythm.

Whilst GPCRs are also known for their complex signalling cascades, it is not yet known whether G protein independent pathways can also interact with the mammalian clock. Despite the apparent inability of F139A JellyOp to induce or suppress cAMP signalling in mammalian cells, Type 0 phase response curve was reported in F139A JellyOp expressing cells following exposure to the same light stimuli (Figure 4.3 B), the profile of which was markedly different from wildtype JellyOp, but reminiscent of the phase shifting data derived from melanopsin expressing *per2::luc* fibroblasts (Ukai et al. 2012). The same authors reported that exposure of *per2::luc* melanopsin expressing fibroblasts to various durations of light (0.5-12 h) lead to phase responses, in which light onset tending towards CT 17-18, a midpoint of the *per2* falling limb, produced the largest response magnitudes. In contrast, minimal phase changes were elicited at CT6, which coincides with the mid-point of the rising limb. Phase delays were triggered early during phases in the subjective night and these become more prominent towards CT17, whereas advances were observed later in the subjective night. The similarity between the PRCs of melanopsin and F139A JellyOp is indeed surprising given the divergences in signalling interface; melanopsin is predominantly $G\alpha_q$-coupled (Matsuyama et al. 2012) whereas the F139A JellyOp lacks the ability to induce mitochondrial aequorin activity in HEK cells.

It appears that the most dramatic light induced phase responses occur in F139A JellyOp expressing cells during the auto-inhibition of *per2*, that is, on the falling limb between CT12 and 0 (Figure 3.4 B). In other words, the fibroblast clock is most responsive during phases of F139A JellyOp when CLOCK and BMAL1 are inhibited, presumably due to high levels of PER and CRY protein. Elucidating the molecular interactions between F139A JellyOp and the clock would provide further insight into the mechanism of entrainment.

4.4.2 Transient changes in period correlate with phase responses

I observed that light triggered phase responses were accompanied by transient changes in period of oscillatory *per2* expression before a new stable phase was established (Figure 4.5). In both JellyOp and F139A JellyOp cell lines, most phase delays were preceded by lengthening of the circadian period respectively (Figure 4.7). This reinforces the notion that circadian entrainment requires a transient modulation in period, irrespective of the different signalling pathways. This association has also been observed at behavioural level, where changes in period following single light pulses are matched by phase shifts, such that period acceleration is often associated with phase advances and deceleration with phase delays (Taylor et al. 2010, Comas et al. 2006). Taken together, the data suggest that phase and period response curves are intrinsically connected and that phase is strongly dependent on adjustments in period, the mechanisms of which can also be recapitulated in a light entrainable fibroblast model of the mammalian clock.

4.4.3 Photostimulation of JellyOp and F139A JellyOp yielded differential amplitude responses in fibroblast rhythms

A shown in Figure 4.4 A, light stimulation of JellyOp expressing fibroblasts was sufficient to substantially induce rhythm amplitude when delivered at certain phases of the circadian day. Furthermore, the amplitude response curve was comparable to that obtained from melanopsin expressing *per2::luc* fibroblasts following exposure to light across the circadian day (Ukai et al. 2007). The same authors demonstrated through single cell imaging techniques, that overall amplitude was dependent on the level of synchronisation between rhythms of individual cells. Thus, it would be of great interest to conduct similar imaging techniques on JellyOp expressing fibroblasts following light exposure at appropriate phases, to test whether this principle also applies. Post-stimulus rhythm amplitude in F139A JellyOp expressing fibroblasts showed a range of enhancements, however, these were only a fraction of what was achieved by 200 nM dexamethasone. Thus, it would be interesting to test whether longer pulse durations could further induce rhythms amplitudes.

4.4.4 Circadian rhythms of cAMP in fibroblasts

Several reports have shown that endogenous levels of cAMP oscillate in SCN and peripheral clocks across the circadian day (Prosser and Gillette. 1991, Hong et al. 2012). I thus sought to investigate the relationship between endogenous cAMP levels and the circadian output of $G\alpha_s$ signalling. The fibroblast cAMP rhythm profile was comparable to rhythmic cAMP levels in the free-running mouse SCN where cAMP levels were high in the early subjective day (CT2), and low in the early subjective light (CT16) (Doi et al. 2011). The authors were also the first to demonstrate that circadian cAMP production in the SCN was tied to the activities of RGS16, a negative regulator of $G\alpha_i$ proteins, as genetic deletion of RGS16 abolished cAMP rhythms in the SCN. Oscillatory expression levels of RGS16 also mirrored that of cAMP signalling in the SCN. This indicates the $G\alpha_i$ activity is more prominent during high levels of *per* and *cry* expression, and at such phases, the magnitude of JellyOp induced phase responses are also minimal. This raises the speculation that circadian regulation of endogenous cAMP contributes significantly to the responsiveness of the clock.

4.4.5 Light induced phase, amplitude and period responses in JellyOp expressing fibroblasts are duration dependent

Many studies have previously demonstrated that the duration or intensity of an entraining stimulus at a given phase plays an important role in shaping circadian response magnitudes within cellular and *in vivo* models (Sharma et al. 1999; Comas et al. 2006). In addition, it is likely that sustained JellyOp phototransduction is also accompanied by negative feedback mechanisms that could diminish the photosensitivity of JellyOp or attenuate downstream signalling components. Thus, I sought to assess the effective duration of JellyOp photoactivation on *per2* phase and amplitude.

I set out to investigate whether different durations of JellyOp photoactivation could trigger a spectrum of response magnitudes. To this end, JellyOp expressing fibroblasts were exposed to 0 - 4 hours of light between CT2-4, a phase which was previously shown to elicit high amplitude phase responses. I report that extending the pulse between 15 minutes - 2 hours produced a dose dependent increase in phase, suggesting that sustained signalling to the molecular clock is necessary for clock manipulation (Figure 4.10 A). The contributions of JellyOp to phase responses varied minimally between 2 - 4 hours, which implies that the 2 hours was sufficient to elicit a saturating phase response. This also suggests that 2 hours of acute induction is sufficient to elicit maximal phase responses. It is also likely that sustained JellyOp photoactivation may initiate negative feedback mechanisms that could diminish sensitivity of JellyOp or attenuate downstream signalling components after 2 hours of activation.

I also reported that changes in rhythm phase were preceded by transient compressions in period. Like phase responses, 4h of light elicited the same level of period compression as 2 hours, further supporting the close relationship between period and phase responses (Figure 4.10 C). Rhythm amplitude was also induced, especially with 4 hours of light, where phase responses were already saturated (Figure 4.10, B). This suggests that sustained activation of JellyOp signalling over 4 hours is capable of increasing the level of synchrony between individual fibroblast clocks, however, bioluminescence imaging assays would further confirm this speculation. Nonetheless, this shows that JellyOp signalling is effective in regulating clock parameters even after 4 hours of light activation.

It would be interesting to investigate whether the duration of light impacts on the magnitude of acute *per* induction, and also how the latter correlates with circadian responses, as these relationships are not well understood. An et al. 2011 showed that 100 µM VIP induced larger phase responses than 10 µM VIP in SCN cultures at CT12 of the PER2 rhythm; however, both concentrations were able to acutely induce comparable levels of PER2 protein over baseline.

4. Optogenetic manipulation of the mammalian clock

5. Investigating mechanisms that entrain the RPE clock

5.1 Introduction

The suprachiasmatic nucleus (SCN) entrains the circadian physiology of peripheral oscillators *in vivo* and *in vitro* (Moore and Eichler. 1972, Li et al. 2008). Within the SCN tissue, individual neurons express intrinsic rhythms of clock gene expression and electrical activity. Many studies have shown that such circadian precision relies on intercellular coupling mechanisms consisting of multiple neurotransmitters, paracrine signalling molecules and gap junctions in synchronisation of cells in the SCN (Shirakawa et al. 2001, Aton et al. 2005, Maywood et al. 2011).

Despite the abundance of such mechanisms, they are by no means redundant, as pharmacological blockade or genetic ablation of individual signalling pathways between neurons is sufficient to compromise the intercellular synchrony of rhythmic neurons in SCN cultures. Hughes et al. 2008 demonstrated using a *per1::GFP* reporter *vipr2*$^{-/-}$ mouse model, that the rhythmic expression of *per1* in SCN neurons showed a wider variation of peak times in culture than those in wildtype mice. Furthermore, application of the $VPAC_2$ inhibitor PG 99-465 at 10 nM to SCN cultures of wildtype mice resulted in a circadian phenotype similar to that of the *vipr2*$^{-/-}$ mouse, with respect to phase clustering.

Many studies have shown that circadian precision also relies on tissue organisation. By recording *per1::luc* reporter activity in SCN neurons as organotypic cultures or as dispersed cell cultures, Herzog et al. 2004 demonstrated that the variation in free-running period of individual dispersed neurons was markedly higher than those in explant culture. Furthermore, the variability in the free-running period of dispersed cells was also greater than neurons in explant culture, thus signifying the importance of anatomical integrity in the maintenance of stable rhythm parameters in individual oscillators. Taken together, the source of precise and stable rhythm parameters appears to be due to anatomical alignment as well as intercellular communication.

5. Investigating mechanisms that entrain the RPE clock

Many types of peripheral cells such as fibroblasts express the same complement of clock genes as neurons of the SCN *in vitro* and *in vivo*, however, individual oscillators appear to be much less coupled (Izumo et al. 2003, Stratmann and Schibler. 2006, Leise al. 2012). Nagoshi et al. 2004 reported that cultured fibroblast cells oscillated independently of others within the same culture and were unable to influence the rhythm parameters of neighbouring cells. This was demonstrated in co-cultures of BMAL1-luciferase reporter NIH3T3 cells and feeder fibroblast cells which exhibited different circadian properties. Following exposure to 10 nM dexamethasone for 15 minutes, rhythms of clock gene expression in rat1 fibroblasts were normally phase advanced by 6h compared to NIH3T3 cells. Furthermore, in a co-culture of 20:1 rat1 fibroblasts and baml1-luciferase reporter NIH3T3 cells, NIH3T3 cells did not show a significant deviation in phasing of baml1-luciferase activity. Similarly, when co-cultured with mutant *per1* Knockout primary fibroblasts, which exhibit a relatively short free-running period of 20 hours, the pace of the feeder cells did not impact the period of the rhythmic bioluminescence in *per1* knockout cells.

However, other reports claim that in the retina, a rhythmic tissue with complex anatomical organisation and circuitry, circadian rhythm parameters are indeed governed by intercellular communication. When Ruan et al. 2008 examined the impact of stimulating GABA signalling in the retina, they reported dose dependent suppression in rhythm amplitude of PER2::LUC reporter. Conversely, pharmacological blockade of $GABA_A$ and $GABA_B$ receptors with antagonist SR 95552 and TPMPA enhanced the rhythm amplitude of the PER2::LUC bioluminescence. The authors also showed that pharmacological induction of dopaminergic neurotransmission can stably reset the phase of the retinal circadian rhythm. Application of 50 µM Dopamine D1 receptor agonist SKF38398 to the retinal explant early in the subjective day (CT3) induced a phase advance of 1.5 hours. Also when pharmacological inhibition was delivered at CT18, a phase delay was observed. Taken together, these data suggested that rhythm parameters in the retinal tissue are governed by local GABAergic and dopaminergic intercellular signalling pathways.

Such studies contrasted greatly with the findings of Tierstein et al. 1980, who reported that circadian ocular physiology was not susceptible to direct photoentraiment and required an entraining signal originating from the suprachiasmatic nucleus. In contrast to previous reports, Ruan et al. 2008 recently described light dependent influences of the retinal clock *in vitro*. The authors observed that exposure of retinal explants to 1 hour pulses of 500 lux light at different times of the circadian day shifted the circadian phase of PER2::LUC bioluminescence in a dopamine dependent manner. Light treatment at CT13 induced a 2.3 hour delay in the phase of the PER2::LUC rhythm whereas a 1.5 hour advance was observed at CT19.5. However, application of 50 µM D1 antagonist, SCA-23390, for 15 minutes prior to light treatment severely attenuated the responses. Thus, the data are consistent with previous reports that dopamine regulates the phasing of the retinal clock and signifies the role of intercellular communication in mediating photoentrainment of the retinal circadian clock.

It is noteworthy that the secretion of dopamine from amacrine cells of the retina is driven by circadian rhythm and also, directly by light transduction (Iuvone et al. 1978, Parkinson and Rando. 1983, Umino and Dowling, 1991). Cameron et al. 2009 demonstrated that when mice were subjected to 90 minutes light exposure at CT6 or CT18, substantial quantities of dopamine were released from both wildtype and melanopsin deficient retinas. However, in retinas of *gnat1*$^{-/-}$ mice which lack rod transducin, a critical component of the phototransduction cascade in rods, dopamine release was significantly impaired. Thus, dopamine release, which relies predominantly on rod photoreception, is a critical mediator of light evoked circadian shifting in the retina.

5. Investigating mechanisms that entrain the RPE clock

Another type of rhythmic peripheral tissue that exhibits structural organisation and an array of opsin photopigments and photoisomerases is the retinal pigmented epithelium (RPE) (Peirson et al. 2004, Tarttelin et al. 2003, Sun et al. 1997, Pandey et al. 1994) These cells form a monolayer which underlies the retina and plays an important role in the maintenance and function of rod and cone photoreceptors. The RPE also forms a structural component in the blood-retina barrier, and serves as the main conduit for the exchange of substances between the retina and choroidal capillaries (Strauss. 2005). Little is known regarding mechanisms of intercellular signalling between RPE cells. A recent study revealed the presence of tunnelling nanotubes (TNTs), intercellular membrane channels, between individual cells in the RPE cell line ARPE-19 (Wittig et al. 2012). Here, TNTs have been shown to facilitate calcium signalling between coupled cells following mechanical stimulation. Other studies reported the presence of gap junction proteins such as connexin 43 (Cx43), which has been shown to allow calcium

Following exposure to saturating levels of dexamethasone, circadian rhythms in transcription levels of clock gene *bmal1* have been reported in human RPE1 cell lines harbouring *hbmal1::luciferase* reporters (Yoshikawa et al. 2008). Similarly, circadian rhythms in clock protein expression have also been detected in RPE-choroid explant cultures. Baba et al. 2010 first demonstrated that RPE-choroid tissue isolated from PER2::LUC reporter mice produced robust rhythms of relative bioluminescence in culture with an average free-running period of 23.9 ± 0.1 hours. Although the explant contained a mixed population of cell types, the authors confirmed that rhythmicity was predominantly due to RPE layer. Interestingly, the PER2::LUC rhythm amplitude of intact cells in tissue culture declined to baseline over the course of 6-7 days following media induced synchronisation, whereas RPE cells have been cultured as enzyme-dissociated cells in culture produced low amplitude rhythms of relative bioluminescence relative to explant cultures. This could be attributed a lack of intercellular synchrony between individual oscillatory cells.

5. Investigating mechanisms that entrain the RPE clock

There is much evidence for circadian and light dependent changes in RPE physiology within its native ocular environment. One prominent rhythmic activity is the phagocytic disposal of rod photoreceptor outer segments. It has been proposed that interactions with the retina directly influences retinal pigment physiology; the binding of shed rod outer segments (ROS) to the RPE surface and subsequent phagocytic uptake is thought to generate an intracellular cascade of inositol phosphate (Heth and Marescalchi. 1993). This has been demonstrated in *in vitro* assays where challenging primary cultured rat retinal pigment epithelial cells with ROS resulted in generation of intracellular inositol phosphate (IP_3). Furthermore, this induction of IP_3 was specific to rat ROS, as an equivalent challenge with polystyrene latex spheres produced no detectable changes in levels of inositol phosphates. Interestingly, exposure of primary cultured RPE cells to rod outer segments also resulted in a 6-fold accumulation of *c-fos* mRNA after 30 minutes. The authors further demonstrated that such transcriptional responses were specific to ROS uptake, as latex spheres resembling the shape of outer segments did not induce such *c-fos* expression (Ershov et al. 1996). The onset of an IP_3 signal transduction cascade and the subsequent induction of immediate response genes are strongly associated with entrainment of the mammalian clock to extrinsic signals (Earnest et al. 1990, Hamada et al. 1999).

Whilst immunohistochemical and RT-PCR studies by Peirson et al. 2004 and Tarttelin et al 2003 have respectively confirmed the expression of opsin photopigments melanopsin and neuropsin in retinal pigment epithelium, it has not been confirmed however, that these endogenous pigments are functionally active. This is unlikely to be due to defective downstream signalling components, as heterologous expression of mouse melanopsin in the RPE cell line D407 enabled light evoked intracellular calcium mobilisation within transfected cells (Giesbers et al. 2008, Pulivarthy et al. 2008). However, the phototransduction cascade of endogenous melanopsin has not yet been characterised.

Another opsin photopigment OPN5, also known as neuropsin, was identified in the various mammalian tissues and includes the retinal pigment epithelium cell line ARPE-19 (Tarttelin et al. 2003). Sequence alignment of the opsin amino acid revealed the equivalent lysine (K296) residue involved in forming the Schiff covalent linkage to a chromophore. Mammalian OPN5 appears to form a functional photopigment upon expression in *Xenopus* oocytes whilst Yamashita et al 2010 first described the bistable nature of the opsin photopigment through spectroscopic and G protein activation studies.

5. Investigating mechanisms that entrain the RPE clock

Few studies have investigated the role of anatomical structure and intercellular synchronisation in regulating circadian rhythms within a peripheral tissue. I hypothesised that due to the recently discovered intercellular mechanisms that regulate overall circadian rhythms of retinal tissues, factors such as tissue anatomy and structure could also play a role in regulating intercellular synchronisation of individual RPE oscillators. To this end, I therefore set out to investigate whether such mechanisms are relevant to RPE cells, by conducting a comparative analysis of rhythm parameters between RPE cells in tissue explant and dispersed cell culture. To capture the rhythm parameters, I sought to perform bioluminescence imaging of individual RPE oscillators in explant tissue and dispersed cell cultures isolated from PER2::LUC reporter mice.

I also aimed to assess whether activation of endogenous opsins in RPE cells is sufficient to drive synchronisation of clock gene expression or directly phase shift the RPE clock. Due to the reported presence of endogenous melanopsin photopigments in RPE cells, my hypothesis was that this pigment could render the RPE cells light responsive that was akin to fibroblasts engineered to express heterologous melanopsin. To probe for acute effects of light on RPE cells in their native ocular environment, I also investigated the effect of photostimulation on the expression of the immediate early response protein, C-FOS.

5.2 Materials and methods

5.2.1 Maintenance of mPER2::LUC mice

Adult mPER2::LUC knockin mice were housed in the at the University of Manchester, under a 12 hour LD cycle with *ad libidum* access to standard lab chow (B&K Universal) and water. Temperature was maintained at 18°C and humidity at 40 %. All procedures were carried out in accordance with the UK Animals (Scientific Procedures) Act 1986.

5.2.2 RPE primary culture medium

Culture medium for primary RPE cells consisted of Dulbecco's modified Eagle's medium/F12 (Sigma Aldrich) to a ratio of 1:1, supplemented with 20 % foetal calf serum (Sigma Aldrich) and 1 % penicillin and 1 % streptomycin (Sigma Aldrich).

5.2.3 Recording medium for primary RPE cells and explant tissue

The recording medium for bioluminescence recordings of RPE cultures consisted of supplemented Dulbecco's modified Eagle's medium (10 g/l DMEM with 3.5 g/l D- Glucose, 350 mg/ml Sodium Bicarbonate (Sigma Aldrich), 10 mM Hepes buffer, 2 % B27 (Life Technologies), 20 U/ml Penicillin and 25 µg/ml Streptomycin (Sigma Aldrich), 200 µM beetle Luciferin (Promega) and 10 µM Forskolin (Sigma Aldrich).

5.2.4 RPE tissue dissection and primary culture preparation

The PER2::LUC reporter mice were culled by cervical dislocation at CT7, their eyeballs were immediately removed after cull with spring scissors (World Precision Instruments, USA) and incubated in chilled HBSS (Sigma Aldrich) supplemented with 0.75 % sodium bicarbonate, 100 mM HEPES buffer (Sigma Aldrich) and 1 % penicillin and 1% streptomycin. The eye balls were dissected with the aid of a dissecting microscope in a laminar flow hood. The cornea of the eyeball was sliced open with a razor blade (Swann Morton) to release the intraocular pressure. The anterior ocular tissues including the cornea, iris pigment epithelium and ora serrata were subsequently removed with Vannas scissors and forceps (World Precision Instruments). The eye cup was then incubated in filter sterilised 2.5 U/ml Dispase II (Sigma Aldrich) in Ca^{2+}/Mg^{2+} free PBS at 37°C for 30 minutes before wash in Ca^{2+}/Mg^{2+} free PBS (Sigma Aldrich).

Dissociated RPE cells were then lifted from the choroid and sclera with a paintbrush, collected in 200 µl RPE culture medium (as described above) and aspirated with a 200 µl micropipettor (Gilson), followed by centrifugation at 300 g for 5 minutes. Pelleted cells were resuspended in RPE culture medium and plated into 35 mm cell culture dishes containing 2 ml RPE culture. Cells were cultured at 37°C in a 5 % CO_2 atmosphere, with culture medium replaced every 2 days.

5.2.5 Photomicroscopy of RPE primary cultures

Cells were visualised with a Leica DM LED inverted microscope (Leica Microsystems) through a phase contrast filter. Images were captured with a fitted Canon Powershop S70 digital camera (Canon) using Canon Zoombrowser EX image browser software and processed on Corel photoshop X3 (Corel).

5.2.6 Immunocytochemical labelling for RPE65 in primary RPE cells.

RPE primary cells cultured on glass coverslips (VWR international, USA) were fixed with 4 % PFA (Sigma Aldrich) at 4^{o}C for 30 minutes in between washings in ice cold PBS. Cells were permeablised in 0.025 % Triton-X 100 in PBS at room temperature for 10 minutes, and blocked in 1 ml BSA, 10 % normal goat serum (Vector Laboratories) in PBS for 30 minutes and then incubate in anti-RPE65 Ig (1:1000, Abcam) in 1 % BSA for 2 hours at room temperature. After 3 washings in PBS, cells were incubated in 2 µg/ml goat anti-mouse Ig conjugated to Alexa 555 Fluor® (Life Technologies) in 1 % BSA for 90 minutes in the dark at room temperature. After rinsing in PBS, coverslips were mounted on a poly-L-lysine slide using vectashield mounting medium with DAPI. Stained cells were observed with a fluorescence microscope with DAPI and Texas red filters. All images were captured with a digital camera (Canon) and processed using the bio-imaging software MetaVue Imaging system (Molecular Devices).

5.2.7 Bioluminescence recordings for PER2::LUC RPE explant cultures and primary cultured cells

Mice which harboured the PER2::LUC reporter were culled by cervical dislocation and the eyes enucleated as described above. Upon dissection of the eye, the lens and retina was gently removed with a fine paintbrush and the remaining eye cup was flattened with radial slits on a Millicell-CM low height culture insert (Millipore) within a 35 mm culture dish (corning) containing 1 ml recording medium supplemented with 200 µM beetle. The culture dish was sealed air-tight with a 40 mm coverslip (VWR international) and high vacuum grease (Dow Corning).

All RPE samples, including explant cultures and confluent P0 primary RPE cells were recorded from the lumicycle (Actimetrics) housed in a light tight incubator at 37°C. The average photon count was sampled for 75 seconds per sample. To change the recording medium, the samples were removed from the lumicycle and transferred to a Class I tissue culture hood. The coverslip was lifted from the culture dish and the old medium was removed with a P1000 pipette (Gilson). 1 ml fresh medium was placed into the culture dish and resealed with the original coverslip and the culture dish protected from light, and returned to their respective wells in the lumicycle.

5.2.8 Bioluminescence imaging for PER2::LUC RPE explant cultures

RPE explants were prepared and cultured as mentioned above, and recorded in the lumicycle for free-running PER2:LUC expression. The tissue and transwell insert were transferred to a glass bottom culture dish (Sigma Aldrich) containing 1.2 ml recording medium, and re-sealed with the original coverslip. The sample was placed under the microscope and focussed onto the x20 lens firstly with brightfield microscope. Bioluminescence imaging was performed using a self-contained Olympus luminoview LV200 luminescence microscopy system (Olympus) fitted with a cooled Hamamatsu ImageEM C9100-13 EM-CCD camera and a 20 x 0.4 NA Plan Apo objective (Olympus). Time-lapse images were captured with an exposure time of 30 minute per frame over for 8 days consecutively at 37^{o}C in darkness and transferred to IMAGEJ software (National Institute of Health) for analysis.

5. Investigating mechanisms that entrain the RPE clock

5. Investigating mechanisms that entrain the RPE clock

5.3 Results

5.3.1 Intercellular desynchronisation of individual RPE oscillators in explant culture

I initially sought to investigate the role of local intercellular signals in regulating individual RPE oscillators. To this end a bioluminescence imaging protocol was developed to enable surveillance of luciferase reporter activity within individual oscillators in explant culture. Such recordings allowed me to sample bioluminescence near single-cell resolution, and reveal the spatiotemporal dynamics of oscillations at the level of the cell as well as the whole population.

I report that 10 µM forskolin was sufficient to induce robust rhythms of bioluminescence in RPE tissue explants with a period of 23.7 ± 0.4 hours, (Figure 5.1 A). Rhythm amplitude damped consistently to baseline levels over 6-7 days, but could be restored by further forskolin treatment at day 9 and 15. This oscillatory damping is reminiscent of other peripheral tissues (Welsh et al. 2004, Izumo et al. 2003) and in those cases has been shown to reflect a gradual loss of synchrony among individual cellular oscillators. To confirm whether that is also the case for the RPE, I next attempted to track oscillations at the single cell level. Using a Hamamatsu ImageEM C9100-13 EM-CCD camera, I continuously recorded 30 minute time-lapse bioluminescence images of the RPE explant consecutively over 8 days. The high resolution of the recording revealed the punctuate nature of the PER2:LUC signal, suggesting that bioluminescence was emerging from individual cells (Figure 5.1 C). Furthermore, the geographic distribution of bioluminescence was consistent with the anatomy of the cultured tissue explant, as shown by phase contrast image of the tissue, thus confirming the cellular origin of the bioluminescence (Figure 5.1 B). Following 10 µM forskolin treatment, robust circadian oscillations in the overall bioluminescence emission were captured at the level of the tissue as well as the individual cell (Figure 5.1 D and E).

5. Investigating mechanisms that entrain the RPE clock

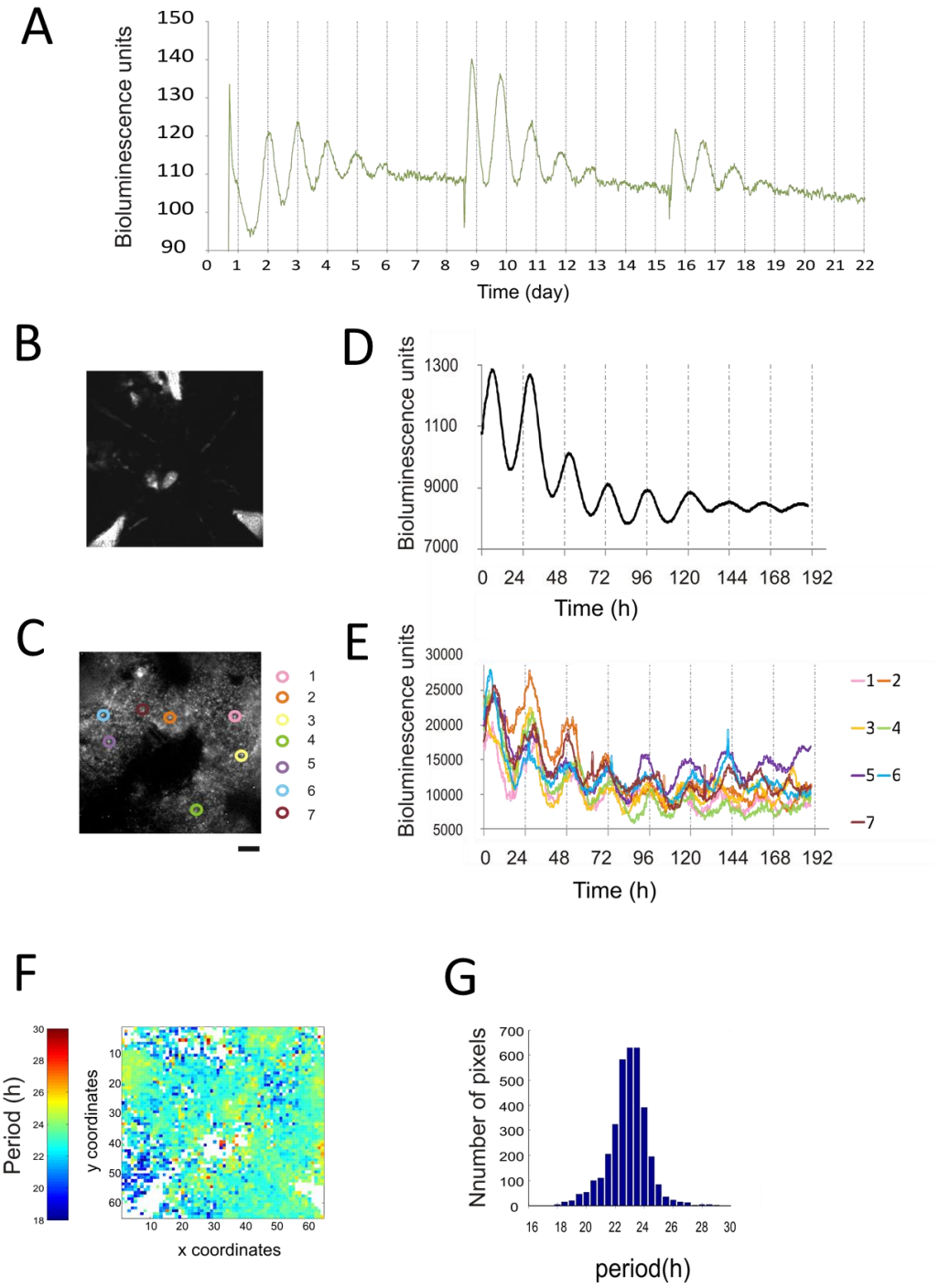

Figure 5.1 Bioluminescence imaging of the RPE-choroid tissue

A) Bioluminescent rhythms captured from cultured RPE-choroid explants from PER2::LUC mice, pre-treated with 10 µM forskolin. During the assay, 10 µM forskolin was administered with media change at days 9 and 15. (B-G) Further analysis of these rhythms in PER2::LUC reporter activity was undertaken using a cooled Hamamatsu ImageEM C9100-13 EM-CCD camera to track patterns of luminescence with near single-cell resolution and time lapse imaging techniques. Phase contrast (B) and 30 minutes time lapse (C) images of the recorded RPE explant. D) An overall bioluminescence trace was captured from the tissue over 8 days of recording. E) Bioluminescence sampled from 7 individual cells within the tissue, with their respective locations highlighted in (C). F) A spatial distribution of free-running periods within regular sub regions across the tissue. This was reconstructed from each time-lapse bioluminescence image as a 64x 64 pixel image, where the average free-running period was sampled as the time lag between oscillatory peaks and troughs of 6 consecutive oscillations. G.) A histogram representing the distribution of free-running period across the tissue, modelled to a normal distribution with a mean of 23.04 hours and standard deviation of 1 hours. Scalebar = 1 mm

5. Investigating mechanisms that entrain the RPE clock

By comparing the phasing of bioluminescence peaks in selected individual cells, I also observed that for individual cells, the timing of the bioluminescence peaks were tightly clustered immediately after forskolin treatment, but exhibited progressively wider temporal distributions of bioluminescent acrophases over time in culture (Figure 5.1 E). It follows that this preparation lacks an efficient mechanism for ensuring global synchrony among cellular oscillators. To assess the global distribution of free-running period, I reconstructed each time-lapse image as a 64x 64 pixel image and sampled the average free-running period in each pixel by measuring the temporal intervals between consecutive rhythm peaks. To calculate the free running period, I measured the time interval between each bioluminescent peak over 6 days of recording in each pixel area. Figure 5.1 F shows a heat map representing the spatial distribution of free-running periods across the tissue. Interestingly, a diffuse circular spread of homogenous periods was observed across the tissue. Figure 5.1 G shows a temporal distribution of free-running period sampled in each square. This temporal variation in period can be modelled by a normal distribution with a mean free-running period of 23 hours and standard deviation of 1 hour. Thus indicates intrinsic heterogeneity in rhythm pacing, reported in multiple types of oscillatory cells including SCN neurons and fibroblasts. It would be interesting to compare this distribution to that of RPE cells dispersed in culture.

In order to analyse intercellular desynchronisation, I constructed heat maps from the same time lapse images to quantify the spatial distribution of cellular acrophases in each pixel. The heat map for day 2 reflected broad areas of homogeneous phasing with diffuse scattering of phase advanced oscillators in the top left quadrant of the tissue (Figure 5.2 A). However, by day 7 the distribution of phasing is very much randomised. I illustrate through frequency histograms (Figure 5.2 G-L) that there was an overall increase in temporal distribution of phase between individual cells over time, suggesting that cells undergo desynchronisation. The standard deviation of the modelled normal distributions is lowest on day 2 of recording at 1.9 hours (Figure 5.2 G). However, with each consecutive day the standard deviation increases up to 7.016 hours by day 7 in culture (Figure 5.2 L). Overall, the histograms reveal the global and progressive spread in temporal distribution of phases.

5. Investigating mechanisms that entrain the RPE clock

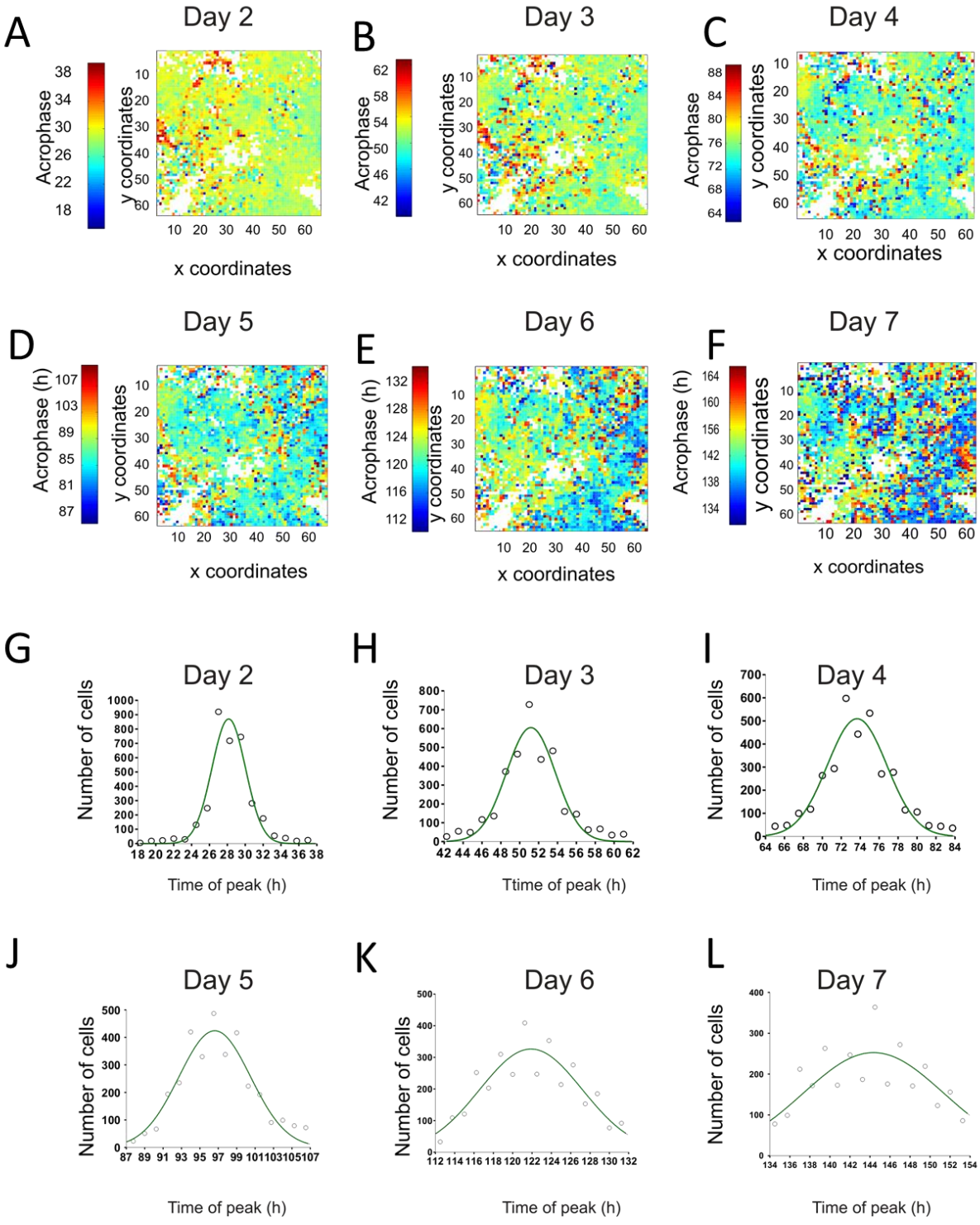

Figure 5.2 Intercellular synchrony of RPE oscillators in explant culture

(A-F) Heat maps showing spatial distribution of cells in the time since culture establishment at which each pixel exhibited peak bioluminescence (rhythm acrophase) for the *Per2::luc* RPE-choroid explant on days 2-7 in culture. (G-L) Histograms representing the distribution in timing of acrophases across the tissue explant for each day. The distributions were fitted with normal distributions to derive the mean and standard deviation of distribution. The distribution at (G) day 2 is 28.2 ±1.9 hours, (H) day 3 is 51.2 ± 2.6 hours, (I) day 4 is 73.7 ± 3.1 hours, (J) day 5 is 96.6 ± 3.9 hours, (K) day 6 is 121.9 ± 5.3 hours (L) day 7 is 244.4 ± 7 hours.

5.3.2 RPE primary culture and rhythm recordings

One way of determining whether there is any discernible coupling between oscillators in the intact tissue is to define whether individual oscillators drift out of phase more rapidly when the tissue organisation is disrupted. I therefore also developed a protocol for the recording PER2::LUC bioluminescence of dispersed RPE cultures. Individual RPE cells were isolated and cultured from PER2::LUC reporter mice, and upon reaching confluence, conducted bioluminescence recordings of P0 RPE cells. Figure 5.3 A represents a trace of bioluminescence captured from the primary cells over 5 days pre-treated with 10 µM forskolin. I observed a circadian rhythm sustained over three days despite rapid damping of rhythm amplitude. However, subsequent treatment failed to initiate bioluminescence rhythms, indicating loss of cells in culture. Thus, my recording protocol did not sufficiently sustain cell viability in culture.

Whilst our recording paradigms were detrimental to cell survival, our primary culture conditions were conducive to RPE growth and proliferation. Upon harvesting primary RPE cells, cell proliferation occurred as early as day 4 in culture, accompanied by morphological changes and reduced levels of pigmentation (Figure 5.3 B). By day 13 where cells were post confluent, pigmentation was heterogeneous and morphologies were mixed with fibroblastic and cobblestone shaped cells (Figure 5.3 C). I utilised RPE65 specific immunolabelling techniques to identify RPE cells in culture and observed strong fluorescence signals in the cytoplasm and membrane of cultured cells, which also contained pigmentation. As RPE65 is exclusively expressed in RPE cells, I could confirm that these pigmented cells were of RPE origin (Figure 5.3 G). RPE immunolabelling was localised to the plasma membrane and also within the cytoplasm but absent from the nucleus. Nevertheless, the poor rhythmicity exhibited by these dispersed cultures makes this an inappropriate preparation for studying the circadian organisation of this tissue.

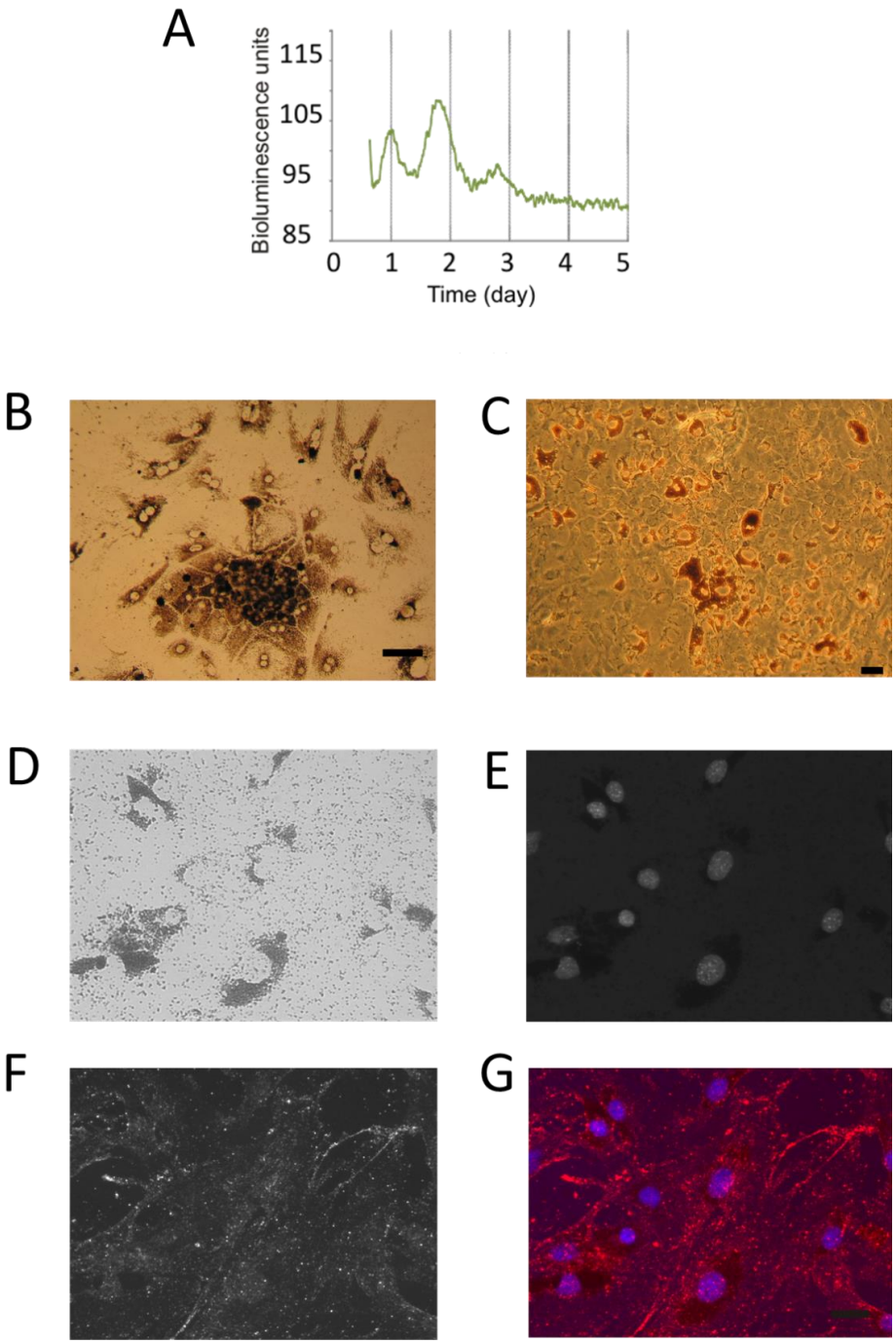

Figure 5.3 Circadian rhythms of bioluminescence in PER2::LUC RPE primary cultures

(A) Bioluminescence rhythms captured from PER2::LUC RPE cells after 14 days of primary culture, pre-treated with 10 μM forskolin. (B) Phase contrast micrograph of an RPE culture similar to that used to produce the data in panel (A) at day 4 of culture shows cells undergoing cell division and morphological changes. Scalebar = 100 μm (C) primary P0 RPE cells are highly confluent in culture by day 13. Scale bar = 100 μm (D) Bright field micrograph of cultured RPE cells at day 13, showing reduced pigmentation compared to day 4. (E-G) Immunofluorescence micrographs of respective cells labelled with (E) the fluorescent nuclear marker, DAPI, (F) and RPE65. (G) A merged image of DAPI and RPE65 fluorescence in co-labelled RPE cells, where the blue represents DAPI labelling and red, RPE65 labelling. Scale bar = 50 μm

5.3.3 Investigating light induced circadian responses in the RPE

One explanation for the absence of mechanisms that ensure strong local coupling of RPE oscillators is that these cells experience the main entraining signal (the light/dark cycle) directly every day. Hence, one might expect that this would be sufficient to ensure coherent oscillations across the tissue. I next sought to investigate whether this entraining signal could rely on inherent photoreception within the RPE cells themselves using melanopsin or one of the other photopigments that they are reported to express (Pierson et al. 2004). To this end I assayed for rhythmic expression of bioluminescence in RPE-choroid explant culture, and delivered a 90 minute pulse of bright white light at 37^{o}C to the tissue near the circadian trough (Figure 5.4 A-B) and peak (Figure 5.4 D-E). A rapid and transient spike in bioluminescence was observed immediately after the light pulse, the kinetics of which strongly implies luciferin oxidation.

To examine phase shifting effects of light on circadian PER2 expression, I measured the phasing of bioluminescence before and after the light pulse. To quantify the phase change, I modelled a sine wave over the pre-pulsed rhythm and measured the time lag between the peak of the sine wave and *per2::luc* bioluminescence after the light pulse. I reported a modest phase advance of 1.9 ± 1.5 hours in RPE-tissue cultures pulsed near the circadian trough. A mock treated RPE-tissue also showed a small phase advance of 0.5 ± 0.8 hours. When pulsed at the circadian peak, I observed a small phase advances in the rhythm of the light pulsed tissue at 0.5 ± 0.1 hours. The mock control also showed a comparable phase advance of 0.9 ± 0.2 hours. Overall, based on this lighting paradigm, I was unable to detect any effect of light on circadian rhythms in this tissue.

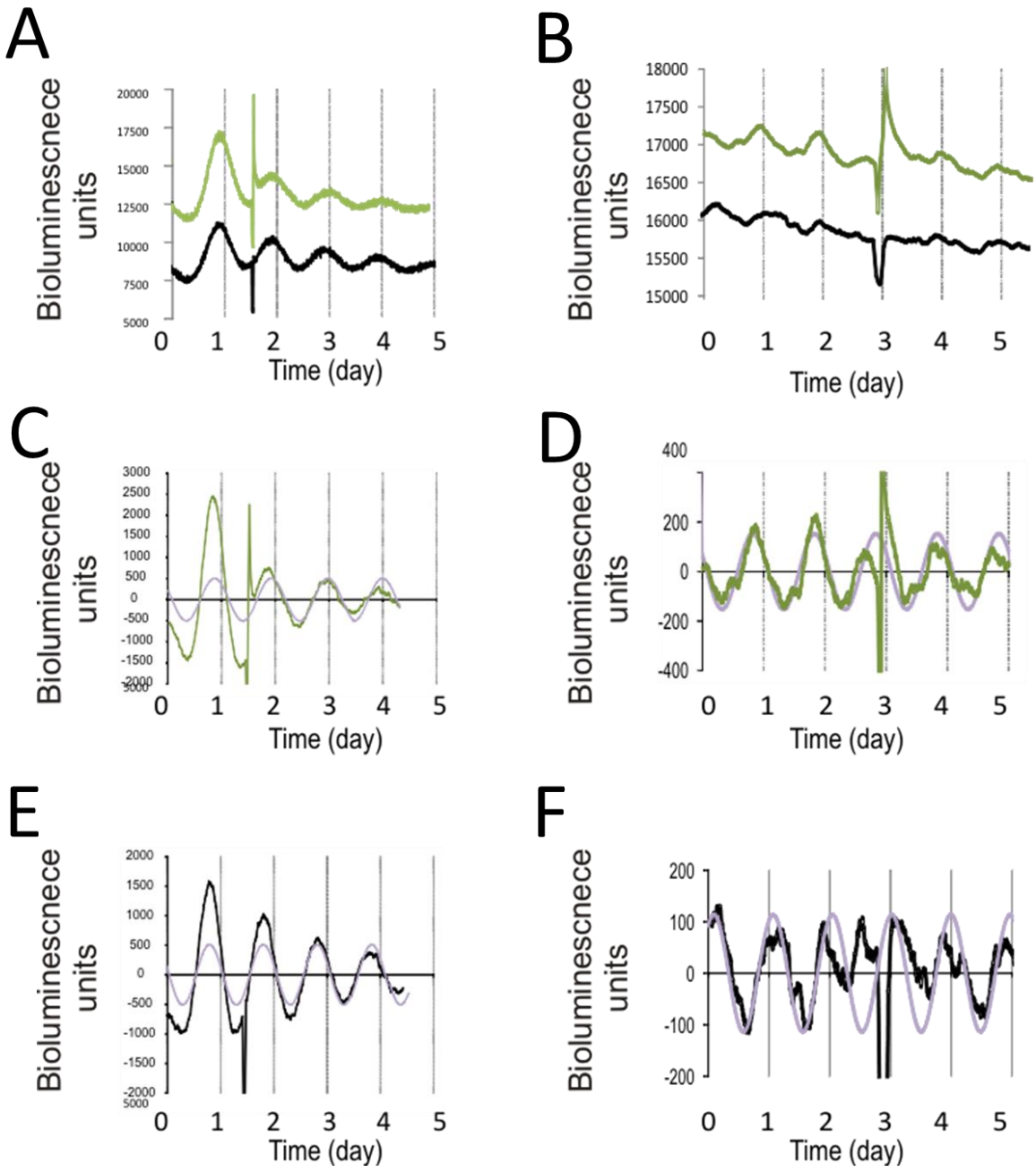

Figure 5.4 Investigating light dependent influences on PER2::LUC bioluminescence rhythm in RPE-choroid explants

(A and C) Bioluminescence recordings of the RPE-choroid explants before and after exposure to 1.5 hours of white light at 37^{o}C near the circadian trough of the *PER2::LUC* rhythm (CT 3.3). Light pulse was delivered on the 2nd day of recording. Green trace shows rhythms from explants that received light at 37°C. (E) Black traces denotes a paired control that was handled similarly, but sham pulsed. To aid calculation of phase shifts, the pre-stimulated luminescence rhythm for light treated (B and D) and sham pulsed (F) traces were modelled with a sine wave that was plotted across the recording period.

5.3.4 Investigating light induced C-FOS expression in the RPE

I also proceeded to investigate the acute effect of light on RPE physiology in its native ocular environment. I used immunohistochemical procedures to detect light induced C-FOS expression in the retina and RPE of dark adapted mice either exposed to 90 minutes room light at ZT6 or continually maintained in the dark. Immunolabelled C-FOS was scattered diffusely across the tissue of both light treated and dark adapted mice and was not localised to cell nuclei, as visualised by a nuclear fluorescent counterstain, DAPI. In addition, the low ratio of signal to noise made it difficult to identify light induced C-FOS expression.

To confirm that the visual system of the mouse of functional and was able to detect room light, I assessed light induction of C-FOS in the retina. In contrast to the RPE, I reported a higher density of C-FOS immunoreactivity in the whole mount retina of the light treated mouse, when imaged from the retinal ganglion layer (Figure 5.5 A top left panel) compared to the dark control mouse (Figure 5.5 A bottom left panel). C-FOS immunorectivity was also characterised as a punctate signal over background autofluorescence in the retina, implying nuclear localisation. I also show that the punctuate labelling is predominantly due to the specific antibody, as labelling with only the secondary florescent antibody produced a diminished level of autofluorescence.

5. Investigating mechanisms that entrain the RPE clock

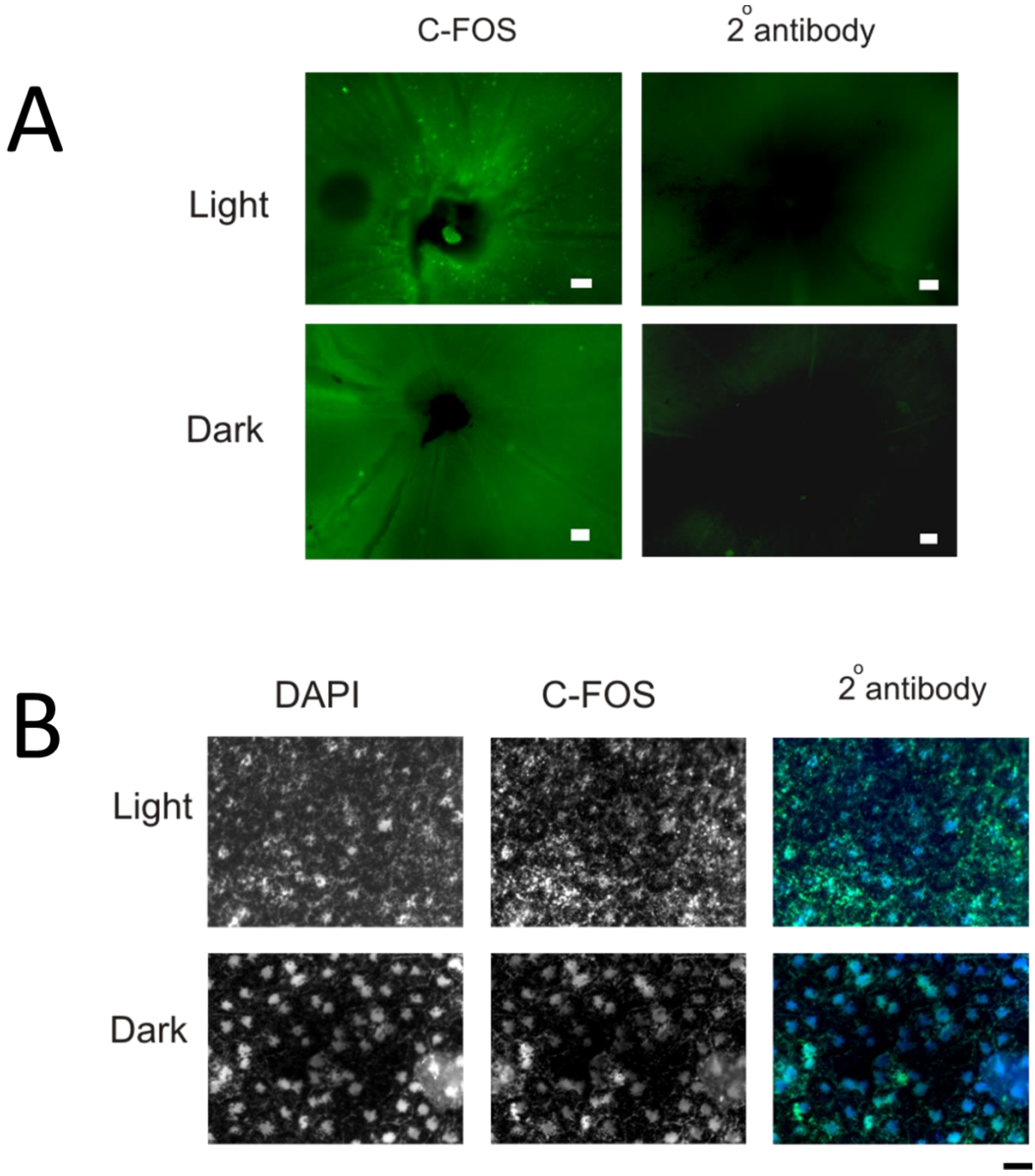

Figure 5.5 Immunocytochemical analysis of light induced C-FOS expression in retinal and RPE tissues

(A) Immunohistochemical examination of C-FOS expression in the retina of mice exposed to 90 minutes room light at ZT7. Light exposure resulted in an induction of C-FOS expression (top left panel) compared to mice maintained in the dark (bottom left panel). C-FOS immunorectivity is characterised as a punctate signal over background autofluorescence in the retina. The nature of the punctate signal is specific to the primary C-FOS antibody as labelling with secondary fluorescence antibody yielded no punctate fluorescence signal in retinas of light exposed and dark control mice (right panels). Scalebar = 1 mm (B) RPE-choroid whole mount tissues from the same mouse eyes of were also labelled for C-FOS expression. Left panels shows whole mount RPE-choroid tissues labelled with DAPI. Centre panels show RPE tissue labelled with both primary anti-C-FOS antibodies and green fluorescent secondary antibodies. Right panels shows merged image of DAPI labelling and C-FOS labelling across the RPE plane, where the blue represents DAPI labelling and green, C-FOS labelling. Scalebar = 50 µm.

5.4 Discussion

There is much evidence that intercellular communication is required for long-term rhythm synchronisation at the level of the SCN tissue. However, few studies have embarked on studying the role of structural organisation and intercellular signalling pathways in the synchronisation of peripheral clocks. Recently however, pharmacological dissection of the retinal circadian network has revealed the importance of GABA in regulating the amplitude of retinal rhythms (Ruan et al. 2008). It would therefore be interesting to further investigate whether amplitude of rhythmicity is generated by collective synchronisation of individual oscillators in the retina. Imaging of individual cellular activity in an intact retina would resolve whether single cells intercellular coupling is influenced by the presence or absence of GABA.

5.4.1 RPE oscillators lack global mechanisms of synchronisation

My initial objective was to determine whether anatomical or intercellular signalling factors were able to govern rhythm parameters of RPE cells in culture. To this end, I established an organotypic tissue culture protocol for bioluminescence recordings of RPE cells. Upon exposing RPE explant culture to 10 µM forskolin, the phasing of PER2::LUC bioluminescence peaks was highly synchronised within the RPE tissue compared to the subsequent days of the recording (Figure 5.2 A). Whilst a high proportion of cells shared a common phase at the start of the recording, such synchrony was gradually lost over several consecutive days as the phasing of cells becomes diversified. This gradual loss of phase clustering is reminiscent of other peripheral clocks such as fibroblasts and SCN neurons of *vipr2*$^{-/-}$ mice (Hughes et al. 2008). Thus, visualising the phasing of PER2 rhythmicity in RPE cells has clarified that RPE cells lack overall coherent phase relationships when cultured as an intact tissue over time.

Whilst I was able to successfully culture RPE cells and confirm the presence of the RPE marker RP65, conducting bioluminescence recordings protocol appeared to be detrimental to cell survival. Thus, I was unable to capture rhythms of primary cultured RPE cells, and consequently unable compare the levels of synchrony between the two cultures. It is clear that further optimisation of the recording protocol is required before bioluminescence imaging can be conducted.

5.4.2 Direct photoentrainment of RPE cells were undetected

To investigate the functionality of endogenous photopigment melanopsin in the RPE, I assayed for light dependent circadian responses in the RPE-choroid explant. Overall, based on the lighting paradigm used, I observed minimal phase responses in both light pulsed tissue and mock control tissues (Figure 5.4). Such light response was negligible compared to the findings of Pulivarthy et al. 2008, where robust amplitude and phase responses were captured in fibroblasts over expressing exogenous mouse melanopsin. When pulsed at the circadian trough, PER2::LUC reporter activity of these fibroblasts exhibited large phase responses of approximately 12 hours. Thus the functional expression of endogenous melanopsin in RPE cells did not match the exogenous overexpression of melanopsin in fibroblasts. The lack of light driven circadian responses reflected the findings by Baba et al. 2010. The authors were the first to report the effect of light on RPE circadian clock gene expression by administering 1 hour pulses of fluorescent light (intensity, 800 $\mu W/cm^2$) across the circadian day and assessing for phases changes in PER2::LUC rhythmicity. Whilst, they reported adjustments in phase of up to 5-6 hours, these phase responses were closely matched by explant cultures that were sham pulsed, thus indicating that light itself was not responsible for the phase deviations of the RPE tissue.

I proceeded to investigate the acute effect of light on RPE physiology in its native ocular environment. Upon exposing a dark adapted mouse to 90 minutes of room light at CT12, I probed for the induction of C-FOS in whole mount RPE-choroid tissue. DAPI fluorescence was localised to RPE nuclei in both light and dark conditions (Figure 5.5 B left panels), whereas the signal arising from immunolabelled C-FOS was scattered diffusely across the tissue of light treated mice only (Figure 5.5 B middle panels) with no clear nuclear localisation. These results are most likely to be due to suboptimal immunohistochemical techniques and not due to the photostimulation protocol. I was able to confirm that retinal phototransduction took place during the light pulse, as shown by an increase in density of C-FOS immuno-reactive cells in the retinas of light treated mice compared to those maintained in the dark (Figure 5.5 A). Light dependent increase in C-FOS expression has also been reported by Hannibal et al. 2001. When 12 hour L:D entrained rats were exposed to light at various times of the circadian day such as ZT0, 6, 14 and 19, an increase in immunoreactivity of C-FOS was observed predominantly in nuclei of retinal ganglion cells. In the absence of light C-FOS immunorectivity was indiscernible. The induction of C-FOS in the retina is likely to be triggered by rod and cone phototransduction. Pickard et al. 2009 reported that light dependent C-FOS activation could be activated in ganglion cells by solely relying on synaptic input from rods and cones in the absence of melanopsin.

5.4.3 Alternative mechanisms of synchronisation

In the present study, I sought to investigate mechanisms of synchronisation between RPE oscillators. There is emerging evidence that peripheral tissues such as the retina, rely on locally secreted signals such as dopamine and GABA to shape the respective phase and amplitude of rhythms (Ruan et al. 2008). I was thus interested to see whether RPE cells are similarly synchronised by local interactions. To this end, I sought to characterise the spatiotemporal distributions of phase and period between RPE cells in explant culture or as isolated cells. I was able to capture rhythms of clock protein expression with high spatial resolution in such a way that was comparable to the single cell level. Unfortunately, I was unable to capture rhythms of primary cultured RPE cells, meaning I was also unable to compare the levels of synchrony between the two cultures. Due to the close association between RPE and retina, the RPE is likely to experience a similar biochemical environment to the outer retina; reports have shown that interactions such as phagocytosis of shed photoreceptor outer segments, lead to transcriptional changes and induction of *c-fos* in the RPE (Ershov et al. 1996). In addition, dopamine receptors are present on the surface of RPE cells, suggesting that endogenous circadian rhythms may also be susceptible to actions of dopamine (Nguyen-Legros et al. 1999).

5. Investigating mechanisms that entrain the RPE clock

6. General discussion

6.1 Advantages of optogenetic actuators

The molecular complexities of an internal signalling network pose a challenge to understanding the functional link between individual receptors and a behavioural response (Nichols and Roth. 2009). In addition, the heterogeneous distribution of receptor subtypes in multicellular systems can also add to the difficulty in selectively activating specific subsets of cells. However, novel optogenetic and pharmacosynthetic technologies have been developed which enable the selective targeting of signaling pathways in a desired subset of tissues (Farrel and Roth. 2013, Deisseroth. 2011). Pharmacogenetic tools such as DREADDs and RASSLs are engineered GPCRs which are exclusively activated by exogenous compounds but not by endogenous ligands. Optogenetic tools however, allow the researcher to circumvent the use of drugs entirely and overcome the temporal resolution of engineered GPCRs.

Light sensitive GPCRs allow for non-invasive manipulation of intercellular molecules in biological systems (Fenno et al. 2011). Due to the selectivity of the photoreceptor protein to light, other endogenous receptors are not activated and the photoreceptor is mutually insensitive to endogenous signals. Thus, cellular responses can solely be attributed to the phototransduction cascade of the optogenetic tool. Opsin based optogenetic tools have been successfully adapted from naturally occurring light sensitive proteins. Other tools have been constructed by extensive splicing of functional domains from light-sensitive and insensitive GPCRs to create light sensitive chimeric receptors (Kim et al. 2005). These tools will enable researchers to command a wide range of intracellular signals in isolation or combination, and ultimately assist with the continuous efforts to delineate the roles of intracellular signalling pathways in mammalian physiology and disease.

6.2 JellyOp mediated phototransduction impacts on the mammalian clock

I sought to study the contribution of GPCR induced cAMP under precisely defined times on the transcriptional regulation of clock genes. In light of its natural $G\alpha_s$ interactions, I sought to employ JellyOp for remotely inducing cAMP and observe the consequences on clock gene dynamics. In particular, I was interested in whether temporally controlled activities of JellyOp could reflect the pharmacological manipulation of cAMP signalling on the mammalian clock, in the context of GPCR signalling. Light induced JellyOp photo activation indeed yielded many aspects of pharmacologically induced circadian responses, as I was able to manipulate the phase, period and amplitude of the *per2* rhythm in a phase and duration dependent manner (An et al. 2011). Phase responses elicited between at CT12 are minimal, whereas, as *per2* approaches CT0, the light pulse also elicited progressively larger phase responses. The simplest interpretation is that the fibroblast clock is most sensitive to JellyOp signalling at CT0. This could arise from the circadian regulation of JellyOp induced cAMP signalling.

In particular, acute induction of clock genes may also be temporally gated such that as the *per2* rhythm approaches CT12, acute induction of clock genes is increasingly suppressed, which results in reduced phase responses. Phase responses imply that clock genes are acutely induced so as to allow for phase responses. It would be useful to quantify the levels of PER protein between CT12 and CT0 to verify whether level of acute induction reflect overall phase responses. It would also be useful to confirm whether CREB was the principal conduit between intracellular signals and acute activation of clock genes, as frequently reported in previous reports.

The PRC derived from WT JellyOp was also dissimilar from the findings of Koinuma et al. 2009, who systematically applied forskolin, a cyclic adenylate cyclase activator, to the C6 glioma cell across the circadian day. They reported that forskolin induced maximal phase responses during CT12 and minimal responses at CT0 or 24. Similarly, the phase response waveform of JellyOp expressing fibroblasts also differed from VIP induced phase responses in SCN slices of PER2::LUC knock-in mice (An et al. 2011).

6. General discussion

The molecular determinants of phase advances and delays are not well understood. However, It is conceivable that JellyOp mediated acute upregulation of clock genes *per* and *cry* at phases between CT0 and 12, leads to premature increase in levels of clock proteins in the cell, which results to accelerated inhibition of CLOCK and BMAL1 activities. Earlier the auto-inhibition is likely to impose higher amplitude phase advances. In contrast, acute induction of genes between 12-24 hours, where clock proteins are rhythmically accumulated in the cell, may lead to an excessive surplus of clock proteins PER and CRY into the cell. This overaccumulation may then immediately cause sustained repression of BMAL1 and CLOCK such that takes it longer for repressor proteins to be degraded, thus delaying the speed in which CLOCK and BMAL1 are disinhibited. This could lead to transient lengthening of the rhythm period, thereby inducing phase delays.

The temporal precision of JellyOp mediated cAMP signalling is likely to be limited by the inactivation time of JellyOp and homeostatic mechanisms involving endogenous cyclic nucleotide phosphodiesterases and possibly β-arrestins. Thus I sought to assess the effective duration of JellyOp signal transduction on clock parameters. In these investigations, light activation between 0–2 hours produced duration dependent phase and period changes in JellyOp expressing fibroblasts. This also mirrored the effect of dosing VIP (10-100 μM) on SCN neurons (An et al. 2011) and applying a range of light durations (0-30 minutes) on melanopsin expressing fibroblasts (Pulivarthy et al. 2007). Light pulses lasting between 2-4 hours produced saturating phase responses, whilst further enhancing the rhythm amplitude of fibroblasts. Taken together, these findings imply that sustained JellyOp phototransduction is necessary to manipulate the clock.

The functional expression of JellyOp in fibroblasts has allowed me to probe the impact of $G\alpha_s$ dependent pathways on various clock parameters including period, phase and amplitude. Based on these investigations, I am confident that wildtype JellyOp will become valuable addition to the established “toolbox” of optogenetic manipulators for studying mammalian physiology.

6. General discussion

6.3 Development of a $G\alpha_s$-decoupled JellyOp

Previously considered only to regulate the GPCRs, β-arrestins have recently been shown to have an extensive impact on cellular behaviour including regulation of insulin secretion, cell cycle and adipocyte differentiation (Hara et al. 2011, Kong et al. 2010, Santos-Zas et al. 2013). These studies are currently performed with pharmacological and genetic tools, but none have yet implemented optogenetics. To address the deficit, I sought to generate various structural variants of JellyOp which favoured β-arrestins signalling independently of G proteins.

I first embarked on designing and constructing a G protein decoupled variant of wildtype JellyOp to favour a β-arrestin biased signal transduction cascade. Upon expression of the F139A JellyOp mutant receptor in HEK and fibroblast cells, I was able to demonstrate an absence of light induced $G\alpha_s$ and $G\alpha_i$ signalling as well as lack of calcium signalling. Furthermore, light induced inhibition of MAPK was evident in fibroblast with delayed kinetics compared to wildtype JellyOp. This raised speculation on whether the mutant could influence signaling pathways by means other than G proteins. I thus turned sought to investigate the role of β-arrestin in mediating the MAPK response.

Upon examining the amino acid sequence, it appears that JellyOp contains several serine and threonine residues on the C-terminus as well as a conserved proline downstream of the DRY motif, all of which have been previously implicated in accelerating β-arrestin recruitment (Marion et al. 2006, Bouvier et al. 1988). However, the cell-based assays failed to detect interactions between JellyOp and β-arrestin. The additional lack of interaction between β-arrestins and β2 adrenergic receptors further highlighted the flaws in the current system and thus warranted further optimisation before any conclusions can be drawn. Hence, future studies should primarily be concerned with deciphering whether or not JellyOp interacts with β-arrestin.

6. General discussion

Few studies have explored the regulatory roles of β-arrestins over opsin phototransduction, nor the binding affinity between β-arrestins and visual opsins. Cell based assays performed by Gurevich et al.1995 have shown that vertebrate rhodopsins exhibited less affinity for visual arrestins. However, a recent report by Kawano-Yamashita et al. 2011 described the light dependent recruitment of β-arrestin to parapinopsin in lamprey pineal organs. Although β-arrestin interactions were not detected, presumably due to a suboptimal assay, I sought to investigate the functional roles of the C-terminus in regulation of G proteins. I therefore proceeded to eliminate the presence of serine and threonine residues from the C-terminus of JellyOp. Following C-terminal truncation, I was unable to detect discernible differences in the kinetics of light induced Glosensor™20F between mutant and wildtype JellyOp expressing cells with all lighting paradigms tested. This again raises further questions about the role of the C-terminus in JellyOp

6.4 JellyOp mediated $G\alpha_s$ independent pathways regulate the circadian clock

One potential means of validating the role of JellyOp mediated cAMP in regulating circadian organisation is to repeat the circadian entrainment experiments using photoactivated adenylate cyclase (PACs), a cytoplasmic enzyme which consists of a photoreceptive BLUF domain and the catalytic domain. However, the kinetics and regulatory mechanisms of PAC signalling may not fully reflect that of GPCRs. To provide a comparable control for JellyOp, I utilised the F139A JellyOp; due to its selective signalling interface, F139A JellyOp pigment represents a suitable control for evaluating the effect cAMP over background signals induced by $G\alpha_s$ coupled GPCRs.

Light induced phase responses were unexpectedly reported in the *per2* rhythms of F139A JellyOp expressing fibroblasts. F139A JellyOp triggered phase response profiles are divergent from wildtype JellyOp, which reflects inherent differences in the phase-responsiveness of the clock to cAMP dependent and independent cascades. Furthermore the PRC of the mutant JellyOp was more comparable to that of melanopsin expressing fibroblasts rather than wildtype JellyOp. However, given a lack of G protein responses from previous studies, it can be presume that the F139A JellyOp signalling pathways are dissimilar to that of melanopsin. It is likely that high amplitude responses are due to unknown interactions between the clock and F139A JellyOp that do not involve cAMP. It would be interesting to test whether G protein independent pathways can also be reproduced with other opsin photopigments such as melanopsin or G protein decoupled non-visual GPCRs such as a $G\alpha_s$ decoupled β2 adrenergic receptor (Shenoy et al. 2006).

6. General discussion

It is tempting to speculate the role of β-arrestins in mediating such G protein independent responses. However, previous cell-based assays failed to shed light on this matter. Thus, future studies should be aimed at deciphering whether β-arrestins have an impact on the clock. This can be evaluated by implementing siRNA technology to suppress β-arrestin expression in host cells. It would also be interesting to decipher whether MAPK inhibition plays a significant role in regulation of the clock. Whilst there is much evidence for MAPK activation on circadian entrainment, little is known for MAPK inhibition (Butcher et al. 2002). This could be achieved by time-delimited application of a pharmacological MAPK inhibitor to the fibroblast clock across the circadian day.

6.5 Future work

One of the aims my investigation, which was not fully addressed, was delineating the ability of JellyOp to bind to mammalian beta-arrestina in cell based assays. Whilst we have concluded that F139A JellyOp does not couple to the $G\alpha_s$ pathway, my next set of aims will be to clarify the immediate downstream effectors of the mutant opsin. Despite current assays failing to detect such as interactions between β-arrestin and F139A JellyOp, I still suspect that β-arrestin is relevant to F139A JellyOp signalling based on the observation that F139A JellyOp was capable of electing light dependent reduction in MAPK phosphorylation in fibroblasts. This event is not likely to be mediated by cAMP as the mutant opsin is not able to activate $G\alpha_s$ signalling pathways that lead to elevation of cAMP. That said, I cannot rule out the possibility that other effectors such as βγ subunits of hetertrimeric G proteins are involved. Nonetheless, it is worth pursuing an alternative experimental strategy for elucidating β-arrestin interactions as my current assay protocols were suboptimal for this purpose.

The next set of aims will be to elucidate the molecular signalling conduits involved in F139A JellyOp mediated phase shifting of the mammalian clock. It was an unexpected but intriguing finding that F139A JellyOp was able to robustly reset the mammalian clock. More interesting still is the divergence of circadian responses elicited between F139A JellyOp and wildtype JellyOp, and thus suggests that the presence of an alternative signalling cascade that interacts with the transcriptional translational feedback loop. In future investigations, I intend to identify the nature of this interaction and the components involved. To this end, I will conduct RT-PCR studies to elucidate whether clock genes *per* and *cry* have been acutely induced following JellyOp and F139A JellyOp stimulation. Induction of clock genes would indicate transcriptional activation, presumably though transcription factors CREB or CLOCK/BMAL1. If clock genes are not activated, this might indicate an alternative mechanism.

6. General discussion

Another one of my aims is to adapt JellyOp for investigating mechanisms of intercellular synchronisation in RPE cells. In this new approach, I will target the expression of JellyOp in RPE cells, photostimulate a localised area of the tissue and investigate the impact of intercellular synchronisation in surrounding, unstimulated RPE oscillators. Having confirmed that JellyOp triggers a cAMP signalling pathway in mammalian cells, it would be conceivable that this cascade can be recapitulated in host RPE cells expressing the opsin photopigment. I will therefore utilise single cell imaging techniques to investigate the impact of localised JellyOp photostimulation on intercellular circadian synchronisation at global and local levels.

6. General discussion

7. References

Airan, R. D., et al. (2009). "Temporally precise in vivo control of intracellular signalling." Nature 458(7241): 1025-9.

Akimzhanov, A. M. And Boehning, D. (2011). "Monitoring dynamic changes in mitochondrial calcium levels during apoptosis using a genetically encoded calcium sensor." J Vis Exp(50).

Alvarez, C. E. (2008). "On the origins of arrestin and rhodopsin." BMC Evol Biol 8: 222.

Alvarez-Curto, E., et al. (2011). "Developing chemical genetic approaches to explore G protein-coupled receptor function: validation of the use of a receptor activated solely by synthetic ligand (RASSL)." Mol Pharmacol 80(6): 1033-46.

An, S., et al. (2011). "Vasoactive intestinal polypeptide requires parallel changes in adenylate cyclase and phospholipase C to entrain circadian rhythms to a predictable phase." J Neurophysiol 105(5): 2289-96.

Ardawatia, V. V., et al. (2010). "Galpha(12) binds to the N-terminal regulatory domain of p120(ctn), and downregulates p120(ctn) tyrosine phosphorylation induced by Src family kinases via a RhoA independent mechanism." Exp Cell Res 317(3): 293-306.

Armbruster, B. N., et al. (2007). "Evolving the lock to fit the key to create a family of G protein-coupled receptors potently activated by an inert ligand." Proc Natl Acad Sci U S A 104(12): 5163-8.

Aton, S. J. and Herzog, E. D. (2005). "Come together, right...now: synchronization of rhythms in a mammalian circadian clock." Neuron 48(4): 531-4.

Azzi, M., et al. (2003). "B-arrestin-mediated activation of MAPK by inverse agonists reveals distinct active conformations for G protein-coupled receptors." Proc Natl Acad Sci U S A 100(20): 11406-11.

Baba, K., A. et al. (2010). "Circadian regulation of the PERIOD 2::LUCIFERASE bioluminescence rhythm in the mouse retinal pigment epithelium-choroid." Mol Vis 16: 2605-11.

Badura, L., et al. (2007). "An inhibitor of casein kinase I epsilon induces phase delays in circadian rhythms under free-running and entrained conditions." J Pharmacol Exp Ther 322(2): 730-8.

Bailes, H. J. and Lucas, R. J. (2013). "Human melanopsin forms a pigment maximally sensitive to blue light (lambdamax approximately 479 nm) supporting activation of G(q/11) and G(i/o) signalling cascades." Proc Biol Sci 280(1759): 20122987.

Bailes, H. J., et al. (2012). "Reproducible and sustained regulation of Galphas signalling using a metazoan opsin as an optogenetic tool." PLoS One 7(1): e30774.

7. References

Baker, J. G. and Hill, S. J. (2007). "Multiple GPCR conformations and signalling pathways: implications for antagonist affinity estimates." Trends Pharmacol Sci 28(8): 374-81.

Ballesteros, J. A., et al. (2001). "Activation of the beta 2-adrenergic receptor involves disruption of an ionic lock between the cytoplasmic ends of transmembrane segments 3 and 6." J Biol Chem 276(31): 29171-7.

Bandyopadhyay, M. and Rohrer, B. (2010). "Photoreceptor structure and function is maintained in organotypic cultures of mouse retinas." Mol Vis 16: 1178-85.

Bauer, C. K., et al. (1996). "An endogenous inactivating inward-rectifying potassium current in oocytes of Xenopus laevis." Pflugers Arch 432(5): 812-20.

Baylor, D. (1996). "How photons start vision." Proc Natl Acad Sci U S A 93(2): 560-5.

Berson, D. M., et al. (2002). "Phototransduction by retinal ganglion cells that set the circadian clock." Science 295(5557): 1070-3.

Binkowski, B. F., et al. (2011). "A luminescent biosensor with increased dynamic range for intracellular cAMP." ACS Chem Biol 6(11): 1193-7.

Binkowski, B., et al. (2009). "Engineered luciferases for molecular sensing in living cells." Curr Opin Biotechnol 20(1): 14-8.

Borhan, B., et al. (2000). "Movement of retinal along the visual transduction path." Science 288(5474): 2209-12.

Bouvier, M., et al. (1988). "Removal of phosphorylation sites from the beta 2-adrenergic receptor delays onset of agonist-promoted desensitization." Nature 333(6171): 370-3.

Boyden, E. S., et al. (2005). "Millisecond-timescale, genetically targeted optical control of neural activity." Nat Neurosci 8(9): 1263-8.

Brown, R. L. and Robinson, P. R. (2004). "Melanopsin--shedding light on the elusive circadian photopigment." Chronobiol Int 21(2): 189-204.

Butcher, A. J., et al. (2012). "Physiological role of G-protein coupled receptor phosphorylation." Handb Exp Pharmacol(208): 79-94.

Butcher, G. Q., et al. (2002). "The p42/44 mitogen-activated protein kinase pathway couples photic input to circadian clock entrainment." J Biol Chem 277(33): 29519-25.

Camacho, F., et al. (2001). "Human casein kinase Iδ phosphorylation of human circadian clock proteins period 1 and 2." FEBS Lett 489(2-3): 159-65.

Cameron, M. A., et al. (2009). "Light regulation of retinal dopamine that is independent of melanopsin phototransduction." Eur J Neurosci 29(4): 761-7.

7. References

Cao, P., et al. 2012. (2011). "Light-sensitive coupling of rhodopsin and melanopsin to G(i/o) and G(q) signal transduction in Caenorhabditis elegans." FASEB J 26(2): 480-91.

Cassel, D. and Selinger, Z. (1978). "Mechanism of adenylate cyclase activation through the beta-adrenergic receptor: catecholamine-induced displacement of bound GDP by GTP." Proc Natl Acad Sci U S A 75(9): 4155-9.

Ceresa, B. P. and Limbird, L. E. (1994). "Mutation of an aspartate residue highly conserved among G-protein-coupled receptors results in nonreciprocal disruption of alpha 2-adrenergic receptor-G-protein interactions. A negative charge at amino acid residue 79 forecasts alpha 2A-adrenergic receptor sensitivity to allosteric modulation by monovalent cations and fully effective receptor/G-protein coupling." J Biol Chem 269(47): 29557-64.

Cervantes, D., et al. (2009). "Arrestin orchestrates crosstalk between G protein-coupled receptors to modulate the spatiotemporal activation of ERK MAPK." Circ Res 106(1): 79-88.

Chang, W. C., et al. (2007). "Modifying ligand-induced and constitutive signaling of the human 5-HT4 receptor." PLoS One 2(12): e1317.

Chen, C. K. (2005). "The vertebrate phototransduction cascade: amplification and termination mechanisms." Rev Physiol Biochem Pharmacol 154: 101-21.

Chen, P., et al. (2001). "A photic visual cycle of rhodopsin regeneration is dependent on Rgr." Nat Genet 28(3): 256-60.

Chen, Q., et al. (2010). "Role of N-linked glycosylation in biosynthesis, trafficking, and function of the human glucagon-like peptide 1 receptor." Am J Physiol Endocrinol Metab 299(1): E62-8.

Cheng, C. Y., et al. (2009). "Sensing domain dynamics in protein kinase A-I{alpha} complexes by solution X-ray scattering." J Biol Chem 284(51): 35916-25.

Cherezov, V., et al. (2007). "High-resolution crystal structure of an engineered human β2-adrenergic G protein-coupled receptor." Science 318(5854): 1258-65.

Christopoulos, A. and Kenakin, T. (2002). "G protein-coupled receptor allosterism and complexing." Pharmacol Rev 54(2): 323-74.

Clack, J. W., et al. (2006). "Transducin subunit stoichiometry and cellular distribution in rod outer segments." Cell Biol Int 30(10): 829-35.

Clapham, D. E. (1995). "Calcium signaling." Cell 80(2): 259-68.

Clapham, D. E. (2007). "Calcium signaling." Cell 131(6): 1047-58.

Cohen, G. B., et al. (1992). "Mechanism of activation and inactivation of opsin: role of Glu113 and Lys296." Biochemistry 31(50): 12592-601.

7. References

Comas, M., et al. (2006). "Phase and period responses of the circadian system of mice (Mus musculus) to light stimuli of different duration." J Biol Rhythms 21(5): 362-72.

de Rooij, J., et al. (2000). "Mechanism of regulation of the Epac family of cAMP-dependent RapGEFs." J Biol Chem 275(27): 20829-36.

Decoursey, P. J. (1960). "Phase control of activity in a rodent." Cold Spring Harb Symp Quant Biol 25: 49-55.

Deisseroth, K. (2011) "Optogenetics." Nat Methods 8(1): 26-9.

Deisseroth, K., et al. (2006). "Next-generation optical technologies for illuminating genetically targeted brain circuits." J Neurosci 26(41): 10380-6.

Doi, M., et al. (2011). "Circadian regulation of intracellular G-protein signalling mediates intercellular synchrony and rhythmicity in the suprachiasmatic nucleus." Nat Commun 2: 327.

Dupriez, V. J., et al. (2002). "Aequorin-based functional assays for G-protein-coupled receptors, ion channels, and tyrosine kinase receptors." Receptors Channels 8(5-6): 319-30.

Earnest, D. J., et al. (1990). "Photic regulation of c-fos expression in neural components governing the entrainment of circadian rhythms." Exp Neurol 109(3): 353-61.

Edwards, R. B. and Adler, A. J. (1994). "Exchange of retinol between IRBP and CRBP." Exp Eye Res 59(2): 161-70.

Ershov, A. V., et al. (1996). "Selective transcription factor induction in retinal pigment epithelial cells during photoreceptor phagocytosis." J Biol Chem 271(45): 28458-62.

Fan, F., et al. (2008). "Novel genetically encoded biosensors using firefly luciferase." ACS Chem Biol 3(6): 346-51.

Fan, H. Y., et al. (2004). "Protein kinase C and mitogen-activated protein kinase cascade in mouse cumulus cells: cross talk and effect on meiotic resumption of oocyte." Biol Reprod 70(4): 1178-87.

Fan, J. Y., et al. (2009). "Drosophila and vertebrate casein kinase Iδ exhibits evolutionary conservation of circadian function." Genetics 181(1): 139-52.

Farrell, M. S. and Roth, B. L. (2013). "Pharmacosynthetics: Reimagining the pharmacogenetic approach." Brain Res 1511: 6-20.

Fenno, L., et al. (2011). "The development and application of optogenetics." Annu Rev Neurosci 34: 389-412.

Fredriksson, R., et al. (2003). "Seven evolutionarily conserved human rhodopsin G protein-coupled receptors lacking close relatives." FEBS Lett 554(3): 381-8.

7. References

Fu, Y. and Yau, K. W. (2007). "Phototransduction in mouse rods and cones." Pflugers Arch 454(5): 805-19.

Fukuda, H., et al. (2011). "Quantitative analysis of phase wave of gene expression in the mammalian central circadian clock network." PLoS One 6(8): e23568.

Fukuhara, S., et al. (1999). "A novel PDZ domain containing guanine nucleotide exchange factor links heterotrimeric G proteins to Rho." J Biol Chem 274(9): 5868-79.

Galione, A. and Churchill, G. C. (2002). "Interactions between calcium release pathways: multiple messengers and multiple stores." Cell Calcium 32(5-6): 343-54.

Gallego, M., et al. (2006). "An opposite role for tau in circadian rhythms revealed by mathematical modeling." Proc Natl Acad Sci U S A 103(28): 10618-23.

Garriga, P., et al. (1996). "Structure and function in rhodopsin: correct folding and misfolding in point mutants at and in proximity to the site of the retinitis pigmentosa mutation Leu-125-->Arg in the transmembrane helix C." Proc Natl Acad Sci U S A 93(10): 4560-4.

Gau, D., et al. (2002). "Phosphorylation of CREB Ser142 regulates light-induced phase shifts of the circadian clock." Neuron 34(2): 245-53.

Gesty-Palmer, D. and Luttrell, L. M. (2008). "Heptahelical terpsichory. Who calls the tune?" J Recept Signal Transduct Res 28(1-2): 39-58.

Gesty-Palmer, et al. (2006). "Distinct beta-arrestin- and G protein-dependent pathways for parathyroid hormone receptor-stimulated ERK1/2 activation." J Biol Chem 281(16): 10856-64.

Gibson, S. K., et al. (2000). "Phosphorylation modulates the affinity of light-activated rhodopsin for G protein and arrestin." Biochemistry 39(19): 5738-49.

Giesbers, M. E., et al. (2008). "Functional expression, targeting and Ca2+ signaling of a mouse melanopsin-eYFP fusion protein in a retinal pigment epithelium cell line." Photochem Photobiol 84(4): 990-5.

Gillette, M. U. and Prosser, R. A. (1988). "Circadian rhythm of the rat suprachiasmatic brain slice is rapidly reset by daytime application of cAMP analogs." Brain Res 474(2): 348-52.

Ginty, D. D., et al. (1993). "Regulation of CREB phosphorylation in the suprachiasmatic nucleus by light and a circadian clock." Science 260(5105): 238-41.

Goddard, A. D. and Watts, A. (2012). "Regulation of G protein-coupled receptors by palmitoylation and cholesterol." BMC Biol 10: 27.

Godinho, S. I., et al. (2007). "The after-hours mutant reveals a role for Fbxl3 in determining mammalian circadian period." Science 316(5826): 897-900.

7. References

Golombek, D. A. and Rosenstein, R. E. (2010). "Physiology of circadian entrainment." Physiol Rev 90(3): 1063-102.

Gomez, M. P. and Nasi, E. (2000). "Light transduction in invertebrate hyperpolarizing photoreceptors: possible involvement of a Go-regulated guanylate cyclase." J Neurosci 20(14): 5254-63.

Gonzalez, G. A. and Montminy, M. R. (1989). "Cyclic AMP stimulates somatostatin gene transcription by phosphorylation of CREB at serine 133." Cell 59(4): 675-80.

Govardhan, C. P. and Oprian, D. D. (1994). "Active site-directed inactivation of constitutively active mutants of rhodopsin." J Biol Chem 269(9): 6524-7.

Grewal, S. S., et al. (2000). "Calcium and cAMP signals differentially regulate cAMP-responsive element-binding protein function via a Rap1-extracellular signal-regulated kinase pathway." J Biol Chem 275(44): 34433-41.

Grone, B. P., et al. (2011). "Acute light exposure suppresses circadian rhythms in clock gene expression." J Biol Rhythms 26(1): 78-81.

Guettier, J. M., et al. (2009). "A chemical-genetic approach to study G protein regulation of beta cell function in vivo." Proc Natl Acad Sci U S A 106(45): 19197-202.

Gunther, E. C., et al. (2000). "The G-protein inhibitor, pertussis toxin, inhibits the secretion of brain-derived neurotrophic factor." Neuroscience 100(3): 569-79.

Gurevich, E. V. And Gurevich, V. V. (2006). "Arrestins: ubiquitous regulators of cellular signaling pathways." Genome Biol 7(9): 236.

Gurevich, V. V. and Benovic, J. L.. (1995). "Visual arrestin binding to rhodopsin. Diverse functional roles of positively charged residues within the phosphorylation-recognition region of arrestin." J Biol Chem 270(11): 6010-6.

Gutierrez, D. V., et al. (2011). "Optogenetic control of motor coordination by Gi/o protein-coupled vertebrate rhodopsin in cerebellar Purkinje cells." J Biol Chem 286(29): 25848-58.

Hamada, T., et al. (1999). "The role of inositol trisphosphate-induced Ca2+ release from IP3-receptor in the rat suprachiasmatic nucleus on circadian entrainment mechanism." Neurosci Lett 263(2-3): 125-8.

Hannibal, J., et al. (2001). "Light-dependent induction of cFos during subjective day and night in PACAP-containing ganglion cells of the retinohypothalamic tract." J Biol Rhythms 16(5): 457-70.

Hao, W. and Fong, H. K. (1999). "The endogenous chromophore of retinal G protein-coupled receptor opsin from the pigment epithelium." J Biol Chem 274(10): 6085-90.

Hara, M. R., et al. (2011). "A stress response pathway regulates DNA damage through β2-adrenoreceptors and β-arrestin-1." Nature 477(7364): 349-53.

7. References

Hargrave, P. A. and McDowell, J. H. (1992). "Rhodopsin and phototransduction: a model system for G protein-linked receptors." FASEB J 6(6): 2323-31.

Harmar, A. J., et al. (2002). "The VPAC(2) receptor is essential for circadian function in the mouse suprachiasmatic nuclei." Cell 109(4): 497-508.

Hart, M. J., et al. (1998). "Direct stimulation of the guanine nucleotide exchange activity of p115 RhoGEF by Galpha13." Science 280(5372): 2112-4.

Hata, J. A. and Koch, W. J. (2003). "Phosphorylation of G protein-coupled receptors: GPCR kinases in heart disease." Mol Interv 3(5): 264-72.

Hattar, S., et al. (2002). "Melanopsin-containing retinal ganglion cells: architecture, projections, and intrinsic photosensitivity." Science 295(5557): 1065-70.

Hattar, S., et al. (2003). "Melanopsin and rod-cone photoreceptive systems account for all major accessory visual functions in mice." Nature 424(6944): 76-81.

He, P. J., et al. (2006). "Real-time monitoring of cAMP response element binding protein signaling in porcine granulosa cells modulated by ovarian factors." Mol Cell Biochem 290(1-2): 177-84.

Heck, M. and Hofmann, K. P. (1993). "G-protein-effector coupling: a real-time light-scattering assay for transducin-phosphodiesterase interaction." Biochemistry 32(32): 8220-7.

Herzog, E. D., et al. (2004). "Temporal precision in the mammalian circadian system: a reliable clock from less reliable neurons." J Biol Rhythms 19(1): 35-46.

Heth, C. A. and Marescalchi, P. A. (1994). "Inositol triphosphate generation in cultured rat retinal pigment epithelium." Invest Ophthalmol Vis Sci 35(2): 409-16.

Hirota, T. and Fukada, Y. (2004). "Resetting mechanism of central and peripheral circadian clocks in mammals." Zoolog Sci 21(4): 359-68.

Hong, J. H., et al. (2012). "Circadian waves of cytosolic calcium concentration and long-range network connections in rat suprachiasmatic nucleus." Eur J Neurosci 35(9): 1417-25.

Hughes, A. T., et al. (2008). "Live imaging of altered period1 expression in the suprachiasmatic nuclei of Vipr2-/- mice." J Neurochem 106(4): 1646-57.

Hunt, N. H. and Evans, T. (1980). "RMI 12330A, an inhibitor of cyclic nucleotide phosphodiesterases and adenylate cyclase in kidney preparations." Biochim Biophys Acta 613(2): 499-506.

Imanishi, Y., et al. (2004). "Noninvasive two-photon imaging reveals retinyl ester storage structures in the eye." J Cell Biol 164(3): 373-83.

Inouye, S., et al. (1985). "Cloning and sequence analysis of cDNA for the luminescent protein aequorin." Proc Natl Acad Sci U S A 82(10): 3154-8.

7. References

Iseki, M., et al. (2002). "A blue-light-activated adenylyl cyclase mediates photoavoidance in Euglena gracilis." Nature 415(6875): 1047-51.

Ishikawa, Y. and Homcy, C. J. (1997). "The adenylyl cyclases as integrators of transmembrane signal transduction." Circ Res 80(3): 297-304.

Isojima, Y., et al. (2009). "CKIepsilon/δ-dependent phosphorylation is a temperature-insensitive, period-determining process in the mammalian circadian clock." Proc Natl Acad Sci U S A 106(37): 15744-9.

Iuvone, P. M., et al. (1978). "Light stimulates tyrosine hydroxylase activity and dopamine synthesis in retinal amacrine neurons." Science 202(4370): 901-2.

Izumo, M., et al. (2003). "Circadian gene expression in mammalian fibroblasts revealed by real-time luminescence reporting: temperature compensation and damping." Proc Natl Acad Sci U S A 100(26): 16089-94.

Jensen, A. D., et al. (2001). "Agonist-induced conformational changes at the cytoplasmic side of transmembrane segment 6 in the beta 2 adrenergic receptor mapped by site-selective fluorescent labeling." J Biol Chem 276(12): 9279-90.

Jiang, M., et al. (1993). "An opsin homologue in the retina and pigment epithelium." Invest Ophthalmol Vis Sci 34(13): 3669-78.

Johnson, C. H. (1999). "Forty years of PRCs--what have we learned?" Chronobiol Int 16(6): 711-43.

Johnson, C. H., et al. (2003). "Entrainment of circadian programs." Chronobiol Int 20(5): 741-74.

Johnson, E. N., et al. (2003). "RGS16 inhibits signalling through the G alpha 13-Rho axis." Nat Cell Biol 5(12): 1095-103.

Jud, C., et al. (2010). "High amplitude phase resetting in rev-erbalpha/per1 double mutant mice." PLoS One 5(9).

Karnik, S. S. and Khorana, H. G. (1990). "Assembly of functional rhodopsin requires a disulfide bond between cysteine residues 110 and 187." J Biol Chem 265(29): 17520-4.

Kaupp, U. B. and Seifert, R. (2002). "Cyclic nucleotide-gated ion channels." Physiol Rev 82(3): 769-824.

Kawano-Yamashita, E., et al. (2011). "β-arrestin functionally regulates the non-bleaching pigment parapinopsin in lamprey pineal." PLoS One 6(1): e16402.

Kelly, P., et al. (2007). "Biologic functions of the G12 subfamily of heterotrimeric g proteins: growth, migration, and metastasis." Biochemistry 46(23): 6677-87.

Keravis, T. and Lugnier, C. (2012) "Cyclic nucleotide phosphodiesterase (PDE) isozymes as targets of the intracellular signalling network: benefits of PDE inhibitors in various diseases and perspectives for future therapeutic developments." Br J Pharmacol 165(5): 1288-305.

7. References

Kim, J. M., et al. (2005). "Light-driven activation of beta 2-adrenergic receptor signaling by a chimeric rhodopsin containing the beta 2-adrenergic receptor cytoplasmic loops." Biochemistry 44(7): 2284-92.

Ko, H. W., et al. (2007). "Cis-combination of the classic per(S) and per(L) mutations results in arrhythmic Drosophila with ectopic accumulation of hyperphosphorylated PERIOD protein." J Biol Rhythms 22(6): 488-501.

Kojima, A., et al. (2008). "Connexin 43 contributes to differentiation of retinal pigment epithelial cells via cyclic AMP signaling." Biochem Biophys Res Commun 366(2): 532-8.

Kojima, D., et al. (1997). "A novel Go-mediated phototransduction cascade in scallop visual cells." J Biol Chem 272(37): 22979-82.

Kong, K. C., et al. (2010). "M3-muscarinic receptor promotes insulin release via receptor phosphorylation/arrestin-dependent activation of protein kinase D1." Proc Natl Acad Sci U S A 107(49): 21181-6.

Konig, B., et al. (1989). "Three cytoplasmic loops of rhodopsin interact with transducin." Proc Natl Acad Sci U S A 86(18): 6878-82.

Konopka, R. J. and Benzer, S. (1971). "Clock mutants of Drosophila melanogaster." Proc Natl Acad Sci U S A 68(9): 2112-6.

Kornhauser, J. M., et al. (1996). "Light, immediate-early genes, and circadian rhythms." Behav Genet 26(3): 221-40.

Koyanagi, M., et al. (2008). "Jellyfish vision starts with cAMP signaling mediated by opsin-G(s) cascade." Proc Natl Acad Sci U S A 105(40): 15576-80.

Krasel, C., et al. (2008). "Dual role of the β2-adrenergic receptor C terminus for the binding of β-arrestin and receptor internalization." J Biol Chem 283(46): 31840-8.

Kristiansen, K. (2004). "Molecular mechanisms of ligand binding, signaling, and regulation within the superfamily of G-protein-coupled receptors: molecular modeling and mutagenesis approaches to receptor structure and function." Pharmacol Ther 103(1): 21-80.

Kristiansen, K., et al. (2000). "A highly conserved aspartic acid (Asp-155) anchors the terminal amine moiety of tryptamines and is involved in membrane targeting of the 5-HT(2A) serotonin receptor but does not participate in activation via a "salt-bridge disruption" mechanism." J Pharmacol Exp Ther 293(3): 735-46.

Kubo, T., et al. (2008). "The therapeutic effects of Rho-ROCK inhibitors on CNS disorders." Ther Clin Risk Manag 4(3): 605-15.

Kurose, H. (2003). "Galpha12 and Galpha13 as key regulatory mediator in signal transduction." Life Sci 74(2-3): 155-61.

7. References

Lagerstrom, M. C. and Schioth, H. B. (2008). "Structural diversity of G protein-coupled receptors and significance for drug discovery." Nat Rev Drug Discov 7(4): 339-57.

Laporte, S. A., et al. (2000). "The interaction of beta-arrestin with the AP-2 adaptor is required for the clustering of beta 2-adrenergic receptor into clathrin-coated pits." J Biol Chem 275(30): 23120-6.

Laroche-Joubert, N., et al. (2002). "Protein kinase A-independent activation of ERK and H,K-ATPase by cAMP in native kidney cells: role of Epac I." J Biol Chem 277(21): 18598-604.

Le Poul, E., et al. (2002). "Adaptation of aequorin functional assay to high throughput screening." J Biomol Screen 7(1): 57-65.

Lee, C. H., et al. (1992). "Members of the Gq alpha subunit gene family activate phospholipase C beta isozymes." J Biol Chem 267(23): 16044-7.

Lee, Y., et al. (2010). "Coactivation of the CLOCK-BMAL1 complex by CBP mediates resetting of the circadian clock." J Cell Sci 123(Pt 20): 3547-57.

Leise, T. L., et al. (2012). "Persistent cell-autonomous circadian oscillations in fibroblasts revealed by six-week single-cell imaging of PER2::LUC bioluminescence." PLoS One 7(3): e33334.

Li, J., et al. (2012). "Lithium impacts on the amplitude and period of the molecular circadian clockwork." PLoS One 7(3): e33292.

Li, N., et al. (2008). "Suprachiasmatic nucleus slices induce molecular oscillations in fibroblasts." Biochem Biophys Res Commun 377(4): 1179-84.

Lin, S. C., et al. (2011). "Optogenetics: background and concepts for neurosurgery." Neurosurgery 69(1): 1-3.

Lipp, P. and Reither, G. (2011). "Protein kinase C: the "masters" of calcium and lipid." Cold Spring Harb Perspect Biol 3(7).

Liu, A. C., et al. (2007). "Mammalian circadian signaling networks and therapeutic targets." Nat Chem Biol 3(10): 630-9.

Loirand, G., et al. (2006). "Rho kinases in cardiovascular physiology and pathophysiology." Circ Res 98(3): 322-34.

Lowrey, P. L. and Takahashi, J. S. (2004). "Mammalian circadian biology: elucidating genome-wide levels of temporal organization." Annu Rev Genomics Hum Genet 5: 407-41.

Lowrey, P. L., et al. (2000). "Positional syntenic cloning and functional characterization of the mammalian circadian mutation tau." Science 288(5465): 483-92.

Lozier, R. H., et al. (1975). "Bacteriorhodopsin: a light-driven proton pump in Halobacterium Halobium." Biophys J 15(9): 955-62.

7. References

Lucas, R. J., S. et al. (2003). "Diminished pupillary light reflex at high irradiances in melanopsin-knockout mice." Science 299(5604): 245-7.

Luttrell, L. M. and Lefkowitz, R. J. (2002). "The role of beta-arrestins in the termination and transduction of G-protein-coupled receptor signals." J Cell Sci 115(Pt 3): 455-65.

Maeda, T., et al. (2003). "Rhodopsin phosphorylation: 30 years later." Prog Retin Eye Res 22(4): 417-34.

Malik, S., et al. (1995). "The role of the CANNTG promoter element (E box) and the myocyte-enhancer-binding-factor-2 (MEF-2) site in the transcriptional regulation of the chick myogenin gene." Eur J Biochem 230(1): 88-96.

Mao, L. M., et al. (2007). "Protein kinase C-regulated cAMP response element-binding protein phosphorylation in cultured rat striatal neurons." Brain Res Bull 72(4-6): 302-8.

Marinissen, M. J. and Gutkind, J. S. (2001). "G-protein-coupled receptors and signaling networks: emerging paradigms." Trends Pharmacol Sci 22(7): 368-76.

Marion, S., et al. (2006). "A beta-arrestin binding determinant common to the second intracellular loops of rhodopsin family G protein-coupled receptors." J Biol Chem 281(5): 2932-8.

Masseck, O. A., et al. (2011). "Light- and drug-activated G-protein-coupled receptors to control intracellular signalling." Exp Physiol 96(1): 51-6.

Mata, N. L., et al. (1992). "Hydrolysis of 11-cis- and all-trans-retinyl palmitate by retinal pigment epithelium microsomes." J Biol Chem 267(14): 9794-9.

Matsuyama, T., et al. (2012). "Photochemical properties of mammalian melanopsin." Biochemistry 51(27): 5454-62.

Mawad, K. and Van Gelder, R. N. (2008). "Absence of long-wavelength photic potentiation of murine intrinsically photosensitive retinal ganglion cell firing in vitro." J Biol Rhythms 23(5): 387-91.

Maywood, E. S., et al. (2011). "A diversity of paracrine signals sustains molecular circadian cycling in suprachiasmatic nucleus circuits." Proc Natl Acad Sci U S A 108(34): 14306-11.

McBee, J. K., et al. (2001). "Confronting complexity: the interlink of phototransduction and retinoid metabolism in the vertebrate retina." Prog Retin Eye Res 20(4): 469-529.

Melyan, Z., et al. (2005). "Addition of human melanopsin renders mammalian cells photoresponsive." Nature 433(7027): 741-5.

Meng, Q. J., et al. (2008). "Setting clock speed in mammals: the CK1 epsilon tau mutation in mice accelerates circadian pacemakers by selectively destabilizing PERIOD proteins." Neuron 58(1): 78-88.

7. References

Meng, Q. J., et al. (2010). "Entrainment of disrupted circadian behavior through inhibition of casein kinase 1 (CK1) enzymes." Proc Natl Acad Sci U S A 107(34): 15240-5.

Miesenbock, G. (2004). "Genetic methods for illuminating the function of neural circuits." Curr Opin Neurobiol 14(3): 395-402.

Miller, G. (2006). "Optogenetics. Shining new light on neural circuits." Science 314(5806): 1674-6.

Miller, W. E. and Lefkowitz, R. J. (2001). "Arrestins as signaling molecules involved in apoptotic pathways: a real eye opener." Sci STKE 2001(69): pe1.

Milligan, G. (2003). "Constitutive activity and inverse agonists of G protein-coupled receptors: a current perspective." Mol Pharmacol 64(6): 1271-6.

Mohawk, J. A., et al. (2012). "Central and peripheral circadian clocks in mammals." Annu Rev Neurosci 35: 445-62.

Moiseyev, G., et al. (2003). "Retinyl esters are the substrate for isomerohydrolase." Biochemistry 42(7): 2229-38.

Montell, C. (2012). "Drosophila visual transduction." Trends Neurosci 35(6): 356-63.

Moore, R. Y. and Eichler, V. B. (1972). "Loss of a circadian adrenal corticosterone rhythm following suprachiasmatic lesions in the rat." Brain Res 42(1): 201-6.

Moro, O., et al. (1993). "Hydrophobic amino acid in the i2 loop plays a key role in receptor-G protein coupling." J Biol Chem 268(30): 22273-6.

Nagano, M., et al. (2009). "rPer1 and rPer2 induction during phases of the circadian cycle critical for light resetting of the circadian clock." Brain Res 1289: 37-48.

Nagarathnam, B., et al. (2011). "Insights from the analysis of conserved motifs and permitted amino acid exchanges in the human, the fly and the worm GPCR clusters." Bioinformation 7(1): 15-20.

Nagel, G., et al. (2003). "Channelrhodopsin-2, a directly light-gated cation-selective membrane channel." Proc Natl Acad Sci U S A 100(24): 13940-5.

Nagel, G., et al. (2005). "Light activation of channelrhodopsin-2 in excitable cells of Caenorhabditis elegans triggers rapid behavioral responses." Curr Biol 15(24): 2279-84.

Nagoshi, E., et al. (2004). "Circadian gene expression in individual fibroblasts: cell-autonomous and self-sustained oscillators pass time to daughter cells." Cell 119(5): 693-705.

Nakajima, K. and Wess, J. (2012). "Design and functional characterization of a novel, arrestin-biased designer G protein-coupled receptor." Mol Pharmacol 82(4): 575-82.

Nakata, H. and Kozasa, T. (2005). "Functional characterization of Galphao signaling through G protein-regulated inducer of neurite outgrowth 1." Mol Pharmacol 67(3): 695-702.

7. References

Nathans, J., C. et al. (1989). "Production of bovine rhodopsin by mammalian cell lines expressing cloned cDNA: spectrophotometry and subcellular localization." Vision Res 29(8): 907-14.

Nathans, J., et al. (1989). "Production of bovine rhodopsin by mammalian cell lines expressing cloned cDNA: spectrophotometry and subcellular localization." Vision Res 29(8): 907-14.

Nelson, C. P. and Challiss, R. A. (2007). ""Phenotypic" pharmacology: the influence of cellular environment on G protein-coupled receptor antagonist and inverse agonist pharmacology." Biochem Pharmacol 73(6): 737-51.

Nguyen-Legros, J., et al. (1999). "Dopamine receptor localization in the mammalian retina." Mol Neurobiol 19(3): 181-204.

Nichols, C. D. and Roth, B. L. (2009). "Engineered G-protein Coupled Receptors are Powerful Tools to Investigate Biological Processes and Behaviors." Front Mol Neurosci 2: 16.

Nobles, K. N., et al. (2007). "The active conformation of beta-arrestin1: direct evidence for the phosphate sensor in the N-domain and conformational differences in the active states of beta-arrestins1 and -2." J Biol Chem 282(29): 21370-81.

Norum, J. H., et al. (2003). "Ras-dependent ERK activation by the human G(s)-coupled serotonin receptors 5-HT4(b) and 5-HT7(a)." J Biol Chem 278(5): 3098-104.

Ntefidou, M., et al. (2003). "Photoactivated adenylyl cyclase controls phototaxis in the flagellate Euglena gracilis." Plant Physiol 133(4): 1517-21.

Oakley, R. H., et al. (2000). "Differential affinities of visual arrestin, beta arrestin1, and beta arrestin2 for G protein-coupled receptors delineate two major classes of receptors." J Biol Chem 275(22): 17201-10.

Oh, E., et al. (2010). "Substitution of 5-HT1A receptor signaling by a light-activated G protein-coupled receptor." J Biol Chem 285(40): 30825-36.

Oldham, W. M. and Hamm, H. E. (2008). "Heterotrimeric G protein activation by G-protein-coupled receptors." Nat Rev Mol Cell Biol 9(1): 60-71.

O'Neill, J. S. and Reddy, A. B. (2012). "The essential role of cAMP/Ca2+ signalling in mammalian circadian timekeeping." Biochem Soc Trans 40(1): 44-50.

O'Neill, J. S., et al. (2008). "cAMP-dependent signaling as a core component of the mammalian circadian pacemaker." Science 320(5878): 949-53.

Page, K. M., C. A. Curtis, et al. (1995). "The functional role of the binding site aspartate in muscarinic acetylcholine receptors, probed by site-directed mutagenesis." Eur J Pharmacol 289(3): 429-37.

Palczewski, K., et al. (2000). "Crystal structure of rhodopsin: A G protein-coupled receptor." Science 289(5480): 739-45.

7. References

Pandey, S., et al. (1994). "Cytoplasmic retinal localization of an evolutionary homolog of the visual pigments." Exp Eye Res 58(5): 605-13.

Parkinson, D. and Rando, R. R. (1983). "Effect of light on dopamine turnover and metabolism in rabbit retina." Invest Ophthalmol Vis Sci 24(3): 384-8.

Pearson, R. A., et al. (2004). "Ca(2+) signalling and gap junction coupling within and between pigment epithelium and neural retina in the developing chick." Eur J Neurosci 19(9): 2435-45.

Peirson, S. N., et al. (2004). "Expression of the candidate circadian photopigment melanopsin (Opn4) in the mouse retinal pigment epithelium." Brain Res Mol Brain Res 123(1-2): 132-5.

Perlman, J. H., et al. (1995). "A disulfide bond between conserved extracellular cysteines in the thyrotropin-releasing hormone receptor is critical for binding." J Biol Chem 270(42): 24682-5.

Pickard, G. E., et al. (2009). "Light-induced fos expression in intrinsically photosensitive retinal ganglion cells in melanopsin knockout (opn4) mice." PLoS One 4(3): e4984.

Pierce, K. L. and Lefkowitz, R. J. (2001). "Classical and new roles of β-arrestins in the regulation of G-protein-coupled receptors." Nat Rev Neurosci 2(10): 727-33.

Pierce, K. L., et al. (2002). "Seven-transmembrane receptors." Nat Rev Mol Cell Biol 3(9): 639-50.

Piggins, H. D. and Cutler, D. J. (2003). "The roles of vasoactive intestinal polypeptide in the mammalian circadian clock." J Endocrinol 177(1): 7-15.

Pittendrigh, C. S. and Takamura, T. (1989). "Latitudinal clines in the properties of a circadian pacemaker." J Biol Rhythms 4(2): 217-35.

Plachetzki, D. C., et al. (2005). "New insights into the evolutionary history of photoreceptor cells." Trends Ecol Evol 20(9): 465-7.

Plachetzki, D. C., et al. (2010). "The evolution of phototransduction from an ancestral cyclic nucleotide gated pathway." Proc Biol Sci 277(1690): 1963-9.

Porter, M. L., et al. (2011). "Shedding new light on opsin evolution." Proc Biol Sci 279(1726): 3-14.

Prosser, R. A. and Gillette, M. U. (1989). "The mammalian circadian clock in the suprachiasmatic nuclei is reset in vitro by cAMP." J Neurosci 9(3): 1073-81.

Prosser, R. A. and Gillette, M. U. (1991). "Cyclic changes in cAMP concentration and phosphodiesterase activity in a mammalian circadian clock studied in vitro." Brain Res 568(1-2): 185-92.

Pulivarthy, S. R., et al. (2007). "Reciprocity between phase shifts and amplitude changes in the mammalian circadian clock." Proc Natl Acad Sci U S A 104(51): 20356-61.

Rajagopal, S., K. et al. (2010). "Teaching old receptors new tricks: biasing seven-transmembrane receptors." Nat Rev Drug Discov 9(5): 373-86.

7. References

Ralph, M. R. and Menaker, M. (1988). "A mutation of the circadian system in golden hamsters." Science 241(4870): 1225-7.

Rao, V. R. and Oprian, D.D. (1996). "Activating mutations of rhodopsin and other G protein-coupled receptors." Annu Rev Biophys Biomol Struct 25: 287-314.

Rapacciuolo, A., et al. (2003). "Protein kinase A and G protein-coupled receptor kinase phosphorylation mediates beta-1 adrenergic receptor endocytosis through different pathways." J Biol Chem 278(37): 35403-11.

Rasmussen, S. G., et al. (2007). "Crystal structure of the human β2 adrenergic G-protein-coupled receptor." Nature 450(7168): 383-7.

Rasmussen, S. G., et al. (2011). "Crystal structure of the β2 adrenergic receptor-Gs protein complex." Nature 477(7366): 549-55.

Rattner, A., et al. (2000). "Identification and characterization of all-trans-retinol dehydrogenase from photoreceptor outer segments, the visual cycle enzyme that reduces all-trans-retinal to all-trans-retinol." J Biol Chem 275(15): 11034-43.

Reed, H. E., et al. (2001). "Vasoactive intestinal polypeptide (VIP) phase-shifts the rat suprachiasmatic nucleus clock in vitro." Eur J Neurosci 13(4): 839-43.

Reischl, S., et al. (2007). "Beta-TrCP1-mediated degradation of PERIOD2 is essential for circadian dynamics." J Biol Rhythms 22(5): 375-86.

Richard, E. A. and Lisman, J. E. (1992). "Rhodopsin inactivation is a modulated process in Limulus photoreceptors." Nature 356(6367): 336-8.

Rittling, S. R. (1996). "Clonal nature of spontaneously immortalized 3T3 cells." Exp Cell Res 229(1): 7-13.

Rizzuto, R., et al. (1989). "A gene specifying subunit VIII of human cytochrome c oxidase is localized to chromosome 11 and is expressed in both muscle and non-muscle tissues." J Biol Chem 264(18): 10595-600.

Ronnett, G. V. and Moon, C. (2002). "G proteins and olfactory signal transduction." Annu Rev Physiol 64: 189-222.

Rosenbaum, D. M., et al. (2009). "The structure and function of G-protein-coupled receptors." Nature 459(7245): 356-63.

Ruan, G. X., et al. (2008). "An autonomous circadian clock in the inner mouse retina regulated by dopamine and GABA." PLoS Biol 6(10): e249.

Ruby, N. F., et al. (2002). "Role of melanopsin in circadian responses to light." Science 298(5601): 2211-3.

7. References

Sabath, E., et al. (2008). "Galpha12 regulates protein interactions within the MDCK cell tight junction and inhibits tight-junction assembly." J Cell Sci 121(Pt 6): 814-24.

Salom, D., et al. (2006). "Crystal structure of a photoactivated deprotonated intermediate of rhodopsin." Proc Natl Acad Sci U S A 103(44): 16123-8.

Santos-Zas, I., et al. (2013). "β-arrestin signal complex plays a critical role in adipose differentiation." Int J Biochem Cell Biol 45(7): 1281-1292.

Sassone-Corsi, P. (1998). "Molecular clocks: mastering time by gene regulation." Nature 392(6679): 871-4.

Scearce-Levie, K., et al. (2005). "Engineered G protein coupled receptors reveal independent regulation of internalization, desensitization and acute signaling." BMC Biol 3: 3.

Schoenlein, R. W., et al. (1991). "The first step in vision: femtosecond isomerization of rhodopsin." Science 254(5030): 412-5.

Seifert, R., et al. (2001). "Functional differences between full and partial agonists: evidence for ligand-specific receptor conformations." J Pharmacol Exp Ther 297(3): 1218-26.

Sellix, M. T., et al. (2010). "Fluorescence/luminescence circadian imaging of complex tissues at single-cell resolution." J Biol Rhythms 25(3): 228-32.

Semo, M., et al. (2003). "Light-induced c-fos in melanopsin retinal ganglion cells of young and aged rodless/coneless (rd/rd cl) mice." Eur J Neurosci 18(11): 3007-17.

Sharma, V. K. and Chandrashekaran, M. K. (1999). "Precision of a mammalian circadian clock." Naturwissenschaften 86(7): 333-5.

Shenoy, S. K. and Lefkowitz, R. J. (2011). "β-arrestin-mediated receptor trafficking and signal transduction." Trends Pharmacol Sci 32(9): 521-33.

Shenoy, S. K., et al. (2006). "β-arrestin-dependent, G protein-independent ERK1/2 activation by the β2 adrenergic receptor." J Biol Chem 281(2): 1261-73.

Shi, L. and Javitch, J. A. (2002). "The binding site of aminergic G protein-coupled receptors: the transmembrane segments and second extracellular loop." Annu Rev Pharmacol Toxicol 42: 437-67.

Shichida, Y. and Imai, H. (1998). "Visual pigment: G-protein-coupled receptor for light signals." Cell Mol Life Sci 54(12): 1299-315.

Shichida, Y. and Matsuyama, T. (2009). "Evolution of opsins and phototransduction." Philos Trans R Soc Lond B Biol Sci 364(1531): 2881-95.

Shim, H. S., et al. (2007). "Rapid activation of CLOCK by Ca2+-dependent protein kinase C mediates resetting of the mammalian circadian clock." EMBO Rep 8(4): 366-71.

7. References

Shimomura, O., et al. (1990). "Recombinant aequorin and recombinant semi-synthetic aequorins. Cellular Ca2+ ion indicators." Biochem J 270(2): 309-12.

Shiraishi, A., S. et al. (2013). "Chemical genomics approach for GPCR-ligand interaction prediction and extraction of ligand binding determinants." J Chem Inf Model 53(6): 1253-62.

Shirakawa, T., S. et al. (2001). "Multiple oscillators in the suprachiasmatic nucleus." Chronobiol Int 18(3): 371-87.

Sibley, D. R., et al. (1987). "Regulation of transmembrane signaling by receptor phosphorylation." Cell 48(6): 913-22.

Smith, S. O. (2010). "Structure and activation of the visual pigment rhodopsin." Annu Rev Biophys 39: 309-28.

Spiering, D. and Hodgson, L. (2011). "Dynamics of the Rho-family small GTPases in actin regulation and motility." Cell Adh Migr 5(2): 170-80.

Stables, J., et al. (1997). "A bioluminescent assay for agonist activity at potentially any G-protein-coupled receptor." Anal Biochem 252(1): 115-26.

Stephan, F. K. and Zucker, I. (1972). "Circadian rhythms in drinking behavior and locomotor activity of rats are eliminated by hypothalamic lesions." Proc Natl Acad Sci U S A 69(6): 1583-6.

Stevens, R. C., et al. (2012). "The GPCR Network: a large-scale collaboration to determine human GPCR structure and function." Nat Rev Drug Discov 12(1): 25-34.

Stierl, M., et al. (2010). "Light modulation of cellular cAMP by a small bacterial photoactivated adenylyl cyclase, bPAC, of the soil bacterium Beggiatoa." J Biol Chem 286(2): 1181-8.

Stork, P. J. and J. M. Schmitt (2002). "Crosstalk between cAMP and MAP kinase signaling in the regulation of cell proliferation." Trends Cell Biol 12(6): 258-66.

Stork, P. J. and Schmitt, J. M. (2002). "Crosstalk between cAMP and MAP kinase signaling in the regulation of cell proliferation." Trends Cell Biol 12(6): 258-66.

Stratmann, M. and Schibler, U. (2006). "Properties, entrainment, and physiological functions of mammalian peripheral oscillators." J Biol Rhythms 21(6): 494-506.

Strauss, O. (2005). "The retinal pigment epithelium in visual function." Physiol Rev 85(3): 845-81.

Stryer, L. (1986). "Cyclic GMP cascade of vision." Annu Rev Neurosci 9: 87-119.

Stryer, L. and Bourne, H. R. (1986). "G proteins: a family of signal transducers." Annu Rev Cell Biol 2: 391-419.

Sun, H., et al. (1997). "Peropsin, a novel visual pigment-like protein located in the apical microvilli of the retinal pigment epithelium." Proc Natl Acad Sci U S A 94(18): 9893-8.

7. References

Takahashi, J. S., et al. (2008). "Searching for genes underlying behavior: lessons from circadian rhythms." Science 322(5903): 909-12.

Tarttelin, E. E., et al. (2003). "Neuropsin (Opn5): a novel opsin identified in mammalian neural tissue." FEBS Lett 554(3): 410-6.

Taussig, R. and Gilman, A. G.(1995). "Mammalian membrane-bound adenylyl cyclases." J Biol Chem 270(1): 1-4.

Taussig, R., J. A. et al. (1993). "Inhibition of adenylyl cyclase by Gi alpha." Science 261(5118): 218-21.

Taylor, S. R., et al. (2010). "Velocity response curves support the role of continuous entrainment in circadian clocks." J Biol Rhythms 25(2): 138-49.

Teirstein, P. S., et al. (1980). "Evidence for both local and central regulation of rat rod outer segment disc shedding." Invest Ophthalmol Vis Sci 19(11): 1268-73.

Terakita, A., et al. (2004). "Counterion displacement in the molecular evolution of the rhodopsin family." Nat Struct Mol Biol 11(3): 284-9

Terman, J. S., et al. (1993). "Rod outer segment disk shedding in rats with lesions of the suprachiasmatic nucleus." Brain Res 605(2): 256-64.

Toh, K. L., et al. (2001). "An hPer2 phosphorylation site mutation in familial advanced sleep phase syndrome." Science 291(5506): 1040-3.

Tsai, S. C., et al. (1984). "Effects of guanyl nucleotides and rhodopsin on ADP-ribosylation of the inhibitory GTP-binding component of adenylate cyclase by pertussis toxin." J Biol Chem 259(24): 15320-3.

Tsukamoto, H. and Terakita, A. (2010). "Diversity and functional properties of bistable pigments." Photochem Photobiol Sci 9(11): 1435-43.

Ukai, H., et al. (2007). "Melanopsin-dependent photo-perturbation reveals desynchronization underlying the singularity of mammalian circadian clocks." Nat Cell Biol 9(11): 1327-34.

Umino, O., et al. (1991). "Effects of light stimuli on the release of dopamine from interplexiform cells in the white perch retina." Vis Neurosci 7(5): 451-8.

van Veen, T., et al. (1986). "alpha-Transducin immunoreactivity in retinae and sensory pineal organs of adult vertebrates." Proc Natl Acad Sci U S A 83(4): 912-6.

Venkatakrishnan, A. J., et al. (2013). "Molecular signatures of G-protein-coupled receptors." Nature 494(7436): 185-94.

Vitaterna, M. H., et al. (1994). "Mutagenesis and mapping of a mouse gene, Clock, essential for circadian behavior." Science 264(5159): 719-25.

7. References

Vitaterna, M. H., et al. (2006). "The mouse Clock mutation reduces circadian pacemaker amplitude and enhances efficacy of resetting stimuli and phase-response curve amplitude." Proc Natl Acad Sci U S A 103(24): 9327-32.

Wald, G. (1968). "Molecular basis of visual excitation." Science 162(3850): 230-9.

Wald, G. (1968). "The molecular basis of visual excitation." Nature 219(5156): 800-7.

Welsh, D. K., et al. (2004). "Bioluminescence imaging of individual fibroblasts reveals persistent, independently phased circadian rhythms of clock gene expression." Curr Biol 14(24): 2289-95.

Wess, J. (1997). "G-protein-coupled receptors: molecular mechanisms involved in receptor activation and selectivity of G-protein recognition." FASEB J 11(5): 346-54.

West, R. E., et al. (1985). "Pertussis toxin-catalyzed ADP-ribosylation of transducin. Cysteine 347 is the ADP-ribose acceptor site." J Biol Chem 260(27): 14428-30.

Whalen, E. J., et al. (2011). "Therapeutic potential of beta-arrestin- and G protein-biased agonists." Trends Mol Med 17(3): 126-39.

Wise, A., et al. (2002). "Target validation of G-protein coupled receptors." Drug Discov Today 7(4): 235-46.

Wittig, D., et al. (2012). "Multi-level communication of human retinal pigment epithelial cells via tunneling nanotubes." PLoS One 7(3): e33195.

Wittinghofer, A. (1996). "Deciphering the alphabet of G proteins: the structure of the alpha, beta, gamma heterotrimer." Structure 4(4): 357-61.

Won, J. H. and Ghil S. H. (2009). "The GTPase domain of Galphao contributes to the functional interaction of Galphao with the promyelocytic leukemia zinc finger protein." Cell Mol Biol Lett 14(1): 46-56.

Xu, J., et al. (1997). "Prolonged photoresponses in transgenic mouse rods lacking arrestin." Nature 389(6650): 505-9.

Xu, Y., et al. (2005). "Functional consequences of a CKIδ mutation causing familial advanced sleep phase syndrome." Nature 434(7033): 640-4.

Yamazaki, S. and Takahashi, J. S. (2005). "Real-time luminescence reporting of circadian gene expression in mammals." Methods Enzymol 393: 288-301.

Yau, K. W. and Hardie, R. C. (2009). "Phototransduction motifs and variations." Cell 139(2): 246-64.

Yizhar, O., et al. (2011). "Optogenetics in neural systems." Neuron 71(1): 9-34.

Yoshikawa, A., et al. (2008). "Establishment of human cell lines showing circadian rhythms of bioluminescence." Neurosci Lett 446(1): 40-4.

7. References

Zemelman, B. V., et al. (2002). "Selective photostimulation of genetically chARGed neurons." Neuron 33(1): 15-22.

Zhang, E. E., et al. (2010). "Cryptochrome mediates circadian regulation of cAMP signaling and hepatic gluconeogenesis." Nat Med 16(10): 1152-6.

Zhang, W., et al. (2007). "A toolbox for light control of Drosophila behaviors through Channelrhodopsin 2-mediated photoactivation of targeted neurons." Eur J Neurosci 26(9): 2405-16.

Zhukovsky, E. A., et al. (1991). "Transducin activation by rhodopsin without a covalent bond to the 11-cis-retinal chromophore." Science 251(4993): 558-60.

Zidar, D. A., et al. (2009). "Selective engagement of G protein coupled receptor kinases (GRKs) encodes distinct functions of biased ligands." Proc Natl Acad Sci U S A 106(24): 9649-54

8. Appendix

Appendix 1: Minimal promoter sequence for the mouse *per2* genes, cloned into pGL4.12

(-519) 5'-

Ctctgccggctgtgagttgcgcagcggccaagcaccattcccccgcgccgcagtggtacgcgccactcc
ggggctgcacgagcgggccaccgccgtgccaggtgaatggaagtcccgcaggccggaagtggacgagcc
tactcgcccgggcgcgggggggcgcaagagcgcgcagcatcttcattgaggaacccgggcggcgaacat
ggagttccatgtgcgtcttatgtaaagagagcgacgggcgtctccaccaattgatgagcgtagctctca
ggttccgccccgccagtatgcaaatgaggtggcactccgaccaatggcgcgcgcaggggcgggctcagc
gcgcgcggt**<u>cacgtt</u>**ttccac**<u>tatgtg</u>**acagcggagggcgacgcggcggcagcggcgctactgggacta
gcgg -3'

Double E box-like elements are underlined and in bold

Appendix 2: Mitochondrial targeting and aequorin encoding sequence

5'-

atgtccgtcctgacgccgctgctgctgcggggcttgacaggctcggcccggcggctcccagtgccgcgcgccaaga
tccattcgttgccgccggaggggaagcttacatcagacttcgacaacccaagatggattggacgacacaagc
atatgttcaatttccttgatgtcaaccacaatggaaaaatctctcttgacgagatggtctacaaggcat
ctgatattgtcatcaataaccttggagcaacacctgagcaagccaaacgacacaaagatgctgtagaag
ccttcttcggaggagctggaatgaaatatggtgtggaaactgattggcctgcatatattgaaggatgga
aaaaattggctactgatgaattggagaaatacgccaaaaacgaaccaacgctcatccgtatatggggtg
atgctttgtttgatatcgttgacaaagatcaaaatggagccattacactggatgaatggaaagcataca
ccaaagctgctggtatcatccaatcatcagaagattgcgaggaaacattcagagtgtgcgatattgatg
aaagtggacaactcgatgttgatgagatgacaagacaacatttaggattttggtacaccatggatcctg
cttgcgaaaagctctacggtggagctgtcccctaa -3'

Bases highlighted in yellow and in bold encode a 25 amino acid sequence which serves as a mitochondria targeting sequence (Rizzuto et al. 1989). The mature aequorin coding region is highlighted in blue (Inouye et al. 1985).

8. Appendix

Appendix 3: Publication

OPEN ACCESS Freely available online

PLoS one

Reproducible and Sustained Regulation of Gαs Signalling Using a Metazoan Opsin as an Optogenetic Tool

Helena J. Bailes, Ling-Yu Zhuang, Robert J. Lucas*

Faculty of Life Sciences, The University of Manchester, Manchester, United Kingdom

Abstract

Originally developed to regulate neuronal excitability, optogenetics is increasingly also used to control other cellular processes with unprecedented spatiotemporal resolution. Optogenetic modulation of all major G-protein signalling pathways (Gq, Gi and Gs) has been achieved using variants of mammalian rod opsin. We show here that the light response driven by such rod opsin-based tools dissipates under repeated exposure, consistent with the known bleaching characteristics of this photopigment. We continue to show that replacing rod opsin with a bleach resistant opsin from *Carybdea rastonii*, the box jellyfish, (JellyOp) overcomes this limitation. Visible light induced high amplitude, reversible, and reproducible increases in cAMP in mammalian cells expressing JellyOp. While single flashes produced a brief cAMP spike, repeated stimulation could sustain elevated levels for 10s of minutes. JellyOp was more photosensitive than currently available optogenetic tools, responding to white light at irradiances ≥1 μW/cm^2. We conclude that JellyOp is a promising new tool for mimicking the activity of Gs-coupled G protein coupled receptors with fine spatiotemporal resolution.

Citation: Bailes HJ, Zhuang L-Y, Lucas RJ (2012) Reproducible and Sustained Regulation of Gαs Signalling Using a Metazoan Opsin as an Optogenetic Tool. PLoS ONE 7(1): e30774. doi:10.1371/journal.pone.0030774

Editor: Paul A. Bartell, Pennsylvania State University, United States of America

Received November 4, 2011; **Accepted** December 26, 2011; **Published** January 24, 2012

Copyright: © 2012 Bailes et al. This is an open-access article distributed under the terms of the Creative Commons Attribution License, which permits unrestricted use, distribution, and reproduction in any medium, provided the original author and source are credited.

Funding: This work was supported by a Milstein Award, Medical Research Council UK to RJL and HJB (G0801731) and a BBSRC doctoral training account. The funders had no role in study design, data collection and analysis, decision to publish, or preparation of the manuscript.

Competing Interests: The authors have declared that no competing interests exist.

* E-mail: robert.lucas@manchester.ac.uk

Introduction

G protein coupled receptors (GPCRs) are the largest family of metazoan cell surface receptors and contribute to inter- and intracellular communication in all major body systems. They are also important therapeutic targets, with as many as a third of top-selling pharmaceutical drugs regulating their activity[1]. Improved tools to regulate GPCR activity are thus of great interest from both experimental and therapeutic perspectives.

Optogenetics is one of the most exciting recent technological developments in neuroscience. In brief, cell types of interest are engineered to express light-sensitive proteins (photopigments), allowing light to be used to regulate their activity remotely and with unprecedented spatial and temporal precision. The most widely used photopigments in optogenetics are microbial light-gated ion channels, which have been extensively exploited to allow direct control of neuronal membrane potential (e.g. [2,3,4] for reviews). More recently, attention has turned to non-excitable cells, and to photopigments capable of regulating cellular systems other than ionic permeability.

The opsin photopigments that support vision across the animal kingdom are GPCRs whose signalling activity is regulated by light. They thus represent natural candidates for optogenetic control of G-protein signalling. *Drosophila* Rh1 and, more recently, mammalian melanopsin have been used to provide photic control of Gαq signalling [5,6]. However, the most flexible tools in this area have been based upon rod opsin, the photopigment of vertebrate rods. Rod opsin's cognate G-protein is transducin, a member of the Gαi subclass, and it has been exploited to regulate Gαi signalling for experimental purposes [7,8]. However, thanks to the extensive structural information available for this protein, chimeric receptors (recently termed OptoXRs) comprising the light sensitive elements of rod opsin fused to intracellular signalling components of other GPCRs have been used to gain access also to the third major class of G protein, Gαs [9,10].

Rod opsin has many advantages as a starting point for designing optogenetic tools: 1.) It expresses efficiently in non-native environments without adding specialist chaperones/folding factors. 2.) Its signalling characteristics are well described and specific [11,12]. 3.) Its basic structure is well-defined, as are many structure:function relationships [13,14,15,16], facilitating the design of chimera and site-directed mutants aimed at optimising its use for particular cell types and modifying its signalling activity. However, it has one potentially important limitation - its reliance upon *cis*-isoforms of retinaldehyde to recover from bleach. In the vertebrate retina an enzymatic pathway ensures a steady supply of such *cis*-isoforms, but this pathway is absent elsewhere in the mammalian body. It seems likely then that the availability of *cis*-retinaldehyde would limit the magnitude of rod-opsin driven responses outside of the eye. Moreover, while application of exogenous *cis*-isoforms could alleviate this problem, the effect of such an approach should steadily decrease during light exposure as *cis*-isoforms are degraded. Previous analyses of OptoXRs have not probed this behaviour because they have relied upon either end-point assays of second messenger or single stimulation protocols [7,10]. Here, using a real time reporter for cAMP, we present evidence that pigment bleach does indeed impose a fundamental limit on the magnitude and reproducibility of rod opsin-based OptoXR activity.

Many opsins from invertebrates (and a very few from vertebrates) do not bleach like rod opsin. These so-called bistable

pigments bind both *cis*- and *trans*- isoforms of retinaldehyde, with light driving isomerisation in both directions. This comprises an intrinsic bleach recovery mechanism that makes bistable pigments much less reliant upon a supply of *cis*-retinaldehydes. Such bistable pigments could therefore provide improved tools for optogenetic control, allowing higher amplitude and more reproducible light responses. Here we show that a bleach-resistant opsin from the box jellyfish, *Carybdea rastonii*, previously shown to be naturally Gαs-coupled [17], does indeed allow much superior control of G protein signalling. The light dependent increase in cAMP induced by this 'JellyOp' is both higher amplitude and, especially, more repeatable than the response driven by currently available OptoXRs. As we also show that JellyOp responds to modest levels of visible light it represents an accessible tool for optogenetic control of GPCR signalling.

Methods

Construction of receptors

Construction of chimeric receptors was carried out following the optimal cytoplasmic boundaries described by Kim et al (2005)[9]. Our version of the 'standard' receptor [9,10] was designed from human rhodopsin and β2AR sequences (Genbank NM_000539.3 and NM_000024, respectively; Figure 1) to maximise any future therapeutic potential of the protein. The sequence also included silent substitutions to introduce unique restriction enzyme recognition sites within each transmembrane region to facilitate cloning different cytoplasmic loops. The nucleotide sequence for Rh1β2AR 1-t with silent substitutions was synthesised by Genscript Corp and supplied in puc57 cloning vector. A phosphorylation mutant (Rh1β2AR 1-t phos mutant) was engineered by exchanging serine residues (7 in total; 261, 262, 345, 346, 355, 356, 364 based on the numbering of residues of the human β2AR) known to be important for PKA and GRK phosphorylation for alanine (following [18]), using site directed mutagenesis (lightning quikchange kit; Stratagene). In addition, a mutant was created from the standard Rh1β2AR 1-t (termed Rh1β2AR 1-t::Gαs) with the stop codon replaced with a 6-base linker and the coding region for a 'short' transcript of the human Gαs protein (Figure 1). The transcript on which the coding region for Gαs was based (GNASS; Genbank NM_080426.2) has been shown to have less constitutive activity than longer forms [19]. A 1D4 epitope was fused at the 3′ end of every receptor construct coding region, composed of the last 9 amino acid codons from bovine rhodopsin followed by a stop codon. All sequences were verified via standard sequencing techniques prior to use. The coding regions of the receptors used were flanked by HindIII and NotI sequences and cloned into the mammalian expression vector pcDNA3.1. The sequence for the opsin of the box jellyfish *Carybdea rastonii* (Genbank AB435549; JellyOp) was also synthesised by Genscript Corp in a puc57 vector and fused with a 1D4 epitope. An HpaI recognition site was introduced into the multiple cloning site of the pcDNA3.1 vector and the jellyfish sequence flanked with HpaI and NotI sites for cloning into pcDNA3.1-HpaI. A jellyfish lysine mutant plasmid was also engineered using site directed mutagenesis to alter the putative chromophore binding site at residue 296 from lysine to alanine (numbering from bovine rhodopsin [14]).

cAMP reporter

A HEK293 cell line expressing the Glosensor™ cAMP biosensor under a tetracycline inducible promoter (FLP-IN™ system, Invitrogen; Glosensor, Promega; [20]) was generated. This biosensor is a modified luciferase that carries the cAMP binding B domain from the RIIβ subunit of cAMP-dependent protein kinase A (PKA). The Glosensor™ region was excised from the pGlosensor plasmid (Promega) and cloned into pcDNA5/FRT/TO, then co-transfected with pOG44 into FLP-IN™-293 cells. Isogenic stable cell lines were selected and maintained with 100 μg/ml hygromycin and 10 μg/ml blasticidin. Cells were maintained at 37°C in Dulbecco's modified Eagle's medium (DMEM), 4,500 mg/ml D-glucose, sodium pyruvate and L-glutamine (Sigma) with 10% foetal bovine serum (Sigma) in a 5% CO_2 atmosphere. Following incubation with 300 ng/ml tetracycline, these cells showed repeatable and robust increases in raw luminescence (RLU) when stimulated with a range of forskolin concentrations (Figure 2).

The reporter was validated by determining the effect of known doses of forskolin on levels of cAMP, determined by ELISA and Glosensor bioluminescence, without any addition of phosphodiesterase inhibitors. Dose response curves of forskolin could be fit by both methods by sigmoidal dose response curves of the form $y = a + b/1+10^{(c-x)}$ where a = bottom, b = top-bottom and c = LogEC50, and yield EC50 values of 51 and 21 μM for ELISA and luminescence assays respectively, confirming the sensitivity of the bioassay. The relationship between cAMP and Glosensor response could then be inferred and fit by a first order polynomial (R^2 value of 0.999), suggesting that, under these conditions, cAMP concentration can therefore be estimated from RLU as follows:
[cAMP] μM = 4.785 + (0.0003971a) + (0.00000526 1aˆ2)
where a = RLU/μl.

Light response assays

7.5 x 10^3 FLP-IN™-293 Glosensor cells in each well of solid white 96 well plates were transfected with plasmids containing opsin based receptors using Lipofectamine 2000 (Invitrogen) in serum-free medium for 6 hours. Immunocytochemistry revealed a transfection efficiency of ~50% using this method. A stable cell line was constructed using a linearised plasmid of pcDNA3-HpaI JellyOp and additionally maintained with 400 μg/ml G418. Following transfection (or plating for the stable line), cells were then incubated for 16 hours with 300 ng/ml tetracycline and 10 μM retinaldehyde (9-*cis* retinal or all-*trans* retinal; Sigma-Aldrich) in CO_2 independent medium without phenol red (L-15, Invitrogen), with 10% FCS. Beetle luciferin potassium salt (Promega) reconstituted in 10mM HEPES buffer was added to a final concentration of 2mM luciferin. All procedures following transfection of cells with opsins were carried out in dim red light.

Raw luminescence units (RLU) in cells were recorded at 37°C with 1s resolution with a top-read 3mm lens in a Fluostar Optima plate reader (BMG Labtech), with cycles of either 30s or 60s and gain of 3600. Following 30 mins equilibration, cells were subjected to repeated flashes from an electronic camera flash (The Jessop Group Ltd, UK; or forskolin application for cAMP biosensor validation) followed by recovery periods where RLU was recorded. Luminescence recordings were analysed with Optima (BMG Labtech) software and Microsoft Office Xcel. All experiments comprised cells plated and treated in triplicate. The average triplicate value for the five minutes prior to light treatment was used to normalise individual well values of the triplicate that were then averaged, except where baseline levels were examined. In the latter case, individual values were normalised to the triplicate average baseline RLU readings for mock transfected cells. Prism (Graphpad) software was used for all statistical analyses.

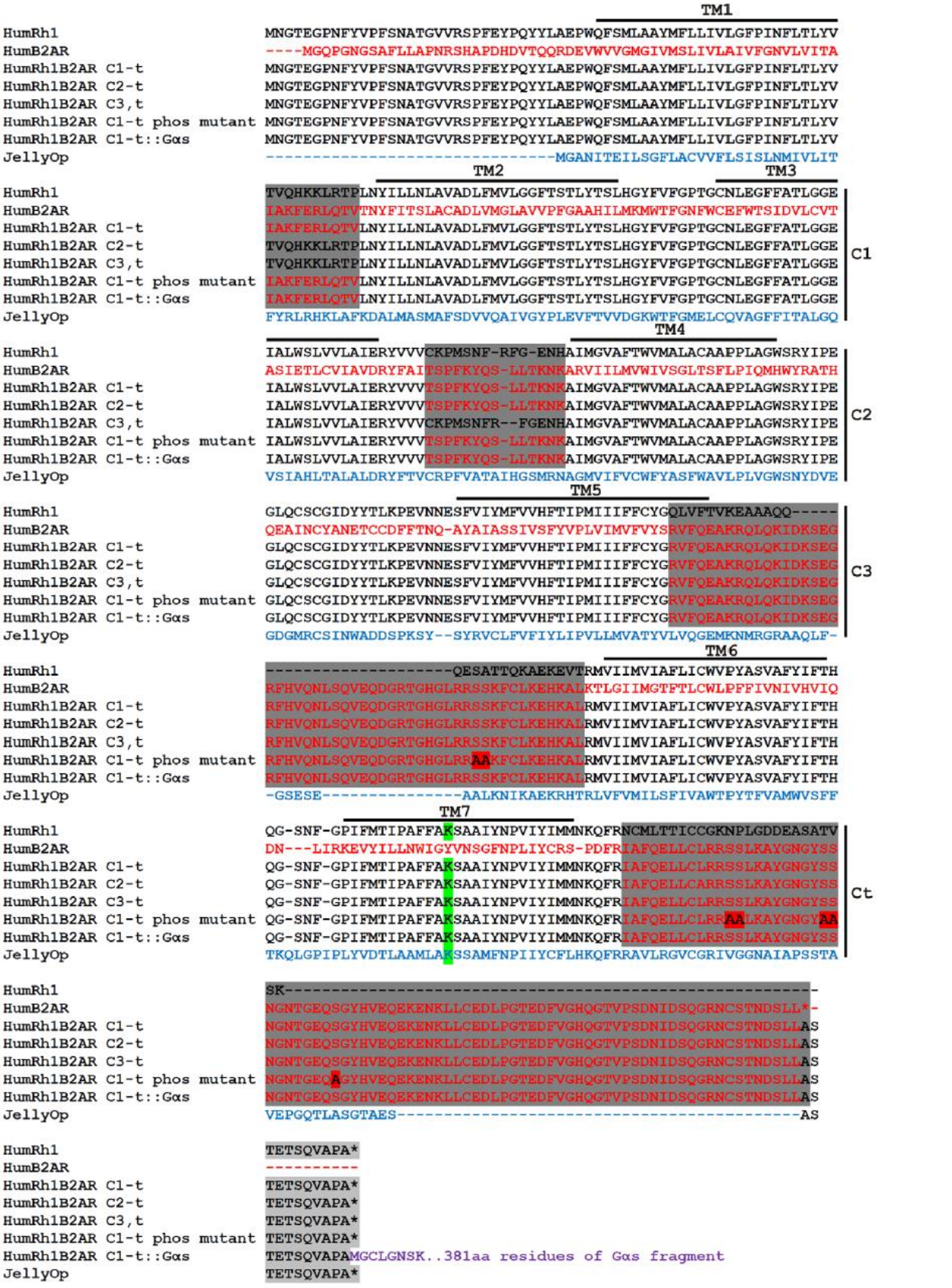
TM1
TM2
TM3
TM4
TM5
TM6
TM7
C1
C2
C3
Ct
HumRh1
HumB2AR
HumRh1B2AR C1-t
HumRh1B2AR C2-t
HumRh1B2AR C3,t
HumRh1B2AR C1-t phos mutant
HumRh1B2AR C1-t::Gαs
JellyOp
HumRh1B2AR C1-t::Gαs ..381aa residues of Gαs fragment

Figure 1. OptoXR sequence alignment. A number of structural variants on a published OptoXR chimera comprising elements of the human β2AR and human rhodopsin sequences were generated in an attempt to increase response amplitude/reproducibility. An amino acid alignment of these variants and, for comparison the human β2AR and rhodopsin (Genbank NM_000539.3, in red and NM_000024, in black), and JellyOp (Genbank AB435549, in blue) sequences are shown. Structural boundaries are based on bovine rhodopsin [14] with putative cytoplasmic regions shaded in dark grey. The lysine residue in TM7, which forms a Schiff-base linkage with retinaldehyde chromophore, is highlighted in green. Note that the terminal 9 amino acids of rod opsin are included as an epitope tag (1D4) in all receptors used in this study (light grey shading). In addition to the published OptoXR in which the entire cytoplasmic surface of rod opsin is replaced by that of the β2AR (Rh1B2AR 1-t), variants in which either 1st or 1st and 2nd intracellular loops from rod opsin were retained (Rh1B2AR 2-t and Rh1B2AR C3,t) in the hope of improving chimera stability were generated. Other variants on Rh1B2AR 1-t employed site directed mutagenesis of phosphorylation sites (highlighted in red) important for arrestin binding and receptor inactivation [18] (Rh1B2AR 1-t phos mutant) or a fusion of the human Gαs subunit at the C-terminal tail in purple (Rh1B2AR 1-t::Gαs).
doi:10.1371/journal.pone.0030774.g001

Light response assays of stably expressing FLP-IN™-293 Glosensor JellyOp cells

7.5×10^4 FLP-IN™-293 Glosensor JellyOp cells in each well of solid white 96 well plates were incubated with tetracycline and retinaldehyde as for temporal responses resulting from transient transfections above. In addition, for one experiment, 4×10^4 FLP-IN™-293 Glosensor JellyOp cells were plated per well following pre-coating the wells with 0.01% poly-L-lysine (Sigma-Aldrich) in PBS for 2 hours. Cells were incubated as before and then treated with vehicle or 100 μM MDL2330A (Tocris Bioscience) for 15 mins before luminescence recordings as above.

An irradiance response curve was created for stable JellyOp expressing cells as follows. Cells were exposed to 10s of light from an array of white LEDs (Low energy floodlight, Palmer Riley Electricals UK) covered with layers of neutral density filter (Lee Filters, UK). Cells were left to recover and luminescence measured for 15 minutes and then exposed to a further light pulse brighter by 1 log unit, and this was repeated up to an irradiance of 4.66 mW cm^{-2}. Spectral irradiance was measured with a spectroradiometer (Bentham Scientific).

Immunocytochemistry

3.5×10^5 cells/ml FLP-IN Glosensor cells were seeded onto coverslips and transfected with receptor constructs as above. 3.5×10^5 cells/ml FLP-IN Glosensor JellyOp cells were seeded onto coverslips in red light. Following transfections, cells for MAPK

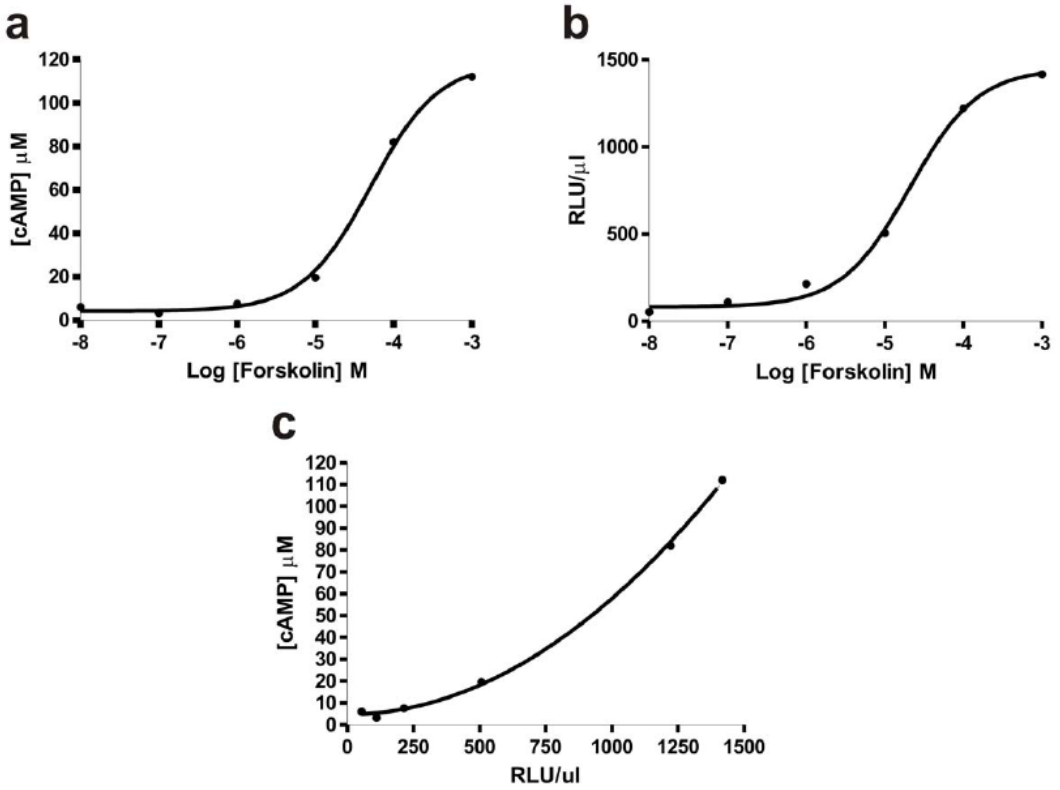

Figure 2. Validating the cAMP biosensor. A HEK293 cell line expressing the Glosensor™ cAMP biosensor under a tetracycline inducible promoter (FLP-IN™ system; Invitrogen) was generated. The reporter was validated by determining the effect of known doses of forskolin on levels of cAMP, determined by ELISA (**a**) and Glosensor bioluminescence (**b**). Data show mean for 2 (ELISA) and 3 (luminescence) separate experiments each of which contained samples in triplicate. Fits show sigmoidal dose response curves of the form $y = a + b/1+10^{(c-x)}$ where a = bottom, b = top-bottom and c = LogEC50, and yield EC50 values of 51 and 21 μM for ELISA and luminescence assays respectively. (**c**) A comparison of cAMP concentration and RLU for each forskolin concentration was used to infer the relationship between these parameters. This could be fit by a first order polynomial (R^2 value of 0.999), suggesting that, under these conditions, cAMP concentration can therefore be estimated from RLU as follows: [cAMP] μM = 4.785 + (0.0003971a) + (0.000005261â2) where a = RLU/μl.
doi:10.1371/journal.pone.0030774.g002

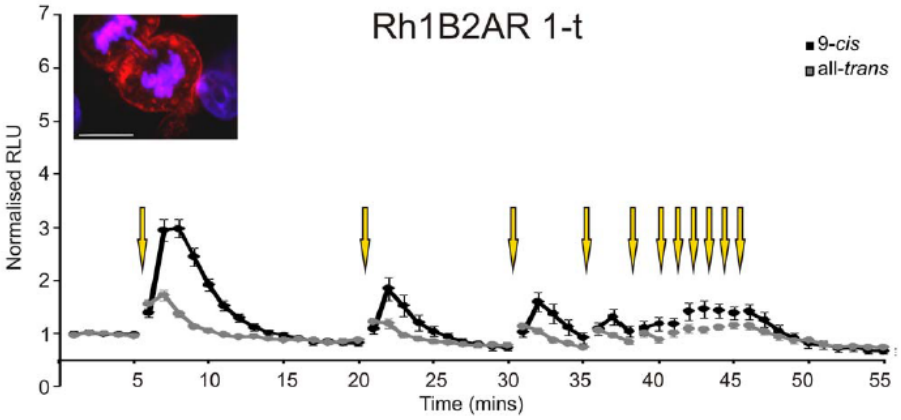

Figure 3 Real time analysis of a standard OptoXR response. Light induced changes in cAMP biosensor (Glosensor) luminescence in HEK293 cells transiently transfected with Rh1B2AR 1-t. Data for cells incubated with 9 *cis* retinaldehyde (black) or all *trans* retinaldehyde (grey) are shown; yellow arrows depict presentation of light flash. Data points show mean ± SEM n = 7. Inset shows immunocytochemical staining for the 1D4 epitope (in red, alexa 555 secondary antibody) of HEK293 cells expressing Rh1B2AR 1-t. DAPI shown in blue, scale bar = 10 μm.
doi:10.1371/journal.pone.0030774.g003

labelling were incubated for 16 hours with 9-*cis* retinal in L-15 medium with 0.5% FCS and no phenol red. Cells were incubated with 100 ng/ml pertussis toxin (PTX, Tocris) for 16 hours, 10 μM U73122 (Tocris) for 30 mins, 100 μM MDL2330A for 15 mins or L-15 only. Dark treated cells were then washed with ice cold PBS and fixed with ice-cold 4% paraformaldehyde (PFA) for 30 mins. Simultaneously, light-treated plates were subject to 2 or 15 minutes exposure to a white LED array (The Litebook Company Ltd, Canada, 2.6 mW cm^{-2} at the level of the cells) and fixed as above. For labelling of the 1D4 epitope, cells were incubated for 16 hours with 9-*cis* retinal in L-15 medium with 10% FCS and fixed in the dark.

Fixed cells were blocked and permeabilised with 0.1% Triton-X 100, 5% BSA, 2% normal goat serum in PBS. Phospho-p44/42 MAPK antibody (CST; #9101) was used at a concentration of 1:500 and rhodopsin 1D4 monoclonal antibody (Thermo Scientific Pearce) at 1:1000. Phospho-MAPK labelled cells were incubated with a biotinylated secondary antibody and ABC streptavidin (Vectalabs) complex and developed with a DAB/Nickel chloride kit (Vectalabs). 1D4 labelling was visualised with Alexa555-conjugated secondary anti-mouse IgG antibody (Molecular Probes) at 1:1000 and cells were mounted with Vectashield with DAPI (Vectalabs). Brightfield images of MAPK labelling were taken with an Axioskop upright microscope with Axiovision CCD camera and software. Fluorescent images were taken on a Nikon Eclipse upright 90i confocal microscope using 405nm and 543nm laser lines.

Results

OptoXR-driven responses have poor reproducibility

Measuring light-dependent cAMP accumulation in optogenetic studies presents a technological challenge. Standard end-point assays fail to capture one of the essential features of optogenetics, the ability for repeated and temporally defined activation. However, real-time assays based upon fluorescent calcium reporters or FRET reporters, which are now in standard use to measure cAMP [21,22,23,24], are inappropriate because the excitation light for the fluorescence reporter will likely also activate the optogenetic photopigment. Here, we hoped to avoid these limitations by using a luciferase-based cAMP reporter, to provide a live-cell readout of this second messenger without impacting receptor activity (Figure 2, Figure, 3, Figure 4, Figure 5). We started by transiently transfecting HEK 293 cells carrying this reporter with a humanised version of a published OptoXR, comprising the trans-membrane and extracellular elements of rod opsin fused to the intracellular components of the β2-adrenergic receptor (termed here Rh1B2AR 1-t; Figure 1). When these cells had been pre-incubated with 9-*cis* retinal, a single brief flash of light induced a rapid and reversible increase in luminescence (Figure 3). The magnitude of this response was robust. Thus, at its peak there was a 3.07±0.2 (mean ± SEM) fold increase in luminescence over background. We estimate a transfection efficiency of ~50% from immunocytochemistry (see Methods; Light response assays). Using the formula derived from the relationship between Glosensor RLU responses to forskolin and measured cAMP values stimulated by forskolin, the peak cAMP light response by the Rh1B2AR 1-t receptor if transfection efficiency is corrected to 100% was ~5.15 μM. This compares to around 7.27 μM cAMP produced in response to 1 μM forskolin or 18.48 μM cAMP produced in response to 10 μM forskolin in these cells. Rh1B2AR 1-t expressing cells pre-incubated with all-*trans* retinaldehyde did also show a light response (presumably because the HEK 293 cell line, unlike primary kidney cells, expresses RPE65 allowing it to generate *cis*-isoforms of retinaldehyde [25,26]), but the associated increase in luminescence was much smaller than in the 9-*cis* retinaldyehyde condition (Figure 3).

The potentiating effect of exogenous 9-*cis* retinaldehyde on the OptoXR light response is consistent with the known dependence of rod opsin on *cis*-isoforms of retinaldehyde. On this basis, however, the effect is predicted not to survive repeated light exposure. This indeed was the case. We found that the light response of cells expressing the published Rh1B2AR 1-t rapidly diminished under these conditions. Thus, the peak response amplitude to a second brief flash was reduced by about 50%, with subsequent responses further diminished. Indeed, by the 5th flash, responses were very small, indicating that the potentiating effect of the exogenous *cis*-retinaldehyde had been largely lost (Figure 3).

We generated a panel of structural variants of the Rh1B2AR chimera in an attempt to improve the magnitude of the OptoXR response. We aimed to obtain a reasonable response amplitude even in the absence of *cis*-retinaldehdyes and/or under repeated light exposure (Figure 4). One, in which the first cytoplasmic loop

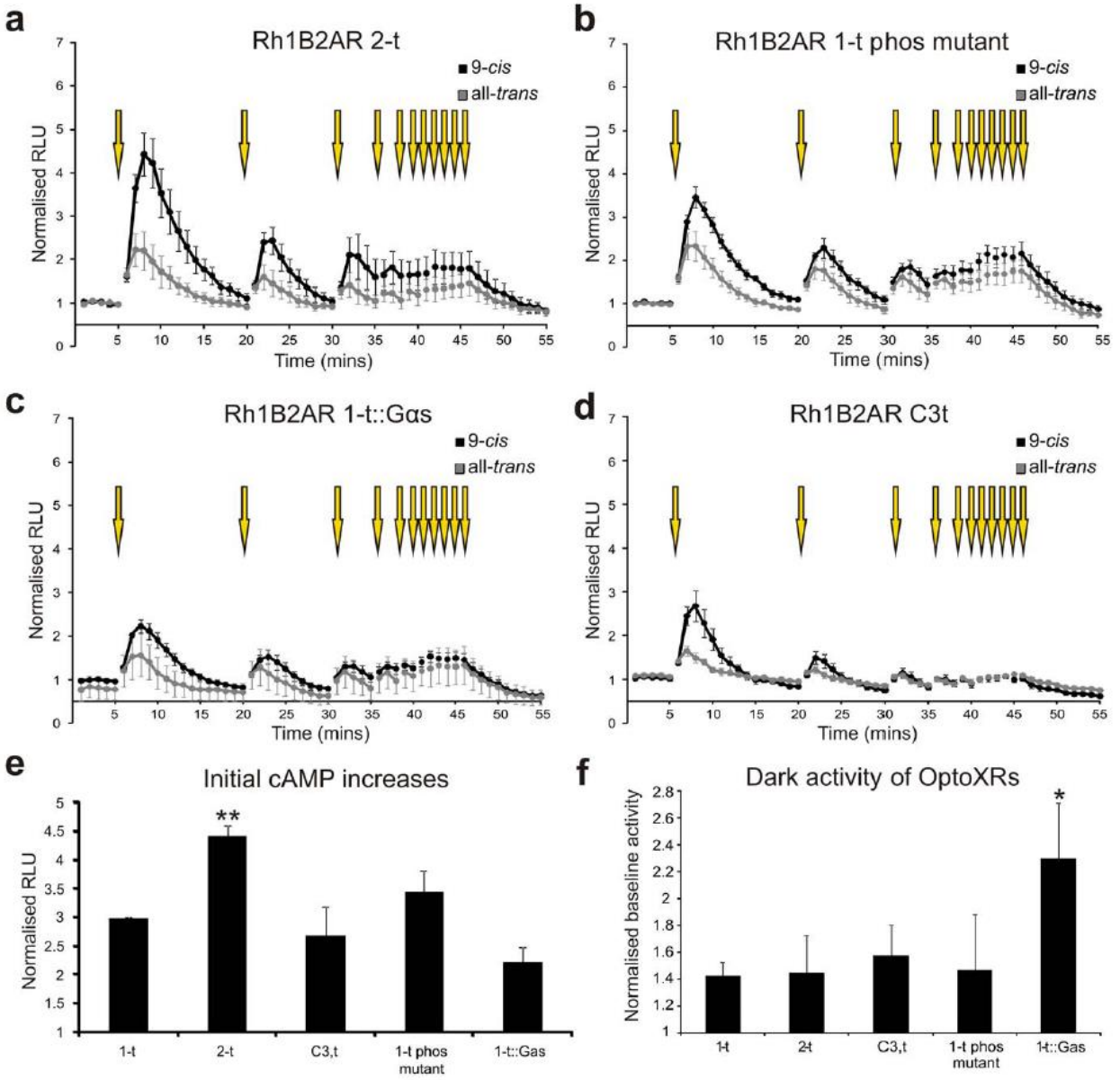

Figure 4. Real time analysis of OptoXR variant responses. (**a**–**d**) Light induced changes in cAMP biosensor (Glosensor) luminescence in HEK293 cells transiently transfected with Rh1B2AR 2-t (**a**) Rh1B2AR 1-t phos mutant (**b**), Rh1B2AR 1-t::Gαs (**c**) or Rh1B2AR C3,t (**d**). Luminescence was measured for 1 second every minute and _ormalized to baseline dark levels. Yellow arrows depict presentation of light flash. (**e**) Quantification of peak response amplitude for the first light flash following incubation with 9 *cis* retinaldehyde reveals that only the Rh1B2AR 2-t chimera shows an improved response amplitude compared to the Rh1B2AR 1-t OptoXR (one-way ANOVA with Dunnett's post hoc comparison to Rh1B2AR 1-t $p<0.01$). (**f**) None of these chimera exhibited reduced dark activity (luminescence prior to light exposure, _ormalized to mock transfected control cells), and indeed this parameter was significantly increased in cells expressing Rh1B2AR 1-t::Gαs when preincubated with 9 *cis* retinaldehyde (one-way ANOVA with Dunnett's post hoc comparisons to mock transfections as control group, $p<0.05$). *$p<0.05$, **$p<0.01$. Data show mean ± SEM ($n\geq4$) shown for cells preincubated overnight with either 9-*cis* retinaldehyde (black) or all *trans* retinaldehyde (grey).
doi:10.1371/journal.pone.0030774.g004

of rod opsin was retained (Rh1B2AR 2-t; Figure 4a), significantly improved the initial light response (peak RLU) following pre-treatment with 9-*cis* retinaldehyde (one-way ANOVA with Dunnett's post hoc comparison to Rh1B2AR 1-t, $p<0.01$, figure 4e). However, none of them overcame the fundamental limitation in response reproducibility.

Improved responses in cells expressing JellyOp

The family of animal opsins contains members who are less susceptible to bleach than rod opsin, and one of these from the box jellyfish *Carybdea rastonii* has recently been shown to couple to Gαs in vitro [17]. We therefore next determined whether this opsin (termed JellyOp here) would allow us to overcome the poor

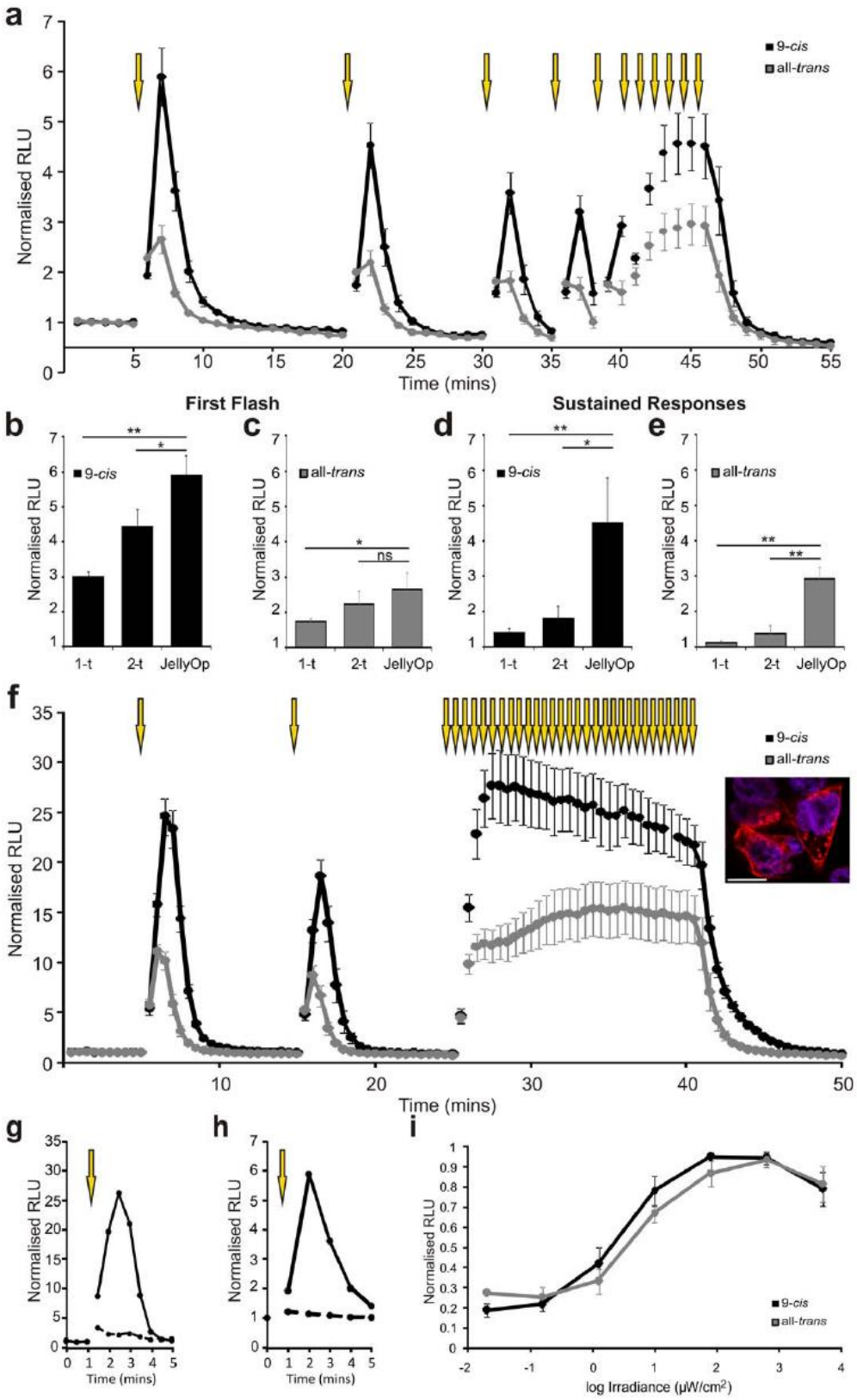
a
Normalised RLU
Time (mins)
9-cis
all-trans
First Flash
Sustained Responses
b
c
d
e
1-t
2-t
JellyOp
ns
f
g
h
i
log Irradiance (μW/cm²)

Figure 5. JellyOp driven light responses. (**a**) Light induced changes in cAMP biosensor luminescence (depicted _ormalized to baseline before light exposure) in HEK293 cells transiently transfected with JellyOp (n = 5). (**b,c**) The peak increase in luminescence following the first light flash was significantly greater for 9-*cis* pretreated cells expressing JellyOp than either the Rh1B2AR 1-t (1-t) or Rh1B2AR 2-t (2-t) chimera. It was also significantly greater for all-*trans* pretreated cells expressing JellyOp than Rh1B2AR 1-t. (**d,e**) Sustained responses were further enhanced, with luminescence over 5 minutes of light exposure (flashes once per minute) reaching a plateau significantly higher in JellyOp than either Rh1B2AR chimera. (**f**) Tracking changes in luminescence with higher temporal resolution (reading every 30s) in HEK293 cells stably transfected with JellyOp revealed high magnitude responses that could be sustained over 15 minutes of repeated stimulation (n = 4). Inset shows immunocytochemical staining for 1D4 epitope (red) in JellyOp expressing HEK293 cells. Nuclei stained blue with DAPI; scale bar 10 μm. (**g**) Cells stably expressing JellyOp show markedly repressed responses to a light flash when treated with 100 μM MDL2330A (adenylate cyclase inhibitor; dashed line), n = 1 (**h**) cAMP biosensor luminescence responses in HEK293 cells transiently transfected with JellyOp (continuous line) are abolished in the JellyOp lysine mutant (dashed line), n = 1 (**i**) Irradiance response curves for cAMP reporter activity in cells stably expressing JellyOp and induced with 10s white light (LED) pulses. RLU values are _ormalized to the peak response (n = 3). **A-I** show cells pre-incubated with either 9-*cis* (black) or all-*trans* (grey) retinaldehyde; mean ± SEM; yellow arrows depict timing of light flash. Data in **b-e** were analysed using one-way ANOVA with Dunnett's post hoc comparisons to JellyOp as control group, *$p<0.05$, **$p<0.01$; $n\geq4$.
doi:10.1371/journal.pone.0030774.g005

reproducibility and sustainability of responses driven by Rh1 based OptoXRs.

When reconstituted overnight with 9-*cis* retinaldehyde, cells transiently transfected with JellyOp showed a 5.9±0.5 fold increase in cAMP reporter activity following a single light flash (Figure 5a&b). This is significantly greater than the best response we achieved with Rh1-based OptoXRs (from Rh1B2AR 2-t; $p<0.05$ one tailed t-test). Interestingly, the kinetics of the JellyOp response were also increased, with a sharper decline in luminescence suggesting that this receptor may allow finer temporal control of the second messenger. The real advantage of using JellyOp was, however, in the response to repeated stimulation. Thus, JellyOp-driven responses to subsequent flashes were only modestly reduced, and a series of 5 flashes maintained cAMP at a much higher level than that obtainable with OptoXRs (one-way ANOVA with Dunnett's post-hoc test, $p<0.01$; Figure 5d). The implication that JellyOp is able to support high amplitude cAMP responses without exogenous *cis*-retinaldehyde was confirmed by the activity of cells pre-incubated with all-*trans* retinal (Figure 5c). In these cells, response amplitude showed no sign of decreasing under repeated stimulation and, if anything, increased. Similarly, the JellyOp response under these conditions was much greater than that of OptoXRs (one-way ANOVA with Dunnett's post-hoc test, $p<0.001$, Figure 5e).

Basal levels of luminescence were modestly increased in cells expressing JellyOp. Thus, cells preincubated with 9-*cis* retinaldehyde had 1.21±0.1 times greater luminescence in the dark than untransfected controls, and 1.81±0.16 times greater luminescence with all-*trans* retinaldehyde. This likely represents genuine basal (dark) activity of the receptor, although given the high photosensitivity of JellyOp (see below), light produced by the luciferase reporter may also have driven some receptor photoactivation.

JellyOp sensory characteristics

In order to further characterise the sensory characteristics of JellyOp in HEK293 cells, we generated a cell line stably expressing this opsin. The first notable feature of this cell line was the magnitude of light responses. We found that a single brief light pulse could increase luminescence by 24.47±2.22 (n = 5) fold in cells pre-incubated with 9-*cis* retinaldehyde (approx. 7.63 μM cAMP). Moreover, we were able to maintain this level of reporter activity for at least 15 mins with repeated stimulation (Figure 5f).

Consistent with the view that JellyOp-dependent increases in luminescence reflect opsin-based activation of adenylate cyclase activity via a Gαs cascade, we found that the light response of these cells was repressed by an adenylyl cyclase inhibitor (MDL2300A) and absent when a JellyOp mutant lacking the lysine critical for chromophore binding was used (Figure 5g,h). Treatment with inhibitors of canonical Gi or Gq cascades (pertussis toxin, a Gi inhibitor or U73122, a PLC inhibitor), however, did not have an effect on the light response (data not shown).

The most commonly used optogenetic tools require very bright light for activation [10,27,28]. We next determined whether this was also true for JellyOp by describing the irradiance dependence of the cAMP response in the stable cell line. We found a measurable increase in luminescence could be induced by 10s pulses of white light (LED source) at irradiances ≥1 μW/cm^2 (Figure 5i). For reference, light levels at bench-top in our laboratory are typically around 200 μW/cm^2. In fact this likely overestimates the light required to activate JellyOp because much of the energy produced by the white LED will be inefficiently absorbed by the pigment. JellyOp is maximally sensitive to light of around 500nm in wavelength [17], and we estimate that responses could be elicited by as little as 11 log photons/cm^2/s (<100 nW/cm^2) if a 500nm narrow band light source were employed. The increase in reporter luminescence at these threshold irradiances corresponds to that induced by around 1 μM forskolin.

Light dependent mitogen activated protein kinase (MAPK) signalling

GPCR signalling is not restricted to conventional Gα/second messenger pathways but may also involve Gβγ and G-protein independent (β-arrestin) pathways that can lead to MAPK phosphorylation and activation of other cascades, typically following a longer time course than the conventional pathways [29]. We found that both JellyOp and all of the OptoXRs used in this study drove a light dependent increase in MAPK phosphorylation in HEK293 cells (Figure 6). Thus, there was a marked increase in immunoreactivity for phospho-MAPK, following 2 or 15 minutes exposure to a white LED based light source (Litebook^{TM}; 2.6 mW cm^{-2}) in HEK293 FLP-IN Glosensor cells transiently expressing any of these receptors. In agreement with data from cAMP Glosensor recordings, treatment of cells expressing JellyOp with inhibitors of canonical Gi or Gq cascades (pertussis toxin or U73122) did not result in measurable reduction of MAPK phosphorylation following light treatment. Conversely, treatment with an adenylate cyclase inhibitor inhibited MAPK phosphorylation at both shorter and longer (15 mins) time points. This indicates that MAPK phosphorylation under these conditions is downstream of an increase in cAMP rather than attributed to G protein independent pathways following light activation.

Discussion

The conventional approach to manipulating GPCR activity is pharmaceutical. However, drugs have a number of well-recognised limitations. Off-target effects on tissues and cell types other

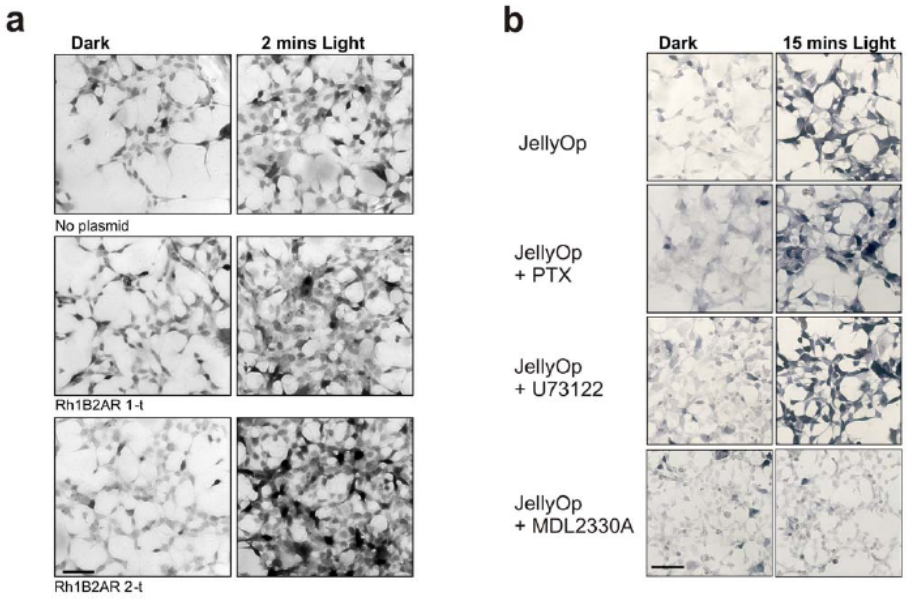

Figure 6. MAPK phosphorylation. Immunohistochemical labelling of phosphorylated MAPK (grey-black stain produced with horseradish peroxidise and diaminobenzidine) in HEK293 cells preincubated with 9-*cis* retinaldehyde and exposed to either 2 minutes of white light or kept in the dark. (**a**) OptoXRs elicit a light dependent increase in MAPK phosphorylation. Photomicrographs for untransfected cells and cells expressing each of the OptoXRs were taken with the same exposure settings. Scale bar = 50 μm. (**b**) Phosphorylated MAPK in HEK293 cells expressing JellyOp exposed to the dark or 15 mins of light. Cells labelled '+PTX' were treated with 100ng/ml pertussis toxin (a Gi inhibitor); '+U73122' with 10 μM U73122 (a Gq inhibitor); '+MDL2330A' with 100 μM (adenylate cyclase inhibitor. MDL inhibits light-induced MAPK phosphorylation following both 2 mins (not shown) and 15 mins of light. The increase in phosphorylation therefore appears to be due to a Gs dependent pathway.
doi:10.1371/journal.pone.0030774.g006

than those of interest occur with even the most localised delivery systems, while the kinetics of drug delivery and clearance impose a limit on the temporal resolution with which systems can be manipulated. Optogenetics provides an exciting opportunity to overcome these problems by using a 'ligand' (light), which can be applied with μm/μsec spatiotemporal resolution, to activate a receptor targeted to specific cell types using the tools of genetic engineering. The ultimate expression of this technology will be to impose natural patterns of GPCR activity. Realising this ambition will, however, require optogenetic tools that allow both repeatable and sustained activation. There is abundant evidence that this level of control is physiologically relevant. Thus, cAMP signalling in units as small as sub-cellular compartments has been described [30,31,32], while pulsatile and oscillatory patterns of cAMP concentration are common and can elicit different downstream responses than continuous cAMP elevations [22,33,34,35]. The data presented here suggests that this is achievable using JellyOp, a bleach resistant visual opsin from the box jellyfish *Carybdea rastonii*.

Optogenetic control of Gαs signalling has previously been achieved using chimeric receptors comprising light absorbing elements of mammalian rod opsin and G-protein interaction domains from other GPCRs [9,10]. Such OptoXRs have been used successfully to regulate cAMP and Ca^{2+} in vitro and in vivo, but the reproducibility and sustainability of activation have not been rigorously interrogated. Here we first set out to achieve this using a new luciferase-based cAMP biosensor to track live cell responses driven by OptoXRs. Our data reveal intrinsic limitations to the currently available rhodopsin/β2 adrenergic receptor chimera (Rh1B2AR 1-t). Thus, although light drove a clear induction of cAMP in HEK293 cells expressing this receptor, responses were low amplitude without preincubation with *cis*-retinaldehyde. We were able to achieve modest improvements in this aspect of performance by changing chimera design. However, the more important deficit was in response reproducibility, and none of our revised OptoXRs were able to recover the precipitous decline in response amplitude over repeated stimulation. This aspect of OptoXR behaviour is predicted by the bleaching characteristics of rod opsin, which requires a ready supply of *cis*-retinaldehyde to remain photosensitive in its native environment. As the enzymatic machinery required to generate large amounts of *cis*-retinaldehyde is restricted to the eye in mammals, this could be an important limitation to optogenetic application. Some researchers have applied exogenous *cis*-retinaldehyde when using rod opsin-based tools for optogenetic control [7]. Our data suggest that this represents only a partial solution to the problem, as its effectiveness should rapidly decline under repeated or continuous light exposure.

Our data suggest that JellyOp overcomes these critical limitations to allow reproducible and sustained cAMP responses. These features are consistent with published evidence that JellyOp is intrinsically bleach-resistant. Many animal opsins have two photo-interconvertible stable states binding either *cis*- or *trans*-isoforms of retinaldehyde. This enables them to remain photosensitive under repeated/continuous light exposure. The photobiology of JellyOp is incompletely understood, but Koyanagi et al (2008 [17]) were able to show that when purified JellyOp was reconstituted with 11-*cis* retinaldehyde, light exposure led to creation of a thermostable pigment binding all-*trans* retinaldehyde and absorbing visible wavelengths. In order to be fully bleach resistant, further light exposure should reconstitute the 11-*cis* isoform. Koyanagi et al (2008 [17]) did

not report this final step in bleach recovery for JellyOp, but this may be due to inadequacies in the *in vitro* environment. Our data support that view. The relatively poor performance of our rod-opsin based OptoXRs except in the presence of exogenous *cis*-retinaldehdye highlights how important such bleach-resistance is likely to be for *in vivo* application. A new generation of optogenetic tools based upon bleach-resistant animal opsins could then be contemplated.

JellyOp is the only animal opsin known to be Gαs coupled. This has enabled us to use it to achieve control of Gαs signalling without OptoXR-like modifications of putative G-protein interaction domains. Nevertheless, future work could usefully concentrate on structural modifications to the receptor. The intracellular surface of GPCRs is responsible not only for defining G-protein specificity, but also for targeting the receptor to specific cellular compartments; defining the rate of receptor deactivation; and coupling to non-canonical signalling pathways. It should therefore be possible in future to adjust these aspects of JellyOp activity by changing its intracellular domains. This potential to approximate multiple aspects of native GPCR activity sets JellyOp aside from other approaches directly targeting cAMP production. A group of microbial photoactivated adenylate cyclases (PACs) have been used to achieve this latter goal [28,36,37,38], although it is not yet clear whether these PACs approach the repeatability/sustainability of JellyOp signalling.

One most notable feature of JellyOp is its high sensitivity. We achieved pharmacological levels of cAMP induction with a white light stimulus as low as 1 $\mu W/cm^2$. This is many orders of magnitude below that required to activate the microbial light gated ion channels used so widely in neuroscience [27] and at least 10x below the threshold for the most sensitive currently available optogenetic tools [38,39,40]. As this means that JellyOp can be activated using simple, inexpensive, white light sources, it makes it a very accessible technology.

Acknowledgments

The authors would like to thank Laura Collins and Christoph Grün for technical assistance.

Author Contributions

Conceived and designed the experiments: HJB RJL. Performed the experiments: HJB L-YZ. Analyzed the data: HJB L-YZ. Contributed reagents/materials/analysis tools: RJL. Wrote the paper: HJB RJL.

References

1. IMS HWR (2000) IMS Industry Ranking of the Top 100 Products. Norwalk: IMS Health.
2. Schoenenberger P, Scharer YP, Oertner TG (2011) Channelrhodopsin as a tool to investigate synaptic transmission and plasticity. Exp Physiol 96: 34–39.
3. Rogan SC, Roth BL (2011) Remote control of neuronal signaling. Pharmacol Rev 63: 291–315.
4. Zhang F, Aravanis AM, Adamantidis A, de Lecea L, Deisseroth K (2007) Circuit-breakers: optical technologies for probing neural signals and systems. Nat Rev Neurosci 8: 577–581.
5. Zemelman BV, Lee GA, Ng M, Miesenbock G (2002) Selective photostimulation of genetically chARGed neurons. Neuron 33: 15–22.
6. Ye H, Daoud-El Baba M, Peng RW, Fussenegger M (2011) A synthetic optogenetic transcription device enhances blood-glucose homeostasis in mice. Science 332: 1565–1568.
7. Oh E, Maejima T, Liu C, Deneris E, Herlitze S (2010) Substitution of 5-HT1A receptor signaling by a light-activated G protein-coupled receptor. J Biol Chem 285: 30825–30836.
8. Gutierrez DV, Mark MD, Masseck O, Maejima T, Kuckelsberg D, et al. (2011) Optogenetic Control of Motor Coordination by Gi/o Protein-coupled Vertebrate Rhodopsin in Cerebellar Purkinje Cells. J Biol Chem 286: 25848–25858.
9. Kim JM, Hwa J, Garriga P, Reeves PJ, RajBhandary UL, et al. (2005) Light-driven activation of beta 2-adrenergic receptor signaling by a chimeric rhodopsin containing the beta 2-adrenergic receptor cytoplasmic loops. Biochemistry 44: 2284–2292.
10. Airan RD, Thompson KR, Fenno LE, Bernstein H, Deisseroth K (2009) Temporally precise in vivo control of intracellular signalling. Nature 458: 1025–1029.
11. Fung BK, Hurley JB, Stryer L (1981) Flow of information in the light-triggered cyclic nucleotide cascade of vision. Proc Natl Acad Sci U S A 78: 152–156.
12. Dickerson CD, Weiss ER (1995) The coupling of pertussis toxin-sensitive G proteins to phospholipase A2 and adenylyl cyclase in CHO cells expressing bovine rhodopsin. Exp Cell Res 216: 46–50.
13. Marin EP, Krishna AG, Zvyaga TA, Isele J, Siebert F, et al. (2000) The amino terminus of the fourth cytoplasmic loop of rhodopsin modulates rhodopsin-transducin interaction. J Biol Chem 275: 1930–1936.
14. Palczewski K, Kumasaka T, Hori T, Behnke CA, Motoshima H, et al. (2000) Crystal structure of rhodopsin: A G protein-coupled receptor. Science 289: 739–745.
15. Jastrzebska B, Tsybovsky Y, Palczewski K (2010) Complexes between photoactivated rhodopsin and transducin: progress and questions. Biochem J 428: 1–10.
16. Mustafi D, Palczewski K (2009) Topology of class A G protein-coupled receptors: insights gained from crystal structures of rhodopsins, adrenergic and adenosine receptors. Mol Pharmacol 75: 1–12.
17. Koyanagi M, Takano K, Tsukamoto H, Ohtsu K, Tokunaga F, et al. (2008) Jellyfish vision starts with cAMP signaling mediated by opsin-G(s) cascade. Proc Natl Acad Sci U S A 105: 15576–15580.
18. Seibold A, Williams B, Huang ZF, Friedman J, Moore RH, et al. (2000) Localization of the sites mediating desensitization of the beta(2)-adrenergic receptor by the GRK pathway. Mol Pharmacol 58: 1162–1173.
19. Seifert R, Wenzel-Seifert K, Lee TW, Gether U, Sanders-Bush E, et al. (1998) Different effects of Gsalpha splice variants on beta2-adrenoreceptor-mediated signaling. The Beta2-adrenoreceptor coupled to the long splice variant of Gsalpha has properties of a constitutively active receptor. J Biol Chem 273: 5109–5116.
20. Fan F, Binkowski BF, Butler BL, Stecha PF, Lewis MK, et al. (2008) Novel genetically encoded biosensors using firefly luciferase. ACS Chem Biol 3: 346–351.
21. DiPilato LM, Cheng X, Zhang J (2004) Fluorescent indicators of cAMP and Epac activation reveal differential dynamics of cAMP signaling within discrete subcellular compartments. Proc Natl Acad Sci U S A 101: 16513–16518.
22. Dunn TA, Wang CT, Colicos MA, Zaccolo M, DiPilato LM, et al. (2006) Imaging of cAMP levels and protein kinase A activity reveals that retinal waves drive oscillations in second-messenger cascades. J Neurosci 26: 12807–12815.
23. Zhang J, Hupfeld CJ, Taylor SS, Olefsky JM, Tsien RY (2005) Insulin disrupts beta-adrenergic signalling to protein kinase A in adipocytes. Nature 437: 569–573.
24. Zaccolo M, Magalhaes P, Pozzan T (2002) Compartmentalisation of cAMP and Ca(2+) signals. Curr Opin Cell Biol 14: 160–166.
25. Ma JX, Zhang D, Laser M, Brownlee NA, Re GG, et al. (1999) Identification of RPE65 in transformed kidney cells. FEBS Lett 452: 199–204.
26. Brueggemann LI, Sullivan JM (2002) HEK293S cells have functional retinoid processing machinery. J Gen Physiol 119: 593–612.
27. Lin JY (2011) A user's guide to channelrhodopsin variants: features, limitations and future developments. Exp Physiol 96: 19–25.
28. Weissenberger S, Schultheis C, Liewald JF, Erbguth K, Nagel G, et al. (2011) PACalpha–an optogenetic tool for in vivo manipulation of cellular cAMP levels, neurotransmitter release, and behavior in Caenorhabditis elegans. J Neurochem 116: 616–625.
29. Shenoy SK, Drake MT, Nelson CD, Houtz DA, Xiao K, et al. (2006) beta-arrestin-dependent, G protein-independent ERK1/2 activation by the beta2 adrenergic receptor. J Biol Chem 281: 1261–1273.
30. Zaccolo M, Pozzan T (2002) Discrete microdomains with high concentration of cAMP in stimulated rat neonatal cardiac myocytes. Science 295: 1711–1715.
31. Hempel CM, Vincent P, Adams SR, Tsien RY, Selverston AI (1996) Spatio-temporal dynamics of cyclic AMP signals in an intact neural circuitm. Nature 384: 166–169.
32. Rich TC, Fagan KA, Tse TE, Schaack J, Cooper DM, et al. (2001) A uniform extracellular stimulus triggers distinct cAMP signals in different compartments of a simple cell. Proc Natl Acad Sci U S A 98: 13049–13054.
33. Dyachok O, Isakov Y, Sagetorp J, Tengholm A (2006) Oscillations of cyclic AMP in hormone-stimulated insulin-secreting beta-cells. Nature 439: 349–352.
34. Dyachok O, Sagetorp J, Isakov Y, Tengholm A (2006) cAMP oscillations restrict protein kinase A redistribution in insulin-secreting cells. Biochem Soc Trans 34: 498–501.
35. Haisenleder DJ, Yasin M, Marshall JC (1992) Enhanced effectiveness of pulsatile 3′,5′-cyclic adenosine monophosphate in stimulating prolactin and alpha-subunit gene expression. Endocrinology 131: 3027–3033.
36. Schroder-Lang S, Schwarzel M, Seifert R, Strunker T, Kateriya S, et al. (2007) Fast manipulation of cellular cAMP level by light in vivo. Nat Methods 4: 39–42.

37. Bucher D, Buchner E (2009) Stimulating PACalpha increases miniature excitatory junction potential frequency at the Drosophila neuromuscular junction. J Neurogenet 23: 220–224.
38. Stierl M, Stumpf P, Udwari D, Gueta R, Hagedorn R, et al. (2011) Light modulation of cellular cAMP by a small bacterial photoactivated adenylyl cyclase, bPAC, of the soil bacterium Beggiatoa. J Biol Chem 286: 1181–1188.
39. Schultheis C, Liewald JF, Bamberg E, Nagel G, Gottschalk A (2011) Optogenetic long-term manipulation of behavior and animal development. PLoS One 6: e18766.
40. Berndt A, Schoenenberger P, Mattis J, Tye KM, Deisseroth K, et al. (2011) High-efficiency channelrhodopsins for fast neuronal stimulation at low light levels. Proc Natl Acad Sci U S A 108: 7595–7600.